PUBLICATIONS OF
THE UNIVERSITY OF EASTERN FINLAND

Dissertations in Health Sciences

LINE LOTTONEN-RAIKASLEHTO

VASCULAR ENDOTHELIAL GROWTH FACTORS IN HEART FAILURE

Cardiovascular Imaging and Gene Therapy Applications

Vascular Endothelial Growth Factors in Heart Failure

Cardiovascular Imaging and Gene Therapy Applications

LINE LOTTONEN-RAIKASLEHTO

Vascular Endothelial Growth Factors in Heart Failure

Cardiovascular Imaging and Gene Therapy Applications

To be presented by permission of the Faculty of Health Sciences, University of Eastern Finland for public examination in Mediteknia Auditorium, Kuopio, on Friday, May 13th 2016, at 12 noon.

Publications of the University of Eastern Finland
Dissertations in Health Sciences
Number 347

Department of Biotechnology and Molecular Medicine
A.I. Virtanen Institute for Molecular Sciences
Faculty of Health Sciences
University of Eastern Finland
Kuopio
2016

Grano Oy
Jyväskylä 2016

Distributor:
University of Eastern Finland
Kuopio Campus Library
P.O.Box 1627
FI-70211 Kuopio, Finland
http://www.uef.fi/kirjasto

ISBN (print): 978-952-61-2089-8
ISBN (pdf): 978-952-61-2090-4
ISSN (print): 1798-5706
ISSN (pdf): 1798-5714
ISSN-L: 1798-5706

Author's address: Department of Biotechnology and Molecular Medicine
A.I. Virtanen Institute for Molecular Sciences
University of Eastern Finland
P.O. Box 1627
FI-70211 Kuopio
FINLAND
E-mail: line.lottonen@uef.fi

Supervisors: Professor Seppo Ylä-Herttuala, M.D., Ph.D.
Docent Timo Liimatainen, Ph.D.
Dr. Jenni Huusko, Ph.D., BSc
Dr. Mari Merentie, M.D., Ph.D., MSc

Department of Biotechnology and Molecular Medicine
A.I. Virtanen Institute for Molecular Sciences
University of Eastern Finland
KUOPIO
FINLAND

Reviewers: Docent Raija Soininen, Ph.D.
Faculty of Biochemistry and Molecular Medicine
Biocenter Oulu
University of Oulu
OULU
FINLAND

Associate Professor Agnieszka Loboda, Ph.D.
Department of Medical Biotechnology
Faculty of Biochemistry
Biophysics and Biotechnology
Jagiellonian University
KRAKÓW
POLAND

Opponent: Professor Risto Kerkelä, M.D., Ph.D.
Research Unit of Biomedicine
University of Oulu
OULU
FINLAND

Lottonen-Raikaslehto, Line
Vascular Endothelial Growth Factors in Heart Failure -Cardiovascular Imaging and Gene Therapy Applications
University of Eastern Finland, Faculty of Health Sciences
Publications of the University of Eastern Finland. Dissertations in Health Sciences Number 347. 2016. 76 p.

ISBN (print): 978-952-61-2089-8
ISBN (pdf): 978-952-61-2090-4
ISSN (print): 1798-5706
ISSN (pdf): 1798-5714
ISSN-L: 1798-5706

ABSTRACT

Heart failure (HF) is a severe syndrome with poor prognosis. Despite improved treatment of cardiovascular diseases, chronic HF is expected to increase in the near future, partly due to an aging population. Left ventricular hypertrophy (LVH) is initially a compensatory mechanism to increased workload in the heart, but prolonged pathological stress induces transition to HF. The mechanisms of this process are unclear, in particular the role of vascular endothelial growth factors (VEGFs), which are the main regulators of vessel growth. Mechanisms underlying HF have been studied in recent years to improve treatments for patients. One treatment possibility being investigated is cardiovascular gene therapy. The main viral vectors studied for the use in gene therapy have been adenoviruses (AdVs), adeno-associated viruses (AAVs) and lentiviruses (LeVs).

In this thesis study expressions of VEGFs were studied in LVH, and their therapeutic potential in treating HF was evaluated in animal model. Furthermore, echocardiography and cardiovascular magnetic resonance imaging (CMR) were compared in the follow-up of LVH progression, and the efficacy and safety of local intramyocardial gene transfer of AdV, AAV and LeV and systemic delivery of AAV9 were investigated.

The results showed that in transverse aortic constriction (TAC)-induced progressive LVH, VEGF-C, VEGF-D and VEGFR-3 were up-regulated in the compensatory phase, whereas VEGF-B was down-regulated, when transition to HF occurred. AAV9-VEGF-B_{186} gene transfer in the compensatory phase of LVH improved systolic function of the heart and reduced apoptosis and metabolic remodelling. Increased angiogenesis and proliferation were also observed. Progressive LVH in mice with cardiac-specific overexpression of VEGF-B_{167} was studied by echocardiography and CMR, both imaging methods revealing similar structural and functional parameters. T_1 relaxation in the rotating frame of reference ($T_{1\rho}$) CMR showed a clear potential in detecting moderate to severe diffuse myocardial fibrosis. AAV and LeV vectors were less effective in transducing cardiomyocytes, but also less harmful compared to the widely used AdV vectors in cardiac gene transfer. Systemic transfer of the AAV9 virus vector led to myocardial fibrosis and deterioration of the LV function.

In conclusion, VEGFs play a central role in LVH development. In mice, VEGF-B gene therapy prevented progression of LVH to HF. Both echocardiography and CMR revealed similar structural and functional changes associated with LVH progression. Careful assessment of viral vectors and delivery routes have to be performed before gene therapy trials can be planned.

National Library of Medicine Classification: QU 107, QU 560, WG 370, WN 180

Medical Subject Headings: Vascular Endothelial Growth Factors; Heart; Myocardium; Heart Failure; Hypertrophy, Left Ventricular; Gene Expression; Echocardiography; Magnetic Resonance Imaging; Genetic Therapy; Gene Transfer Techniques; Genetic Vectors; Adenoviridae; Lentivirus; Safety; Disease Models, Animal

Lottonen-Raikaslehto, Line
Verisuonen endoteelin kasvutekijät sydämen vajaatoiminnassa -Sydän- ja verisuonikuvantaminen ja geeniterapiasovellukset
Itä-Suomen yliopisto, terveystieteiden tiedekunta
Publications of the University of Eastern Finland. Dissertations in Health Sciences Numero 347. 2016. 76 s.

ISBN (print): 978-952-61-2089-8
ISBN (pdf): 978-952-61-2090-4
ISSN (print): 1798-5706
ISSN (pdf): 1798-5714
ISSN-L: 1798-5706

TIIVISTELMÄ

Sydämen vajaatoiminta on vakava ja huonoennusteinen oireyhtymä, jonka esiintyvyys tulee lisääntymään lähitulevaisuudessa, kun ikääntyvän väestön määrä kasvaa ja selviytyminen muista sydän- ja verisuonitaudeista paranee. Vasemman kammion hypertrofia on aluksi kompensatorinen vaste sydämen kasvaneelle työkuormalle, mutta patologisen stressin jatkuessa kompensaatiokyky ylittyy, mistä seuraa sydämen vajaatoiminnan kehittyminen. Verisuonen endoteelin kasvutekijät (VEGF) ovat tärkeimpiä veri- ja lymfasuonten kasvun säätelijöitä, ja niiden rooli sydämen vajaatoiminnan kehittymisessä on epäselvä. Vajaatoimintaan johtavien prosessien tutkimuksessa pyritään löytämään uusia hoitomuotoja, joista virusvälitteinen geeniterapia adenoviruksia (AdV), adeno-assosioituvia viruksia (AAV) ja lentiviruksia (LeV) käyttäen on yksi mahdollisuus.

Tässä väitöskirjatutkimuksessa selvitettiin VEGF:en ilmentymistä vasemman kammion hypertrofiassa ja näiden terapeuttista potentiaalia sydämen vajaatoiminnan hoidossa. Sydämen ultraääni- ja magneettikuvantamisella seurattiin vasemman kammion liikakasvun kehittymistä. Lisäksi pieneläinmallissa selvitettiin AdV:n, AAV:n ja LeV:n tehokkuutta ja turvallisuutta ultraääniohjatuissa sydänlihaksen sisäisissä geeninsiirroissa sekä systeemisen geeninsiirron vaikutuksia AAV9-välitteisesti.

Kirurgisesti aiheutettu aortan kaaren ahtauma johti vasemman kammion hypertrofiaan ja kompensatorisessa vaiheessa VEGF-C:n ja VEGF-D:n sekä VEGFR-3:n ilmentymisen lisääntymiseen. VEGF-B:n ilmentyminen sen sijaan vähentyi sydämen vajaatoiminnan myötä. Hypertrofian kompensatorisessa vaiheessa tehdyn AAV9-VEGF-B_{186} geeninsiirron jälkeen sydämen systolisen toiminnan havaittiin pysyvän normaalilla tasolla. Geeniterapialla vähennettiin apoptoosia ja metabolista uudelleenmuokkausta, sekä lisättiin angiogeneesiä ja sydänlihassolujen jakautumista estäen näin sydämen vajaatoiminnan kehittyminen. Siirtogeenisissä hiirissä, joissa VEGF-B_{167}:ää yli-ilmennettiin sydämessä, voitiin havaita vasemman kammion etenevään hypertrofiaan liittyvät rakenteelliset ja toiminnalliset muutokset sekä ultraääni- että magneettikuvantamisen avulla. Lisäksi havaittiin $T_{1\rho}$ magneettikuvantamismenetelmän potentiaali laaja-alaisen fibroosin osoittamisessa. Geeniterapiakokeet osoittivat AAV ja LeV -vektorien olevan tehottomampia, mutta myös haitattomampia paikallisessa geeninsiirrossa kuin AdV-vektori. Systeemisesti annettuna AAV9 johti sydänlihaksen fibroosiin ja vasemman kammion toiminnan heikentymiseen.

Yhteenvetona voidaan todeta, että VEGF:llä on keskeinen rooli vasemman kammion hypertrofian kehittymisessä. Hiirillä VEGF-B geeniterapia esti hypertrofian kehittymistä sydämen vajaatoiminnaksi. Ultraääni- ja magneettikuvantaminen osoittivat etenevään hypertrofiaan liittyvät rakenteelliset ja toiminnalliset muutokset. Geeniterapiasovellusten suunnitteluvaiheessa virusvektorit ja geeninsiirtoreitit tulee arvioida huolellisesti.

Luokitus: QU 107, QU 560, WG 370, WN 180

Yleinen Suomalainen asiasanasto: kasvutekijät; verisuonet; endoteeli; sydän; sydämen vajaatoiminta; geenilekspressio; kuvantaminen; ultraäänitutkimus; magneettitutkimus; geeniterapia; geenitekniikka; adenovirukset; lentivirukset; turvallisuus; koe-eläinmallit

It always seems impossible until its done.

Nelson Mandela

Acknowledgements

This thesis work was carried out in the Department of Biotechnology and Molecular Medicine, A.I. Virtanen Institute for Molecular Sciences, University of Eastern Finland during the years 2009-2016. Many people have contributed to my studies or made my days otherwise easier at AIVI, for which I'm sincerely grateful for.

First and foremost I wish to thank my main supervisor Professor Seppo Ylä-Herttuala for giving me the opportunity to join your research group as a first-year medical student. You have given me the freedom, but also responsibility to advance research alongside my medical studies. I appreciate your overall optimism, enthusiasm and capability to see the big picture in research.

My second supervisor Docent Timo Liimatainen, I wish to thank you for your expertise in the field of cardiovascular magnetic resonance imaging. I'm grateful, that you too allowed me to advance my research while completing my medical studies.

The mouse team founders, my supervisors and most of all my friends Mari Merentie and Jenni Huusko are warmly thanked for everything related to my research work. Mari, thank you for choosing me to join the mouse team. I will never forget the endless hours you spent in the beginning teaching me almost everything needed for my research work; from animal handling and echocardiography to laboratory methods, and from data analyses to the basics of scientific writing. Within the last half a year you have been available for all my questions and worries regarding this thesis work. Jenni, thank you for letting me participate in your work and providing help whenever needed. I appreciate your strong opinions and effectiveness in work. I'm grateful for your support when completing this thesis.

I wish to thank the official pre-examiners of this thesis Docent Raija Soininen and Associate Professor Agnieszka Loboda. I appreciate your valuable comments and new ideas, which helped me to improve this thesis. Dr. Nihay Laham-Karam, thank you for the excellent and precise English-language proofreading. In addition to that I would like to thank you for being such a caring and helpful office mate for many years. I am grateful for getting to know you.

All the past and present researchers have made the group a unique and inspiring place to work in. I think the best thing in our group is, that people have lots of variety in their background and knowledge about different things. I have had lots of help from many people, but also extremely fun moments outside the labs. I wish to thank all of the mouse team members: Riina Rissanen, Viktor Parviainen, Annakaisa Tirronen, Anssi Laine, Teemu Valkama and Erika Gurzeler. Erika, it has been great to share knowledge, thoughts and sometimes also frustration about the research with you. Venla Olsson, thank you for sharing the office for many years and for the nice chats during the work days. Marike Dijkstra, I appreciate your help with molecular biology methods. Lari Holappa, thank you for the great handling of the animal-related matters and also sharing your knowledge about the vectors. Suvi Jauhiainen and Tiina Nieminen, I wish to thank you for all the help with practical issues and encouraging words regarding the preparation of this thesis. Johanna Laakkonen, thank you for your help especially with microscopy and image processing. Krista Honkonen and Hanna Stedt, thank you for being my friends also outside of the research world and hospital environment.

Elisa Hytönen, it has been a privilege to get to know you. You are such a warm-hearted and reliable friend, having always time to listen and help in whatever is needed. I appreciate all the work you have done for this thesis, in addition to being a great mental support. I have been fortunate to get to know your family too; I hope that we'll have time to meet much more often. Anna-Kaisa Ruotsalainen, thank you for being such a great friend

for many years. We have shared knowledge about the science, but most importantly thoughts about many aspects of life. I also hope to see you and your family more frequently.

The technicians have made the studies possible. I wish to acknowledge Seija Sahrio, Anne Martikainen, Tuula Salonen, Svetlana Laidinen, Tiina Koponen, Sari Järveläinen, Anne Karppinen, Mervi Nieminen, Anneli Miettinen, Joonas Malinen and Maarit Mähönen for their valuable help. My gratitude is extended to Pekka Alakuijala, Jari Nissinen and Jouko Mäkäräinen for their help with many practical issues. Helena Pernu, Marja Poikolainen, Jatta Pitkänen and Marjo-Riitta Salminkoski, thank you for the help with the sometimes extremely confusing bureaucracy of the University.

Mum Pia and dad Jarmo, you have given me multiple opportunities in life and encouraged me to follow my own path. Your support and belief in me have been invaluable throughout the years. I know, that whatever happens, you are there for me. Thank you for everything. Joanna, you are a great little sister. I miss your cooking skills and wish, that we could go for a walk around Töölönlahti much more often. You are dear to me. My grandmother Irma, I appreciate your support and interest in whatever I have decided to do in my life.

Teppo, thank you for sharing the past ten years with me. You have supported and encouraged me to follow my dreams, and have understood my choices. With your help in practical issues, I have been able to combine medical studies, research and motherhood, which I truly appreciate. Ellen, you are the dearest in my life. During the past 2.5 years you have taught me more about myself than anybody else before. I admire your positive curiosity, energy and sincerity. You could not be more right when you sing, "Elämä ei ole hassumpaa, kun saa Epen kanssa asustaa…". Olet ihana!

Kuopio, April 19th 2016

Line Lottonen-Raikaslehto

This work was supported by grants from Finnish Academy, Sigrid Juselius Foundation, Finnish Foundation for Cardiovascular Research, Ida Montin Foundation, Aarne Koskelo Foundation, Center of Excellence and The Finnish Medical Foundation.

List of the original publications

This dissertation is based on the following original publications and manuscript:

I Huusko J, **Lottonen L**, Merentie M, Gurzeler E, Anisimov A, Miyanohara A, Alitalo K, Tavi P, Ylä-Herttuala S. AAV9-mediated VEGF-B gene transfer improves systolic function in progressive left ventricular hypertrophy. Molecular Therapy 20(12):2212-2221, 2012.

II **Lottonen-Raikaslehto L**, Rissanen R, Gurzeler E, Merentie M, Huusko J, Schneider J, Liimatainen T, Ylä-Herttuala S. Left ventricular remodelling leads to heart failure in mouse with cardiac-specific overexpression of VEGF-B_{167} - Echocardiography and magnetic resonance imaging study. Submitted manuscript.

III Merentie M, **Lottonen-Raikaslehto L***, Parviainen V*, Huusko J, Pikkarainen S, Mendel M, Laham-Karam N, Kärjä V, Rissanen R, Hedman M, Ylä-Herttuala S. Efficacy and safety of myocardial gene transfer of adenovirus, adeno-associated virus and lentivirus vectors in the mouse heart. Gene Ther 2016 Mar;23(3):296-305.

* Authors with equal contribution.

Contents

Abbreviations

AAV	Adeno-associated virus
AC	Adenylyl cyclase
ACE	Angiotensin-converting enzyme
ADHF	Acute decompensated heart failure
Ad libitum	Free feeding with unlimited access to food and water
AdV	Adenovirus
Akt	Protein kinase B
Ang-1	Angiopoietin-1
AngII	Angiotensin II
ANOVA	Analysis of Variance
ANP	Atrial natriuretic peptide
ARNI	Angiotensin receptor and neprilysin inhibitor
ATP	Adenosine-5′-triphosphate
AF	Atrial fibrillation
AV node	Atrioventricular node
BNP	B-type natriuretic peptide
Ca^{2+}	Calcium ion
CAD	Coronary artery disease
CAMK	Calcium/calmodulin kinase
cAMP	cAMP Cyclic adenosine cyclic adenosine monophosphate
cGMP	Cyclic guanosine monophosphate
CMR	Cardiovascular magnetic resonance
CMV	Cytomegalovirus
CNP	C-type natriuretic peptide
CO	Cardiac output
CT	Computed tomography
CT-1	Cardiotrophin 1
cTnT	Cardiac troponin T
CVD	Cardiovascular diseases
DAG	Diacylglycerol
DNA	Deoxyribonucleic acid
ECG	Electrocardiography
EDV	End-diastolic volume
EF	Ejection fraction
ELISA	Enzyme-linked immunosorbent assay
Endo-1	Endothelin-1
ERK	Extracellular-signal-regulated kinase
ESV	End-systolic volume
FGF	Fibroblast growth factor
Gα	Subunit of GPCR
Gβγ	Subunit of GPCR
GC-A	Guanyl cyclase-A
GFP	Green fluorescent protein
GMP	Good manufacturing practice
GH	Growth hormone
gp130	Glycoprotein 130
GPCR	G-protein-coupled receptor
GSK-3	Glycogen synthase kinase 3
HE	Hematoxylin-eosin staining
HF	Heart failure
HFpEF	Heart failure with preserved ejection fraction
HFrEF	Heart failure with reduced ejection fraction
hPLAP	Human placental alkaline phosphatase
HT	Hypertension
IGF	Insulin-like growth factor
InsP3	Inositol tris phosphate
In vitro	In an artificial environment outside the living organism
In vivo	Within a living organism
I.v.	Intravenous
JAK	Janus kinase

JNK	c-Jun kinase
LA	Left atrium
LacZ	β-galactosidase
LDH	Lactate dehydrogenase
LeV	Lentivirus
LGE	Late gadolinium enhancement
LV	Left ventricle
LVH	Left ventricular hypertrophy
MAP	Mean arterial pressure
MAPK	Mitogen-activated protein kinase
MHC	Myosin heavy chain
MI	Myocardial infarction
mRNA	Messenger ribonucleic acid
MRS	Magnetic resonance spectroscopy
mTOR	Mammalian target of rapamycin
NFAT	Nuclear factor of activated T cells
NFκB	Nuclear factor κB
NLS	Nuclear localization signal
NPRA	Natriuretic peptide receptor A
Nrp	Neuropilin
NYHA	New York Heart Association
p110γ	Isoform of PI3K
PAD	Peripheral artery disease
PAS	Periodic acid-Schiff´s glycogen staining
PBS	Phosphate-buffered saline
PET	Positron emission tomography
PDGF	Platelet-derived growth factor
PFA	Paraformaldehyde
PGC-1α	Peroxisome proliferator-activated receptor gamma co-activator
PI3K	Phosphoinositide 3′-OH kinase
PIP_3	Phosphatidylinositol tris phosphate
PK-A	Protein kinase A
PK-C	Protein kinase C
PKG I	Protein kinase G I
PLC	Phospholipase C
PlGF	Placental growth factor
PPAR	Peroxisome proliferator-activated receptor
PPIA	Peptidylprolyl isomerase
p38K	p38 kinase
RAAS	Renin-angiotensin-aldosterone system
RAS	Monomeric G-protein
RNA	Ribonucleic acid
RTK	Receptor tyrosine kinase
RT-PCR	Reverse transcriptase polymerase chain reaction
RV	Right ventricle
S.c.	Subcutaneous
SD	Standard deviation
SERCA2	Sarcoplasmic reticulum calcium^{2+}-ATPase
SEM	Standard error of the mean
SNS	Sympathetic nervous system
STAT	Signal transducer and activator of transcription
TAC	Transverse aortic constriction
TGF-β1	Transforming growth factor beta 1
TIA	Transient ischemic attack
VEGF	Vascular endothelial growth factor
VEGFR	Vascular endothelial growth factor receptor

1 Introduction

Prevalence of heart failure (HF) is increasing rapidly and the syndrome has a poor prognosis (Farmakis et al. 2015). Knowledge of the pathophysiology of several diseases causing HF has increased the effort to find new, more effective and targeted treatment strategies. Traditional treatment options or invasive procedures are not suitable for all patients and gene therapy has been under investigation for these no-option patients. (Markkanen et al. 2005.)

Left ventricular hypertrophy (LVH), commonly caused by hypertension, is one major reason for HF. LVH is characterized by progressive structural, functional and metabolic changes, as well as alterations in gene expression profiles. At the end-stage these features lead to accumulation of myocardial fibrosis and dilatation of the LV. (Kerkela, Force 2006.) Early diagnosis of the changes associated with LVH would be beneficial in developing new treatment strategies for delaying LVH progression. Cardiovascular magnetic resonance imaging (CMR) has brought new methods to evaluate diseased and structurally altered LV accurately (Kramer, Hundley 2010).

The role of vascular endothelial growth factor (VEGF)-B in cardiac diseases has been under investigation in the past years. VEGF-B has been shown to have cardioprotective properties after gene transfer to ischemic and nonischemic hearts (Lahteenvuo et al. 2009, Pepe et al. 2010). Altered lipid metabolism and cardiac hypertrophy have been associated with the overexpression of VEGF-B_{167} in the heart (Karpanen et al. 2008).

Gene therapy is based on transferring genetic material into targeted tissues and allowing transgene expression of the therapeutic protein which can then act locally or systemically. Suitable gene delivery route, viral vector and optimal viral dose have been studied in small and large animal models and positive results from safety in clinical gene therapy trials with adenovirus (AdV) have been confirmed. (Yla-Herttuala, Alitalo 2003, Hedman et al. 2009.) AdV, adeno-associated virus (AAV) and lentivirus (LeV) vectors have been studied in cardiovascular gene therapy. AdVs are the most commonly used vectors in gene therapy studies and they induce an effective, but transient expression of the transgene, whereas AAVs demonstrate less effective, but long-term transgene expression. LeVs integrate into the host cell genome and can provide potentially a lifelong transgene expression, however their use in cardiac gene therapy has still been limited. (Kay, Glorioso & Naldini 2001.) Cardiovascular gene therapy has mainly focused on inducing angiogenesis in ischemic regions in the heart or lower extremities (Lahteenvuo et al. 2009, Korpisalo et al. 2011).

The aim of this thesis study was to investigate the expression of different VEGFs and their receptors in LVH progression and to evaluate the potential to treat failing heart with VEGF-B gene therapy. Echocardiography and CMR were compared in following LVH progression in mice with cardiac-specific overexpression of VEGF-B. The effects and safety of AdV, AAV and LeV vectors in mouse heart were also evaluated.

2 Review of the literature

2.1 CARDIOVASCULAR DISEASES

2.1.1 Epidemiology of cardiovascular diseases

Cardiovascular diseases (CVD) are the leading cause of death globally covering over 30 percent of all deaths (WHO, who.int). In Europe over 4 million people die of CVD every year and that represents almost half (46 %) of all deaths. Coronary artery disease and cerebrovascular disease cause the majority of CVD related deaths in Europe. (Nichols et al. 2014.)

Age-adjusted mortality to CVD shows large inequality between European countries, although overall it has decreased (Nichols et al. 2014). Death rates are higher in Central and Eastern Europe than in Northern, Southern and Western Europe (Nichols, M 2012).

Morbidity of CVD reflects on hospitalization, which has increased since the early 2000s according to hospital discharge data. The burden of the CVD is high, this is partly because of the increase in the ageing population. (Nichols et al. 2014.) In the EU almost 196 billion euros per year are used to cover costs from CVD, which include the direct health care costs, productivity losses and informal care of people with CVD (Nichols, M 2012).

The main risk factors affecting CVD are smoking, diet, physical inactivity, alcohol consumption, hypertension, hypercholesterolemia, obesity and diabetes. Especially the prevalence of diabetes has increased rapidly during the last decade, not only as a single risk factor but also as a factor that multiplies the effects of other risk factors. (Nichols, M 2012.) It has been suggested, that 40-50 % of all diabetics are still undiagnosed (Tamayo et al. 2014). Several gene variants have been found to be associated with increased risk of CAD or myocardial infarction (MI; Roberts 2014). Psychosocial factors including depression and continuous stress were shown to be strong risk factors for MI (Yusuf et al. 2004).

Current treatment of CVD focuses on addressing risk factors. Prevention is aimed at by distribution of information about the lifestyle aspects affecting the risk of CVD. Different medications are used to reduce high blood pressure, cholesterol and glucose levels. Furthermore, complications from CVD can also be treated with invasive methods including endovascular procedures (balloon angioplasty and stenting) and cardiac and peripheral bypass surgery. (Piccolo et al. 2015.)

2.2 CARDIOVASCULAR SYSTEM

2.2.1 Anatomy and function of the heart

The heart consists of two pumps, both of which have two chambers called the atrium and ventricle (Figure 1). Deoxygenated blood comes to the right atrium from the body via the superior and inferior vena cava, it continues to the right ventricle and then to the lungs via the pulmonary trunk. The pulmonary veins take the oxygenated blood from the lungs to the left atrium, from where it continues to the left ventricle and then via the aorta to the peripheral organs. (Drake, Vogl & Mitchell 2005.) The pump function of the heart maintains the circulation of the blood; it affects the blood pressure and is important in transferring oxygen and nutrients to the periphery. The right and left coronary arteries originate from the aortic sinuses of the ascending aorta and supply blood to the heart. (Guyton, Hall 2006.)

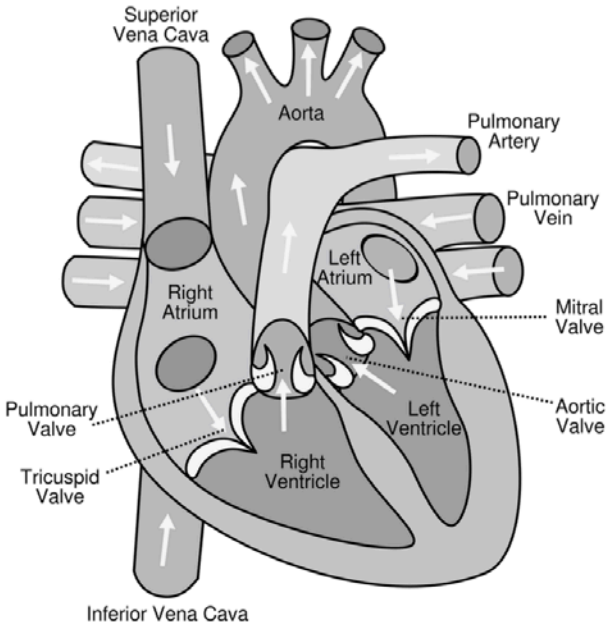

Figure 1. Anatomy of the heart. White arrows indicate the normal direction of the blood flow (Courtesy of Wikipedia.org, used under licence).

The cardiac muscle is striated with some special features in its structure. Actin and myosin are complex protein molecules responsible for the contraction of the sarcomere unit. Actin, tropomyosin and troponin form the actin filament and in the relaxed stage tropomyosin-troponin complex prevents the active sites from connecting with the myosin. The action potential induces an influx of calcium to the cytoplasm via the T tubules, which are connected to the extracellular fluid. Sarcoplasmic reticulum releases also calcium to the cytoplasm due to the action potential, but the amount of ions is not enough to provide full contraction. Calcium in the cytoplasm attaches to troponin C, which activates the crossbridges between the actin and myosin filaments. The actin filament slides inward among the myosin filaments and starts the contraction by shortening the sarcomere unit. The strength of a cardiac contraction highly depends on the concentration of calcium; the more calcium ions bind to troponin and activate crossbridges between the actin and myosin filaments, the higher contractility of the heart is achieved. (Guyton, Hall 2006.)

A unique feature of cardiac muscle is intercalated discs; these are cell membranes which connect cardiac muscle cells in series and in parallel with each other. Gap juctions in intercalated discs allow free diffusion of the ions, which enable the action potentials to travel easily from one cell to another. The atrial and ventricular cell networks, syncytiums, are separated with fibrotic tissue around the openings of aorta, pulmonary trunks and ventricles on both sides. (Guyton, Hall 2006.)

Initiation of the action potential is caused by opening of the fast and slow sodium channels. The slow sodium channels enable calcium and sodium to influx inside the cardiac cell and this maintains a prolonged depolarization (plateau) in the cell. Decreased potassium permeability prevents positively charged potassium ions to outflux from the cells during the action potential plateau and an early return of the action potential voltage to its resting level. Closing of the slow calcium-sodium channels decreases the influx of these ions and permeability for potassium increases rapidly returning the membrane potential to resting level. (Guyton, Hall 2006.)

The sinus node in the wall of the right atrium initiates the action potential spontaneously which is the start for one cardiac cycle. The action potential moves through both atriums

and delays at atrioventricular (AV) node to enable the atriums to contract earlier than the ventricles. The action potential continues towards apex of the heart in the septum and then to all parts of the ventricle. During systole, the heart pumps the blood from the ventricles to the lungs and the periphery. The blood returns to the heart during the diastole. The reason for the separated atrial and ventricular syncytiums is that the atriums contract and fill the ventricles before systole. (Guyton, Hall 2006.)

An electrocardiogram (ECG) can record the electrical voltages of the heart. In the ECG, the P wave is the duration of atrial depolarization, the PQ is the time from the start of atrial depolarization to the beginning of ventricular depolarization, the QRS indicates the ventricular depolarization and the T wave the ventricular repolarization. The QT time refers to the ventricular depolarization and repolarization. (Thaler 2010.) Early repolarization in the murine heart produces a J wave in the ECG, this is due to the T wave merging with the final part of the QRS complex leaving the murine ECG without a clear ST-segment or T wave (Liu et al. 2004). Representative ECGs from a human and a mouse are presented in Figure 2.

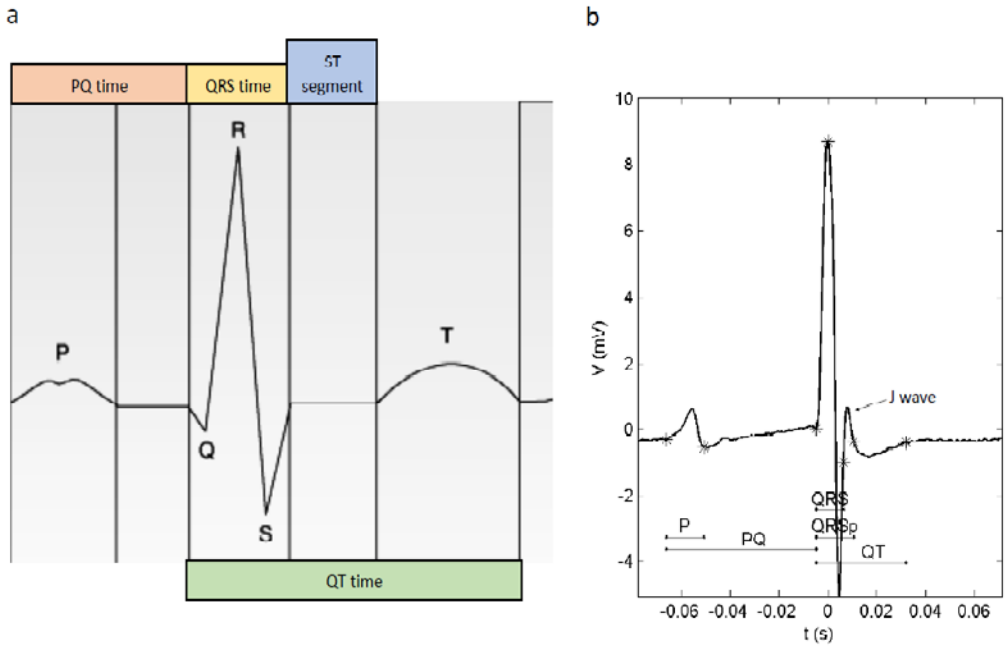

Figure 2. Representative ECG curves from a human (a) and a mouse (b). Atrial depolarization (P) and ventricular depolarization (QRS) are presented in both ECGs. In the human ECG, the T wave can be distinguished at the end of the ventricular repolarization. In the mouse ECG, the J wave after the QRS complex represents early repolarization and the T wave is not distinguishable as it merges with the end of the QRS complex. (a) Modified from http://www.terveysportti.fi/dtk/aho/inf04260, read 30.3.2016. (b) From own studies.

The heart pumps automatically all incoming blood to the arteries. Due to the Frank-Starling mechanism the stronger the stretch of the heart muscle is during filling, the stronger the contraction is. Sympathetic stimulation of the heart increases the heartbeat and force of the contraction resulting in increased cardiac output. The end-diastolic pressure (preload) and the pressure in the artery leading from the ventricle (afterload) influence the contractile properties of the heart and are often affected in abnormal functional states of the heart or in the circulation. (Guyton, Hall 2006.)

2.2.2 Metabolism of the heart

In the healthy adult heart over 95 % of the ATP formation comes from oxidative phosporylation in the mitochondria. At rest, 70 % of the energy is derived from fatty acids, whereas glucose and lactate cover the remaining percentage. 60-70 % of ATP is used for muscle contraction and 30-40 % for the sarcoplasmic reticulum calcium^{2+}-ATPase (SERCA2) and other ion pumps. Mitochondrias are 40 % of the cardiac cell volume and at rest use 15-25 % of the oxidative capacity. During exercise the heart can increase the oxidative capacity to 80-90 % and also utilize lactate, which is released from the skeletal muscles due to heavy training, as an energy source. (Stanley, Recchia & Lopaschuk 2005.)

Contractile performance of the heart at a given rate of myocardial oxygen consumption was shown to be better when more glucose and lactate and less fatty acids were oxidized (Stanley, Chandler 2002). It was shown in dog studies, that increased fatty acid uptake to the heart resulted in increased myocardial oxygen consumption without changing the mechanical power of the LV (Mjos 1971). This indicates, that acquiring a given rate of ATP synthesis from fatty acids, compared to carbohydrates, requires greater rate of oxygen consumption (Mjos 1971, Stanley, Chandler 2002).

Cardiac metabolism depends on the substrates available, the hemodynamic condition and inotropic state. Enzymes, transporters and the amount and activity of mitochondrias all affect the metabolic phenotype of the heart. (Stanley, Recchia & Lopaschuk 2005.) Mitochondrial biogenesis and function are regulated by transcription factors associated with replication and trascription of mitochondrial genome, which allows cellular adaptation to changing energetic and metabolic demands. Peroxisome proliferator-activated receptors (PPARs) are ligand-activated transcription factors, which activate transcription of fatty acid oxidation genes when lipid concentration inside the cell increased. Peroxisome proliferator-activated receptor-gamma coactivator (PGC)-1α and β are transcriptional coactivators that are expressed widely in tissues with high energy demands and they have been found to integrate physiological signals to several transcription factors associated with mitochondrial genes. Overexpression of PGC-1α and PGC-1β was shown to increase mitochondrial content, expression of mitochondrial genes and to improve exercise performance. Increased energy need was shown to induce PGC-1α expression indicating a role for this coactivator in the long-term adaptation to changed energy needs. Several signaling pathways were shown to participate in the posttranslational regulation of PGC-1α activation. (Hock, Kralli 2009.)

Pathological remodelling of the LV due to heart disease was associated with changes in the metabolism, which shifted from using fatty acids to glucose as the main energy source. Normal fatty acid uptake has been detected in the early stage of HF but the fatty acid oxidation decreases significantly in advanced or end-stage HF. In LVH increased glucose uptake and glycolysis result from altered regulation of the metabolism, in which transcription of genes associated with fatty acid oxidation and mitochondrial oxidative phosphorylation is decreased. Lactate dehydrogenase (LDH) activity is increased in LVH, which results in elevated levels of lactate converted from pyruvate and an increased efflux of lactate from the myocardium. (Stanley, Recchia & Lopaschuk 2005, Kolwicz, Tian 2011.)

2.3 HEART FAILURE

2.3.1 Epidemiology of heart failure

HF is a syndrome with typical symptoms and clinical signs, which result from cardiac abnormality in structure or function (McMurray et al. 2012). The failing heart is incapable of providing sufficient blood flow to fulfill the metabolic needs or accommodate the systemic venous return. CAD, MI, hypertension (HT) and atrial fibrillation (AF) are the most common reasons for HF development. Cardiomyopathies, infections, toxins, valvular disease and prolonged arrhythmias are less common reasons for HF. (Kemp, Conte 2012.)

CAD causes 1.8 million deaths in Europe each year and is the single most common reason for death. Hospital discharge rates in Europe for CAD are 800 per 100 000 population. (Nichols M 2012.) CAD reduces the blood flow to the myocardium due to atherosclerotic plaques, which leads to insufficient oxygen supply, reduced availability of nutrients and insufficient removal of metabolites. Atherosclerotic plaques consist of a lipid core with a fibrotic cap protruding into the vessel lumen. A plaque obstructing at least 75 % of the vessel lumen would usually cause angina pectoris as a symptom during exercise. (Kumar et al. 2010.) Angina reduces the quality of life affecting the ability to work, do physical activities and induces mental distress, hospitalization and financial costs (Piccolo et al. 2015). Symptoms at rest develope when 90 % of the vessel lumen is obstructed. Acute coronary syndrome occurs typically when a weakened fibrotic cap of the plaque ruptures and a thrombus occludes the rest of the obstructed lumen preventing the blood flow to the distal part of the vessel. Prolonged obstruction leads to severe ischemia and death of the myocardium, which is refered to as myocardial infarction. (Kumar et al. 2010.)

HT occurs usually with other risk factors for CVD and they may potentiate each other thus leading to increased total risk of CVD. In Europe 30-45 % of the population suffer from high blood pressure, which is an important cause of stroke and HF. The definition for HT is systolic blood pressure over 140 mmHg and/or diastolic blood pressure over 90 mmHg. (Mancia et al. 2014.) Systemic hypertension induces a pressure overloadon the left side of the heart thus activating adaptive mechanisms and leading to cardiac hypertrophy (Kumar et al. 2010). A beneficial effect of using antihypertensive drugs in preventing HF has been shown (Mancia et al. 2014).

AF has become a major public health problem and the prevalence is still increasing. Improved treatment of chronic cardiac diseases has resulted in increased survival of patients, consequently, this longevity is expected to contribute to the prevalence of AF. Aging is a risk factor for AF; 3,7-4,2 % of 60-70 years old and 10-17 % of 80 years old are affected by the disease. In Europe approximately 10 million patients are suffering from AF. It has been estimated, that within the next 15 years there will be 14-17 million individuals in Europe with AF and the increase is 120 000-215 000 new cases per year. (Zoni-Berisso et al. 2014.) AF is a supraventricular tachyarrhythmia that is characterized by uncoordinated atrial contraction. With normal AV conduction, the ventricular response to AF is irregular and usually fast. Palpitations, chest pain, dyspnea, fatigue and lightheadedness are the most common symptoms that patients suffer from, but some patients may not even recognize the arrythmias. Long-term risks of stroke, transient ischemic attac (TIA) and HF are increased among patients with AF. It has been shown, that HF induces AF and AF worsens HF state predicting a poor prognosis for patients with both conditions. (Fuster et al. 2011.)

The prevalence of chronic HF will increase in the near future as a result of an aging population and longer survival with CVDs causing the HF. Over 2 % of the population in the USA and 1-2 % in Europe suffer from HF. It has been estimated, that by the year 2030 the HF prevalence in the USA would increase 46 %. Compared to many cancers HF has a worse prognosis; the overall 5-year mortality rate is approximately 50 %. 30-50 % of the patients hospitalized for acute decompensated heart failure (ADHF) die within a year. The economic burden of HF is significant due to its high prevalence, therapy demands, comorbidity and most importantly frequent hospitalization. (Farmakis et al. 2015.)

2.3.2 Pathophysiology of heart failure

Compensatory mechanisms are activated when the failing heart tries to maintain adequate function. The mean arterial pressure (MAP), resulting from cardiac output (CO) and total peripheral resistance, is carefully regulated. The body has multiple options, which are discussed later, for trying to compensate the reduced MAP affecting the tissue perfusion. Long-term effects of the initially beneficial changes in the heart lead to deterioration of the LV dysfunction in a vicious cycle (Figure 3). (Kemp, Conte 2012.)

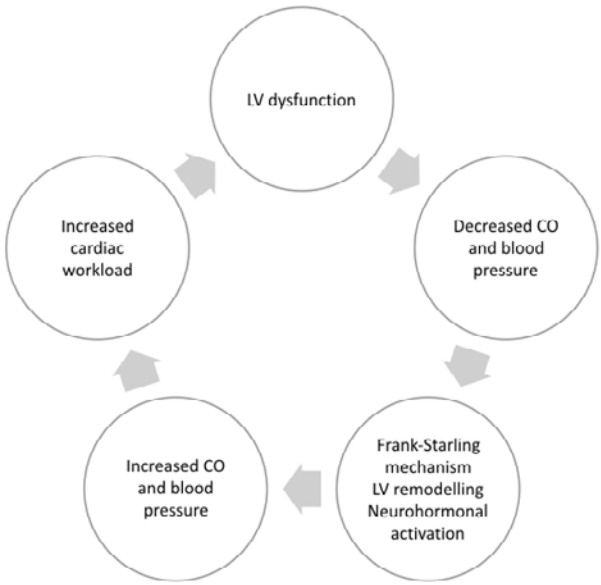

Figure 3. A vicious cycle in HF progression. LV dysfunction activates compensatory mechanisms, which by increasing cardiac output (CO) and blood pressure try to maintain sufficient blood flow to peripheral tissues. Increased workload on the heart leads to deterioration of the LV function and initiation of a new cycle, until the compensatory mechanisms reach their limits. Modified from Kemp et al. (Kemp, Conte 2012).

Increased volume or pressure overload due to physiological or pathological reasons activate the hypertrophic signaling pathway to maintain normal contractility and sufficient blood flow to peripheral tissues (Kemp, Conte 2012). The initial response to increased cardiac stress in pathological conditions, like HT or valvular stenosis, is concentric hypertrophy, which is characterized by a decreased LV internal diameter and an increase in cardiomyocyte thickness more than in length leading to increased LV wall thickness. MI or dilated cardiomyopathy lead to an eccentric type of hypertrophy, in which the ventricular volume increases and LV walls become thinner due to lengthening of cardiomyocytes. (Maillet, van Berlo & Molkentin 2013.) Hypertrophy is also a response to physiological stimulus of volume or pressure overload in athletes or during pregnancy without affecting the cardiac function. Physiological growth is moderate and the mass of the heart increases 10-20 % due to proportional addition in muscular and non-muscular cell compartments. Eccentric and concentric changes are reversible and milder than detected in pathological LVH. (Hunter, Chien 1999, Maillet, van Berlo & Molkentin 2013.)

Continuous pathological stress in the heart eventually leads to failure of the compensatory mechanisms to maintain cardiac function and subsequently LV remodelling proceeds. Neurohumoral factors, mechanical stretch and cytokines affect intracellular hypertrophic signaling pathways, which regulate transcription factors, gene expression profile and protein synthesis. Eventually LV remodelling results in decompensated HF with increased fibrosis, cell death by necrosis or apoptosis, disarray of sarcomeres and LV dilatation. (Kerkela, Force 2006.) Autophagy, the degradation and recycling of damaged cellular components, in HF has been studied in the past years and according to the present knowledge, autophagy is thought to be an adaptive mechanism in HF rather than a suicide pathway for the cardiomyocytes (Nishida, Otsu 2015). Genetic reprogramming towards expression of fetal isoforms of sarcomeric proteins (β-myosin heavy chain and skeletal α-actin) and natriuretic peptides is observed in HF (Kerkela, Force 2006). HF has been

associated with impaired calcium cycling resulting in reduced calcium content in the sarcoplasmic reticulum, deteriorated myofilament activation and decreased contractility. A known phenomenon in HF is the SERCA2a dysfunction, which delays the transport of cytoplasmic calcium to sarcoplasmic reticulum. In addition, the cytosolic calcium content is increased due to its leakage from the sarcoplasmic reticulum. (Gorski, Ceholski & Hajjar 2015.)

A decrease in MAP activates both the sympathetic nervous system (SNS), acting via the norepinephrine and epinephrine, and the renin-angiotensin-aldosterone system (RAAS). The SNS and RAAS are important stimulators of LVH. Prolonged overstimulation of SNS has been connected with the development of chronic HF by defecting excitation-contraction coupling and enhancing apoptosis. In addition, signaling via cardiac $beta_1$-adrenergic receptors has been shown to be dysregulated in HF. (Triposkiadis et al. 2009.) RAAS in the peripheral vasculature participates in the vicious cycle of HF by facilitating the release of norepinephrine, inducing vasopressin release and increasing sodium absorption and cardiac contractility. Angiotensin II (Ang II), converted from angiotensin I by angiotensin-converting enzyme (ACE) was shown to be an important peptide in the process leading to LVH. (Kemp, Conte 2012.)

The mammalian natriuretic peptide (NP) system contains three members. Two of these, the active hormone atrial natriuretic peptide (ANP) and prohormone B-type natriuretic peptide (BNP) are circulating factors, which are measured in serum samples to diagnose HF or follow the efficacy of therapies. The third member, C-type natriuretic peptide (CNP), was shown to be overexpressed in the heart during HF, but levels were very low in the plasma. Mechanical stretch, Ang II, endothelin-1 (Endo-1) and adrenergic agonists are known to induce production of ANP and BNP in the cardiomyocytes. The effects of ANP and BNP in the cardiomyocytes are mediated via activation of guanyl cyclase-A coupled receptor (natriuretic peptide receptor A; NPRA) on the cell surface and leading to signaling via cyclic guanosine monophosphate (cGMP) and protein kinase G I (PKG I; Figure 4). Activation of PKG I inhibits nuclear factor of activated T cell (NFAT)-mediated activation of MEF2C and GATA 4, which are the key transcriptional regulators in the heart. GATA 4 regulates the transcription of ANP and BNP in addition to signaling pathway with mitogen-activated protein kinases (MAPKs) and extracellular receptor-mediated kinases (ERKs). (Kerkela, Ulvila & Magga 2015.) The known effects of NPs include vasodilatation, diuretic and natriuretic actions as well as reduction of blood pressure (Tavi et al. 2001). During cardiac remodelling NPs were shown to inhibit cardiac hypertrophy and fibrosis, decrease apoptosis and enhance angiogenesis. The metabolic effects of NPs include activation of lipolysis and lipid oxidation, increased mitochondrial biogenesis, promotion of white adipose tissue to brown adipose tissue and protection against diet-induced obesity and insulin resistance. (Kerkela, Ulvila & Magga 2015.)

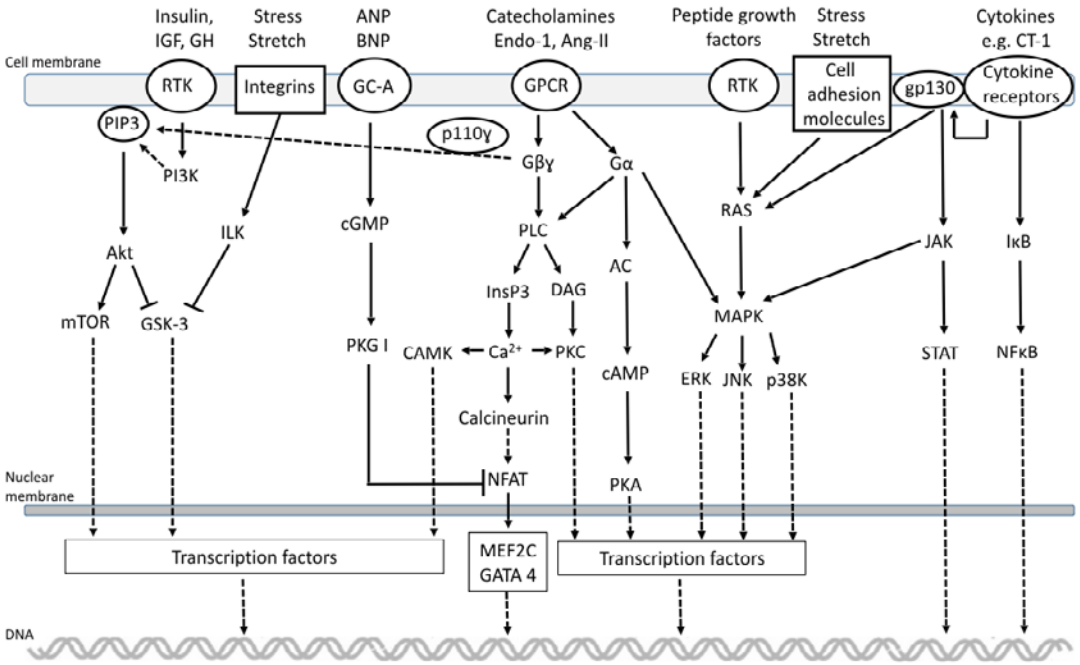

Figure 4. Signaling cascades in the heart during a hypertrophic response. Solid arrows indicate signaling pathways and dashed arrows mark phosphorylation or dephosphorylation reactions. IGF, insulin-like growth factor; GH, growth hormone; ANP, atrial natriuretic peptide; BNP, brain natriuretic peptide; Endo-1, endothelin-1; Ang-II, angiotensin II; CT-1, cardiotrophin-1; RTK, receptor tyrosine kinase; GC-A, guanyl cyclase-A; GPCR, G-protein-coupled receptor; gp130, glycoprotein 130; PIP3, phosphatidylinositol tris phosphate; PI3K, phosphoinositide 3′-OH kinase; Akt, protein kinase B; mTOR, mammalian target of rapamycin; GSK-3, glycogen synthetase kinase 3; ILK, integrin-linked kinase; cGMP, cyclic guanosine monophosphate; PKG I, protein kinase G I; p110γ, isoform of PI3K; Gβγ, subunit of GPCR; Gα, subunit of GPCR; PLC, phospholipase C; InsP3, inositol tris phosphate; DAG, diacylglycerol; Ca^{2+}, calcium ion; CAMK, calcium/calmodulin kinase; PKC, protein kinase C; NFAT, nuclear factor of activated T cell; AC, adenylyl cyclase; cAMP, cyclic adenosine monophosphate; PKA, protein kinase A; RAS, monomeric G-protein; MAPK, mitogen-activated protein kinase; ERK, extracellular receptor-mediated kinases; JNK, c-Jun kinase; p38K, p38 kinase; JAK, Janus kinase; STAT, signal transducer and activator of transcription; IκB, inhibitor of κB; NF-κB, nuclear factor-κB. Modified from Heineke et Molkentin and Katz (Heineke, Molkentin 2006, Katz 2008).

The cardiac hypertrophic response inside the cell involves multiple signal-transduction pathways (Figure 4) resulting in changes in transcription factor activities affecting gene transcription and protein synthesis. Physiological, adaptive hypertrophy is largely mediated by signaling through insulin, insulin-like growth factor (IGF) or growth hormone (GH). Insulin, IGF and GH bind to receptor tyrosine kinases (RTK) and their signaling cascade begins with phosphorylation of phosphatidylinositol tris phosphate (PIP_3) by phosphoinositide 3′-OH kinases (PI3K). PIP3 activates protein kinase B (Akt), which phosporylates mammalian target of rapamycin (mTOR) and inhibits glycogen synthetase kinase 3 (GSK-3). Active GSK-3 inhibits a number of transcription factors associated with cardiac growth and its inhibition was shown to play an important role in the shift towards hypertrophy. Cell adhesion molecules like integrins have been shown to inhibit GSK-3 via integrin-linked kinase (ILK) in response to biomechanical stress and stretch. Catecholamines, Endo-1 and Ang-II activate G-protein-coupled receptors (GPCRs) and their subunits Gβɣ and Gα. Gβɣ associates with PI3K isoform p110γ thus activating PIP3-

Akt pathway. Phospholipase C (PLC), activated by Gβɣ and Gα, leads to activation of inositol tris phosphate (InsP3) and diacylglycerol (DAG). Calcium released by InsP3 activates calcium/calmodulin kinase (CAMK), calcineurin and protein kinase C (PKC), which is also activated by DAG. Calcineurin dephosphorylates NFAT enabling further activation of transcription factors MEF2C and GATA4. Gα activates adenylyl cyclase (AC) to form cyclic adenosine monophosphate (cAMP), which stimulates protein kinase A (PKA). Activated PKC and PKA were shown to be involved in inhibiting GSK-3 thus promoting hypertrophic signaling. This neurohormonal and calcium-activated pathway, including calcineurin and PKCs, appears to be the major determinant of adaptive versus maladaptive hypertrophy. Peptide growth factors bind to RTKs and activate a monomeric G-protein RAS, which stimulates MAPK pathways: ERKs, c-Jun kinase (JNK) and p38K kinase (p38K). Cell adhesion molecules activate RAS due to cell stress and stretch. Cytokines like cardiotrophin-1 (CT-1) activate gp130-mediated signaling pathways leading to activation of RAS and stimulation of signal transducer and activator of transcription (STAT) and MAP kinases via Janus kinase (JAK). Cytokine receptor activation leads to phosphorylation of inhibitor of κB (IκB) and its subsequent dissociation from nuclear factor-κB (NF-κB), hence releasing NF-κB from inhibition. As described, adaptive and maladaptive signaling pathways share common mediators, but the initial activators of the pathways differ. (Selvetella et al. 2004, Dorn, Force 2005, Heineke, Molkentin 2006, Katz 2008, Kerkela, Ulvila & Magga 2015.)

2.3.3 Diagnostics of heart failure

Diagnosis of HF is based on typical symptoms and signs, cardiac imaging and recognizing the pathological process behind the syndrome. Typical symptoms include breathlessness, orthopnea, paroxysmal nocturnal dyspnea, decreased exercise tolerance, fatigue and ankle swellig. Elevated jugular venous pressure, hepatojugular reflux, hepatomegaly, third heart sound, laterally displaced apical impulse, cardiac murmur, pitting oedema and pulmonary crepitations are the signs of HF during examination. (McMurray et al. 2012.) Weight gain is often observed with ADHF especially in cases of HF with reduced ejection fraction (HFrEF; Maisel et al. 2015). The classification from New York Heart Association (NYHA) is used for evaluating HF state based on the severity of symptoms limiting physical activity (Table 1; McMurray et al. 2012).

Table 1. NYHA classification to grade the symptoms of HF patients.

NYHA Class	Symptoms
I	No limitation of physical activity.
II	Mild limitation in ordinary physical activity.
III	Marked limitation in less-than-ordinary physical activity.
IV	Symptoms in all physical activities and possibly also at rest.

Diastolic and systolic HF have been studied during the past years and the aim has been to evaluate whether there are different stages or separated phenotypes of HF. Due to changes in EF the naming of the HF types has changed to HF with reduced EF (HFrEF) and HF with preserved HF (HFpEF). (Bronzwaer, Paulus 2009.)

2.3.3.1 Heart failure with reduced ejection fraction

Diagnosis of HFrEF, formerly called systolic dysfunction, requires typical symptoms and signs of HF and reduced EF (< 50 %). Increased end-diastolic and end-systolic volumes (EDV and ESV) and decreased blood flow velocity to the aorta indicate systolic dysfunction

in echocardiography. (McMurray et al. 2012.) Prior myocardial infarction and left bundle branch block were shown to be predictors for HFrEF. Dilated LV and reduction in EF have been connected with the late-stage hypertensive heart disease and hypertrophic cardiomyopathy, but in many cases coronary events have been involved in the progression of HF. (Bronzwaer, Paulus 2009.) Hearts with HFrEF have more interstitial fibrosis but also replacement fibrosis, shorter and less stiff cardiomyocytes and lower myofibrillar density in cardiomyocytes compared to HFpEF (van Heerebeek et al. 2006). Baseline BNP levels were shown to be higher in HFrEF, but acute rises of BNP predict ADHF better in HFpEF than HFrEF (Maisel et al. 2015).

2.3.3.2 Heart failure with preserved ejection fraction

HFpEF, formerly known as diastolic HF, is a syndrome with typical signs and symptoms for HF, normal EF and evidence of diastolic dysfunction due to relevant structural heart disease (McMurray et al. 2012). Diastolic dysfunction causes elevated left ventricular end-diastolic pressure and pulmonary capillary wedge pressure, changes in mitral valve and pulmonary vein blood flow velocities and increases in LA size or LV mass (Paulus et al. 2007). Compared to HFrEF the patients with HFpEF are usually older, women, more obese, have AF and suffer from hypertension (Mancia et al. 2014, Melenovsky et al. 2015). HFpEF accounts for 50 % of HF patients and the prevalence is rising fast, subsequently it has been predicted to be the major HF type within the next years. Prognosis is similar to HFrEF, but no major improvements in treatment have been made during the last decades. (Borlaug, Paulus 2011.)

In HFpEF, LV relaxation and filling are slow in diastolic dysfunction with increased myocardial stiffness. Collagen type I accumulation to extracellular matrix and cardiomyocyte stiffness due to decreased calcium sensitivity and cross-bridge disengagement were shown to cause LV relaxation abnormalities. (Borlaug, Paulus 2011.) Increased NT-proBNP and BNP levels correlate with abnormalities in LV relaxation indicating diastolic dysfunction, but comorbidities may also affect these values making them nonspecific for HF. NPs can be used along with other diagnostic methods for evaluating the probability of HFpEF. (Paulus et al. 2007.)

2.3.4 Treatment of heart failure

The general measures of treating HF include lifestyle modifications and medical therapy. Weight reduction, smoking cessation, limited alcohol consumption and exercise to improve physical condition are the basic procedures in treating cardiovascular diseases. Medication, which is discussed later in this chapter, is combined with the lifestyle changes and possibly also with endovascular procedures or pacemaker placements. The treatment focuses on the reason behind the HF as well as relieving the symptoms of the syndrome. (Kemp, Conte 2012.)

ADHF or intensification of the chronic HF cause the majority of the hospitalizations among patients with HF (Henes, Rosenberger 2016). In decompensated state of acute or chronic HF the patients typically suffer from pitting oedema, weight gain, breathlessness and decreased excercise tolerance. The treatment in decompensated HF aims to relieve the symptoms and support the heart to maintain adequate cardiac output with medication and technical assistance if needed. (McMurray et al. 2012.)

ACE inhibitors and beta-blockers are used in chronic HF to reduce the LV remodelling and improve EF in HFrEF. Mineralocorticoid receptor blockers were shown to be beneficial among patients with reduced EF. Ivabradine and digoxin are used with certain patients to reduce their heart rate. Diuretics are commonly used with HF patients to relieve signs and symptoms of congestion, although the effects of diuretics on mortality and morbidity have not been studied among HF patients. (McMurray et al. 2012.) In clinical trials a novel drug inhibiting angiotensin receptor and neprilysin, an endopeptidase degrading vasoactive peptides like NPs, was shown to be superior in reducing hospitalization for HF and

mortality compared to an ACE inhibitor in HFrEF (McMurray et al. 2014). The same angiotensin receptor and neprilysin inhibitor (ARNI) for treating HFpEF, is in an ongoing PARAGON-HF trial, which is now in Phase III comparing the morbidity and mortality between patients treated with the new ARNI or old angiotensin receptor blocker valsartan (Macdonald 2015). In addition to medication, cardiac resynchronization therapy with pacemaker was shown to improve LV stucture and function and delay the first hospitalization for HF in patients with prolonged QRS interval (Bristow et al. 2004).

Gene therapy has been widely studied in treating HF in preclinical settings, following identification of the molecules associated with the disease. Several molecules, of which many are associated with calcium handling, are being studied in HF development in order to develop new gene therapy applications. (Yla-Herttuala 2015.) Gene therapy as a concept and clinical trials for HF are further discussed in chapter 2.6.

2.3.5 Mouse models of heart failure

Mouse models are important in studying the pathogenesis of HF. The advantages and limitations of the most commonly used mouse models of HF are listed in the Table 2.

The availability of several transgenic (including inducible and cell type-specific transgene expression) and knockout strains, has been important in studying the molecular and cellular mechanisms behind HF and identifying novel therapeutic targets (Patten, Hall-Porter 2009). For example, deletion of the gene encoding muscle lim protein (Arber et al. 1997), cardiac-specific overexpression of tumor necrosis factor-α (Kubota et al. 1997) and overexpression of cytoplasmic calmodulin kinase II (Zhang et al. 2003) cause LVH and dilatation of the LV, thus leading to HF.

Transverse aortic constriction in mouse is the most common model of aortic stenosis, which induces left ventricular hypertrophy by increasing cardiac afterload. The severity of constriction affects the outcome; tight constriction induces acute hemodynamic instability whereas mild constriction leads to progressive LVH. (Houser et al. 2012.) Surgically induced mouse models of HF also include coronary ligation leading to MI and ischemia-reperfusion injury (Patten, Hall-Porter 2009).

A technically simple and reproducible method of modelling HF is administration of a single cardiotoxin or drug. Ethanol and the cytotoxic drug doxorubicin are known cardiotoxins in humans and have been used to induce HF in mice. Elevated levels of an amino acid homocysteine are associated with an increased risk of HF in humans and have been shown to induce HF also in mice. (Breckenridge 2010.)

β-Adrenergic stimulation with prohypertrophic agents like subcutaneously administered Ang II were shown to induce hypertension, cardiac hypertrophy and diastolic dysfunction in mice. Isoprenaline was also shown to have β-adrenergic properties leading to systolic and diastolic dysfunction and myocardial fibrosis in the heart. (Horgan et al. 2014.)

Table 2. Most commonly used mouse models of HF. Modified from Patten et Hall-Porter and Breckenridge (Patten, Hall-Porter 2009, Breckenridge 2010).

	Model	Advantages	Limitations
Surgical	Coronary ligation	Relevant to human disease (MI)	Significant expertise and expense required for mouse surgery, high mortality, limited myocardial tissue restricts the biochemical and histological analyses that can be performed
	Transverse aortic constriction	Model of human pressure overload (LVH progression), also possible to induce acute HF	Acute onset of hypertension is not clinically relevant, other limitations similar to coronary ligation (row above)
Toxic	Ethanol Doxorubicin Homocysteine	Non-invasive, technically simple, reproducible	High mortality, non-cardiac effects, suitability to model HF is questionable
Genetic	Transgenic	Reproduction of gene expression changes seen in disease	Non-specific effects of overexpression
	Cell type-specific	Reproduction of gene expression changes seen in disease	Developmental effects of null allele
	Inducible knockout/transgenic	Control of time course of deletion/induction	Controlling the level of the transgene expression often difficult

2.4 CARDIAC IMAGING

Cardiac imaging modalities provide information on cardiac and valvular structures and function, myocardial perfusion, metabolism and coronary arteries. Multiple imaging methods have been developed for these purposes. Echocardiography is an inexpensive and readily available method for evaluating cardiac structure and function, whereas cardiovascular magnetic resonance imaging (CMR) is especially useful in patients with suspected or diagnosed myocardial disease. Computed tomography (CT) is used to diagnose CAD and aortic diseases as well as structural abnormalities in the heart. Perfusion imaging by CMR, CT or positron emission tomography (PET) can be used to identify ischemic regions in the heart. Meanwhile, magnetic resonance spectroscopy (MRS) has been assessed for measuring changes in cardiac metabolism. Angiography is used to image coronary arteries in patients, which have a high likelihood to require endovascular procedures for treatment. (Blankstein 2012, McMurray et al. 2012, Al-Mallah et al. 2015.)

2.4.1 Echocardiography

Echocardiography is a non-invasive, radiation-free, affordable, portable and readily available method for investigating heart structure and function. The ultrasound-based echocardiography can be performed transthoracically or via the oesophagus and the most commonly used imaging options contain two-dimensional (2D), M-mode and Doppler imaging. 2D imaging is used for viewing the heart structure and movement in real time, in a cross-section of the heart, typically in the parasternal long axis, parasternal short axis and four-chamber view. Measurements of the structures are done from the 2D or M-mode view and in Doppler imaging the estimation of blood-flow velocity is made by comparing the frequency change between the transmitted and reflected sound waves. The calculations for LV end-diastolic volume (EDV), LV end-systolic volume (ESV), myocardial mass and EF are usually done automatically by the software according to the measurements. The disadvantages in using echocardiography are that it is strongly observer dependent, it relies on assumptions about the heart structure and the acoustic access is limited. (Ashley, Niebauer 2004, Jensen 2007.) Especially the right ventricle (RV) volumes and EF have been difficult to estimate due to the complex RV geometry (Anavekar et al. 2007).

Ultrasound contrast agents are intravenously administered microbubbles, which can be used in perfusion imaging, measuring LV volumes and function, detecting neovascularization and finding possible endoleaks after endograft placement (Abbas et al. 2014, Porter, Xie 2015). Targeted microbubbles, in which specific ligands have been placed onto the surface of the bubble, have been studied in sonothrombolysis, as well as in drug and gene delivery. Microbubbles attach to the target tissue and ultrasound pushes the microbubbles to adhere firmly. (Unger et al. 2014.) BR55 is an example of a targeted microbubble, which detects human VEGFR-2 and have been studied in imaging tumoral angiogenesis (Pochon et al. 2010).

2.4.2 Cardiovascular magnetic resonance imaging

CMR is an accurate and reproducible method for quantifying LV structure and function without using ionizing radiation and is not limited by acoustic access. Technical difficulties in performing echocardiography or abnormal LV size and function are indications for which the three-dimensional (3D) visualization of the LV is especially useful with CMR. In humans, CMR LV evaluation is usually done by using ECG-gated segmented breath-held cine imaging with a steady-state free procession sequence. Different planes of the heart can be imaged depending on the purpose. For complete analysis of the LV structure and function, the laboratories usually analyze a stack of LV short-axis images to avoid geometrical assumptions and to get reliable results. The calculations for EDV, ESV, myocardial mass and EF can be done after analysis. (Kramer, Hundley 2010.)

A contrast agent, usually gadolinium, increases the sensitivity of CMR and late gadolinium enhancement (LGE) is widely used for measuring myocardial fibrosis. Renal failure is commonly associated with HF and it limits the use of exogenous contrast agents. (Rajappan et al. 2000.) T_1 relaxation in the rotating frame of reference ($T_{1\rho}$) was shown to act like an endogenous contrast agent and be a sensitive marker for macromolecular-water interaction (Grohn et al. 2000, Witschey et al. 2012). The use of $T_{1\rho}$ has been studied in osteoarthritis (Borthakur et al. 2006), acute cerebral ischemia (Grohn et al. 2000), liver fibrosis (Wang et al. 2011) and gene therapy applications (Hakumaki et al. 2002), in which the method was shown to bee succesfull in detecting affected areas. A significant increase in $T_{1\rho}$ has been reported 7 and 20 days after acute myocardial infarction (Musthafa et al. 2013) and fibrotic area sizes evaluated from $T_{1\rho}$ and LGE images were shown to correlate significantly in patients suffering from hypertrophic cardiomyopathy (Wang et al. 2015).

CMR perfusion is based on contrast agent accumulation in the field of interest, where the signal changes are detected (Rajappan et al. 2000). Perfusion can be used for determining subendocardial ischemic regions in hypertrophied and dilated hearts, as well as evaluating ischemic burden of the myocardium with ischemic heart disease (Kitsiou et al. 1998).

MRS can be used to measure noninvasively *in vivo* changes in cardiac metabolism. Several metabolites with ^{31}P, ^{1}H or ^{13}C nuclei can be detected with MRS. ^{1}H MRS has proven to be efficient in studying cardiac lipid and creatine metabolism. The results are shown as spectral peaks, from which the absolute or relative concentration to the tissue water peak can be quantified by measuring the peak area. Each metabolite appears at a known frequency or frequencies and can thus be detected from the spectrum by specific peak pattern. (van Ewijk et al. 2015, Bakermans et al. 2015.)

2.4.3 Other cardiac imaging modalities

PET myocardial perfusion imaging provides information about the regional myocardial blood flow of the left ventricle in milliliters per gram per minute. Early and subclinical abnormalities in coronary arterial vascular function and/or structure affect myocardial blood flow and can be assessed noninvasively by PET. The evaluation and quantification of myocardial blood flow and myocardial flow reserve are valuable for the detection of early stages of CAD and microvascular dysfunction. Impaired myocardial blood flow or flow reserve have been associated with increased risk of death or progression of HF regardeless of CAD. PET imaging is based on intravenous administration of a positron-emitting perfusion tracer, like ^{13}N-ammonia, ^{15}O-water or $^{82}Rubidium$, and serial acquisition of images showing the transit of the tracer from systemic circulation to LV myocardium. (Schindler et al. 2010.) ^{15}O-water is considered to be an ideal tracer for noninvasive quantitative measurements of myocardial blood flow, as the water is freely diffusible, it extracts completely to the myocardial tissue and has no metabolic interactions (Knaapen et al. 2010). ^{18}F-labeled PET tracer (^{18}F-FDG, 2-deoxy-2-[fluorine-18]fluoro-D-glucose) was shown to provide excellent image quality, efficient uptake to the myocardium and longer half-life when compared to the above mentioned tracers. ^{18}F-FDG is efficient after a single dose and can be used during treadmill exercise due to its long half-life. (Nekolla et al. 2009, Sherif et al. 2009.)

PET combined with CT can be used to diagnose inflammatory diseases of the heart. PET tracer ^{18}F-FDG is known to collect in tissues, where the cells use glucose as the energy source. Inflammatory cells using glucose can be detected from the heart by PET/CT after fasting and support the diagnosis of sarcoidosis for example. PET/magnetic resonance (MR) is a novel and yet infrequently used method to evaluate the heart. The advantages of PET/MR compared to PET/CT are lower radiation exposure, high soft-tissue contrast and multiparametric assessment of pathologies. (Sarikaya 2015.) The advantage of PET compared to CT and CMR alone is that it allows information about the physiological processes and molecular abnormalities that are the basis of the disease, and not only the end-point effects in the structure or function of the imaged organ (Yao, Lecomte & Crawford 2012).

CT is based on the variable absorption of X-rays by different tissues and provides cross-sectional images of the body. Generally, CT is often recommended when echocardiographic findings are uncertain or as an alternative to CMR in imaging cardiac structure. CT coronary angiography has become useful in detecting CAD in low risk patients and in patients with stable CAD. Fast data acquisition time with CT was proven to be important in imaging patients with suspected aortic dissection or rupture, althought CT can also be used to evaluate patients with other diseases affecting the aorta. (Al-Mallah et al. 2015.) Recently perfusion CT with adenosine was shown to identify patients with flow limiting CAD, offering information about physiological state in the diseased heart (Rochitte et al. 2014).

Angiography is an invasive method to image coronary arteries and to measure pressures in the cardiac chambers or outflow tracts. A catheter is used to administer the contrast agent at the desired area to be visualized and X-ray images show transient distribution of the contrast agent within the blood flow. Angiography offers a method to diagnose and treat the occluded vessel at the same time by balloon angioplasty and stents, but is not suitable for all patients. (Bagai et al. 2014; https://www.heart.org/idc/groups/heartpublic/

@wcm/@hcm/documents/downloadable/ucm_317626.pdf, read 17.3.2016.)

2.4.4 Imaging modalities for mouse heart

Several methods for mouse cardiac imaging have been developed for the visualization and assessment of cardiac structure and function. Mouse cardiac imaging has been technically challenging because of the small size of the heart and high heart rate, as both high spatial and temporal resolutions are required. (Ram et al. 2011.)

Echocardiography has remained the most frequently used modality in mouse cardiac imaging, since high costs, the need for a contrast agent or tracer and limited availability have restricted the use of other imaging methods (Gao et al. 2011). Technical improvements in high-frequency transducers, signal processing and imaging frame rates have been achieved to overcome challenges in this imaging modality. Echocardiography is routinely used in small animals, although intra- and interobserver variability, mouse strain, anaesthesia and imaging technique have been shown to affect the cardiac measurements. (Ram et al. 2011.)

CMR and micro CT have been modified for mouse cardiac imaging, although the acquisition of images comparable to that achieved from humans requires massive increases in spatial and temporal resolutions. In CMR the challenge has been the weak signal from the tissue, which can be strengthened by increasing the magnetic field. Unfortunately, higher magnetic fields have also been associated with increased technical challenges in the imaging. Image generation requires synchronization of the ventilation and cardiac cycle to the used pulse sequence. ECG triggering in mouse is demanding due to the high and variable heart rate and low ECG magnitude. Weak signals and ECG triggering require data acquisition from several respiratory and cardiac cycles, which extends the imaging time. (Badea et al. 2006.)

Micro CT shares the same challenges of cardiac motion and ventilation with CMR and systems with a ventilation and ECG synchronization possibility have been developed. A high dose of x-rays and short exposure time are technical requirements to generate CT images from mouse heart. Soft tissue contrast in CT is known to be low compared to CMR, but exogenous contrast agents are also available for small animal imaging. (Badea et al. 2006.)

Small-animal PET has been widely used in the drug development to measure quantitatively and noninvasively the 3-D distribution of a labeled compound as a function of time, thus providing pharmacokinetic data and facilitating the decision process about the suitability of the compound for further studies. Cardiac physiology and metabolism have been assessed with ECG gated data acquisition to avoid motion artefacts. Clinically available tracers have been adapted for small-animal imaging to meet the limitations in tracer mass and usable maximal injection volume. High spatial resolution requirement is similar to other imaging modalities and it can not be optimally achieved with small-animal PET systems, but high efficacy in detecting emitted photons can be reached. The supporting resources and required equipment, including cyclotron and PET radiochemistry facilities, limit the availability of PET imaging. (Yao, Lecomte & Crawford 2012.)

2.5 VASCULAR ENDOTHELIAL GROWTH FACTORS IN BLOOD VESSEL GROWTH

The human VEGF family consists of five members: VEGF-A, VEGF-B, VEGF-C, VEGF-D and placental growth factor (PlGF). In addition to these, VEGF homologs have been identified from viruses (VEGF-E) and snake venom (VEGF-F). VEGF family members have different properties in vessel development, angiogenesis, vascular homeostasis, lymphangiogenesis and metabolism. The VEGF activities are mediated by three RTKs called VEGF receptor (VEGFR)-1, VEGFR-2 and VEGFR-3. Neuropilin (Nrp)-1 and Nrp-2

act as co-receptors for VEGFRs. (Yla-Herttuala 2007.) VEGFs, their receptors and main functions are summarized in Figure 5.

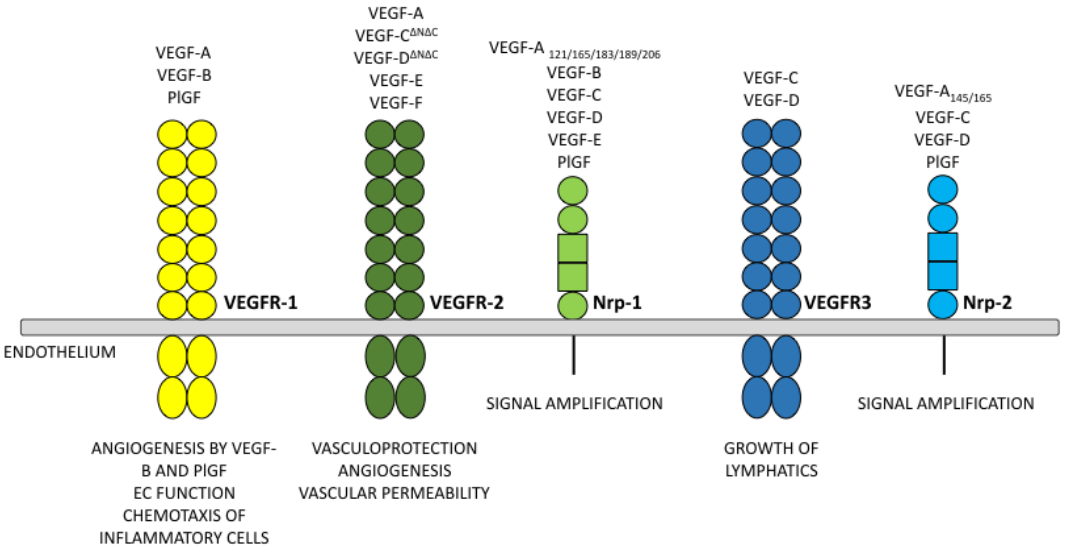

Figure 5. VEGFs and their receptors. VEGFR-1 is mainly expressed in endothelial cells and it binds VEGF-A, VEGF-B and PlGF. VEGFR-2 is the major mediator of angiogenesis and in addition to VEGF-A it binds processed forms of VEGF-C and VEGF-D and invertebrate polypeptides VEGF-E and VEGF-F. Nrp-1 acts as a co-receptor to VEGFR-2 and binds specific isoforms of VEGF-A, VEGF-B, VEGF-C, VEGF-D, VEGF-E and PlGF. VEGFR-3 binds VEGF-C and VEGF-D and promotes lymphagiogenesis. Nrp-2 acts as a co-receptor to VEGFR-3 and binds specific isoforms of VEGF-A, VEGF-C, VEGF-D, and PlGF. Modified from Ylä-Herttuala et al. (Yla-Herttuala 2007).

2.5.1 Angiogenesis

Angiogenesis is the term used to describe the growth and remodelling process of the primitive vasculature into a capillary network. New functional vessels in adults form from pre-existing ones by sprouting, transendothelial cell bridging or pillar-formation by periendothelial cells (intussusception). Endothelial cells initiate the angiogenic process, but pericytes are needed for vascular stabilization and maturation. (Carmeliet 2000.)

Several factors having either a positive or negative regulatory activity on angiogenesis have been identified. An 'Angiogenic switch' results from increased production of factors promoting angiogenesis, especially VEGF-A and its receptors due to hypoxia. (Hanahan, Folkman 1996, Ribatti 2005.) The hypoxic cells secrete VEGF-A protein and by paracrine signaling activate endothelial cells to proliferate and migrate towards the VEGF-A gradient. Migration of endothelial cells requires destabilization of the mature vessel and degradation of the cellular matrix by several factors. Platelet-derived growth factor (PDGF) recruits pericytes and smooth muscle cells around the neovessel meanwhile angiopoietin-1 (Ang-1) together with transforming growth factor beta 1 (TGF-β1) stabilize the vessel. Ang-1 is also a natural inhibitor of vascular permeability thus tightening the vessels. (Carmeliet 2003.)

Regulated angiogenesis is crucial for normal development and growth. Excessive angiogenesis is associated with diseases like cancer, psoriasis and arthritis, whereas insufficient vessel growth can lead to for example ischemia, neurodegeneration, hypertension and pre-eclampsia. Proangiogenic gene therapy has become an interesting and widely studied treatment option for ischemic diseases. (Carmeliet 2003.) Tumor growth above 2-3 mm in diameter requires initiation of angiogenesis and already in the 1970s the anti-angiogenic therapy was thought to be the solution for preventig neovascularization

and thus growth of tumours (Folkman et al. 1971). VEGF-A neutralizing antibodies, inhibitors for several RTKs and soluble VEGFRs binding VEGF-A have been studied to inhibit neovascularization and improve the outcome in cancer (Ribatti 2005, Yadav et al. 2015).

2.5.2 Arteriogenesis

Arteriogenesis means the process, in which the pre-existing arterioles are remodelled into functional arteries. Haemodynamically relevant occlusion in a large artery redirects the blood flow to pre-existing collateral arterioles, in which the blood flow and hydrostatic pressure increase and shear stress occurs. Increased shear stress induces swelling and activates the endothelium to produce chemokines, colony stimulating factors and cell adhesion molecules, which enable monocytes to invade arteriolar collaterals and cause an inflammatory environment. Activated monocytes and platelets produce multiple growth factors, which proceed proliferation of endothelial and smooth muscle cells. Remodelling of the arteriole is also accompanied with remodelling of the extracellular matrix by macrophages. (Buschmann, Schaper 2000.) Compared to angiogenesis, arteriogenesis is initiated by physical forces that activate the endothelium and not hypoxia. Arteriogenesis occurs near the occluded artery, whereas angiogenesis takes place relatively far and downstream from the occlusion. (Schaper, Scholz 2003.)

2.5.3 Vascular endothelial growth factor receptors

VEGFR-1, VEGFR-2 and VEGFR-3 are RTKs, transmembrane glycoproteins, which share similar structure with seven immunoglobulin-like loops in their extracellular part and a split tyrosine-kinase domain in the intracellular part. They have been shown to activate signal transduction pathways, which are essential for embryonic development and adult tissue regeneration and maintenance by affecting cell proliferation, differentation, migration and metabolism. (Hubbard 1999.)

VEGFR-1 was the first receptor cloned for VEGF-A (Shibuya et al. 1989) and later VEGF-B and PlGF were also shown to activate VEGFR-1 (Ferrara, Gerber & LeCouter 2003). VEGFR-1 is mainly expressed in endothelial cells, but also in trophoblast cells, monocytes and renal mesangial cells (Neufeld et al. 1999). Lack of VEGFR-1 during embryogenesis was shown to be lethal, as the receptor is essential in the organization of vasculature (Fong et al. 1995). VEGFR-1 has been proposed to act as negative regulator of mitogenic activity by binding VEGF-A and thus preventing signaling via VEGFR-2 (Neufeld et al. 1999). A naturally occurring soluble form of VEGFR-1 was thought to act similarly and its expression was shown to be increased in pre-eclampsia (Kendall, Wang & Thomas 1996, Koga et al. 2003). VEGFR-1 activation leads to cell proliferation and vascular permeability, but minimally compared to VEGFR-2 activation (Shibuya 2001). In pathological situations, VEGFR-1 activation has been associated with stimulation of endothelial cell function, indirectly recruiting bone marrow progenitor cells and enhancing migration of inflammatory cells (Shibuya, Claesson-Welsh 2006).

VEGFR-2 is the strongest mediator of the mitogenic, angiogenic and permeability-enhancing effects of VEGF-A (Matthews et al. 1991). Furthermore, it mediates the chemotactic and antiapoptotic actions of VEGF-A (Ferrara, Gerber & LeCouter 2003, Waltenberger et al. 1994). In addition to VEGF-A, the processed forms of VEGF-C and VEGF-D and invertebrate polypeptides VEGF-E and VEGF-F can activate VEGFR-2 (Shibuya, Claesson-Welsh 2006, Yamazaki, Morita 2006). VEGFR-2 is expressed in endothelial cells, hematopoietic stem cells, megakaryocytes and retinal progenitor cells (Neufeld et al. 1999). VEGFR2 deficiency caused embryonic lethality, due to the critical role of the receptor in differentiation of endothelial cells and blood vessel formation (Shalaby et al. 1995). VEGFR-2 expression has been linked to developmental and physiological blood vessel growth, but also to tumor angiogenesis and blood vessel-dependent metastasis (Shibuya, Claesson-Welsh 2006).

Activation of VEGFR-3 by VEGF-C has been shown to induce angiogenesis even without the presence of VEGFR-2 indicating a role for VEGFR-3 as a regulator of vascular network formation during development. The inhibition of VEGFR-3 leads to decreased proliferation of endothelial cells, a reduced number of vessel sprouts and branching points and a less dense vascular network. Lack of VEGFR-3 also caused embryonic lethality due to cardiovascular remodelling defects. (Dumont et al. 1998, Tammela et al. 2008.) Suppression of VEGFR-3 signaling during the first two weeks of postnatal life in mice was shown to lead to systemic regression of lymphatic capillaries and medium-sized lymphatic vessels (Karpanen et al. 2006b). In adults, VEGFR-3 is mainly expressed on the lymphatic endothelial cells promoting lymphangiogenesis, but its expression can be up-regulated in angiogenic endothelial cells, for example in tumor vasculature and in endothelial tip cells. A lack of VEGFR-3 in the blood vessel endothelial cells can result in a hypervascular response via up-regulated VEGFR-2 expression indicating that normally VEGFR-3 suppresses the VEGFR-2 expression. (Zarkada et al. 2015.)

2.5.4 Neuropilin receptors

Nrp-1 and Nrp-2 have been thought to be enhancing factors for angiogenesis, lymphangiogenesis and tumor progression (Masuda et al. 1987, Kolodkin et al. 1997, Ellis 2006). Nrp-1 is a cell surface protein, which was first characterized as a receptor for the class 3 semaphorins mediating inhibitory axon guidance signals to neurons during embryogenesis (He, Tessier-Lavigne 1997). Later the importance of Nrp-1 in cardiovascular development was discovered. The overexpression of Nrp-1 caused embryonic lethality due to an excessive formation of blood vessels, hemorrhages and cardiac malformations, whereas deletion of Nrp-1 caused multiple vascular and neuronal defects also leading to death during embryogenesis (Kitsukawa et al. 1995, Kawasaki et al. 1999). Nrp-1 acts as a co-receptor to VEGFR-2 by enhancing the binding of VEGF-A to its receptor and increasing VEGF-A mitogenic activity and chemotaxis (Soker et al. 1998). In addition to VEGF-$A_{121/165/183/189/206}$ isoforms, VEGF-B, VEGF-C, VEGF-D, VEGF-E and PlGF-2 were also shown to activate Nrp-1 (Yla-Herttuala et al. 2007, Wild et al. 2012). Naturally occurring soluble Nrp-1 can bind VEGF-A, and lead to inhibition of VEGF-A mediated effects and antitumor activity (Gagnon et al. 2000).

Nrp-2, expressed during development mainly in the veins and lymphatic vessels, acts as a co-receptor to VEGFR-3 by promoting the lymphatic vessel sprouting in response to VEGF-C (Karpanen et al. 2006a, Xu et al. 2010, Koch et al. 2011). Nrp-2 deficiency causes mild defects in lymphatic vasculature, but does not affect viability (Yuan et al. 2002). VEGF-$A_{145/165}$, VEGF-C, VEGF-D and PlGF-2 have been shown to activate Nrp-2 (Gluzman-Poltorak et al. 2000, Yla-Herttuala et al. 2007, Wild et al. 2012).

2.5.5 Vascular endothelial growth factor-A

The first member identified from the VEGF-family, VEGF-A, exists as isoforms, which are alternatively spliced froms of the VEGF-A gene. Pro-angiogenic isoforms VEGF-$A_{111/121/145/148/165/183/189/206}$ differ in the number of amino acids, their solubility properties and receptor binding. VEGF-A145, VEGF-A165, VEGF-A189 and VEGF-A206 contain the heparin-binding domain and bind tightly to cell surface heparin-containing proteoglycans in the extracellular matrix. VEGF-A isoforms lacking the domain are diffusible. (Hoeben et al. 2004, Dehghanian, Hojati & Kay 2014.) VEGF-$A_{121b/145b/165b/183b/189b}$ are thought to form another subfamily of isoforms, which as opposed to previously mentioned isoforms are anti-angiogenic. The expression patterns of VEGF-A isoforms were shown to alter in health and disease; for example in tumorigenesis, a switching from anti- to pro-angiogenic isoforms occurs. (Dehghanian, Hojati & Kay 2014.) VEGF-A is crucial for the development of the cardiovascular system, as deletion of even a single allele caused death during embryogenesis (Carmeliet et al. 1996). VEGF-A expression is regulated by hypoxia, activated oncogenes and several cytokines. In adults, VEGF-A stimulates endothelial cell

proliferation and migration, inhibits apoptosis, increases vascular permeability, induces vasodilatation and is expressed in practically all vascularized tissues. (Neufeld et al. 1999, Maharaj et al. 2006.) VEGF-A mediates its actions via VEGFR-1, VEGFR-2 and in an isoform-specific manner to Nrp-1 and Nrp-2. VEGF-$A_{121/165/183/189/206}$ have been shown to bind to Nrp-1, whereas VEGF-$A_{145/165}$ bind to Nrp-2. (Soker et al. 1998, Neufeld et al. 1999, Gluzman-Poltorak et al. 2000, Pan et al. 2007.)

2.5.6 Vascular endothelial growth factor-B

VEGF-B was cloned in 1996 and the most abundant expression was found in mouse heart, brain, skeletal muscle and kidney (Olofsson et al. 1996a). The VEGF-B gene encodes for two alternatively spliced secreted protein isoforms consistent of 167 or 186 amino acids. VEGF-B_{167} has strong affinity for cellular and pericellular heparan sulfates, whereas VEGF-B_{186} is freely secreted from cells. The longer isoform can be modified by *O*-linked glycosylation, which increases the solubility of the secreted protein in aqueous solution. (Olofsson et al. 1996b.) The effects of VEGF-B are mediated via VEGFR-1 and Nrp-1 (Olofsson et al. 1998, Makinen et al. 1999). VEGF-B induced capillary growth in the myocardium is dependent on the presence of Nrp-1 (Lahteenvuo et al. 2009).

Two VEGF-B knockout mouse strains exist, both of which are viable and fertile (Bellomo et al. 2000, Aase et al. 2001). Direct comparison of these two strains showed no differences in echocardiographic and electrocardiographic parameters in standard diet. Exposition to a high-fat-diet did not induce changes in cardiac phenotype or metabolism indicating that VEGF-B may be dispensable under non-stressed conditions. (Dijkstra et al. 2014.)

The role of VEGF-B in metabolism and cardiac function has been under investigation during the past years. VEGF-B_{186} has appeared to be cardioprotective by inducing cardiomyocyte proliferation, decreasing apoptosis and increasing lipid and glycogen accumulation (Lahteenvuo et al. 2009). Fatty acid uptake from blood vessels to peripheral tissues is at least partly controlled by VEGF-B (Hagberg et al. 2010). Overexpression of both isoforms in transgenic rat model indicated enhanced coronary vasculature, decreased fatty acid uptake and increased glucose oxidation thus leading to ischemia resistance in the heart (Kivela et al. 2014). Adenovirus-mediated VEGF-B_{186} gene transfer resulted in angiogenic effects, collateral artery growth and improved functional outcome in a pig model of myocardial infarction after adenovirus-mediated VEGF-B_{186} gene transfer (Lahteenvuo et al. 2009). Cardiac hypertrophy in mice with cardiac-specific overexpression of VEGF-B_{167} seemed to result from altered lipid metabolism, in which accumulating ceramides cause mitochondrial damage and eventually lipotoxicity (Karpanen et al. 2008). In humans, VEGF-B expression was shown to be decreased in ischemic heart disease and dilated cardiomyopathy (Kivela et al. 2014), furthermore after myocardial infarction low levels of VEGF-B in plasma have indicated adverse remodelling of LV (Devaux et al. 2012).

2.5.7 Vascular endothelial growth factor-C and vascular endothelial growth factor-D

VEGF-C and VEGF-D are relatively similar in structure and functional properties. Both growth factors are secreted as precursors and are proteolytically processed to their active forms. The full length of VEGF-C and VEGF-D promote mainly lymphangiogenesis by binding to VEGFR-3 and Nrp-2, but in mouse, VEGF-D has been shown to bind only to VEGFR-3. *In vitro* binding studies have shown VEGF-C and VEGF-D to bind also to Nrp-1. Completely processed forms of VEGF-C and VEGF-D (VEGF-C $^{\Delta N\Delta C}$ and VEGF-D $^{\Delta N\Delta C}$) activate VEGFR-2 and induce angiogenic responses with increased vascular permeability. (Joukov et al. 1996, Kukk et al. 1996, Yamada et al. 1997, Achen et al. 1998, Baldwin et al. 2001 Karpanen et al. 2006a.)

VEGF-C deficiency is embryonically lethal due to the defects in lymphangiogenesis and fluid accumulation in the tissues (Karkkainen et al. 2004). As was shown, lymphangiogenesis during embryogenesis is mainly induced by VEGF-C, whereas VEGF-D is the predominant factor affecting lymphangiogenesis after birth (Karpanen et al. 2006b).

VEGF-D deficient mice are viable and fertile with normally developed and functional lymphatic system (Baldwin et al. 2005). Overexpression of VEGF-C and VEGF-D were shown to induce sprouting lymphangiogenesis and was associated with vascular invasion, lymphatic system involvement and distant metastasis in various cancers. Soluble VEGFR-3 transfer was used to block VEGF-C and VEGF-D signaling and to prevent lymphatic metastasis formation in transgenic tumour models. (Lohela et al. 2009.) Adenoviral-mediated VEGF-C gene transfer combined with lymph node transfer was shown to reconstruct lymphatic vasculature in pigs and provide a treatment option for patients suffering from lymphedema (Honkonen et al. 2013).

2.5.8 Placental growth factor

PlGF, first isolated from a placenta, is expressed as isoforms 1-4, but exists only as isoform PlGF-2 in mouse (Maglione et al. 1991, DiPalma et al. 1996, Yang et al. 2003). Although the effects of PlGF are mediated through VEGFR-1, PlGF-2 and PlGF-4 have also Nrp1 and Nrp2 binding properties (De Falco 2012). PlGF gene therapy stimulated angiogenesis and arteriogenesis in ischemic heart and limb possibly by amplifying the angiogenic activity of VEGF-A (Luttun et al. 2002). Formation of PlGF/VEGF-A heterodimers are also capable of stimulating angiogenesis via VEGFR-2 (De Falco 2012).

The absence of PlGF during embryogenesis does not affect the normal development, but in pathological conditions, like tumor growth, lack of PlGF was shown to reduce pathological angiogenesis and the associated inflammation. This observation has led to a search for an inhibitor of PlGF for therapeutic approaches. (De Falco 2012.)

2.6 GENE THERAPY FOR CARDIOVASCULAR DISEASES

2.6.1 Concept of the cardiovascular gene therapy

Gene therapy can be defined as transfer of a functional gene into somatic cells for a therapeutic effect (Yla-Herttuala, Alitalo 2003). Transferring genes into targeted cells requires a transferring tool, either a non-viral or viral vector. Plasmids are the most important non-viral vectors, but they have been shown to achieve a low transfection efficiency and short-term expression in the target cells. Although plasmid-based vectors have been approved in several countries, they have not proved efficient in clinical trials. (Laitinen et al. 1997, Yla-Herttuala, Alitalo 2003, Korpisalo, Yla-Herttuala 2010.) Viral vectors have been made replication-defective by displacing viral coding genes with therapeutic gene cassette (Kay, Glorioso & Naldini 2001). Transduction of cells by viral vectors enables transgenes to be transported to the nucleus for production of the desired therapeutic protein. The advantages of gene therapy include selective local administration and opportunity for long-term effects after a single treatment. (Yla-Herttuala, Alitalo 2003.) Viral vectors are discussed further in chapter 2.6.2.

Several routes for performing cardiovascular gene therapy have been introduced. In the heart, transgenes can be transferred by cathether-mediated intraventricular or intracoronary injection, epicardial injection or during bypass surgery (Sylven et al. 2002, Katz et al. 2012). Intra-arterial, perivascular and intramuscular injections have been used in gene therapy applications for peripheral arterial disease (PAD). Local administration of the gene therapy products prevents side effects, which might occur in systemic delivery of the therapeutic agent. (Yla-Herttuala, Alitalo 2003.) For a successful outcome in gene therapy, the amount of transgene in the target tissue has to be sufficient without being toxic and the expression time has to meet the requirements of the treated disease (Kay, Glorioso & Naldini 2001).

In cardiovascular diseases gene therapy has been studied in treating CAD, PAD, HF and arrhytmias. High gene transfer efficiency and ability to transduce nondividing cells have made adenovirus (AdV), adeno-associated virus (AAV) and lentivirus (LeV) vectors

interesting options for cardiovascular gene therapy. (Laakkonen, Yla-Herttuala 2015.) Several factors that stimulate angiogenesis have been studied. Usually, a transient growth factor expression is desired and potent secreted growth factors may induce sufficient angiogenic response also with low transduction efficiency of the viral vector. (Yla-Herttuala, Alitalo 2003.) Tissue oedema and inflammation can be problematic side effects depending on the viral dose used, subsequently by reducing the dose as low as possible the side effects can be minimized. The correct amount of growth factor is also needed, as too high local concentration of the therapeutic agent like VEGF-A induces abnormal vascular growth. (Korpisalo et al. 2011.) Long-term safety of transient gene therapy with Ads was shown to be good without increasing the risk for other diseases like cancer (Muona et al. 2012).

Gene therapy for HF has focused on improving cardiac function, decreasing symptoms and positively influencing the quality of life. Several transgenes have been used to induce changes at the molecular level in HF. In preclinical settings, for the prevention of arrhythmias, transgenes have been used to increase myocyte refractory properties or conduction velocity of the myocardium. (Sasano et al. 2006, Lau et al. 2009, Greener et al. 2012.) To achieve a therapeutic effect, high transgene expression was needed in arrhythmia studies. Novel therapeutic targets in cardiovascular diseases have been found, as the knowledge about the pathogenesis at the cellular and molecular levels in several diseases has increased. (Wolfram, Donahue 2013.)

2.6.2 Viral vectors

2.6.2.1 Adenovirus

AdVs are human pathogens, which cause mainly respiratory infections, cystitis, gastroenteritis and conjunctivitis. Structurally AdVs are non-enveloped and they have a protein capsid shell covering the viral genome. (Lenaerts, De Clercq & Naesens 2008.) The large double-stranded viral DNA genome (~ 36 kb) can be modified and high transgene capacity (~ 8 kb) can be achieved (Kennedy, Parks 2009). AdVs are frequently used as vectors in gene therapy due to their high gene transfer efficiency in several tissues (Laakkonen, Yla-Herttuala 2015).

AdVs enter dividing and nondividing cells by endocytosis after binding to coxsackie and adenovirus receptors (CARs), which are expressed in different densities in various tissues. In cardiomyocytes CARs were shown to be highly expressed. (Kootstra, Verma 2003.) Inside the targeted cell AdV vectors are present extrachromosomally and induce robust, but transient gene expression peaking a few days after the gene transfer and lasting for 2-4 weeks (Hedman et al. 2003). Strong cellular and humoral immune responses towards AdVs have been documented after vector administration resulting in clearance of the transduced cells and formation of antibodies against AdVs. The latest generation of Ad vectors lacks all of the viral genes, which decreases inflammatory reactions and also increases the transgene capacity. (Kootstra, Verma 2003, Rincon, VandenDriessche & Chuah 2015.)

Over 50 serotypes of AdVs have been found and they differ in their transduction efficiencies in various tissues. Serotypes 2 and 5 are mainly used for vector production and most adults have been exposed to these serotypes. Pre-existing immunity towards the virus due to AdV infection or previously administered AdV vector may complicate the use of the vector in gene therapy applications. (Yla-Herttuala, Alitalo 2003, Rincon, VandenDriessche & Chuah 2015.) In human trials, AdV vectors have caused, in addition to antibody formation, inflammation, transient fever and increased liver transaminases (Yla-Herttuala, Alitalo 2003). Innate and/or adaptive immune responses against the vector may lead to systemic toxicity, reduced transduction or a shortened duration of the therapeutic effect. Immunosuppression or immunomodulation prior to AdV administration and modifications of the capsid proteins have been studied to overcome immunological problems related to AdVs. (Ahi, Bangari & Mittal 2011.)

2.6.2.2. Adeno-associated virus

Adeno-associated viruses (AAVs) are nonpathogenic and can be replicated only when coinfected with a helper virus, usually AdV or herpes virus. They have a small, single-stranded DNA genome (~ 4.7 kb), which limits the size of the transgene possible in AAV vectors. AAVs enter the host cells by endocytosis and are transported to the nucleus. After converting the single-stranded DNA into a stable double-stranded DNA by the host cell machinery AAV vector remains extrachromosomally. AAV vectors can induce long-term transgene expression. (Kootstra, Verma 2003, Zacchigna, Zentilin & Giacca 2014.)

Thirteen AAV serotypes have been identified with differences in the protein capsid structure. Natural tissue-specific tropism varies between the serotypes which can be utilized in vector production. AAV serotype 2 (AAV2) was the first serotype discovered and for that reason it has been most commonly used. AAV8 has shown natural tropism towards liver, smooth muscle, central nervous system, retina, pancreas, heart and kidney in mouse and AAV9 towards lung and testes in addition to the above-mentioned. (Zacchigna, Zentilin & Giacca 2014, Lisowski, Tay & Alexander 2015.) In mouse studies, intravenous administration of AAV8 and AAV9 transduced the liver with similar efficiencies, but in the heart AAV9 has been more efficient in transducing the cardiomyocytes throughout the myocardium (Inagaki et al. 2006).

AAV vectors are widely studied in CVD gene therapy, as their genome is simple to modify, high-titer vector preparations can be generated, long-term transgene expression is achievable and the inflammatory response is low compared to AdV vectors (Zacchigna, Zentilin & Giacca 2014). High prevalence of neutralizing antibodies against AAVs in human populations has restricted the use of AAV vectors in clinical gene therapy. These antibodies prevent successful transduction also with low neutralizing titers. Different species of animals, including naïve mice, had neutralizing antibodies in their sera, with titers varying widely between species and AAV serotypes. (Rapti et al. 2012.) Neutralizing antibody formation after vector administration has also been reported in animals and may complicate the use of this vector in gene therapy (Kootstra, Verma 2003).

2.6.2.3 Lentivirus

Lentivirus (LeV) belongs to the family of retroviruses, which have two copies of the viral RNA genome. They have a lipid envelope covering the protein capsid and viral genome. In vectors, the natural cell-surface receptor is deleted and the particles are pseudotyped with the vesicular stomatitis virus (VSV-G), this modification increases the tropism to a wider range of tissues, as the wildtype virus can only infect CD4-expressing cells. After entering the host cell through membrane fusion, the viral reverse transcriptase enzyme converts the genome into a double-stranded proviral DNA. The newly formed DNA translocates to the nucleus and integrates into the host cell genome. (Kootstra, Verma 2003, Di Pasquale et al. 2012.)

Human immunodeficiency virus type 1 (HIV-1) has been mainly used in LV vector production with transgene capacity of ~ 8 kb. All viral proteins and the majority of the viral genome have been eliminated from the vectors, thus making them replication incompetent and decreasing the possibility of recombination with wildtype viruses. In the third-generation vectors safety has been improved further by changing the wildtype promoter region. (Lyon et al. 2008.) Low titers of virus preparations have been one of the limiting factors for using LeVs more widely in cardiovascular studies (Laakkonen, Yla-Herttuala 2015).

LeV vectors can transduce both dividing and nondividing cells and they have been shown to deliver genes to several tissues, including brain, liver, skeletal muscle, retina and cardiomyocytes. Transgene expression up to 6 months after LeV vector administration has been shown in the rat heart, which indicates that transgenes delivered with LeV vector may have long-term effects. (Niwano et al. 2008b.) By integrating into the host cell genome there

is also potential for life-long transgene expression. The inflammatory response after LeV vector administration has proven to be low (Di Pasquale et al. 2012).

Safety concerns in using LeV vectors include the pathogenity of HIV-1 to humans and random integration of the viral genome, which can lead to abnormal expression of genes and to tumorigenesis (Kootstra, Verma 2003, Laakkonen, Yla-Herttuala 2015).

The most commonly used vectors in cardiovascular gene therapy and their advantages and disadvantages are listed in Table 3.

Table 3. The most commonly used viral vectors in cardiovascular gene therapy. Modified from Rissanen and Ylä-Herttuala (Rissanen, Yla-Herttuala 2007).

Vector	**Advantages**	**Disadvantages**
Adenovirus	- High transduction efficiency - Relatively high transgene capacity - Easy to produce in high titers - Ability to transduce quiescent cells - Natural tropism for multiple cells	- Inflammation with high doses - Transient expression - Antibody formation
Adeno-associated virus	- Long-term gene expression - Moderate immune response - Ability to transduce quiescent cells - High tropism for myocardium (AAV -8 and -9) - WT not pathogenic for humans	- Limited transgene capacity - Production in large quantities - Antibody formation
Lentivirus	- Long-term gene expression - Ability to transduce quiescent cells - Relatively high transgene capacity - Low immune response	- Random integration - Low transduction efficiency - Limited tropism - Production in large quantities is difficult

2.6.3 Clinical trials

The majority of the gene therapy clinical trials have been aimed at treating cancer (Figure 6). Gene therapy for cardiovascular diseases accounts for 7.9 % of the clinical trials. (http://www.abedia.com/wiley/indications.php, read 1.2.2016.) Currently there are five ongoing clinical gene therapy trials aiming to treat patients with CAD, six aiming to treat PAD and three aiming to treat HF. Nine out of 14 trials use viral vectors instead of plasmid DNA to deliver the therapeutic gene. Clinical trials for CVDs focus mainly on inducing therapeutic angiogenesis and/or improving contractility of the failing heart. (Halonen et al. 2014.)

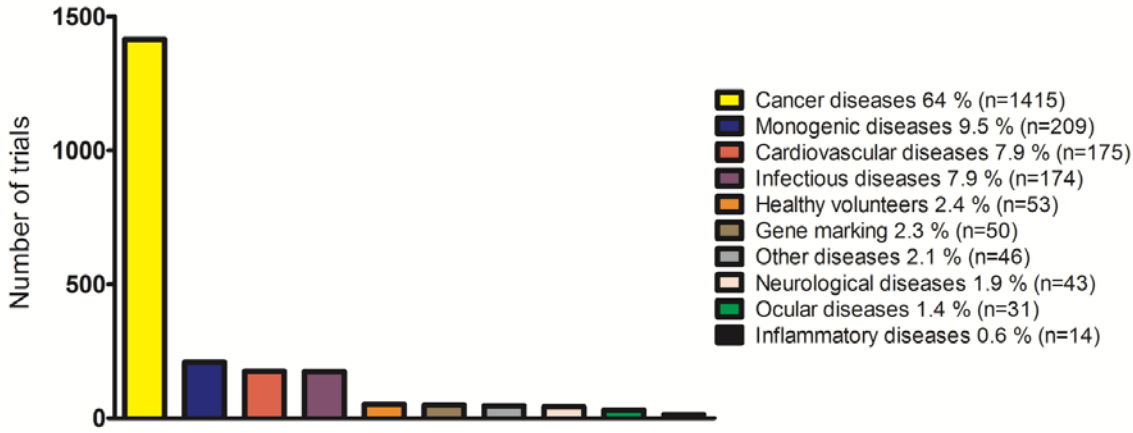

Figure 6. Indications for clinical gene therapy trials. Updated in July 2015. (Modified from http://www.abedia.com/wiley/indications.php.)

In PAD AdV-mediated VEGF-A gene transfer has been shown to induce angiogenesis and long-term safety of the treatment was proven to be very good, but no improvement in general survival or change in amputation frequency were detected. VEGF-D delivered by AdV is currently used in phase I/II study of PAD and the gene transfer route has been changed from intravascular delivery to direct intramuscular injections. (Makinen et al. 2002, Muona et al. 2012, Yla-Herttuala 2013.)

AdV-mediated VEGF-A was demonstrated to improve function of the heart of patients suffering from CAD, but cardiovascular mortality or exercise tolerance was not changed. Intracoronary VEGF-A gene transfer with AdV was shown to be safe in long-term follow-up. (Hedman et al. 2009.) Nowadays catheter-mediated intramyocardial delivery of the transgene is preferred in order to direct the gene transfer accurately and to reduce the needed viral dose (Yla-Herttuala 2013). It has been proposed that very sick end-stage patients may not be the best candidates for studying proangiogenic gene therapy, as they may not have any more a capacity to respond positively to treatment (Gupta, Tongers & Losordo 2009). AdV-VEGF-D is currently used in phase I clinical trial for the treatment of severe CAD with endocardial gene therapy (http://www.abedia.com/wiley/record_detail.php?ID=322, read 31.3.2016). In addition to VEGF-A and VEGF-D, fibroblast growth factor, hepatocyte growth factor and hypoxia-inducible factor (HIF-1α) have been used in clinical gene therapy trials for PAD and CAD (Laakkonen, Yla-Herttuala 2015).

In studies of heart failure SERCA-2a and stromal derived factor-1 (SDF-1) genes have been transferred to the heart (Gupta et al. 2008, Penn et al. 2013, Wolfram, Donahue 2013). Downregulation of SERCA-2a has been associated with HF in experimental animal models and humans, but a clinical trial of AAV1-SERCA2a gene transfer (CUPID-2b) failed to meet the primary endpoint of reducing hospitalization for HF and the secondary endpoint of preventing death or the need for mechanical cardiac support or heart transplant (Yla-Herttuala 2015, http://www.celladon.com/clinical-trials/cupid-2/, read 1.2.2016). SDF-1 gene transfer has shown positive effects on HF symptoms and quality of life in patients with ischemic cardiomyopathy in a phase I trial (Penn et al. 2013). Several molecules, many of which are associated with calcium handling, are being studied to develop new gene therapy applications for HF (Yla-Herttuala 2015).

The first gene medicinal product, which passed the clinical trials and was approved in 2012 for marketing in the Western world, is Glybera®. Intramuscular injections are used to treat patients with hereditary lipoprotein lipase deficiency with AAV1-vectors carrying the LPL gene. Glybera® was shown to be an effective and well-tolerated medicine. (Scott 2015.) The second gene medicine approved for clinical use in EU and USA in 2015 was T-Vec

(talimogene laherparepvec), which is an oncolytic herpes simplex-1 virus armed with an immunostimulatory protein GM-CSF for the treatment of advanced melanoma (http://www.amgen.com/media/news-releases/2015/11/amgen-to-present-imlygic-talimogene-laherparepvec-data-at-the-2015-international-congress-of-the-society-for-melanoma-research/ and http://global.onclive.com/web-exclusives/t-vec-approved-in-europe-for-unresectable-metastatic-melanoma, read 16.2.2016).

3 Aims of the study

The aim of this thesis was to study the expression of VEGFs and functional changes in the heart associated with LVH and HF development, to compare cardiovascular imaging methods and to evaluate the efficacy and safety of AdV, AAV and LeV vectors in cardiac gene therapy.

The specific aims were as follows:

I To study the expression of different VEGFs and their receptors in a pressure overload model of progressive LVH, and to investigate the therapeutic potential of AAV9-VEGF-B_{186} gene transfer in HF in mice.

II To compare echocardiography and CMR in the detection and follow-up of LVH progression in mice with cardiac-specific overexpression of VEGF-B_{167}.

III To compare the effects of direct intramyocardial injections of AdV, AAV and LeV vectors as well as systemic delivery of AAV9 on the transduction efficiency, heart structure, function and electrophysiological properties in mice.

4 Materials and methods

4.1 EXPERIMENTAL ANIMALS

All animal experiments were approved by the National Animal Experiment Board of Finland and carried out in accordance with the guidelines of the Finnish Act on Animal Experimentation. The animal experiments conformed with *the Guide for the Care and Use of Laboratory Animals* published by the US National Institutes of Health (NIH Publication No. 85-23, revised 1996). Mice were kept in group-cages in standard, temperature and humidity controlled environment with a 12 hour light/dark cycle at the National Laboratory Animal Centre in Kuopio. Animals were fed *ad libitum.* Euthanasia was performed with carbon dioxide. Mouse strains, number of mice used in the studies, pathology in the heart and gene transfer method are summarized in Table 4.

Table 4. Mouse models used in the thesis studies.

Study	Strain	Model	Gene transfer method
I	C57BL/6JOlaHsd mice (n=128)	TAC	Echocardiography-guided closed-chest injection
II	αMHC-VEGF-B_{167} mice (n=31)	LVH due to cardiac-specific overexpression of VEGF-B_{167}	-
III	C57BL/6JOlaHsd mice (n=112)	-	Echocardiography-guided closed-chest injection, intravenous injection

4.1.1 Mouse model of transverse aortic constriction (study I)

C57BL/6JOlaHsd mice from Harlan Laboratories Inc., USA underwent a modified transverse aortic constriction (TAC) operation (Rockman et al. 1991) to cause progressive LVH. Mice were anesthetized with a subcutaneously (s.c.) administered mixture of medetomidine (1 mg/kg, Domitor®, Pfizer Inc., NY, USA) and ketamine (75 mg/kg; Ketalar®, Pfizer Inc., NY, USA). To ensure ventilation, mice were intubated with 0.75 mm polyethylene tube (MicroVent, Harvard Apparatus, MA, USA). The thorax was opened from the midline of the sternum and the transverse aorta was visualized by a blunt dissection. A 25-G needle was placed inside the aorta and a 7-0 silk suture was tightened around it between the brachiocephalicus and the arteria carotis communis sinistra. After placing the suture, the needle was removed. Sham mice were operated similarly without the ligation. Analgesics (carprofen 5 mg/kg, s.c; Rimadyl, Pfizer Inc., NY, USA and bubrenorfin 0.05-1 mg/kg, s.c.; Temgesic, RB Pharmaceuticals Limited, UK) were given up to third post-operative day.

4.1.2 Transgenic mouse model for LVH (study II)

αMHC-VEGF-B_{167} mice with cardiac-specific overexpression of human VEGF-B_{167} carry the transgene under heart-specific αMHC-promoter (Karpanen et al. 2008). The mice were provided by Prof. Kari Alitalo, University of Helsinki, and further bred into the C57BL/6JOlaHsd background at the animal facility of the University of Eastern Finland.

4.2 GENE TRANSFER METHODS

4.2.1 Viral vectors (studies I and III)

The bacterial beta galactosidase (LacZ) transgene with nuclear localization signal (NLS) was driven by the cytomegalovirus (CMV) promoter in human clinical grade first-generation serotype 5 replication-deficient AdV vector. An empty vector used as a control contained the CMV promoter without any transgene. Good manufacturing practice (GMP) conditions were used for vector production in 293T cells and preparations were shown to be free from endotoxins and microbiological contaminants (Makinen et al. 2002, Hedman et al. 2003). Spectrophotometry was used for determining the titers of AdV preparations (Laitinen et al. 2000).

In the AAV2 vector, the LacZ transgene was similarily under a CMV promoter and contained a NLS. The AAV2 were produced as previously published (Zolotukhin et al. 1999) with some modifications. 293T cells were transfected with the AAV2 vector plasmid and pDG helper plasmid with calcium phosphate precipitation and the cells were harvested 48-72 h after the transfection. Viral vectors were released from the cells by freeze-thaw cycles and the media with vectors was purified by iodixanol-gradient centrifugation and heparin-affinity chromatography.

Transgenes VEGF-B_{186} and LacZ were under CMV promoter, but did not carry NLS in AAV9 vectors. For AAV9 vector production standard plasmid transfection method in 293T cells was used and the AAV9 particles were purified through sucrose-cushion ultracentrifugation and an anion-exchange column chromatography (Q-Sepharose, GE Healthcare, UK) followed by concentration through a second sucrose-cushion ultracentrifugation (Zolotukhin et al. 1999, Gao et al. 2000). The titers of AAV viral preparations were measured by qPCR method (Rohr et al. 2002).

Green fluorescent protein (GFP) transgene was driven by the human phosphoglycerate kinase-1 (PGK-1) promoter in LeV vector. Third-generation HIV-1 based LeVs were prepared with calcium phosphate transfection method in 293T cells as described earlier (Koponen et al. 2003). The concentration of particles was done with ultracentrifugation. Titers were determined with two methods: by measuring the amount of HIV p24 Gag antigen by enzyme-linked immunosorbent assay (ELISA) (Koponen et al. 2003) and with flow cytometry. Similar magnitude titers were measured with both methods and final viral dose was calculated with the functional titers from the flow cytometry.

All used viral vectors and doses in local and systemic gene transfer are listed in the Table 5.

Table 5. Viral vectors used in the thesis studies. Abbreviations: vp = viral particles, vg = viral genomes, tu = transduction units.

Vector and transgene	Promoter	Viral dose	Total injected volume	Gene transfer method	Study
Ad-LacZ	CMV	1 x 10^{10} vp	10 μl	Closed-chest injection	III
Ad-CMV	CMV	1 x 10^{10} vp	10 μl	Closed-chest injection	III
AAV2-LacZ	CMV	1 x 10^{10} vg	10 μl	Closed-chest injection	III
AAV9-LacZ	CMV	1 x 10^{10} vg	10 μl	Closed-chest injection	I, III
AAV9-LacZ	CMV	1 x 10^{12} vg	200 μl	Intravenous injection	III
		1 x 10^{11} vg	200 μl		
		1 x 10^{10} vg	200 μl		
AAV9-VEGF-B_{186}	CMV	1 x 10^{10} vg	10 μl	Closed-chest injection	I
LeV-GFP	PGK-1	1.3-4 x 10^{7} tu	10 μl	Closed-chest injection	III

4.2.2 Local and systemic delivery of the transgene (studies I and III)

Echocardiography-guided intramyocardial injections were performed as described earlier (Springer et al. 2005). The mice were anesthetized with inhaled isoflurane (induction: 4,5 % isoflurane, 450 ml air, maintenance: 2.0 % isoflurane, 200 ml air, Baxter International Inc., IL, USA) and a 30-G disposable needle attached to a 50 μl Hamilton syringe was connected to a micromanipulator (FujiFilm VisualSonics Inc., ON, Canada). Under visual control the needle penetrated the chest substernally in a 20° angle until it reached the anterior wall of the left ventricle. Viral dose (Table 5) was diluted in sterile 0,9 % NaCl in total volume of 10 μl in local intramyocardial injections. In LeV-GFP gene transfers, 10 μl of non-diluted viral preparations with the highest possible titers were used. Ultrasound video clips were recorded during and after the injection. Analgesic (carprofen, 5 mg/kg, s.c.; Rimadyl, Pfizer Inc. NY, USA) was given after the operation.

In systemic gene transfer 0,9 % sterile NaCl was used for diluting the viral doses (Table 5) for total volume of 200 μl and AAV9-LacZ was administered via tail vein to isoflurane anesthetized mice (induction and maintenance as described above).

4.3 METHODS FOR EVALUATING CARDIAC ANATOMY AND FUNCTION

4.3.1 Echocardiography (studies I-III)

Transthoracic echocardiography (TTE) was performed with high-resolution Vevo770 and Vevo2100 (FujiFilm VisualSonics Inc., ON, Canada) using high-frequency ultrasound probes (RMV-707B in Vevo770 and MS-400 in Vevo2100) operating at 18-38 MHz.

For TTE, mice were anesthetized as described above in 4.2.2. Mice were placed in a supine position on a heated platform and limbs were attached to electrode pads for registering electrocardiographic (ECG) signal. Hair was carefully removed from the chest with depilatory cream (Veet, Reckitt Benckiser, UK) and warm ultrasound gel (Aquasonic 100, Parker Laboratories Inc., NJ, USA) was applied. Ultrasound clips from short-axis view (SAX), long-axis view (LAX), M-mode aortic root and M-mode left atrium were aquired during the imaging.

All LV measurements were done from SAX M-mode images acquired at the mid-papillary level of LV. LV anterior wall thickness, interventricular diameter and posterior wall thickness were measured and LV end-diastolic volume (LV volume), LV mass and EF were calculated with Vevo770 or Vevo2100 programs as follows: LVvolume: [((7.0 / (2.4 + LVID;d)] x LVID;d, LV mass: 1,053 x [(LVEDD;d + LVPW;d + LVAW;d)^3 – LVEDD^3] and EF: 100 x ((LV Vol;d – LV Vol;s) / LV Vol;d). Aortic root and diameter of the left atrium were measured from LAX, which was taken more laterally than normal LAX.

4.3.2 Electrocardiography (studies II-III)

ECG was conducted as described earlier (Merentie et al. 2015). Briefly, ECG (lead II) was registered during TTE and the data was exported as a raw data format for Matlab based ECG analysis software (Kubios HRV, version 2.0 beta 4, Department of Physics, University of Eastern Finland, Kuopio, Finland). A 30 second clip of each mouse was analyzed and measurements for defining time intervals (P wave duration, PQ-time, QRS-time, QRSp-time, QT-time and QTc-time) were collected.

4.3.3 Cardiovascular magnetic resonance imaging (study II)

CMR experiments were performed at 9.4 T magnet, which was equipped with Varian DirectDriveTM console (Varian Inc., Palo Alto, CA). Mice were in a prone position on a pad, which was filled with circulating warm water. The pad was placed inside the quadrature volume radiofrequency (RF) transceiver with a coil diameter of 35 mm (Rapid Biomed, Rimpar, Germany). Multi-slice SAX gradient echo cine imaging, $T_{1\rho}$ mapping and T_2 mapping were included in the CMR protocol, which is carefully described in manuscript II.

Analyses were done with Matlab based software (Aedes software package, aedes.ue.fi). LV contours in diastole and systole were drawn in each slice from the apex to the valve level of the heart and calculated together to get LV end-diastolic volume (EDV, in results used LV volume), end-systolic volume (ESV) and myocardial wall volume. Manual calculation for EF [(1-ESV/EDV)*100] and LV mass (myocardium wall volume in diastole x conversion coefficient 1,05g/cm^3) was performed. $T_{1\rho}$ and T_2 relaxation times were determined from reconstructed $T_{1\rho}$ and T_2 maps.

4.4 HISTOLOGICAL METHODS (STUDIES I-III)

During the sacrifications plasma was collected by puncturing the right auricle and the heart was perfused via LV with phosphate buffered saline (PBS) or 1 % PFA in PBS (pH 7.4). The hearts were immersed and fixed in 4 % PFA in 7.5 % or 15 % sucrose for 4 hours and kept in 15 % sucrose overnight before further processing. Mounted paraffin blocks were cut to 5 μm thick sections. LeV-GFP transduced heart samples were frozen with OCT (Optimal Cutting Temperature, Tissue-Tek, Sakura Finetek, Torrance, CA, USA) and cut to 8 μm thick sections.

Tissue morphology was observed from hematoxylin-eosin (HE) stained paraffin sections and fibrotic tissue and inflammation from Masson trichrome stained sections (Masson Trichrome, Accustain trichrome stains, Sigma-Aldrich, USA) at X 12.5 magnification.
Fibrosis and inflammation were graded in a blinded fashion on a scale of 0-3, in which 0 =

no fibrosis/inflammation, 1 = mild fibrosis/inflammation, 2 = moderate fibrosis/inflammation and 3 = severe fibrosis/inflammation. Periodic acid Schiff´s glycogen staining (Periodic acid Schiff´s glycogen staining, Sigma-Aldrich, USA) was used to evaluate glycogen accumulation in the cells from three microscopic fields at X 200 magnification for each animal. Capillary area, capillary/myocyte, capillary/mm^2 and myocyte/mm^2 were analyzed from five microscopic fields of Biotinylated Griffonia (Bandeiraea) Simplicifolia Lectin I stained sections at X 400 magnification for each animal. Analysis of immunostained sections for proliferating (Ki-67), apoptotic (Cleaved Caspase-3) and transgene positive cells (LacZ or GFP), as well as ANP expression were likewise calculated. Green fluorescence from LeV-GFP transduced hearts was evaluated with a fluorescence microscope from frozen sections mounted in Vectashield Hard-Set Mounting Medium with DAPI (Vector Laboratories, Inc., Burlingame, CA, USA). The primary antibodies used are listed in Table 6.

Table 6. Primary antibodies used in immunohistochemistry.

Antibody	Manufacturer	Dilution	Target	Study
ANP (N-20, SC-18811)	Santa Cruz Biotechnologies, (Santa Cruz, CA)	1:100	ANP positive cells	I
Ki-67 (ab15580)	Abcam (Cambridge, UK)	1:200	Proliferating cells	I, II
Cleaved Caspase-3 (Asp175)	Cell Signaling Technology (Danvers, MA)	1:250	Apoptotic cells	I, II
Biotinylated Griffonia (Bandeiraea) Simplicifolia Lectin I	Vector Laboratories (Burlingame, CA)	1:100	Endothelium; detection of angiogenesis	I
LacZ (Beta-galactosidase)	Merck Millipore (Darmstadt, Germany)	1:2500	LacZ positive transduced cells after gene transfer	III
GFP (ab290)	Abcam (Cambridge, UK)	1:1500	GFP positive transduced cells after gene transfer	III

4.5 PROTEIN AND GENE EXPRESSION ANALYSES

4.5.1 Clinical chemistry (study II)

Cardiac troponin T (cTnT), sodium, potassium and lactatedehydrogenase (LDH) plasma concentrations were measured by Movet Oy, Kuopio, Finland.

4.5.2 Reverse transcription (RT) quantitative PCR (studies I-III)

Total RNA was isolated with GenElute Mammalian Total RNA Miniprep Kit (Sigma-Aldrich, St Louis, MO, USA; study I) or with TRI-reagent (Sigma-Aldrich, St Louis, MO, USA; studies II and III) and reverse transcribed into cDNA by using M-MuLV reverse transcriptase (MBI Fermentas, NY, USA; study I) or RevertAid™ (Thermo Fischer Scientific,

Waltham, MA, USA; studies II and III). The amount of cDNA was quantitated using real time qPCR, either using specific primer sets with SYBR Green chemistry or specific Taqman® gene expression assays (Applied Biosystems, Life Technologies Corporation, CA, USA). The real time PCR was processed on StepOnePlus Real-Time PCR System or ABI 7700 Sequence Detection System (Applied Biosystems, Life Technologies Corporation, CA, USA; studies I-III). The measured mRNA expression, corresponding to the proteins of interest, was normalized to 18S ribosomal RNA (study I) or peptidylprolyl isomerase A (PPIA; studies II and III). In Table 7 all Assays-On-Demand and primers used are listed.

Table 7. Taqman® gene expression assays and primers used in the studies.

Gene	Taqman® gene expression assay (Applied Biosystems)	Forward primer 5´ -> 3´	Reverse primer 5´-> 3´	Study
ANP	Mm01255747_g1			II
BNP	Mm01255770_g1			II
cTnT	Mm01290256_m1			II
PPIA	Mm03302254_g1			II, III
LacZ	Mr03987581_mr			III
mVEGF-A		GATCCGCAGACGTGTAAATGTTC	TTAACTCAAGCTGCCTCGCC	I
hVEGF-B		GCCCAGGCCCCTGTCT	ACATCTATCCATGACACCACTTTCC	I
mVEGF-B		CCACTGGGCAACACCAAGTC	GCTGTGTTCTTCCAGGGACATC	I
mVEGF-C		TCAGCAAGACGTTGTTTG AAATTAC	TGATTGGCAAAACTGATTGTGACT	I
mVEGF-D		TGGACCAGTGAAGGATTTTTCTTT	TGCTCGGATCTGTTGTTCAGA	I
mVEGFR-1		CTTTTCAAGGACGGCTTTGC	GCTCATGAATTTGAAAGCGTTTAC	I
mVEGFR-2		AAAACTCTGGAAGACAGGAACAAATT	GCCACAGACTCCCTGCTTTTA	I
mVEGFR-3		TCTCCAACTTCTTGCGTGTCA	CGTTGCTCCGGAGACTTCTC	I
Nrp-1		CTATGACCGGCTGGAGATCTG	GCCCACAATAACGCCCAAT	I
CytB		CCACTTCATCTTACCATTTATC	TGATCCTGTTTCGTGGAGGAA	I
PGC-1α		AGCGACCAATCGGAAATCAT	GCAAGTTTGCCTCATTCTCTTCA	I
ANP		GAAAAGCAAACTGAGGGCTCTG	CCTACCCCCGAAGCAGCT	I
18S		TGGTTGCAAAGCTGAAACTTAAAG	AGTCAAATTAAGCCGCAGGC	I

4.6 STATISTICAL ANALYSES (STUDIES I-III)

The following statistical analyses were used: Student´s t-test (Excel software) when two groups were compared (studies I-III), GraphPadPrism 5 software (GraphPad Software, Inc., La Jolla, CA, USA) with one-way analysis of variance with a suitable post hoc test when three or more groups per timepoint were compared (I, III) or with repeated measures two-way ANOVA when the follow-up data from the same mice was analyzed (I). Linear mixed

model analysis (IBM Corp. Released 2010. IBM SPSS Statistics for Windows, Version 19.0. Armonk, NY: IBM Corp.) was used when follow-up data with variable number of mice was analyzed (II). Results are presented as mean ± standard deviation (SD) or mean ± standard error of the mean (SEM). The following symbols are used in the figures: * $P < 0.05$, ** $P < 0.01$, *** $P < 0.001$.

5 Results

In this section, selected results showing the main findings from the original publications and manuscript are presented. The order of the results may vary from the original publications and manuscript.

5.1 THE PROGRESSION OF LEFT VENTRICULAR HYPERTROPHY (STUDIES I, II)

In this thesis study two mouse models, which developed LVH and HF, were used. LVH was induced by pressure-overload due to TAC-operation (study I) or by cardiac-specific overexpression of VEGF-B_{167} (study II) and changes associated with LVH progression were measured by echocardiography, CMR, molecular biology methods and histology. Progression of LVH led to increased LV mass, increased LV volume or internal diameter and decreased function of the LV as measured by EF in both mouse models. Changes in the above mentioned measurements occurred within weeks in TAC operated mice (Figure 7 a-d), whereas VEGF-B_{167} overexpression in the heart led to pathological remodelling within months (Figure 8 a-f). Comparison of echocardiography and CMR in following LVH progression was performed with mice having cardiac-specific overexpression of VEGF-B_{167} (Figure 8 a-j).

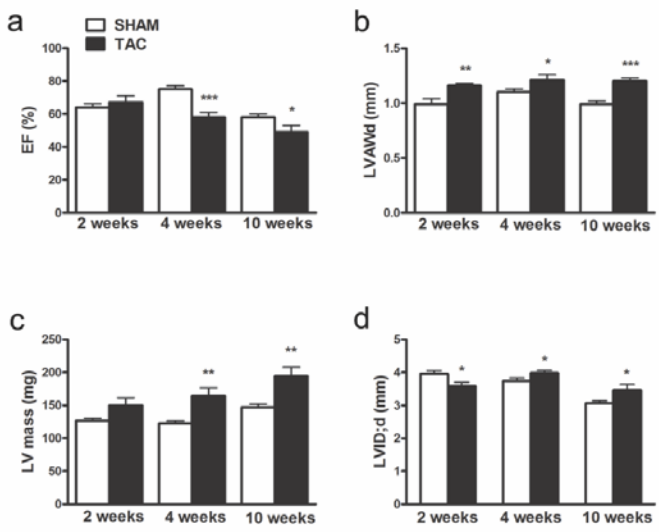

Figure 7. The effects of pressure-overload after TAC operation on cardiac structure and function. LV function was preserved in the compensatory phase of LVH at the two weeks timepoint, but decreased four and ten weeks after the TAC operation (a). Increased LV anterior wall thickness (LVAWd) and LV mass indicated the development of LVH in TAC operated mice (b-c). Increased LV internal diameter (LVID; d) was associated with LV dysfunction at the four and ten weeks timepoints (d). Mean ± SD, statistical analyses with Student´s t-test (comparison of SHAM and TAC groups in each timepoint). *P < 0.05, **P < 0.01, ***P < 0.001. Modified from figure 1 in publication I.

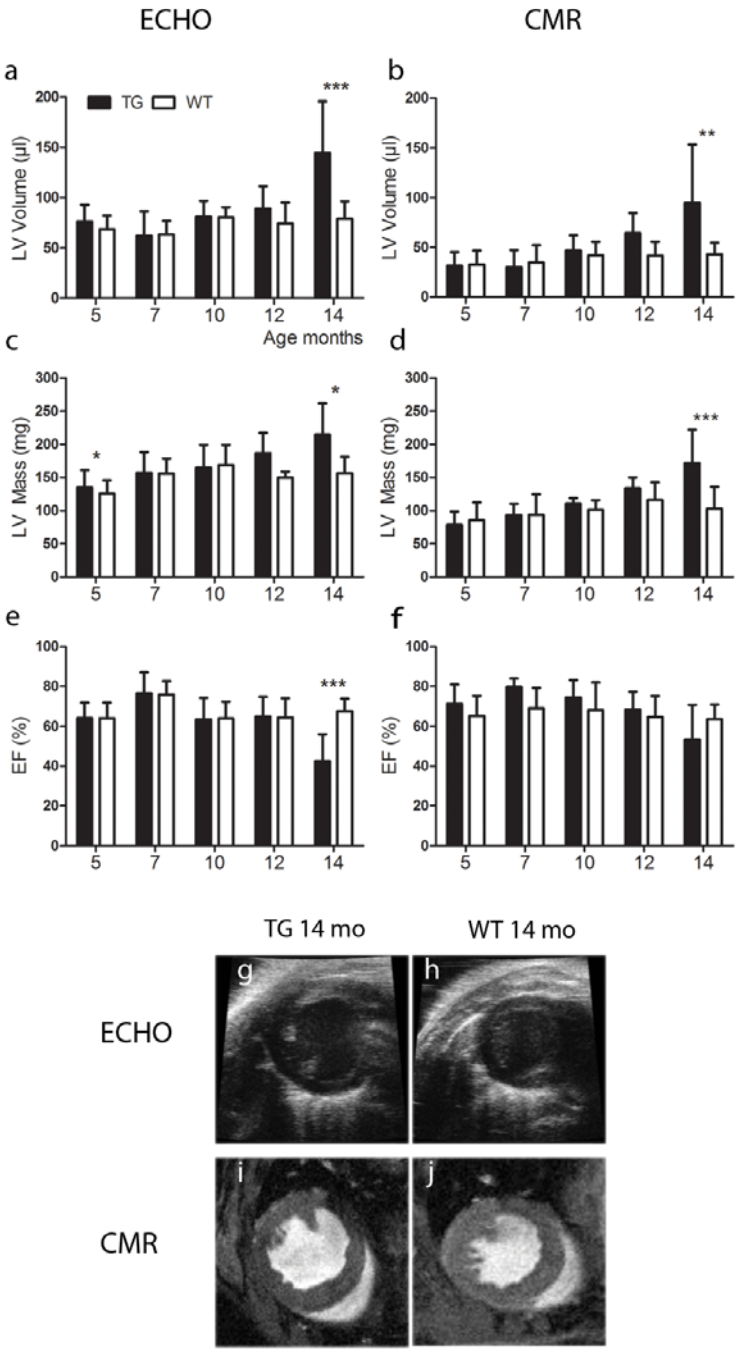

Figure 8. Comparison of echocardiography and cardiovascular magnetic resonance imaging (CMR) in following LVH progression. Cardiac-specific overexpression of VEGF-B_{167} led to dilatation of the LV (a, b), an increase in LV mass (c, d) and LV dysfunction as measured by decreased EF (e, f) by the age of 14 months compared to WT mice. Both echocardiography and CMR showed structural and functional changes associated with LVH progression and HF. Representative images from the echocardiography (g, h) and CMR (i, j) at the age of 14 months, when TG mice had markedly dilated LVs and decreased EF compared to WT mice. Mean ± SD, statistical analyses with SPSS Linear Mixed Model Analysis. *P < 0.05, **P < 0.01, ***P < 0.001. Modified from the figure 1 in manuscript II.

Fibrosis has been connected to LVH progression and HF. Accumulation of fibrosis was evaluated from Masson Trichrome stained sections 2, 4 and 10 weeks after TAC-operation and compared to intact mice. Fibrosis was associated with LVH progression 4 and 10 weeks after TAC operation (data not shown). As with the TAC operated mice, fibrosis was evaluated from TG mice overexpressing VEGF-B_{167} in the heart and compared to WT mice at the age of 5, 10 and 14 months (Figure 9 a-h). Severity of the diffuse fibrosis increased in TG group within aging and a significant difference compared to WT mice was observed at the age of 10 and 14 months (Figure 9 i). The average $T_{1\rho}$ relaxation time from the LV measured with CMR was shown to correlate with the severity of diffuse fibrosis in the myocardium of TG mice (Figure 9 j-k).

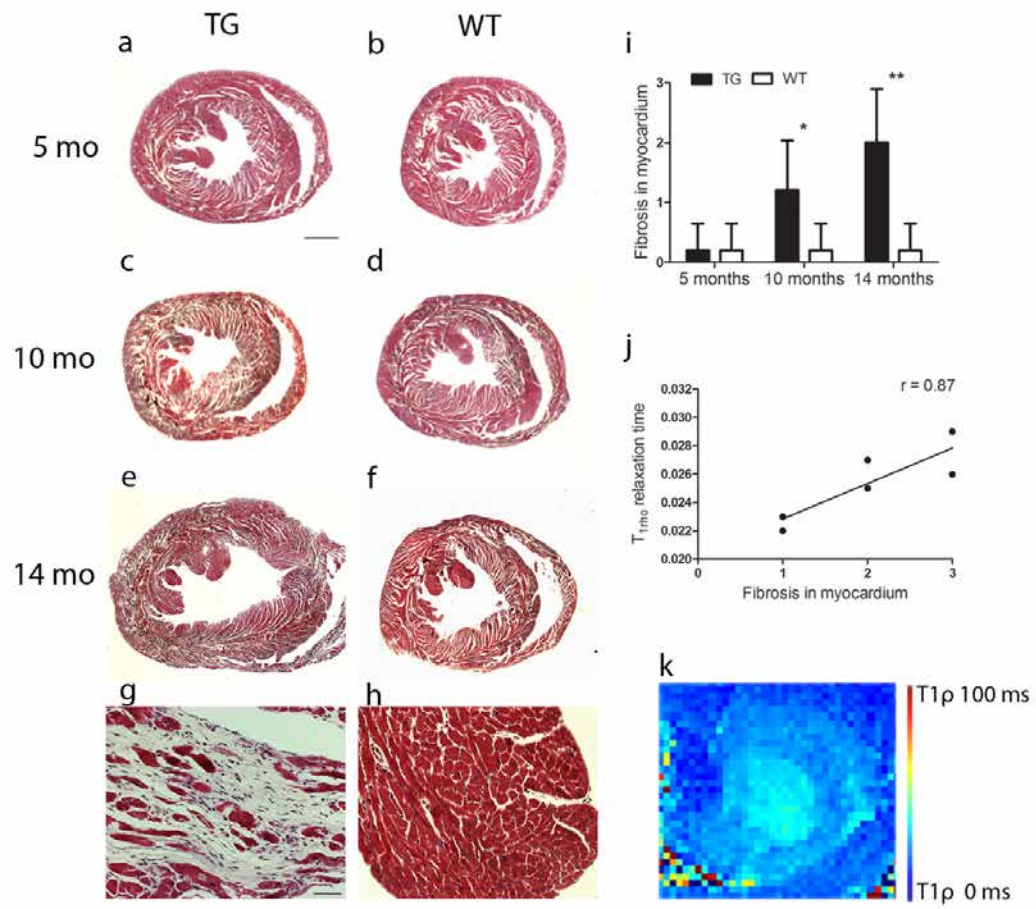

Figure 9. Accumulation of myocardial fibrosis in mice with VEGF-B_{167} overexpression in the heart. Diffuse fibrosis was detected from TG mice at the age of 10 and 14 months, whereas WT mice maintained normal morphology (a-i) Fibrosis was graded from Masson Trichrome stained sections on a scale of 0-3, in which 0 = no fibrosis, 1 = mild fibrosis, 2 = moderate fibrosis and 3 = severe fibrosis (i). The amount of fibrosis correlated with $T_{1\rho}$ relaxation time measured from the LV in TG mice (Pearson r=0.87, *P < 0.03; j). Representative reconstructed $T_{1\rho}$ map from 14 months old TG mouse (k). Scale bar 1000 μm (a-f) and 50 μm (g, h). Mean ± SD, TG and WT mice were compared with Student´s t-test at each timepoint (i). Pearson correlation coefficient (r) was calculated with GraphPad Prism5 software *P < 0.05, **P < 0.01. Modified from figure 2 in manuscript II.

ECG was registered during echocardiography from the TG mice with cardiac-specific overexpression of VEGF-B_{167} and WT mice, because electrophysiological properties have been shown to be affected in LVH and HF and they had not been studied before in this TG mouse strain. ECG was further analyzed with a Matlab based analysis program, which has been specially made for measuring time intervals from the mouse ECG. An increase in LV mass, LV dilatation and accumulation of fibrosis affected the electrophysiological properties of the heart by delaying conduction times of PQ (the time from the beginning of atrial depolarization to the beginning of ventricular depolarization), QRSp (ventricular depolarization and early repolarization) and QT (ventricular depolarization and repolarization; Figure 10 a-c). Heart rate was markedly decreased in TG mice after 5 months of age compared to WT mice (Figure 10 d). QRS time referring to ventricular depolarization was markedly increased at the 14 months timepoint (data not shown).

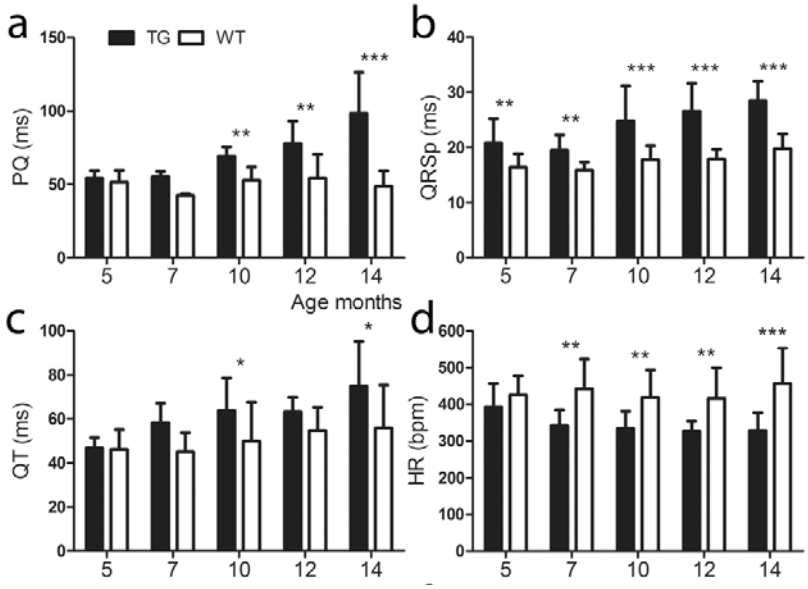

Figure 10. Changes in ECG during LVH progression in mice with VEGF-B_{167} overexpression in the heart. PQ time, measuring the time from the beginning of atrial depolarization to the beginning of ventricular depolarization, started to prolong after seven months of age (a) and QRSp time referring to LV depolarization and early repolarization (b) was significantly longer at all ages in TG mice compared to WT mice. QT time, measuring ventricular depolarization and repolarization, was increased at the age of 10 and 14 months (c) and heart rate (HR) decreased (d) in all timepoints after five months of age compared to WT mice. Mean ± SD, statistical analyses with SPSS Linear Mixed Model Analysis. *P < 0.05, **P < 0.01, ***P < 0.001. Modified from figure 3 in manuscript II.

The roles of VEGFs had not been fully clarified in progressive LVH, so in study I the aim was to determine the mRNA expression profile of VEGFs and their related receptors in compensatory LVH and HF. VEGF-C, VEGF-D and VEGFR-3 were shown to be upregulated in the heart in compensatory phase of LVH two weeks after TAC operation (Figure 11 a-c). Four weeks after TAC operation cardiac VEGF-B expression was downregulated and similarly LV function started to deteriorate (Figure 11 d).

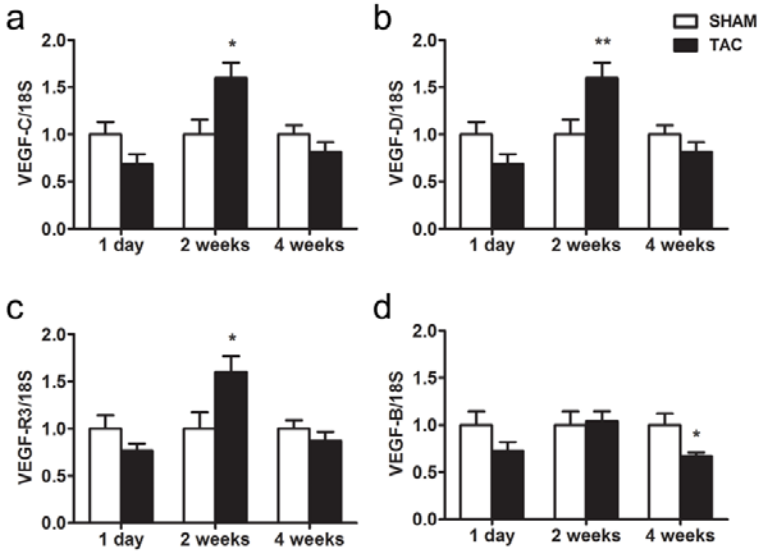

Figure 11. Expression of selected VEGFs in the heart during LVH progression. Upregulation of VEGF-C, VEGF-D and VEGF-R3 expression occurred two weeks after TAC operation (a-c). VEGF-B expression was shown to be downregulated at four weeks timepoint (d). Mean ± SEM, SHAM and TAC mice were compared with Student´s t-test at each timepoint. *P < 0.05, **P < 0.01. Modified from figure 4 in publication I.

5.2 GENE THERAPY FOR TREATING LEFT VENTRICULAR HYPERTROPHY (STUDY I)

A decrease in the cardiac VEGF-B expression was detected four weeks after TAC operation, when transition from compensatory LVH towards HF occurred and systolic function of LV as measured with EF had deteriorated. Echocardiography-guided closed-chest injection of AAV9-VEGF-B_{186} to the anterior wall of the LV in the compensatory phase of LVH improved the systolic function of the heart 4 weeks after the gene transfer (Figure 12 a). Anterior wall thickness, mass and internal diameter of the LV did not change in the VEGF-B_{186} treated group within the four-week follow-up time compared to LacZ treated group, in which the LVH progressed (Figure 12 b-d).

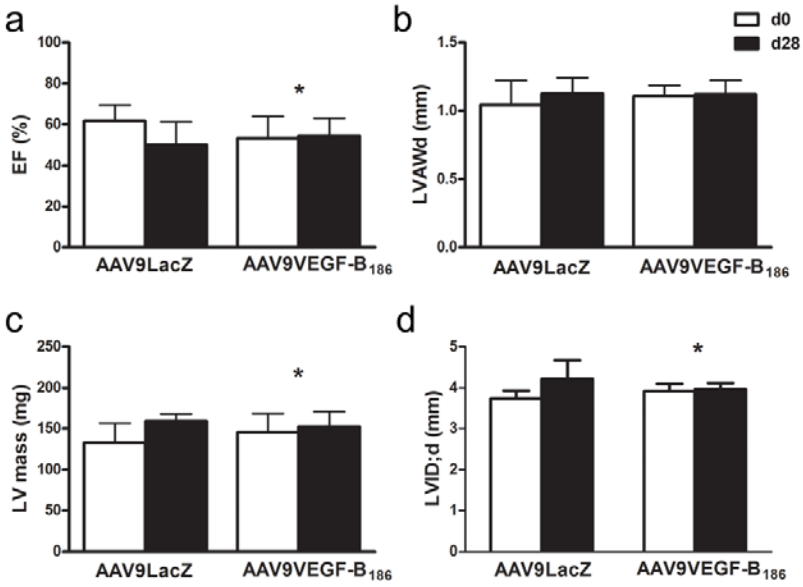

Figure 12. Effects of AAV9-VEGF-B_{186} gene transfer on structure and function of the heart. Gene transfer in compensatory phase of LVH improved systolic function of the LV four weeks after the VEGF-B administration compared to AAV9-LacZ treated group (a). LVH did not progress in VEGF-B treated group measured by LV anterior wall thickness, mass or internal diameter, when compared to LacZ treated group (b-d). Statistical analyses with repeated measurements two-way ANOVA. *P < 0.05. Modified from figure 5 in publication I.

The effects of AAV9-VEGF-B_{186} gene transfer on cardiomyocyte proliferation and apoptosis were determined from Ki67 stained sections and Cleaved Caspase -3 stained sections, respectively. Gene transfer of VEGF-B_{186} increased the number of proliferating cardiomyocytes (Figure 13 a-c) and decreased the amount of apoptotic cardiomyocytes (Figure 13 d-f) in the heart compared to AAV9-LacZ treated mice.

Progressive LVH led to decreased expressions of PGC-1α (data not shown) and endogenous VEGF-B in mouse heart four weeks after TAC operation, when the systolic function also deteriorated. After AAV9-VEGF-B_{186} gene transfer the expressions of PGC-1α and mVEGF-B were upregulated indicating a delay in metabolic remodelling associated with HF development compared to AAV9-LacZ treated mice (Figure 14 a, b). ANP was shown to be upregulated during LV remodelling and decreased expression in the heart after AAV9-VEGF-B_{186} gene transfer compared to mice treated with LacZ may indicate a delay in the transition towards HF (Figure 14 c).

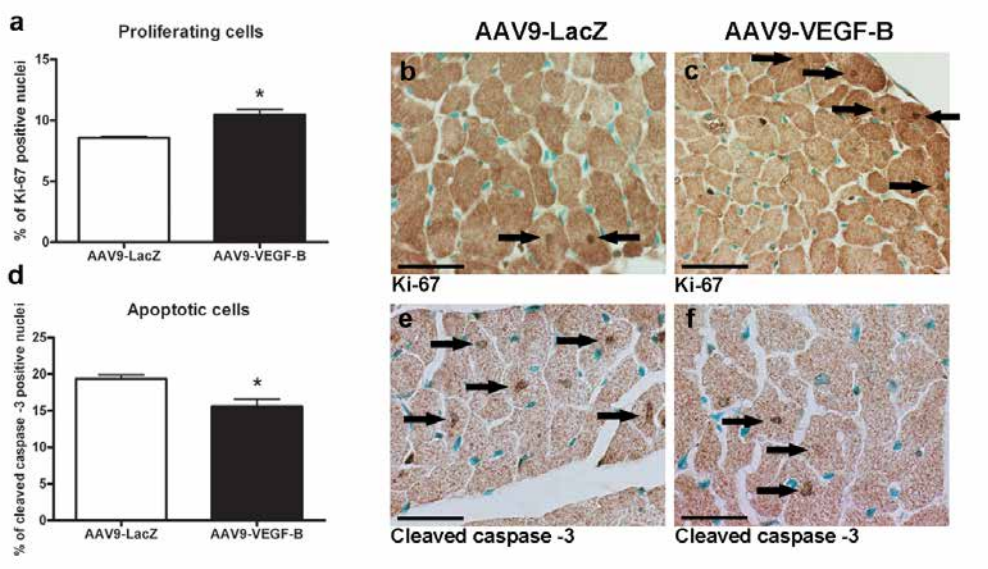

Figure 13. Effects of AAV9-VEGF-B_{186} gene transfer on cardiomyocyte proliferation and apoptosis. VEGF-B treated mice had more proliferating cardiomyocytes (Ki-67, a, c) and less apoptotic cardiomyocytes (Cleaved Caspase-3, d, f) compared to LacZ treated mice (a, b, d, e). Scale bars 25 μm. Mean ± SEM, statistical analyses with Student´s t-test. *P < 0.05. Modified from figure 7 in publication I.

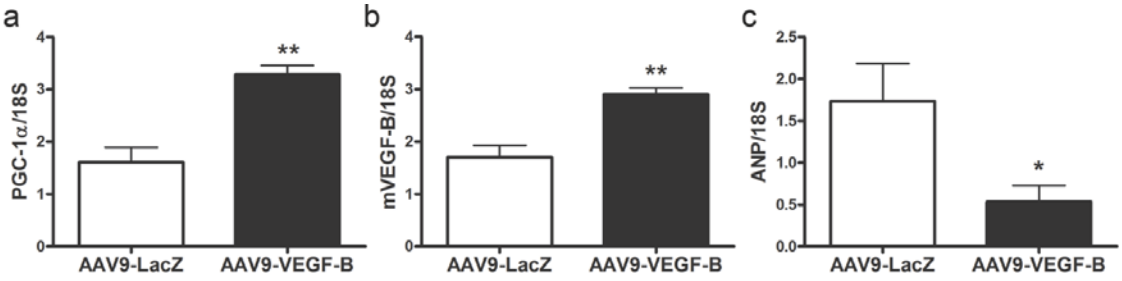

Figure 14. Comparison of the effects of AAV9-VEGF-B_{186} and AAV9-LacZ gene transfer on expression of PGC-1α, endogenous VEGF-B and ANP in the heart. PGC-1α and mouse endogenous VEGF-B expressions were increased four weeks after VEGF-B_{186} administration (a, b) and ANP expression was decreased at the same timepoint (c) when compared to LacZ treated mice. Mean ± SEM, statistical analyses with Student´s t-test. *P < 0.05, **P < 0.01. Modified from figure 8 in publication I.

5.3 SAFETY AND EFFICACY OF VIRAL VECTORS IN CARDIOVASCULAR GENE THERAPY (STUDY III)

Viral vectors are the most efficient tools in transferring genes to other cells. AdV, AAV2, AAV9 and LeV were compared to find an efficient and safe vector for cardiac gene therapy. The effects of closed-chest intramyocardial injection method were evaluated from needle punctured or NaCl injected hearts and transduction efficiencies, inflammation and fibrosis after viral vector administration were determined histologically from the heart. LacZ and CMV as marker genes were compared after AdV vector administration and the effects of AAV9 were also determined after systemic gene transfer. Echocardiographic data were used to evaluate the effects of different viral vectors to cardiac structure and function 28 days after the vector administration.

5.3.1 Transduction efficiency of AdV, AAV2, AAV9 and LeV vectors

Transduction efficiencies were determined 28 days after vector administration using immunohistochemistry of LacZ stained sections of AdV, AAV2 and AAV9 injected hearts (Figure 15 a-f) and hearts after intravenous AAV9-mediated gene transfer (Figure 15 i, j) or GFP stained sections of LeV injected hearts (Figure 15 g, h). Transgene positive cardiomyocytes were measured from the maximally transduced area near the needle tract, and the greatest number was measured in AdV treated hearts, demonstrating that AdV was the most efficient vector administered locally (Figure 16 a). Whereas AAV9 transduced the largest area of the LV, LeV transduced the smallest area as measured 28 days after the local intramyocardial gene transfer (Figure 16 b). In addition to immunohistochemical quantification, fluorescent microscopy of GFP was also used to quantitate GFP-positive cells in LeV injected hearts, both these methods gave similar localization (data not shown).

The transduced area of the LV with intravenously administered AAV9 was dependent on the viral dose used, but even with the highest viral dose only an area size comparable to local LeV gene transfer was observed (Figure 16 b).

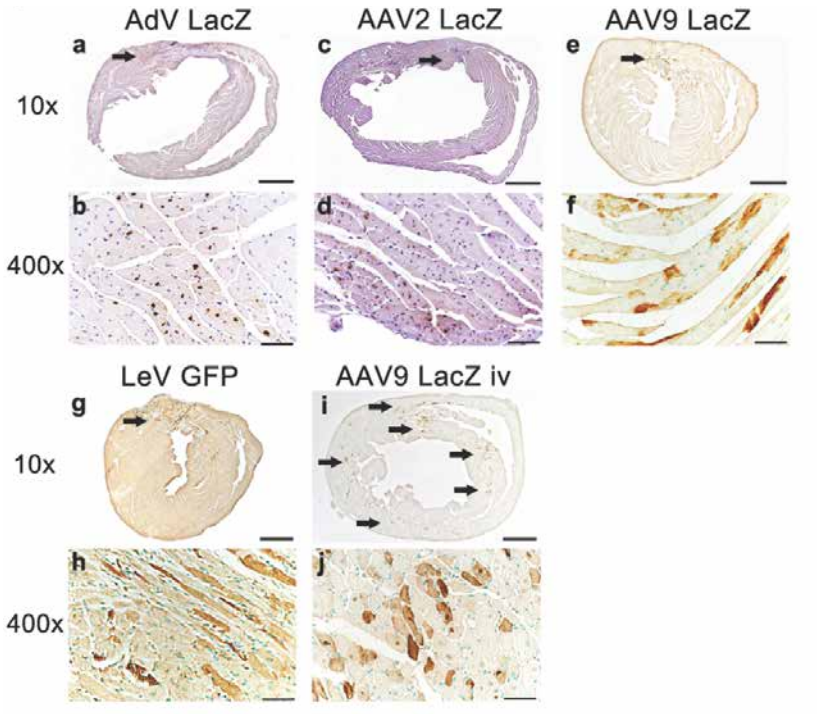

Figure 15. Transduced cardiomyocytes 28 days after local or systemic viral vector administration. Transgene positive cells were detected by immunohistochemical stainings for LacZ from AdV (a, b), AAV2 (c, d) and AAV9 (e, f) injected hearts or for GFP from LeV (g, h) injected hearts. Transgene positive cells after intravenous injection of AAV9 were detected by immunohistochemical staining for LacZ (i, j). Scale bar 1000 μm (a, c, e, g, i) and 50 μm (b, d, f, h, j). Modified from the figure 1 in publication III.

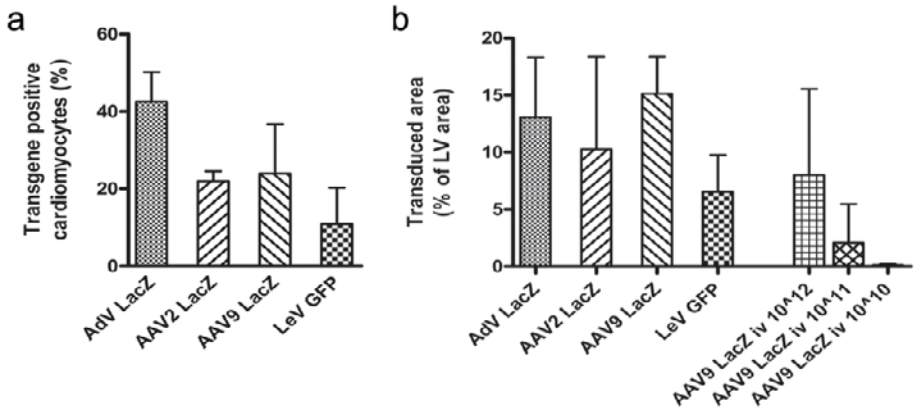

Figure 16. Gene transfer efficiencies 28 days after local or systemic delivery of different viral vectors. Transgene positive cardiomyocytes at the maximally transduced area of the LV were determined from LacZ or GFP stained sections. AdV transduced more cardiomyocytes around the needle tract than AAV2, AAV9 and LeV (a), although AAV9 transduced cardiomyocytes over a wider area than AdV (b). The transduced area of the LV after intravenous gene transfer of AAV9 was dose dependent (b). Modified from the figure 1 in publication III.

5.3.2 Scar area and inflammation after intramyocardial and intravenous gene transfer with viral vectors

Intramyocardial gene transfer of AdV, AAV2, AAV9 and LeV vectors to the anterior wall of LV produced a local scar and inflammatory reaction around the needle tract 28 days after the gene delivery. Measurements of the scar areas and inflammation gradings were done in a blinded fashion from Masson Trichrome stained sections at X 12.5 magnification. The largest scar and strongest lymphocyte-intensive inflammatory reactions were observed in AdV and AAV9 injected hearts compared to NaCl injected hearts (Figure 17 a-e). The smallest scar with minor inflammation at the injection site was observed in LeV injected hearts (Figure 17 a, b, f). A small scar, counting approximately 1 % of the LV area, was detected from the needle puncture and NaCl injection groups (Figure 17 a-c). Intravenous administration of AAV9 vector with the dose of $1x10^{12}$ vg induced diffuse fibrosis with lymphocyte-intensive inflammation throughout the myocardium, which were graded in a blinded fashion from Masson Trichrome stained sections at X 12.5 magnification. With lower doses ($1x10^{11}$ vg and $1x10^{10}$ vg) only minor fibrosis and inflammation were detected from the myocardium (Figure 18 a-d).

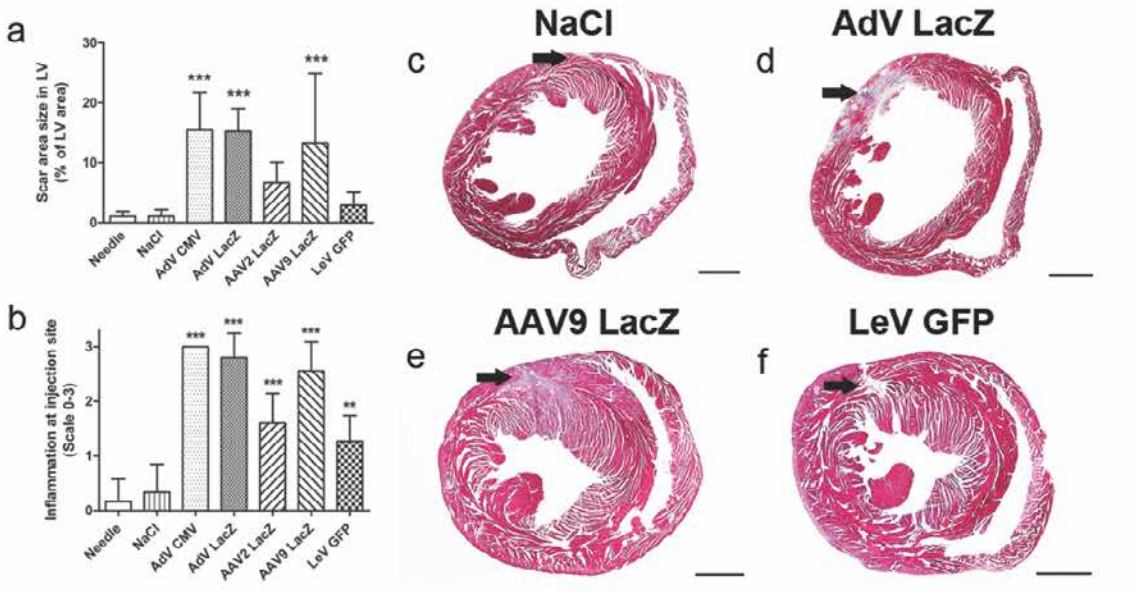

Figure 17. Scar area and inflammation in the myocardium 28 days after viral vector injection. The largest local scar and lymphocyte-intensive inflammatory reactions after intramyocardial injection were measured in AdV and AAV9 injected hearts (a, b, d, e), followed by AAV2 and LeV injected hearts (a, b, f). The needle puncture and NaCl caused a minor scar and inflammatory reaction at the injection site (a, b, c). Comparison was done to NaCl injected group. Masson Trichrome stained sections at magnification X 12.5 (c, d, e, f) were used to quantify scar area size and to the grade inflammation in the myocardium (scale 0 = no inflammation, 1 = minor inflammation, 2 = moderate inflammation, 3 = severe inflammation). Scale bar 1000 μm. Mean ± SD, statistical analyses with one-way ANOVA with Dunnet´s post hoc test. **P < 0.01, ***P < 0.001. Modified from figure 2 in publication III.

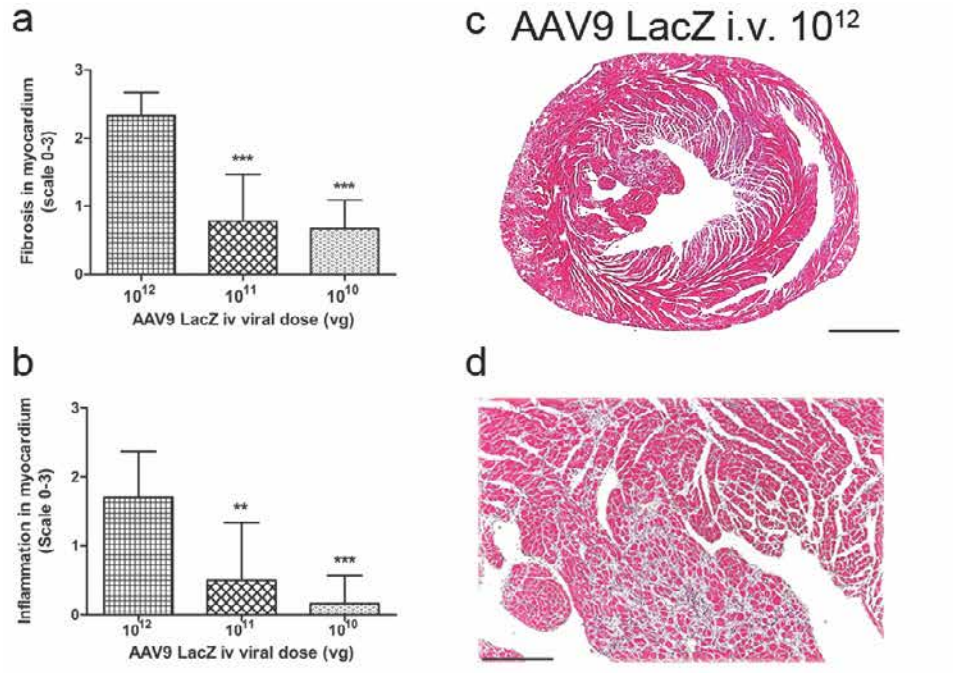

Figure 18. Fibrosis in the myocardium 28 days after intravenous (i.v.) gene transfer of AAV9. Diffuse myocardial fibrosis and inflammation were graded from Masson Trichrome stained sections on a scale of 0-3, in which 0 = no fibrosis/inflammation, 1 = mild fibrosis/inflammation, 2 = moderate fibrosis/inflammation and 3 = severe fibrosis/inflammation. Amount of fibrosis and inflammation were dose-dependent and comparison was done to the highest viral dose ($1x10^{12}$ vg; a, b). Representative images of Masson Trichrome stained sections of AAV9-LacZ i.v. (dose $1x10^{12}$ vg; c, d). Scale bar 1000 μm (whole heart, c) and 250 μm (100x magnification, d). Mean ± SD, statistical analyses with one-way ANOVA with Dunnet´s post hoc test. **P < 0.01, ***P < 0.001. Modified from figure 2 in publication III.

5.3.3 Effects of intramyocardial and intravenous gene transfer with viral vectors on cardiac structure and function

Echocardiography was used to measure changes in the thickness of the injection site at the LV anterior wall, the left atrium (LA) area size and the systolic and diastolic functions as measured by EF, and mitral valve E/A ratio, respectively. The strongest increase in the LV anterior wall thickness was observed 6 days after the gene transfer in AdV injected groups due to acute edema at the injection site (Figure 19 a). AdV-LacZ gene transfer caused thinning of the anterior wall of LV and systolic dysfunction as measured by decreased EF due to fibrosis, which was detected 28 days after the vector administration. The trend was similar after AdV-CMV gene transfer in the anterior wall thickness and EF at day 28 (Figure 19 a, b). An increase in the LV anterior wall thickness was observed after AAV9-LacZ and LeV-GFP intramyocardial gene transfers (Figure 19 a). Despite the presence of only a minor scar and inflammation at the injection site, 28 days after the intramyocardial injection of NaCl, a marked decrease in EF was observed in this group indicating a systolic dysfunction of the LV (Figure 19 b). Decreased EF, increased left atrium area size and increased E/A ratio in the mitral valve velocities were observed in the AAV9-LacZ group treated with $1x10^{12}$ vg dose intravenously (Figure 19, b-h).

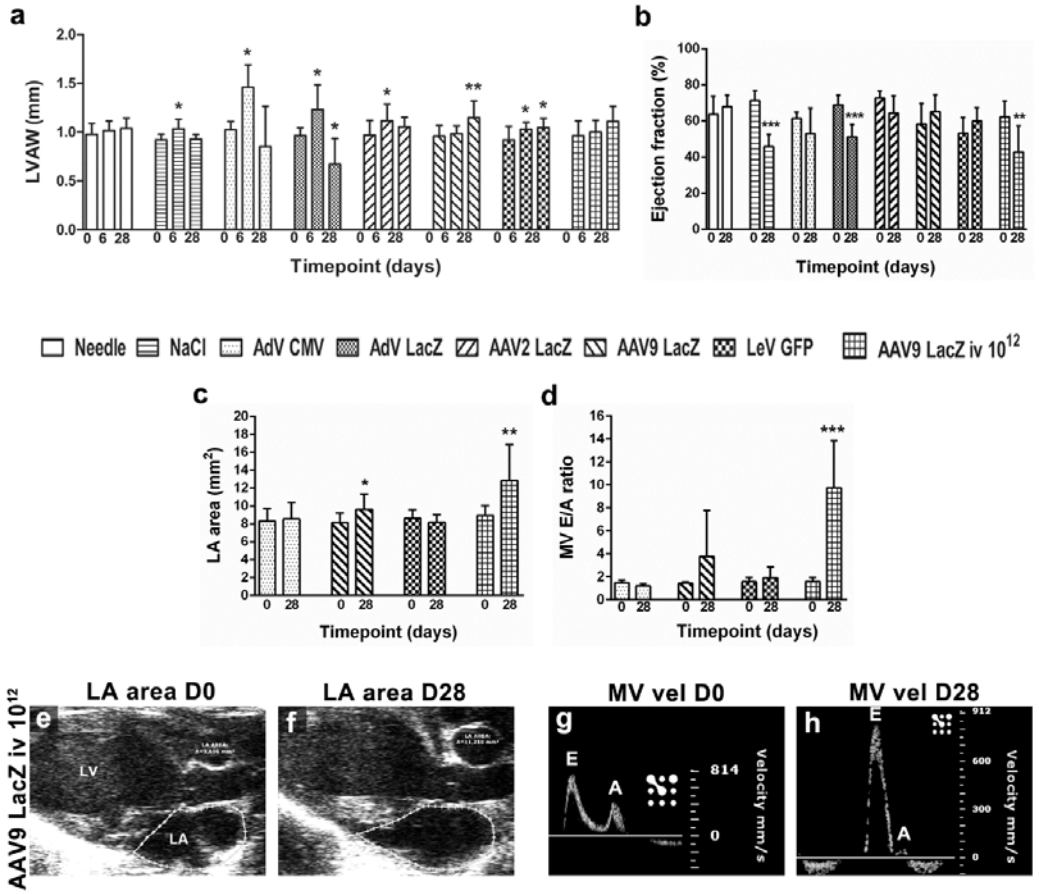

Figure 19. Effects of viral gene transfer to cardiac structure and function. LV anterior wall thickness in diastole (LVAW; a), EF (b), left atrium (LA) area (c) and mitral valve (MV) E/A ratio (d) were measured with echocardiography and compared to day 0 value within each group. Representative images of LA area and MV flow velocities at day 0 and 28 after the intravenous gene transfer of the highest dose of AAV9-LacZ ($1x10^{12}$ vg). Mean ± SD, statistical analyses with one-way ANOVA with Dunnet´s post hoc test (a) or Student´s t-test (b-d). *P < 0.05, **P < 0.01, ***P < 0.001. Modified from figure 3 in publication III.

6 Discussion

6.1 CARDIOVASCULAR IMAGING METHODS

Echocardiography is widely used in measuring structural and functional parameters from the heart. It is an easily available, fast, non-invasive and cheap method for cardiac analysis; however, it relies on assumptions about the cardiac structure and is strongly dependent on the observers skills. (Ashley, Niebauer 2004, Jensen 2007.) 3D visualization of the heart with CMR was shown to be especially useful, when there are technical difficulties in performing echocardiography, for example the heart structure is abnormal due to disease process or a geometrically challenging right ventricle is imaged (Kramer, Hundley 2010).

In this thesis study, echocardiography and CMR were compared in LVH and HF progression in TG mice with cardiac-specific overexpression of VEGF-B_{167}. The LV volume and LV mass increased and EF decreased within months and marked systolic dysfunction occurred at the age of 14 months in TG mice. Changes associated with LVH progression and HF development were measurable with both echocardiography and CMR. Echocardiographic measurements are more prone to errors than CMR measurements, as the slice selection for M-mode measurements during imaging highly impacts the results. The whole of the LV is taken into consideration in the CMR analyses and objective measurements can be performed without making assumptions about the heart structure (Stuckey et al. 2008). In previous studies with rats and patients, echocardiography has shown to underestimate all measurements in diseased heart (Stuckey et al. 2008, Gardner et al. 2009). Contrary to previous findings, higher measurements of absolute values of LV volume and LV mass were obtained by echocardiography in comparison to CMR in TG mice. The EF data were consistent with the previous finding, that echocardiography shows lower values than CMR in diseased heart. In TG mice an increase in LV volume and LV mass from 5 to 14 months of age was markedly higher as measured by CMR in comparison to echocardiography. This indicates that since the CMR measures the whole myocardium then hypertrophic changes in the septum or lateral wall of LV are not missed, as is potentially the case in echocardiography.

Although the CMR is thought to be the best imaging method for diseased heart, it also has its limitations. The equipment needed is expensive and not widely available. The high heart and breathing rate in mice combined with the small cardiac size induced marked motion artifacts to the CMR images. These artifacts were reduced by using ECG-triggered sequences. ECG-triggering allows CMR sequence to be synchronized to the cardiac cycle using data collection from spins at a certain region and phase within a R-R interval in the ECG. In mice, the high and variable heart rate and low ECG magnitude complicate the ECG-triggering, which make dection of R-R intervals difficult and extend the imaging time. (Sabbah et al. 2007.)

Long imaging time (~ 2 hours per mouse) with CMR reduced the number of mice studied in this thesis work and restricted the use of additional CMR protocols. In addition to cine imaging for cardiac structure and function, $T_{1\rho}$ and T_2 maps were only done from one 1mm thick slice in the middle of the LV for TG mice suffering from LVH. It would have been beneficial to reconstruct $T_{1\rho}$ maps from several slices of the heart to be able to evaluate the fibrosis in the myocardium. However, this would have prohibited the acquisition of other images due to the limited anaesthesia time for the mice. $T_{1\rho}$ map could also be taken from LAX view to better cover the whole LV in detecting fibrosis.

Besides long imaging time, the data processing with CMR is time consuming (~ 1 hour per mouse). The amount of pixels in LV and myocardium in diastole and systole are determined from each slice of the LV by manually drawing the contours. The pixel

numbers are converted to end-diastolic and end-systolic LV volumes and the slices are summed together to obtain the results from the whole LV. Functional parameters like EF, SV and LV mass are calculated manually. Automatic methods for measuring LV dimensions and calculating structural and functional parameters were shown to be accurate and reproducible compared to manual evaluations (Lu et al. 2013). In clinical practise, time saving by using automated analysing programs would be very beneficial.

In conclusion, CMR is a challenging and time consuming method in imaging mouse heart, but the evaluation of LV structure with CMR is superior to echocardiography. Echocardiography due to its availability and relatively fast data acquisition (20-30 minutes per mouse) and analysis (15 minutes per mouse) can be used to screen the hearts for further imaging with CMR, which can not be performed to all patients or mice.

6.2 DIAGNOSTICS OF HEART FAILURE

The diagnosis of HF in patients requires an identified cardiac pathology, typical symptoms and recognized signs of the syndrome (McMurray et al. 2012). Ejection fraction is a standard measurement for the cardiac function, although it should always be connected with the structure and function visualized during echocardiography. Skills of the operator, the chosen analysis method to evaluate LV and the heart structure assumption during measurements affect to the reliability of the calculated EF (Ashley, Niebauer 2004, Jensen 2007). In this thesis study LVH leading to HF was induced by pressure overload after TAC operation and by cardiac-specific overexpression of VEGF-B_{167}. A decrease in EF is a clinical parameter, which can be detected from mice with HF. Other clinical symptoms and signs (McMurray et al. 2012), like breathlessness, changes in cardiac sounds or pulmonary crepitations are difficult, or impossible to examine from the mice. Neither TAC operated nor TG mice with VEGF-B_{167} overexpression in the heart suffered from pulmonary oedema or swelling in the lower extremities, which could have been detected during sacrifications. In addition to decreased EF, the HF diagnosis in TG mice was supported by LV dilatation, increased expression of ANP and BNP and contractility defects measured by decreased expression of cTnT. TAC operated mice and TG mice suffered from diffuse myocardial fibrosis, which is also associated with LV remodelling (Kerkela, Force 2006) and may at least partly explain the function loss indicated by the decreased EF.

Myocardial fibrosis has been associated with an increased risk of hospitalization for HF, death or both, with increasing risk depending on the level of fibrosis (Diez et al. 2002). There is a clear need to develop methods to identify fibrosis from the myocardium. Novel imaging methods would be important in diagnosing heart diseases, following their progression and enabling therapies to possibly reduce accumulation of fibrosis (Diez et al. 2002). Late-gadolinium enhancement (LGE) has traditionally been used for the tissue characterization in CMR, but contraindications to exogenous contrast agents often restrict its usage. T1 relaxation in the rotating frame of reference ($T_{1\rho}$) was shown to be a sensitive marker for collagen and proteoglygan accumulation to extracellular space (Grohn et al. 2000, Witschey et al. 2012). In cardiovascular studies, $T_{1\rho}$ relaxation time has shown high contrast similarly to LGE between remote myocardium and myocardial infarction or fibrosis associated with hypertrophic cardiomyopathy (Witschey et al. 2012, Musthafa et al. 2013, Wang et al. 2015). In this thesis work, a correlation between the amount of fibrosis in the myocardium and $T_{1\rho}$ relaxation time was found in mice with cardiac-specific overexpression of VEGF-B_{167}. This suggests, that $T_{1\rho}$ CMR has a clear potential in detecting moderate to severe diffuse myocardial fibrosis and that this protocol could be utilized in the clinic.

6.3 VEGF-B IN LEFT VENTRICULAR HYPERTROPHY AND HEART FAILURE

The role of VEGF-B in metabolism and cardiac function has been under investigation during the past years. VEGF-B exists in two alternatively spliced isoforms, VEGF-B_{167} and VEGF-B_{186}. VEGF-B_{167} binds to heparan sulfate proteoglycans in the extracellular matrix, but VEGF-B_{186} is freely soluble. Both isoforms of VEGF-B are co-expressed in various metabolically active tissues and their effects are mediated via VEGFR-1 and Nrp-1. (Olofsson et al. 1996b, Makinen et al. 1999.) Both isoforms of VEGF-B have been shown to control fatty acid uptake from blood vessels to peripheral tissues and similarly the expression of mitochondrial genes to ensure oxidative capacity of the tissue (Hagberg et al. 2010). Cardiac-specific overexpression of VEGF-B_{167} in mice was shown to induce LVH by altered lipid metabolism, in which ceramides accumulate in the heart causing mitochondrial dysfunction and lipotoxicity (Karpanen et al. 2008). Overexpression of both VEGF-B isoforms specifically in rat heart induced LVH without LV dysfunction or lipotoxicity. Strong arteriogenesis has been observed in the rat, but not in the mouse heart with cardiac-specific overexpression of VEGF-B gene. (Bry et al. 2010.)

In this thesis work both isoforms of VEGF-B were studied. Cardiac-specific overexpression of VEGF-B_{167} in mice induced LVH without affecting the systolic function until one year of age, but longer follow-up in this thesis study showed the appearance of LV dysfunction and marked dilatation of the LV. Contrary to the concentric LVH reported earlier (Karpanen et al. 2008), we did not detect increases in LV wall thicknesses at any timepoint indicating an eccentric type of LVH. The remodelling process in the LV progressed within months. Expressions of ANP and BNP were upregulated and cTnT expression in the heart was downregulated already from 5 months of age. The heart rate in TG mice was previously shown to be lower than in WT mice (Karpanen et al. 2008), but further studies on the effects of VEGF-B overexpression on ECG measurements have not otherwise been performed. Ventricular repolarization was prolonged already at 5 months of age as measured from the QRSp interval, but ventricular depolarization defects occurred only at the age of 14 months. Accumulation of fibrosis is likely to explain the delay in ventricular conduction in that timepoint.

Both isoforms of VEGF-B were shown to have beneficial effects in gene therapy; AdV mediated VEGF-B_{186} was shown to have cardioprotective properties by inducing cardiac angiogenesis, improving cardiomyocyte survival and decreasing apoptosis in a myocardium-specific manner (Lahteenvuo et al. 2009). Likewise, AAV9-VEGF-B_{167} delayed the progression toward HF in dilated cardiomyopathy (Pepe et al. 2010). In this thesis study, VEGF-B was downregulated in LVH four weeks after TAC operation and simultaneously LV function started to deteriorate. AAV9 mediated VEGF-B_{186} gene transfer in compensatory phase of LVH delayed the progression of HF, improved systolic function, induced angiogenesis, decreased apoptotic cells and altered the expression of metabolism-associated genes in the heart. PGC-1α and endogenous VEGF-B expression were upregulated in the heart after VEGF-B_{186} administration and possibly an increased fatty acid utilization could have reduced energy deprivation in the failing heart. A recent publication has shown, that in the skeletal muscle, PGC-1α coordinates VEGF-A and VEGF-B expression, thus controlling vessel growth and regulating lipid uptake. Overexpressed PGC-1α resulted in upregulation of VEGF-B expression, which increased fatty acid accumulation to tissues and induced insulin resistance. (Mehlem et al. 2016.)

Short-term overexpression of VEGF-B after gene therapy has been shown to be cardioprotective by several mechanisms in ischemic and nonischemic conditions (Lahteenvuo et al. 2009, Pepe et al. 2010). However, TG mice overexpressing VEGF-B_{167} showed adverse effects of long-term deviation from the normal gene expression pattern, by leading to HF via LVH as shown in this thesis study. Insulin resistance has also been observed after upregulation of endogenous VEGF-B expression (Mehlem et al. 2016), which highlights the importace of having adequate levels of growth factors in the body.

6.4 VIRAL VECTORS IN CARDIOVASCULAR GENE THERAPY

Gene therapy is a promising new treatment for cardiovascular diseases, such as CAD or HF. A better understanding of the mechanisms behind several diseases have introduced new molecules, some of these have recently been studied in gene therapy settings in addition to the angiogenic factors. (Wolfram, Donahue 2013, Laakkonen, Yla-Herttuala 2015.) Still, there has also been a need to develop minimally invasive, but efficient gene transfer methods and to compare the viral vectors available for gene transfer studies.

In the clinical setting, catheter-mediated intramyocardial delivery of the transgene has proven to be accurate, safe and a minimally invasive method. The local administration of the transgene has reduced the required viral dose and prevented possible side effects associated with systemic gene transfer. (Hedman et al. 2009, Yla-Herttuala 2013.) In this thesis study we used the closed-chest intramyocardial injection technique for gene transfer, in which the needle was punctured through the chest under echocardiography guidance. In previous studies, this has proven to be a feasible and well tolerated method in mice (Springer et al. 2005, Huusko et al. 2010). Indeed, the needle puncture caused a minor scar without affecting the cardiac structure or function. Interestingly, NaCl injection caused a minor scar comparable to needle puncture, but a marked LV dilatation and global hypokinesia without major ECG changes 28 days after the injection. Adverse effects of intramyocardial saline injections have not been reported earlier, but systemic delivery of NaCl has been found to be safe without inducing LV dysfunction (Zincarelli et al. 2008).

Viral vectors differ from their transgene capacity, tropism towards tissues, expression profile and side effects. High transduction efficiency and transient expression make AdVs a suitable vector choice after acute ischemic situation, when a rapid response to therapy is needed. The highest expression of AdVs occurs around 6 days after the gene transfer and lasts up to 2-4 weeks, which is a reasonable time for inducing an angiogenic response. (Markkanen et al. 2005.) The transgene expression with AdVs is limited due to direct toxicity of the viral capsid and stimulation of an immune response towards AdV gene products (Ahi, Bangari & Mittal 2011). In this thesis study AdV transduced approximately 40 % of the cardiomyocytes around the needle tract and the transduced area matched with the scar area size of approximately 15 % of the LV. Similar transduction efficiencies have been shown before in the heart after echocardiography-guided AdV-LacZ injection (Toivonen et al. 2012). In AdV transduced hearts, inflammation at the injection site was most severe compared to AAV or LeV injected groups. The present findings support the known fact, that AdVs induce a strong immune response (Korpisalo et al. 2011, Ahi, Bangari & Mittal 2011, Toivonen et al. 2012). A transient increase in the anterior wall thickness of LV due to oedema was observed in AdV injected hearts 6 days after gene transfer. Twenty-eight days after AdV-LacZ injection, the diastolic diameter of the LV was increased and the EF decreased due to accumulation of fibrosis at the injection site. To evaluate the possible effects of the chosen marker gene on the scar formation, inflammatory response, cardiac function and electrophysiological properties after gene transfer, an empty AdV carrying the CMV promoter and no transgene was used and compared to AdV-LacZ group. Studies in this thesis work indicated, that the LacZ gene itself did not affect the safety profile of the viral vector, at least in the case of AdV.

AAVs are present extrachromosomally and can produce long-term transgene expression after only one delivery. AAV expression in the heart has been shown to peak 8-26 weeks after gene transfer and to last up to one year. The transduction efficiency has been shown to be lower with AAVs than AdVs in the heart. (Vassalli et al. 2003.) The finding in this thesis study was similar, as AAVs reached approximately 20 % transduction efficiency around the needle tract. AAV9 transduced a larger area from the LV than AAV2, and similarly the scar area and inflammation in the LV were more severe in AAV9 than in AAV2 injected hearts. AAVs do not express any viral genes, but a cellular immune response can be induced against the viral capsid. A more difficult type of immunity is the precence of neutralizing

antibodies, especially found against AAV2 serotype, which can even at very low levels prevent successful transduction. (Louis Jeune et al. 2013.)

Systemic delivery of the viral vector is not a feasible method in clinic, but widely used in preclinical studies. AAV9 previously achieved efficient transduction in cardiomyocytes after systemic gene transfer in small animals (Zincarelli et al. 2008, Fang et al. 2012) and no major adverse effects were reported. The systemic AAV9 gene transfers in this thesis study were done with the generally used dose of $1x10^{12}$ vg, which surprisingly induced severe diffuse fibrosis and marked inflammation in the heart and led to impaired systolic function 28 days after the vector administration. The adverse effects of systemic AAV9 application were highly dose-dependent, as 10- and 100-fold decreased viral doses, reduced the tissue damage significantly. Unfortunately, with lower doses expression of the transgene was barely detectable. A $1x10^{12}$ vg dose of systemic AAV9 transduced also several other organs, which is a known side effect after systemic vector administration (Zincarelli et al. 2008). Systemic administration of AAV9 produced severe effects in a dose-dependent manner and cannot be considered as a safe choice for systemic gene therapy studies.

LeV integrate into host cell genome, thus leading to potentially life-long expression of the transgene (Kootstra, Verma 2003). Few preclinical trials have reported efficient transduction of the adult cardiomyocytes *in vitro and in vivo* after LeV administration (Zhao et al. 2002, Niwano et al. 2008b). Low titers of virus preparations in addition to safety aspects concerning the random integration into the host cell genome have limited the use of LeV vectors in cardiovascular studies (Laakkonen, Yla-Herttuala 2015). In this thesis study, lower LeV vector doses were used compared to AdV and AAV vectors, due to the low titers in virus preparations. In addition, in LeV vector, GFP was used as the transgene in comparison to LacZ in AdV and AAV vectors, as it was not possible to produce high enough titers with LacZ in LeV vector. The differences in dose, transgene and promoter (PGK in LeV and CMV in AdV and AAV) made LeV vector comparison more complicated than comparison of AdV and AAV, in which the promoter, transgene and dose were similar.

LeV transduced approximately 11 % of the cardiomyocytes around the needle tract and induced the smallest scar and least inflammation compared to AdV and AAV injected hearts. Similar transduction efficiency has been reported after LeV-EGFP intramyocardial injection (Fleury et al. 2003) and higher transduction efficiencies after intraventricular delivery of LeV-hPLAP (human placental alkaline phosphatase; Metcalfe et al. 2004) or intracoronary injection of LeV-SERCA2 (Niwano et al. 2008a). A minor increase in the anterior wall thickness of LV was detected 28 days after LeV gene transfer, but functional and electrophysiological parameters were not changed.

Gene transfer with a chosen vector is optimal, when transduction of the target cells is efficient, transgene expression time and level are suitable for the treated disease, no major side effects are induced in the target or other tissues and gene transfer route is minimally invasive (Thomas, Ehrhardt & Kay 2003). All of the above mentioned aspects and the treated species should be concidered, when gene therapy applications are planned. We found, that intramyocardial closed-chest injection was suitable and well-tolerated gene transfer method in mice. AdV was the most efficient in transducing cardiomyocytes, although fibrosis and inflammation leading to reduced function of the heart were the most severe side effects compared to AAV and LeV. In clinical trials, AdV has proven to be well-tolerated and safe also in long follow-up (Hedman et al. 2009). Mouse tissues are much less prone to transduction by AdVs than human tissues (Rissanen, Yla-Herttuala 2007) and the small heart size in mouse combined with the relatively high viral dose used may explain the marked changes in morphology and function of the heart shown in this thesis study. AAV was found to be less efficient, but also less harmful than AdV when delivered intramyocardially. Systemically delivered AAV induced severe diffuse fibrosis and LV dysfunction, and cannot be considered as a safe gene transfer concept. It would be interesting to study further the potential of LeV, although improvements in LeV production

are needed to achieve higher viral titers. In this study, the GFP expression from LeV was transcribed from a PGK promoter. The different promoter activities could influence the level of GFP expression, in particular, CMV has been shown to drive higher GFP expression than PGK in cultured rat cardiomyocytes (Fleury et al. 2003). Hence, the choice of promoter used in vectors is important, and needs to be taken into account when planning gene therapy studies.

7 Conclusions

Based on this thesis study, the following conclusions can be made:

(I) In the compensatory phase of LVH, the expressions of VEGF-C, VEGF-D and their primary receptor VEGFR-3 are increased. VEGF-B expression is decreased in the transition from LVH to HF. Furthermore, systolic function of the heart can be improved by AAV9-VEGF-B_{186} gene transfer, indicating an important role of VEGFs in LVH. Gene transfer of VEGF-B_{186} in AAV9 vector delayed the progression of HF by increasing angiogenesis and proliferating cells, decreasing apoptosis and promoting beneficial changes in gene expression.

(II) Life-long cardiac-specific overexpression of VEGF-B_{167} leads to LVH and HF in mice. Changes in expression of natriuretic peptides and cTnT can be detected in the early phase of LV remodelling. The LV mass, LV size and EF changes that occur due to the progression of LVH can be followed by echocardiography and CMR. Correlation between the amount of diffuse myocardial fibrosis and $T_{1\rho}$ relaxation time in CMR was found in this thesis study, indicating a clear potential in detecting moderate to severe fibrosis by CMR.

(III) AdV vector was the most efficient in transducing cardiomyocytes after echocardiography-guided closed-chest injection, but it also induced marked myocardial fibrosis and LV dysfunction when compared to AAV and LeV vectors. The lower transduction efficiency of AAV2, AAV9 and LeV was associated with less harmful side effects than after AdV injection. Systemic delivery of AAV9 was less efficient than local intramyocardial injection and induced significant myocardial fibrosis and LV dysfunction in a dose-dependent manner, which makes the local delivery of the vector a preferable gene transfer method.

Graphical abstract (Figure 20) summarises the most important findings of this thesis work.

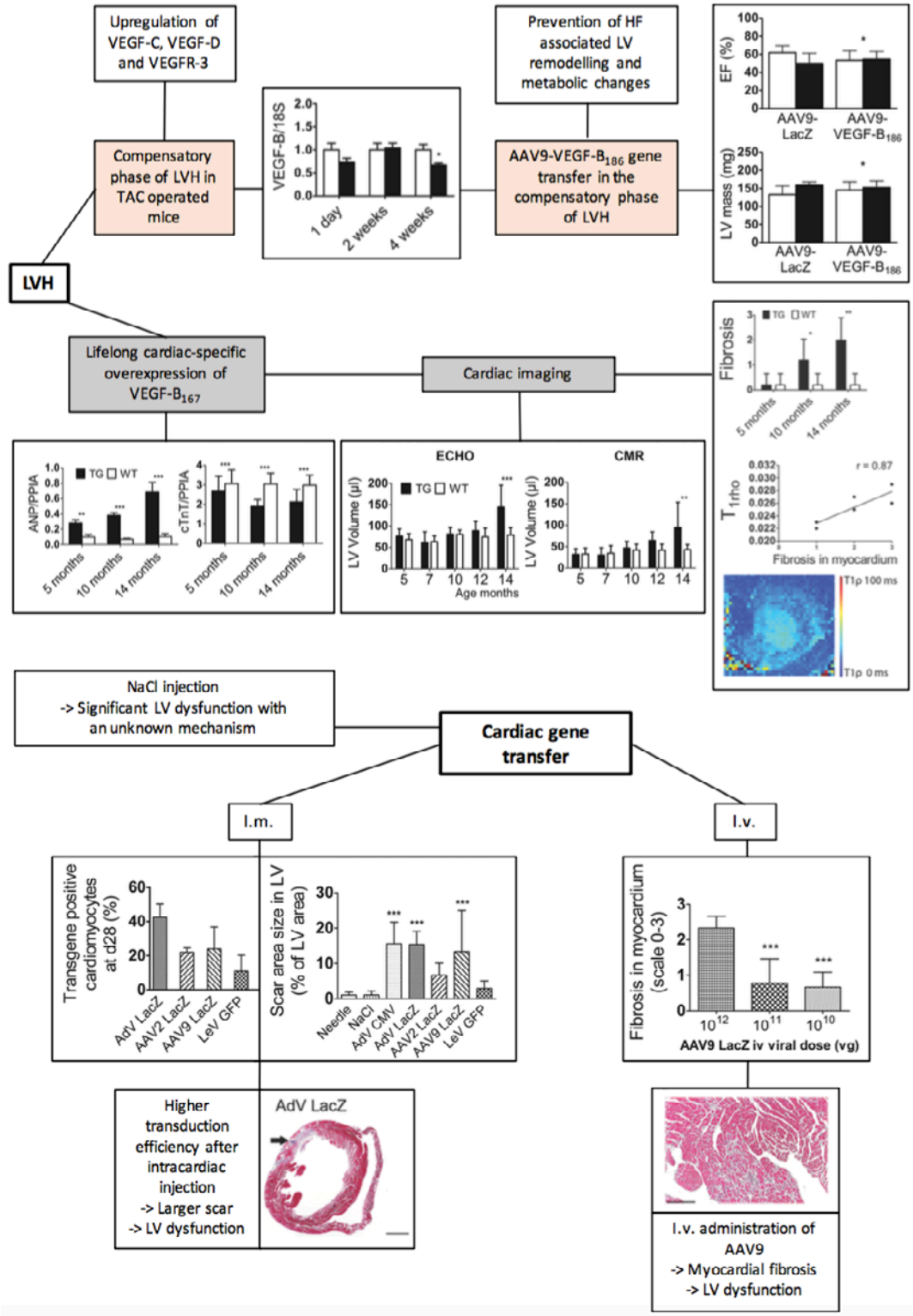

Figure 20. Graphical abstract.

8 References

Aase, K., von Euler, G., Li, X., Ponten, A., Thoren, P., Cao, R., Cao, Y., Olofsson, B., Gebre-Medhin, S., Pekny, M., Alitalo, K., Betsholtz, C. & Eriksson, U. 2001, "Vascular endothelial growth factor-B-deficient mice display an atrial conduction defect", *Circulation,* vol. 104, no. 3, pp. 358-364.

Abbas, A., Hansrani, V., Sedgwick, N., Ghosh, J. & McCollum, C.N. 2014, "3D contrast enhanced ultrasound for detecting endoleak following endovascular aneurysm repair (EVAR)", *European journal of vascular and endovascular surgery : the official journal of the European Society for Vascular Surgery,* vol. 47, no. 5, pp. 487-492.

Achen, M.G., Jeltsch, M., Kukk, E., Makinen, T., Vitali, A., Wilks, A.F., Alitalo, K. & Stacker, S.A. 1998, "Vascular endothelial growth factor D (VEGF-D) is a ligand for the tyrosine kinases VEGF receptor 2 (Flk1) and VEGF receptor 3 (Flt4)", *Proceedings of the National Academy of Sciences of the United States of America,* vol. 95, no. 2, pp. 548-553.

Ahi, Y.S., Bangari, D.S. & Mittal, S.K. 2011, "Adenoviral vector immunity: its implications and circumvention strategies", *Current gene therapy,* vol. 11, no. 4, pp. 307-320.

Al-Mallah, M.H., Aljizeeri, A., Villines, T.C., Srichai, M.B. & Alsaileek, A. 2015, "Cardiac computed tomography in current cardiology guidelines", *Journal of cardiovascular computed tomography,* vol. 9, no. 6, pp. 514-523.

Anavekar, N.S., Gerson, D., Skali, H., Kwong, R.Y., Yucel, E.K. & Solomon, S.D. 2007, "Two-dimensional assessment of right ventricular function: an echocardiographic-MRI correlative study", *Echocardiography (Mount Kisco, N.Y.),* vol. 24, no. 5, pp. 452-456.

Arber, S., Hunter, J.J., Ross, J.,Jr, Hongo, M., Sansig, G., Borg, J., Perriard, J.C., Chien, K.R. & Caroni, P. 1997, "MLP-deficient mice exhibit a disruption of cardiac cytoarchitectural organization, dilated cardiomyopathy, and heart failure", *Cell,* vol. 88, no. 3, pp. 393-403.

Ashley, E.A. & Niebauer, J. 2004, *Cardiology Explained*, Remedica, London.

Badea, C.T., Bucholz, E., Hedlund, L.W., Rockman, H.A. & Johnson, G.A. 2006, "Imaging methods for morphological and functional phenotyping of the rodent heart", *Toxicologic pathology,* vol. 34, no. 1, pp. 111-117.

Bagai, A., Dangas, G.D., Stone, G.W. & Granger, C.B. 2014, "Reperfusion strategies in acute coronary syndromes", *Circulation research,* vol. 114, no. 12, pp. 1918-1928.

Bakermans, A.J., Abdurrachim, D., Moonen, R.P., Motaal, A.G., Prompers, J.J., Strijkers, G.J., Vandoorne, K. & Nicolay, K. 2015, "Small animal cardiovascular MR imaging and spectroscopy", *Progress in Nuclear Magnetic Resonance Spectroscopy,* vol. 88-89, pp. 1-47.

Baldwin, M.E., Halford, M.M., Roufail, S., Williams, R.A., Hibbs, M.L., Grail, D., Kubo, H., Stacker, S.A. & Achen, M.G. 2005, "Vascular endothelial growth factor D is dispensable for development of the lymphatic system", *Molecular and cellular biology,* vol. 25, no. 6, pp. 2441-2449.

Baldwin, M.E., Roufail, S., Halford, M.M., Alitalo, K., Stacker, S.A. & Achen, M.G. 2001, "Multiple forms of mouse vascular endothelial growth factor-D are generated by RNA splicing and proteolysis", *The Journal of biological chemistry,* vol. 276, no. 47, pp. 44307-44314.

Bellomo, D., Headrick, J.P., Silins, G.U., Paterson, C.A., Thomas, P.S., Gartside, M., Mould, A., Cahill, M.M., Tonks, I.D., Grimmond, S.M., Townson, S., Wells, C., Little, M., Cummings, M.C., Hayward, N.K. & Kay, G.F. 2000, "Mice lacking the vascular endothelial growth factor-B gene (Vegfb) have smaller hearts, dysfunctional coronary vasculature, and impaired recovery from cardiac ischemia", *Circulation research,* vol. 86, no. 2, pp. E29-35.

Blankstein, R. 2012, "Cardiology patient page. Introduction to noninvasive cardiac imaging", *Circulation,* vol. 125, no. 3, pp. e267-71.

Borlaug, B.A. & Paulus, W.J. 2011, "Heart failure with preserved ejection fraction: pathophysiology, diagnosis, and treatment", *European heart journal,* vol. 32, no. 6, pp. 670-679.

Borthakur, A., Mellon, E., Niyogi, S., Witschey, W., Kneeland, J.B. & Reddy, R. 2006, "Sodium and T1rho MRI for molecular and diagnostic imaging of articular cartilage", *NMR in biomedicine,* vol. 19, no. 7, pp. 781-821.

Breckenridge, R. 2010, "Heart failure and mouse models", *Disease models & mechanisms,* vol. 3, no. 3-4, pp. 138-143.

Bristow, M.R., Saxon, L.A., Boehmer, J., Krueger, S., Kass, D.A., De Marco, T., Carson, P., DiCarlo, L., DeMets, D., White, B.G., DeVries, D.W., Feldman, A.M. & Comparison of Medical Therapy, Pacing, and Defibrillation in Heart Failure (COMPANION) Investigators 2004, "Cardiac-resynchronization therapy with or without an implantable defibrillator in advanced chronic heart failure", *The New England journal of medicine,* vol. 350, no. 21, pp. 2140-2150.

Bronzwaer, J.G. & Paulus, W.J. 2009, "Diastolic and systolic heart failure: different stages or distinct phenotypes of the heart failure syndrome?", *Current heart failure reports,* vol. 6, no. 4, pp. 281-286.

Bry, M., Kivela, R., Holopainen, T., Anisimov, A., Tammela, T., Soronen, J., Silvola, J., Saraste, A., Jeltsch, M., Korpisalo, P., Carmeliet, P., Lemstrom, K.B., Shibuya, M., Yla-Herttuala, S., Alhonen, L., Mervaala, E., Andersson, L.C., Knuuti, J. & Alitalo, K. 2010, "Vascular endothelial growth factor-B acts as a coronary growth factor in transgenic rats without inducing angiogenesis, vascular leak, or inflammation", *Circulation,* vol. 122, no. 17, pp. 1725-1733.

Buschmann, I. & Schaper, W. 2000, "The pathophysiology of the collateral circulation (arteriogenesis)", *The Journal of pathology,* vol. 190, no. 3, pp. 338-342.

Carmeliet, P. 2003, "Angiogenesis in health and disease", *Nature medicine,* vol. 9, no. 6, pp. 653-660.

Carmeliet, P. 2000, "Mechanisms of angiogenesis and arteriogenesis", *Nature medicine,* vol. 6, no. 4, pp. 389-395.

Carmeliet, P., Ferreira, V., Breier, G., Pollefeyt, S., Kieckens, L., Gertsenstein, M., Fahrig, M., Vandenhoeck, A., Harpal, K., Eberhardt, C., Declercq, C., Pawling, J., Moons, L., Collen, D., Risau, W. & Nagy, A. 1996, "Abnormal blood vessel development and lethality in embryos lacking a single VEGF allele", *Nature,* vol. 380, no. 6573, pp. 435-439.

De Falco, S. 2012, "The discovery of placenta growth factor and its biological activity", *Experimental & molecular medicine,* vol. 44, no. 1, pp. 1-9.

Dehghanian, F., Hojati, Z. & Kay, M. 2014, "New Insights into VEGF-A Alternative Splicing: Key Regulatory Switching in the Pathological Process", *Avicenna journal of medical biotechnology,* vol. 6, no. 4, pp. 192-199.

Devaux, Y., Vausort, M., Azuaje, F., Vaillant, M., Lair, M.L., Gayat, E., Lassus, J., Ng, L.L., Kelly, D., Wagner, D.R. & Squire, I.B. 2012, "Low levels of vascular endothelial growth factor B predict left ventricular remodeling after acute myocardial infarction", *Journal of cardiac failure,* vol. 18, no. 4, pp. 330-337.

Diez, J., Querejeta, R., Lopez, B., Gonzalez, A., Larman, M. & Martinez Ubago, J.L. 2002, "Losartan-dependent regression of myocardial fibrosis is associated with reduction of left ventricular chamber stiffness in hypertensive patients", *Circulation,* vol. 105, no. 21, pp. 2512-2517.

Dijkstra, M.H., Pirinen, E., Huusko, J., Kivela, R., Schenkwein, D., Alitalo, K. & Yla-Herttuala, S. 2014, "Lack of cardiac and high-fat diet induced metabolic phenotypes in two independent strains of Vegf-b knockout mice", *Scientific reports,* vol. 4, pp. 6238.

Di Pasquale, E., Latronico, M.V., Jotti, G.S. & Condorelli, G. 2012, "Lentiviral vectors and cardiovascular diseases: a genetic tool for manipulating cardiomyocyte differentiation and function", *Gene therapy,* vol. 19, no. 6, pp. 642-648.

DiPalma, T., Tucci, M., Russo, G., Maglione, D., Lago, C.T., Romano, A., Saccone, S., Della Valle, G., De Gregorio, L., Dragani, T.A., Viglietto, G. & Persico, M.G. 1996, "The placenta growth factor gene of the mouse", *Mammalian genome : official journal of the International Mammalian Genome Society,* vol. 7, no. 1, pp. 6-12.

Dorn, G.W.,2nd & Force, T. 2005, "Protein kinase cascades in the regulation of cardiac hypertrophy", *The Journal of clinical investigation,* vol. 115, no. 3, pp. 527-537.

Drake, R.L., Vogl, W. & Mitchell, A.W.M. (eds) 2005, *Gray´s Anatomy for Students*, 1st edn, Elsevier Inc., Philadelphia.

Dumont, D.J., Jussila, L., Taipale, J., Lymboussaki, A., Mustonen, T., Pajusola, K., Breitman, M. & Alitalo, K. 1998, "Cardiovascular failure in mouse embryos deficient in VEGF receptor-3", *Science (New York, N.Y.),* vol. 282, no. 5390, pp. 946-949.

Ellis, L.M. 2006, "The role of neuropilins in cancer", *Molecular cancer therapeutics,* vol. 5, no. 5, pp. 1099-1107.

Fang, H., Lai, N.C., Gao, M.H., Miyanohara, A., Roth, D.M., Tang, T. & Hammond, H.K. 2012, "Comparison of adeno-associated virus serotypes and delivery methods for cardiac gene transfer", *Human gene therapy methods,* vol. 23, no. 4, pp. 234-241.

Farmakis, D., Stafylas, P., Giamouzis, G., Maniadakis, N. & Parissis, J. 2015, "The medical and socioeconomic burden of heart failure: A comparative delineation with cancer", *International journal of cardiology,* vol. 203, pp. 279-281.

Ferrara, N., Gerber, H.P. & LeCouter, J. 2003, "The biology of VEGF and its receptors", *Nature medicine,* vol. 9, no. 6, pp. 669-676.

Fleury, S., Simeoni, E., Zuppinger, C., Deglon, N., von Segesser, L.K., Kappenberger, L. & Vassalli, G. 2003, "Multiply attenuated, self-inactivating lentiviral vectors efficiently deliver and express genes for extended periods of time in adult rat cardiomyocytes in vivo", *Circulation,* vol. 107, no. 18, pp. 2375-2382.

Folkman, J., Merler, E., Abernathy, C. & Williams, G. 1971, "Isolation of a tumor factor responsible for angiogenesis", *The Journal of experimental medicine,* vol. 133, no. 2, pp. 275-288.

Fong, G.H., Rossant, J., Gertsenstein, M. & Breitman, M.L. 1995, "Role of the Flt-1 receptor tyrosine kinase in regulating the assembly of vascular endothelium", *Nature,* vol. 376, no. 6535, pp. 66-70.

Fuster, V., Ryden, L.E., Cannom, D.S., Crijns, H.J., Curtis, A.B., Ellenbogen, K.A., Halperin, J.L., Kay, G.N., Le Huezey, J.Y., Lowe, J.E., Olsson, S.B., Prystowsky, E.N., Tamargo, J.L., Wann, L.S., Smith, S.C.,Jr, Priori, S.G., Estes, N.A.,3rd, Ezekowitz, M.D., Jackman, W.M., January, C.T., Lowe, J.E., Page, R.L., Slotwiner, D.J., Stevenson, W.G., Tracy, C.M., Jacobs, A.K., Anderson, J.L., Albert, N., Buller, C.E., Creager, M.A., Ettinger, S.M., Guyton, R.A., Halperin, J.L., Hochman, J.S., Kushner, F.G., Ohman, E.M., Stevenson, W.G., Tarkington, L.G., Yancy, C.W. & American College of Cardiology Foundation/American Heart Association Task Force 2011, "2011 ACCF/AHA/HRS focused updates incorporated into the ACC/AHA/ESC 2006 guidelines for the management of patients with atrial fibrillation: a report of the American College of Cardiology Foundation/American Heart Association Task Force on practice guidelines", *Circulation,* vol. 123, no. 10, pp. e269-367.

Gagnon, M.L., Bielenberg, D.R., Gechtman, Z., Miao, H.Q., Takashima, S., Soker, S. & Klagsbrun, M. 2000, "Identification of a natural soluble neuropilin-1 that binds vascular endothelial growth factor: In vivo expression and antitumor activity", *Proceedings of the National Academy of Sciences of the United States of America,* vol. 97, no. 6, pp. 2573-2578.

Gao, G., Qu, G., Burnham, M.S., Huang, J., Chirmule, N., Joshi, B., Yu, Q.C., Marsh, J.A., Conceicao, C.M. & Wilson, J.M. 2000, "Purification of recombinant adeno-associated virus vectors by column chromatography and its performance in vivo", *Human Gene Therapy,* vol. 11, no. 15, pp. 2079-2091.

Gao, S., Ho, D., Vatner, D.E. & Vatner, S.F. 2011, "Echocardiography in Mice", *Current protocols in mouse biology,* vol. 1, pp. 71-83.

Gardner, B.I., Bingham, S.E., Allen, M.R., Blatter, D.D. & Anderson, J.L. 2009, "Cardiac magnetic resonance versus transthoracic echocardiography for the assessment of cardiac volumes and regional function after myocardial infarction: an intrasubject comparison using simultaneous intrasubject recordings", *Cardiovascular ultrasound,* vol. 7, pp. 38-7120-7-38.

Gluzman-Poltorak, Z., Cohen, T., Herzog, Y. & Neufeld, G. 2000, "Neuropilin-2 is a receptor for the vascular endothelial growth factor (VEGF) forms VEGF-145 and VEGF-165 [corrected", *The Journal of biological chemistry,* vol. 275, no. 24, pp. 18040-18045.

Gorski, P.A., Ceholski, D.K. & Hajjar, R.J. 2015, "Altered myocardial calcium cycling and energetics in heart failure-a rational approach for disease treatment", *Cell metabolism,* vol. 21, no. 2, pp. 183-194.

Greener, I.D., Sasano, T., Wan, X., Igarashi, T., Strom, M., Rosenbaum, D.S. & Donahue, J.K. 2012, "Connexin43 gene transfer reduces ventricular tachycardia susceptibility after myocardial infarction", *Journal of the American College of Cardiology,* vol. 60, no. 12, pp. 1103-1110.

Grohn, O.H.J., Kettunen, M.I., Makela, H.I., Penttonen, M., Pitkanen, A., Lukkarinen, J.A. & Kauppinen, R.A. 2000, "Early detection of irreversible cerebral ischemia in the rat using dispersion of the magnetic resonance imaging relaxation time, T1rho", *Journal of cerebral blood flow and metabolism : official journal of the International Society of Cerebral Blood Flow and Metabolism,* vol. 20, no. 10, pp. 1457-1466.

Gupta, D., Palma, J., Molina, E., Gaughan, J.P., Long, W., Houser, S. & Macha, M. 2008, "Improved exercise capacity and reduced systemic inflammation after adenoviral-mediated SERCA-2a gene transfer", *The Journal of surgical research,* vol. 145, no. 2, pp. 257-265.

Gupta, R., Tongers, J. & Losordo, D.W. 2009, "Human studies of angiogenic gene therapy", *Circulation research,* vol. 105, no. 8, pp. 724-736.

Guyton, A.C. & Hall, J.E. 2006, *Textbook of Medical Physiology,* 11th edn, Elsevier Inc., Philadelphia, http://vet.uokufa.edu.iq/staff/falah/Textbook%20of%20Medical%20Physiology.pdf, read 30.10.2015.

Hagberg, C.E., Falkevall, A., Wang, X., Larsson, E., Huusko, J., Nilsson, I., van Meeteren, L.A., Samen, E., Lu, L., Vanwildemeersch, M., Klar, J., Genove, G., Pietras, K., Stone-Elander, S., Claesson-Welsh, L., Yla-Herttuala, S., Lindahl, P. & Eriksson, U. 2010, "Vascular endothelial growth factor B controls endothelial fatty acid uptake", *Nature,* vol. 464, no. 7290, pp. 917-921.

Hakumaki, J.M., Grohn, O.H., Tyynela, K., Valonen, P., Yla-Herttuala, S. & Kauppinen, R.A. 2002, "Early gene therapy-induced apoptotic response in BT4C gliomas by magnetic resonance relaxation contrast T1 in the rotating frame", *Cancer gene therapy,* vol. 9, no. 4, pp. 338-345.

Halonen, P.J., Nurro, J., Kuivanen, A. & Yla-Herttuala, S. 2014, "Current gene therapy trials for vascular diseases", *Expert opinion on biological therapy,* vol. 14, no. 3, pp. 327-336.

Hanahan, D. & Folkman, J. 1996, "Patterns and emerging mechanisms of the angiogenic switch during tumorigenesis", *Cell,* vol. 86, no. 3, pp. 353-364.

He, Z. & Tessier-Lavigne, M. 1997, "Neuropilin is a receptor for the axonal chemorepellent Semaphorin III", *Cell,* vol. 90, no. 4, pp. 739-751.

Hedman, M., Hartikainen, J., Syvanne, M., Stjernvall, J., Hedman, A., Kivela, A., Vanninen, E., Mussalo, H., Kauppila, E., Simula, S., Narvanen, O., Rantala, A., Peuhkurinen, K., Nieminen, M.S., Laakso, M. & Yla-Herttuala, S. 2003, "Safety and feasibility of catheter-based local intracoronary vascular endothelial growth factor gene transfer in the prevention of postangioplasty and in-stent restenosis and in the treatment of chronic myocardial ischemia: phase II results of the Kuopio Angiogenesis Trial (KAT)", *Circulation,* vol. 107, no. 21, pp. 2677-2683.

Hedman, M., Muona, K., Hedman, A., Kivela, A., Syvanne, M., Eranen, J., Rantala, A., Stjernvall, J., Nieminen, M.S., Hartikainen, J. & Yla-Herttuala, S. 2009, "Eight-year safety follow-up of coronary artery disease patients after local intracoronary VEGF gene transfer", *Gene therapy,* vol. 16, no. 5, pp. 629-634.

Heineke, J. & Molkentin, J.D. 2006, "Regulation of cardiac hypertrophy by intracellular signalling pathways", *Nature reviews, Molecular cell biology,* vol. 7, no. 8, pp. 589-600.

Henes, J. & Rosenberger, P. 2016, "Systolic heart failure: diagnosis and therapy", *Current opinion in anaesthesiology,* vol. 29, no. 1, pp. 55-60.

Hock, M.B. & Kralli, A. 2009, "Transcriptional control of mitochondrial biogenesis and function", *Annual Review of Physiology,* vol. 71, pp. 177-203.

Hoeben, A., Landuyt, B., Highley, M.S., Wildiers, H., Van Oosterom, A.T. & De Bruijn, E.A. 2004, "Vascular endothelial growth factor and angiogenesis", *Pharmacological reviews,* vol. 56, no. 4, pp. 549-580.

Honkonen, K.M., Visuri, M.T., Tervala, T.V., Halonen, P.J., Koivisto, M., Lahteenvuo, M.T., Alitalo, K.K., Yla-Herttuala, S. & Saaristo, A.M. 2013, "Lymph node transfer and perinodal lymphatic growth factor treatment for lymphedema", *Annals of Surgery,* vol. 257, no. 5, pp. 961-967.

Horgan, S., Watson, C., Glezeva, N. & Baugh, J. 2014, "Murine models of diastolic dysfunction and heart failure with preserved ejection fraction", *Journal of cardiac failure,* vol. 20, no. 12, pp. 984-995.

Houser, S.R., Margulies, K.B., Murphy, A.M., Spinale, F.G., Francis, G.S., Prabhu, S.D., Rockman, H.A., Kass, D.A., Molkentin, J.D., Sussman, M.A., Koch, W.J. & American Heart Association Council on Basic Cardiovascular Sciences, Council on Clinical Cardiology, and Council on Functional Genomics and Translational Biology 2012, "Animal models of heart failure: a scientific statement from the American Heart Association", *Circulation research,* vol. 111, no. 1, pp. 131-150.

Hubbard, S.R. 1999, "Structural analysis of receptor tyrosine kinases", *Progress in biophysics and molecular biology,* vol. 71, no. 3-4, pp. 343-358.

Hunter, J.J. & Chien, K.R. 1999, "Signaling pathways for cardiac hypertrophy and failure", *The New England journal of medicine,* vol. 341, no. 17, pp. 1276-1283.

Huusko, J., Merentie, M., Dijkstra, M.H., Ryhanen, M.M., Karvinen, H., Rissanen, T.T., Vanwildemeersch, M., Hedman, M., Lipponen, J., Heinonen, S.E., Eriksson, U., Shibuya, M. & Yla-Herttuala, S. 2010, "The effects of VEGF-R1 and VEGF-R2 ligands on angiogenic responses and left ventricular function in mice", *Cardiovascular research,* vol. 86, no. 1, pp. 122-130.

Inagaki, K., Fuess, S., Storm, T.A., Gibson, G.A., Mctiernan, C.F., Kay, M.A. & Nakai, H. 2006, "Robust systemic transduction with AAV9 vectors in mice: efficient global cardiac gene transfer superior to that of AAV8", *Molecular therapy : the journal of the American Society of Gene Therapy,* vol. 14, no. 1, pp. 45-53.

Jensen, J.A. 2007, "Medical ultrasound imaging", *Progress in biophysics and molecular biology,* vol. 93, no. 1-3, pp. 153-165.

Joukov, V., Pajusola, K., Kaipainen, A., Chilov, D., Lahtinen, I., Kukk, E., Saksela, O., Kalkkinen, N. & Alitalo, K. 1996, "A novel vascular endothelial growth factor, VEGF-C, is a ligand for the Flt4 (VEGFR-3) and KDR (VEGFR-2) receptor tyrosine kinases", *The EMBO journal,* vol. 15, no. 2, pp. 290-298.

Joukov, V., Sorsa, T., Kumar, V., Jeltsch, M., Claesson-Welsh, L., Cao, Y., Saksela, O., Kalkkinen, N. & Alitalo, K. 1997, "Proteolytic processing regulates receptor specificity and activity of VEGF-C", *The EMBO journal,* vol. 16, no. 13, pp. 3898-3911.

Karkkainen, M.J., Haiko, P., Sainio, K., Partanen, J., Taipale, J., Petrova, T.V., Jeltsch, M., Jackson, D.G., Talikka, M., Rauvala, H., Betsholtz, C. & Alitalo, K. 2004, "Vascular endothelial growth factor C is required for sprouting of the first lymphatic vessels from embryonic veins", *Nature immunology,* vol. 5, no. 1, pp. 74-80.

Karpanen, T., Bry, M., Ollila, H.M., Seppanen-Laakso, T., Liimatta, E., Leskinen, H., Kivela, R., Helkamaa, T., Merentie, M., Jeltsch, M., Paavonen, K., Andersson, L.C., Mervaala, E., Hassinen, I.E., Yla-Herttuala, S., Oresic, M. & Alitalo, K. 2008, "Overexpression of vascular endothelial growth factor-B in mouse heart alters cardiac lipid metabolism and induces myocardial hypertrophy", *Circulation research,* vol. 103, no. 9, pp. 1018-1026.

Karpanen, T., Heckman, C.A., Keskitalo, S., Jeltsch, M., Ollila, H., Neufeld, G., Tamagnone, L. & Alitalo, K. 2006a, "Functional interaction of VEGF-C and VEGF-D with neuropilin receptors", *FASEB journal : official publication of the Federation of American Societies for Experimental Biology,* vol. 20, no. 9, pp. 1462-1472.

Karpanen, T., Wirzenius, M., Makinen, T., Veikkola, T., Haisma, H.J., Achen, M.G., Stacker, S.A., Pytowski, B., Yla-Herttuala, S. & Alitalo, K. 2006b, "Lymphangiogenic growth factor responsiveness is modulated by postnatal lymphatic vessel maturation", *The American journal of pathology,* vol. 169, no. 2, pp. 708-718.

Katz, A.M. 2008, "The "modern" view of heart failure: how did we get here?", *Circulation.Heart failure,* vol. 1, no. 1, pp. 63-71.

Katz, M.G., Fargnoli, A.S., Pritchette, L.A. & Bridges, C.R. 2012, "Gene delivery technologies for cardiac applications", *Gene therapy,* vol. 19, no. 6, pp. 659-669.

Kawasaki, T., Kitsukawa, T., Bekku, Y., Matsuda, Y., Sanbo, M., Yagi, T. & Fujisawa, H. 1999, "A requirement for neuropilin-1 in embryonic vessel formation", *Development (Cambridge, England),* vol. 126, no. 21, pp. 4895-4902.

Kay, M.A., Glorioso, J.C. & Naldini, L. 2001, "Viral vectors for gene therapy: the art of turning infectious agents into vehicles of therapeutics", *Nature medicine,* vol. 7, no. 1, pp. 33-40.

Kemp, C.D. & Conte, J.V. 2012, "The pathophysiology of heart failure", *Cardiovascular pathology : the official journal of the Society for Cardiovascular Pathology,* vol. 21, no. 5, pp. 365-371.

Kendall, R.L., Wang, G. & Thomas, K.A. 1996, "Identification of a natural soluble form of the vascular endothelial growth factor receptor, FLT-1, and its heterodimerization with KDR", *Biochemical and biophysical research communications,* vol. 226, no. 2, pp. 324-328.

Kennedy, M.A. & Parks, R.J. 2009, "Adenovirus virion stability and the viral genome: size matters", *Molecular therapy : the journal of the American Society of Gene Therapy,* vol. 17, no. 10, pp. 1664-1666.

Kerkela, R. & Force, T. 2006, "Recent insights into cardiac hypertrophy and left ventricular remodeling", *Current heart failure reports,* vol. 3, no. 1, pp. 14-18.

Kerkela, R., Ulvila, J. & Magga, J. 2015, "Natriuretic Peptides in the Regulation of Cardiovascular Physiology and Metabolic Events", *Journal of the American Heart Association,* vol. 4, no. 10, pp. e002423.

Kitsiou, A.N., Srinivasan, G., Quyyumi, A.A., Summers, R.M., Bacharach, S.L. & Dilsizian, V. 1998, "Stress-induced reversible and mild-to-moderate irreversible thallium defects: are they equally accurate for predicting recovery of regional left ventricular function after revascularization?", *Circulation,* vol. 98, no. 6, pp. 501-508.

Kitsukawa, T., Shimono, A., Kawakami, A., Kondoh, H. & Fujisawa, H. 1995, "Overexpression of a membrane protein, neuropilin, in chimeric mice causes anomalies in the cardiovascular system, nervous system and limbs", *Development (Cambridge, England),* vol. 121, no. 12, pp. 4309-4318.

Kivela, R., Bry, M., Robciuc, M.R., Rasanen, M., Taavitsainen, M., Silvola, J.M., Saraste, A., Hulmi, J.J., Anisimov, A., Mayranpaa, M.I., Lindeman, J.H., Eklund, L., Hellberg, S., Hlushchuk, R., Zhuang, Z.W., Simons, M., Djonov, V., Knuuti, J., Mervaala, E. & Alitalo, K. 2014, "VEGF-B-induced vascular growth leads to metabolic reprogramming and ischemia resistance in the heart", *EMBO molecular medicine,* vol. 6, no. 3, pp. 307-321.

Knaapen, P., de Haan, S., Hoekstra, O.S., Halbmeijer, R., Appelman, Y.E., Groothuis, J.G., Comans, E.F., Meijerink, M.R., Lammertsma, A.A., Lubberink, M., Gotte, M.J. & van Rossum, A.C. 2010, "Cardiac PET-CT: advanced hybrid imaging for the detection of coronary artery disease", *Netherlands heart journal : monthly journal of the Netherlands Society of Cardiology and the Netherlands Heart Foundation,* vol. 18, no. 2, pp. 90-98.

Koch, S., Tugues, S., Li, X., Gualandi, L. & Claesson-Welsh, L. 2011, "Signal transduction by vascular endothelial growth factor receptors", *The Biochemical journal,* vol. 437, no. 2, pp. 169-183.

Koga, K., Osuga, Y., Yoshino, O., Hirota, Y., Ruimeng, X., Hirata, T., Takeda, S., Yano, T., Tsutsumi, O. & Taketani, Y. 2003, "Elevated serum soluble vascular endothelial growth factor receptor 1 (sVEGFR-1) levels in women with preeclampsia", *The Journal of clinical endocrinology and metabolism,* vol. 88, no. 5, pp. 2348-2351.

Kolodkin, A.L., Levengood, D.V., Rowe, E.G., Tai, Y.T., Giger, R.J. & Ginty, D.D. 1997, "Neuropilin is a semaphorin III receptor", *Cell,* vol. 90, no. 4, pp. 753-762.

Kolwicz, S.C.,Jr & Tian, R. 2011, "Glucose metabolism and cardiac hypertrophy", *Cardiovascular research,* vol. 90, no. 2, pp. 194-201.

Kootstra, N.A. & Verma, I.M. 2003, "Gene therapy with viral vectors", *Annual Review of Pharmacology and Toxicology,* vol. 43, pp. 413-439.

Koponen, J.K., Kankkonen, H., Kannasto, J., Wirth, T., Hillen, W., Bujard, H. & Yla-Herttuala, S. 2003, "Doxycycline-regulated lentiviral vector system with a novel reverse transactivator rtTA2S-M2 shows a tight control of gene expression in vitro and in vivo", *Gene therapy,* vol. 10, no. 6, pp. 459-466.

Korpisalo, P., Hytonen, J.P., Laitinen, J.T., Laidinen, S., Parviainen, H., Karvinen, H., Siponen, J., Marjomaki, V., Vajanto, I., Rissanen, T.T. & Yla-Herttuala, S. 2011, "Capillary enlargement, not sprouting angiogenesis, determines beneficial therapeutic effects and side effects of angiogenic gene therapy", *European heart journal,* vol. 32, no. 13, pp. 1664-1672.

Korpisalo, P. & Yla-Herttuala, S. 2010, "Stimulation of functional vessel growth by gene therapy", *Integrative biolog : quantitative biosciences from nano to macro,* vol. 2, no. 2-3, pp. 102-112.

Kramer, C.M. & Hundley, W.G. (eds) 2010, *Atlas of Cardiovascular Magnetic Resonance Imaging*, 1st edn, Saunders, Philadelphia.

Kubota, T., McTiernan, C.F., Frye, C.S., Slawson, S.E., Lemster, B.H., Koretsky, A.P., Demetris, A.J. & Feldman, A.M. 1997, "Dilated cardiomyopathy in transgenic mice with cardiac-specific overexpression of tumor necrosis factor-alpha", *Circulation research,* vol. 81, no. 4, pp. 627-635.

Kukk, E., Lymboussaki, A., Taira, S., Kaipainen, A., Jeltsch, M., Joukov, V. & Alitalo, K. 1996, "VEGF-C receptor binding and pattern of expression with VEGFR-3 suggests a role in lymphatic vascular development", *Development (Cambridge, England),* vol. 122, no. 12, pp. 3829-3837.

Kumar, V., Abbas, A.K., Fausto, N. & Aster, J.C. (eds) 2010, *Robbins and Cotran Pathologic Basis of Disease*, 8th edn, Saunders, Philadelphia.

Laakkonen, J.P. & Yla-Herttuala, S. 2015, "Recent Advancements in Cardiovascular Gene Therapy and Vascular Biology", *Human Gene Therapy,* vol. 26, no. 8, pp. 518-524.

Lahteenvuo, J.E., Lahteenvuo, M.T., Kivela, A., Rosenlew, C., Falkevall, A., Klar, J., Heikura, T., Rissanen, T.T., Vahakangas, E., Korpisalo, P., Enholm, B., Carmeliet, P., Alitalo, K., Eriksson, U. & Yla-Herttuala, S. 2009, "Vascular endothelial growth factor-B induces myocardium-specific angiogenesis and arteriogenesis via vascular endothelial growth factor receptor-1- and neuropilin receptor-1-dependent mechanisms", *Circulation,* vol. 119, no. 6, pp. 845-856..

Laitinen, M., Hartikainen, J., Hiltunen, M.O., Eranen, J., Kiviniemi, M., Narvanen, O., Makinen, K., Manninen, H., Syvanne, M., Martin, J.F., Laakso, M. & Yla-Herttuala, S. 2000, "Catheter-mediated vascular endothelial growth factor gene transfer to human coronary arteries after angioplasty", *Human Gene Therapy,* vol. 11, no. 2, pp. 263-270.

Laitinen, M., Pakkanen, T., Donetti, E., Baetta, R., Luoma, J., Lehtolainen, P., Viita, H., Agrawal, R., Miyanohara, A., Friedmann, T., Risau, W., Martin, J.F., Soma, M. & Yla-Herttuala, S. 1997, "Gene transfer into the carotid artery using an adventitial collar: comparison of the effectiveness of the plasmid-liposome complexes, retroviruses, pseudotyped retroviruses, and adenoviruses", *Human Gene Therapy,* vol. 8, no. 14, pp. 1645-1650.

Lau, D.H., Clausen, C., Sosunov, E.A., Shlapakova, I.N., Anyukhovsky, E.P., Danilo, P.,Jr, Rosen, T.S., Kelly, C., Duffy, H.S., Szabolcs, M.J., Chen, M., Robinson, R.B., Lu, J., Kumari, S., Cohen, I.S. & Rosen, M.R. 2009, "Epicardial border zone overexpression of skeletal muscle sodium channel SkM1 normalizes activation, preserves conduction, and suppresses ventricular arrhythmia: an in silico, in vivo, in vitro study", *Circulation,* vol. 119, no. 1, pp. 19-27.

Lenaerts, L., De Clercq, E. & Naesens, L. 2008, "Clinical features and treatment of adenovirus infections", *Reviews in medical virology,* vol. 18, no. 6, pp. 357-374.

Lisowski, L., Tay, S.S. & Alexander, I.E. 2015, "Adeno-associated virus serotypes for gene therapeutics", *Current opinion in pharmacology,* vol. 24, pp. 59-67.

Liu, G., Iden, J.B., Kovithavongs, K., Gulamhusein, R., Duff, H.J. & Kavanagh, K.M. 2004, "In vivo temporal and spatial distribution of depolarization and repolarization and the illusive murine T wave", *The Journal of physiology,* vol. 555, no. Pt 1, pp. 267-279.

Lohela, M., Bry, M., Tammela, T. & Alitalo, K. 2009, "VEGFs and receptors involved in angiogenesis versus lymphangiogenesis", *Current opinion in cell biology,* vol. 21, no. 2, pp. 154-165.

Louis Jeune, V., Joergensen, J.A., Hajjar, R.J. & Weber, T. 2013, "Pre-existing anti-adeno-associated virus antibodies as a challenge in AAV gene therapy", *Human gene therapy methods,* vol. 24, no. 2, pp. 59-67.

Lu, Y.L., Connelly, K.A., Dick, A.J., Wright, G.A. & Radau, P.E. 2013, "Automatic functional analysis of left ventricle in cardiac cine MRI", *Quantitative imaging in medicine and surgery,* vol. 3, no. 4, pp. 200-209.

Luttun, A., Tjwa, M., Moons, L., Wu, Y., Angelillo-Scherrer, A., Liao, F., Nagy, J.A., Hooper, A., Priller, J., De Klerck, B., Compernolle, V., Daci, E., Bohlen, P., Dewerchin, M., Herbert, J.M., Fava, R., Matthys, P., Carmeliet, G., Collen, D., Dvorak, H.F., Hicklin, D.J. & Carmeliet, P. 2002, "Revascularization of ischemic tissues by PlGF treatment, and inhibition of tumor angiogenesis, arthritis and atherosclerosis by anti-Flt1", *Nature medicine,* vol. 8, no. 8, pp. 831-840.

Lyon, A.R., Sato, M., Hajjar, R.J., Samulski, R.J. & Harding, S.E. 2008, "Gene therapy: targeting the myocardium", *Heart (British Cardiac Society),* vol. 94, no. 1, pp. 89-99.

Macdonald, P.S. 2015, "Combined angiotensin receptor/neprilysin inhibitors: a review of the new paradigm in the management of chronic heart failure", *Clinical therapeutics,* vol. 37, no. 10, pp. 2199-2205.

Maglione, D., Guerriero, V., Viglietto, G., Delli-Bovi, P. & Persico, M.G. 1991, "Isolation of a human placenta cDNA coding for a protein related to the vascular permeability factor", *Proceedings of the National Academy of Sciences of the United States of America,* vol. 88, no. 20, pp. 9267-9271.

Maharaj, A.S., Saint-Geniez, M., Maldonado, A.E. & D'Amore, P.A. 2006, "Vascular endothelial growth factor localization in the adult", *The American journal of pathology,* vol. 168, no. 2, pp. 639-648.

Maillet, M., van Berlo, J.H. & Molkentin, J.D. 2013, "Molecular basis of physiological heart growth: fundamental concepts and new players", *Nature reviews.Molecular cell biology,* vol. 14, no. 1, pp. 38-48.

Maisel, A.S., Shah, K.S., Barnard, D., Jaski, B., Frivold, G., Marais, J., Azer, M., Miyamoto, M.I., Lombardo, D., Kelsay, D., Iqbal, N., Taub, P.R., Kupfer, K., Lee, E., Clopton, P., Zile, M. & Greenberg, B. 2015, "How B-Type Natriuretic Peptide (BNP) and Body Weight Changes Vary in Heart Failure With Preserved Ejection Fraction Compared With Reduced Ejection Fraction: Secondary Results of the HABIT (HF Assessment With BNP in the Home) Trial", *Journal of cardiac failure,* .

Makinen, K., Manninen, H., Hedman, M., Matsi, P., Mussalo, H., Alhava, E. & Yla-Herttuala, S. 2002, "Increased vascularity detected by digital subtraction angiography after VEGF gene transfer to human lower limb artery: a randomized, placebo-controlled, double-blinded phase II study", *Molecular therapy : the journal of the American Society of Gene Therapy,* vol. 6, no. 1, pp. 127-133.

Makinen, T., Olofsson, B., Karpanen, T., Hellman, U., Soker, S., Klagsbrun, M., Eriksson, U. & Alitalo, K. 1999, "Differential binding of vascular endothelial growth factor B splice and

proteolytic isoforms to neuropilin-1", *The Journal of biological chemistry,* vol. 274, no. 30, pp. 21217-21222.

Mancia, G., Fagard, R., Narkiewicz, K., Redon, J., Zanchetti, A., Bohm, M., Christiaens, T., Cifkova, R., De Backer, G., Dominiczak, A., Galderisi, M., Grobbee, D.E., Jaarsma, T., Kirchhof, P., Kjeldsen, S.E., Laurent, S., Manolis, A.J., Nilsson, P.M., Ruilope, L.M., Schmieder, R.E., Sirnes, P.A., Sleight, P., Viigimaa, M., Waeber, B., Zannad, F. & Task Force for the Management of Arterial Hypertension of the European Society of Hypertension and the European Society of Cardiology 2014, "2013 ESH/ESC Practice Guidelines for the Management of Arterial Hypertension", *Blood pressure,* vol. 23, no. 1, pp. 3-16.

Markkanen, J.E., Rissanen, T.T., Kivela, A. & Yla-Herttuala, S. 2005, "Growth factor-induced therapeutic angiogenesis and arteriogenesis in the heart--gene therapy", *Cardiovascular research,* vol. 65, no. 3, pp. 656-664.

Masuda, K., Funayama, S., Komiyama, K., Umezawa, I. & Ito, K. 1987, "Antitumor acidic polysaccharide NRP-1 isolated from starfish; Asterias amurensis Lutken", *The Kitasato archives of experimental medicine,* vol. 60, no. 3, pp. 95-103.

Matthews, W., Jordan, C.T., Gavin, M., Jenkins, N.A., Copeland, N.G. & Lemischka, I.R. 1991, "A receptor tyrosine kinase cDNA isolated from a population of enriched primitive hematopoietic cells and exhibiting close genetic linkage to c-kit", *Proceedings of the National Academy of Sciences of the United States of America,* vol. 88, no. 20, pp. 9026-9030.

McMurray, J.J., Adamopoulos, S., Anker, S.D., Auricchio, A., Bohm, M., Dickstein, K., Falk, V., Filippatos, G., Fonseca, C., Gomez-Sanchez, M.A., Jaarsma, T., Kober, L., Lip, G.Y., Maggioni, A.P., Parkhomenko, A., Pieske, B.M., Popescu, B.A., Ronnevik, P.K., Rutten, F.H., Schwitter, J., Seferovic, P., Stepinska, J., Trindade, P.T., Voors, A.A., Zannad, F., Zeiher, A., Task Force for the Diagnosis and Treatment of Acute and Chronic Heart Failure 2012 of the European Society of Cardiology, Bax, J.J., Baumgartner, H., Ceconi, C., Dean, V., Deaton, C., Fagard, R., Funck-Brentano, C., Hasdai, D., Hoes, A., Kirchhof, P., Knuuti, J., Kolh, P., McDonagh, T., Moulin, C., Popescu, B.A., Reiner, Z., Sechtem, U., Sirnes, P.A., Tendera, M., Torbicki, A., Vahanian, A., Windecker, S., McDonagh, T., Sechtem, U., Bonet, L.A., Avraamides, P., Ben Lamin, H.A., Brignole, M., Coca, A., Cowburn, P., Dargie, H., Elliott, P., Flachskampf, F.A., Guida, G.F., Hardman, S., Iung, B., Merkely, B., Mueller, C., Nanas, J.N., Nielsen, O.W., Orn, S., Parissis, J.T., Ponikowski, P. & ESC Committee for Practice Guidelines 2012, "ESC guidelines for the diagnosis and treatment of acute and chronic heart failure 2012: The Task Force for the Diagnosis and Treatment of Acute and Chronic Heart Failure 2012 of the European Society of Cardiology. Developed in collaboration with the Heart Failure Association (HFA) of the ESC", *European journal of heart failure,* vol. 14, no. 8, pp. 803-869.

McMurray, J.J., Packer, M., Desai, A.S., Gong, J., Lefkowitz, M.P., Rizkala, A.R., Rouleau, J.L., Shi, V.C., Solomon, S.D., Swedberg, K., Zile, M.R. & PARADIGM-HF Investigators and Committees 2014, "Angiotensin-neprilysin inhibition versus enalapril in heart failure", *The New England journal of medicine,* vol. 371, no. 11, pp. 993-1004.

Mehlem, A., Palombo, I., Wang, X., Hagberg, C.E., Eriksson, U. & Falkevall, A. 2016, "PGC-1alpha coordinates mitochondrial respiratory capacity and muscular fatty acid uptake via regulation of VEGF-B", *Diabetes,* .

Melenovsky, V., Hwang, S.J., Redfield, M.M., Zakeri, R., Lin, G. & Borlaug, B.A. 2015, "Left atrial remodeling and function in advanced heart failure with preserved or reduced ejection fraction", *Circulation.Heart failure,* vol. 8, no. 2, pp. 295-303.

Metcalfe, B.L., Huentelman, M.J., Parilak, L.D., Taylor, D.G., Katovich, M.J., Knot, H.J., Sumners, C. & Raizada, M.K. 2004, "Prevention of cardiac hypertrophy by angiotensin II type-2 receptor gene transfer", *Hypertension,* vol. 43, no. 6, pp. 1233-1238.

Migdal, M., Huppertz, B., Tessler, S., Comforti, A., Shibuya, M., Reich, R., Baumann, H. & Neufeld, G. 1998, "Neuropilin-1 is a placenta growth factor-2 receptor", *The Journal of biological chemistry,* vol. 273, no. 35, pp. 22272-22278.

Mjos, O.D. 1971, "Effect of free fatty acids on myocardial function and oxygen consumption in intact dogs", *The Journal of clinical investigation,* vol. 50, no. 7, pp. 1386-1389.

Muona, K., Makinen, K., Hedman, M., Manninen, H. & Yla-Herttuala, S. 2012, "10-year safety follow-up in patients with local VEGF gene transfer to ischemic lower limb", *Gene therapy,* vol. 19, no. 4, pp. 392-395.

Musthafa, H.S., Dragneva, G., Lottonen, L., Merentie, M., Petrov, L., Heikura, T., Yla-Herttuala, E., Yla-Herttuala, S., Grohn, O. & Liimatainen, T. 2013, "Longitudinal rotating frame relaxation time measurements in infarcted mouse myocardium in vivo", *Magnetic resonance in medicine,* vol. 69, no. 5, pp. 1389-1395.

Nekolla, S.G., Reder, S., Saraste, A., Higuchi, T., Dzewas, G., Preissel, A., Huisman, M., Poethko, T., Schuster, T., Yu, M., Robinson, S., Casebier, D., Henke, J., Wester, H.J. & Schwaiger, M. 2009, "Evaluation of the novel myocardial perfusion positron-emission tomography tracer 18F-BMS-747158-02: comparison to 13N-ammonia and validation with microspheres in a pig model", *Circulation,* vol. 119, no. 17, pp. 2333-2342.

Neufeld, G., Cohen, T., Gengrinovitch, S. & Poltorak, Z. 1999, "Vascular endothelial growth factor (VEGF) and its receptors", *FASEB journal : official publication of the Federation of American Societies for Experimental Biology,* vol. 13, no. 1, pp. 9-22.

Nichols, M., Townsend, N., Luengo-Fernandez, R., Leal, J., Gray, A., Scarborough, P., Rayner, M. 2012, "European Cardiovascular Disease Statistics 2012", European Heart Network, Brussels, European Society of Cardiology, Sophia Antipolis.

Nichols, M., Townsend, N., Scarborough, P. & Rayner, M. 2014, "Cardiovascular disease in Europe 2014: epidemiological update", *European heart journal,* vol. 35, no. 42, pp. 2950-2959.

Nishida, K. & Otsu, K. 2015, "Autophagy during cardiac remodeling", *Journal of Molecular and Cellular Cardiology.*

Niwano, K., Arai, M., Koitabashi, N., Watanabe, A., Ikeda, Y., Miyoshi, H. & Kurabayashi, M. 2008a, "Lentiviral vector-mediated SERCA2 gene transfer protects against heart failure and left ventricular remodeling after myocardial infarction in rats", *Molecular therapy : the journal of the American Society of Gene Therapy,* vol. 16, no. 6, pp. 1026-1032.

Olofsson, B., Korpelainen, E., Pepper, M.S., Mandriota, S.J., Aase, K., Kumar, V., Gunji, Y., Jeltsch, M.M., Shibuya, M., Alitalo, K. & Eriksson, U. 1998, "Vascular endothelial growth factor B (VEGF-B) binds to VEGF receptor-1 and regulates plasminogen activator activity in endothelial

cells", *Proceedings of the National Academy of Sciences of the United States of America,* vol. 95, no. 20, pp. 11709-11714.

Olofsson, B., Pajusola, K., Kaipainen, A., von Euler, G., Joukov, V., Saksela, O., Orpana, A., Pettersson, R.F., Alitalo, K. & Eriksson, U. 1996a, "Vascular endothelial growth factor B, a novel growth factor for endothelial cells", *Proceedings of the National Academy of Sciences of the United States of America,* vol. 93, no. 6, pp. 2576-2581.

Olofsson, B., Pajusola, K., von Euler, G., Chilov, D., Alitalo, K. & Eriksson, U. 1996b, "Genomic organization of the mouse and human genes for vascular endothelial growth factor B (VEGF-B) and characterization of a second splice isoform", *The Journal of biological chemistry,* vol. 271, no. 32, pp. 19310-19317.

Patten, R.D. & Hall-Porter, M.R. 2009, "Small animal models of heart failure: development of novel therapies, past and present", *Circulation.Heart failure,* vol. 2, no. 2, pp. 138-144.

Paulus, W.J., Tschope, C., Sanderson, J.E., Rusconi, C., Flachskampf, F.A., Rademakers, F.E., Marino, P., Smiseth, O.A., De Keulenaer, G., Leite-Moreira, A.F., Borbely, A., Edes, I., Handoko, M.L., Heymans, S., Pezzali, N., Pieske, B., Dickstein, K., Fraser, A.G. & Brutsaert, D.L. 2007, "How to diagnose diastolic heart failure: a consensus statement on the diagnosis of heart failure with normal left ventricular ejection fraction by the Heart Failure and Echocardiography Associations of the European Society of Cardiology", *European heart journal,* vol. 28, no. 20, pp. 2539-2550.

Penn, M.S., Mendelsohn, F.O., Schaer, G.L., Sherman, W., Farr, M., Pastore, J., Rouy, D., Clemens, R., Aras, R. & Losordo, D.W. 2013, "An open-label dose escalation study to evaluate the safety of administration of nonviral stromal cell-derived factor-1 plasmid to treat symptomatic ischemic heart failure", *Circulation research,* vol. 112, no. 5, pp. 816-825.

Pepe, M., Mamdani, M., Zentilin, L., Csiszar, A., Qanud, K., Zacchigna, S., Ungvari, Z., Puligadda, U., Moimas, S., Xu, X., Edwards, J.G., Hintze, T.H., Giacca, M. & Recchia, F.A. 2010, "Intramyocardial VEGF-B167 gene delivery delays the progression towards congestive failure in dogs with pacing-induced dilated cardiomyopathy", *Circulation research,* vol. 106, no. 12, pp. 1893-1903.

Piccolo, R., Giustino, G., Mehran, R. & Windecker, S. 2015, "Stable coronary artery disease: revascularisation and invasive strategies", *Lancet (London, England),* vol. 386, no. 9994, pp. 702-713.

Pochon, S., Tardy, I., Bussat, P., Bettinger, T., Brochot, J., von Wronski, M., Passantino, L. & Schneider, M. 2010, "BR55: a lipopeptide-based VEGFR2-targeted ultrasound contrast agent for molecular imaging of angiogenesis", *Investigative radiology,* vol. 45, no. 2, pp. 89-95.

Porter, T.R. & Xie, F. 2015, "Contrast echocardiography: latest developments and clinical utility", *Current cardiology reports,* vol. 17, no. 3, pp. 569-015-0569-9.

Rajappan, K., Bellenger, N.G., Anderson, L. & Pennell, D.J. 2000, "The role of cardiovascular magnetic resonance in heart failure", *European journal of heart failure,* vol. 2, no. 3, pp. 241-252.

Ram, R., Mickelsen, D.M., Theodoropoulos, C. & Blaxall, B.C. 2011, "New approaches in small animal echocardiography: imaging the sounds of silence", *American journal of physiology.Heart and circulatory physiology,* vol. 301, no. 5, pp. H1765-80.

Rapti, K., Louis-Jeune, V., Kohlbrenner, E., Ishikawa, K., Ladage, D., Zolotukhin, S., Hajjar, R.J. & Weber, T. 2012, "Neutralizing antibodies against AAV serotypes 1, 2, 6, and 9 in sera of commonly used animal models", *Molecular therapy : the journal of the American Society of Gene Therapy,* vol. 20, no. 1, pp. 73-83.

Ribatti, D. 2005, "The crucial role of vascular permeability factor/vascular endothelial growth factor in angiogenesis: a historical review", *British journal of haematology,* vol. 128, no. 3, pp. 303-309.

Rincon, M.Y., VandenDriessche, T. & Chuah, M.K. 2015, "Gene therapy for cardiovascular disease: advances in vector development, targeting, and delivery for clinical translation", *Cardiovascular research,* vol. 108, no. 1, pp. 4-20.

Rissanen, T.T. & Yla-Herttuala, S. 2007, "Current status of cardiovascular gene therapy", *Molecular therapy : the journal of the American Society of Gene Therapy,* vol. 15, no. 7, pp. 1233-1247.

Roberts, R. 2014, "Genetics of coronary artery disease", *Circulation research,* vol. 114, no. 12, pp. 1890-1903.

Rochitte, C.E., George, R.T., Chen, M.Y., Arbab-Zadeh, A., Dewey, M., Miller, J.M., Niinuma, H., Yoshioka, K., Kitagawa, K., Nakamori, S., Laham, R., Vavere, A.L., Cerci, R.J., Mehra, V.C., Nomura, C., Kofoed, K.F., Jinzaki, M., Kuribayashi, S., de Roos, A., Laule, M., Tan, S.Y., Hoe, J., Paul, N., Rybicki, F.J., Brinker, J.A., Arai, A.E., Cox, C., Clouse, M.E., Di Carli, M.F. & Lima, J.A. 2014, "Computed tomography angiography and perfusion to assess coronary artery stenosis causing perfusion defects by single photon emission computed tomography: the CORE320 study", *European heart journal,* vol. 35, no. 17, pp. 1120-1130.

Rohr, U.P., Wulf, M.A., Stahn, S., Steidl, U., Haas, R. & Kronenwett, R. 2002, "Fast and reliable titration of recombinant adeno-associated virus type-2 using quantitative real-time PCR", *Journal of virological methods,* vol. 106, no. 1, pp. 81-88.

Sabbah, M., Alsaid, H., Fakri-Bouchet, L., Pasquier, C., Briguet, A., Canet-Soulas, E. & Fokapu, O. 2007, "Real-time gating system for mouse cardiovascular MR imaging", *Magnetic resonance in medicine,* vol. 57, no. 1, pp. 29-39.

Sarikaya, I. 2015, "Cardiac applications of PET", *Nuclear medicine communications,* vol. 36, no. 10, pp. 971-985.

Sasano, T., McDonald, A.D., Kikuchi, K. & Donahue, J.K. 2006, "Molecular ablation of ventricular tachycardia after myocardial infarction", *Nature medicine,* vol. 12, no. 11, pp. 1256-1258.

Schaper, W. & Scholz, D. 2003, "Factors regulating arteriogenesis", *Arteriosclerosis, Thrombosis, and Vascular Biology,* vol. 23, no. 7, pp. 1143-1151.

Schindler, T.H., Schelbert, H.R., Quercioli, A. & Dilsizian, V. 2010, "Cardiac PET imaging for the detection and monitoring of coronary artery disease and microvascular health", *JACC.Cardiovascular imaging,* vol. 3, no. 6, pp. 623-640.

Scott, L.J. 2015, "Alipogene tiparvovec: a review of its use in adults with familial lipoprotein lipase deficiency", *Drugs,* vol. 75, no. 2, pp. 175-182.

Selvetella, G., Hirsch, E., Notte, A., Tarone, G. & Lembo, G. 2004, "Adaptive and maladaptive hypertrophic pathways: points of convergence and divergence", *Cardiovascular research,* vol. 63, no. 3, pp. 373-380.

Shalaby, F., Rossant, J., Yamaguchi, T.P., Gertsenstein, M., Wu, X.F., Breitman, M.L. & Schuh, A.C. 1995, "Failure of blood-island formation and vasculogenesis in Flk-1-deficient mice", *Nature,* vol. 376, no. 6535, pp. 62-66.

Sherif, H.M., Saraste, A., Weidl, E., Weber, A.W., Higuchi, T., Reder, S., Poethko, T., Henriksen, G., Casebier, D., Robinson, S., Wester, H.J., Nekolla, S.G. & Schwaiger, M. 2009, "Evaluation of a novel (18)F-labeled positron-emission tomography perfusion tracer for the assessment of myocardial infarct size in rats", *Circulation.Cardiovascular imaging,* vol. 2, no. 2, pp. 77-84.

Shibuya, M. 2001, "Structure and dual function of vascular endothelial growth factor receptor-1 (Flt-1)", *The international journal of biochemistry & cell biology,* vol. 33, no. 4, pp. 409-420.

Shibuya, M. & Claesson-Welsh, L. 2006, "Signal transduction by VEGF receptors in regulation of angiogenesis and lymphangiogenesis", *Experimental cell research,* vol. 312, no. 5, pp. 549-560.

Shibuya, M., Matsushime, H., Yamane, A., Ikeda, T., Yoshida, M.C. & Tojo, A. 1989, "Isolation and characterization of new mammalian kinase genes by cross hybridization with a tyrosine kinase probe", *Princess Takamatsu symposia,* vol. 20, pp. 103-110.

Soker, S., Takashima, S., Miao, H.Q., Neufeld, G. & Klagsbrun, M. 1998, "Neuropilin-1 is expressed by endothelial and tumor cells as an isoform-specific receptor for vascular endothelial growth factor", *Cell,* vol. 92, no. 6, pp. 735-745.

Springer, M.L., Sievers, R.E., Viswanathan, M.N., Yee, M.S., Foster, E., Grossman, W. & Yeghiazarians, Y. 2005, "Closed-chest cell injections into mouse myocardium guided by high-resolution echocardiography", *American journal of physiology.Heart and circulatory physiology,* vol. 289, no. 3, pp. H1307-14.

Stanley, W.C. & Chandler, M.P. 2002, "Energy metabolism in the normal and failing heart: potential for therapeutic interventions", *Heart failure reviews,* vol. 7, no. 2, pp. 115-130.

Stanley, W.C., Recchia, F.A. & Lopaschuk, G.D. 2005, "Myocardial substrate metabolism in the normal and failing heart", *Physiological Reviews,* vol. 85, no. 3, pp. 1093-1129.

Stuckey, D.J., Carr, C.A., Tyler, D.J. & Clarke, K. 2008, "Cine-MRI versus two-dimensional echocardiography to measure in vivo left ventricular function in rat heart", *NMR in biomedicine,* vol. 21, no. 7, pp. 765-772.

Sylven, C., Sarkar, N., Insulander, P., Kenneback, G., Blomberg, P., Islam, K. & Drvota, V. 2002, "Catheter-based transendocardial myocardial gene transfer", *Journal of interventional cardiology,* vol. 15, no. 1, pp. 7-13.

Tamayo, T., Rosenbauer, J., Wild, S.H., Spijkerman, A.M., Baan, C., Forouhi, N.G., Herder, C. & Rathmann, W. 2014, "Diabetes in Europe: an update", *Diabetes research and clinical practice,* vol. 103, no. 2, pp. 206-217.

Tammela, T., Zarkada, G., Wallgard, E., Murtomaki, A., Suchting, S., Wirzenius, M., Waltari, M., Hellstrom, M., Schomber, T., Peltonen, R., Freitas, C., Duarte, A., Isoniemi, H., Laakkonen, P., Christofori, G., Yla-Herttuala, S., Shibuya, M., Pytowski, B., Eichmann, A., Betsholtz, C. & Alitalo, K. 2008, "Blocking VEGFR-3 suppresses angiogenic sprouting and vascular network formation", *Nature,* vol. 454, no. 7204, pp. 656-660.

Tavi, P., Laine, M., Weckstrom, M. & Ruskoaho, H. 2001, "Cardiac mechanotransduction: from sensing to disease and treatment", *Trends in pharmacological sciences,* vol. 22, no. 5, pp. 254-260.

Thaler, M.S. 2010, *The Only EKG Book You´ll Ever Need,* 6th edn, Lippincott Williams & Wilkins, Philadelphia.

Thomas, C.E., Ehrhardt, A. & Kay, M.A. 2003, "Progress and problems with the use of viral vectors for gene therapy", *Nature reviews.Genetics,* vol. 4, no. 5, pp. 346-358.

Toivonen, R., Koskenvuo, J., Merentie, M., Soderstrom, M., Yla-Herttuala, S. & Savontaus, M. 2012, "Intracardiac injection of a capsid-modified Ad5/35 results in decreased heart toxicity when compared to standard Ad5", *Virology journal,* vol. 9, pp. 296-422X-9-296.

Triposkiadis, F., Karayannis, G., Giamouzis, G., Skoularigis, J., Louridas, G. & Butler, J. 2009, "The sympathetic nervous system in heart failure physiology, pathophysiology, and clinical implications", *Journal of the American College of Cardiology,* vol. 54, no. 19, pp. 1747-1762.

Unger, E., Porter, T., Lindner, J. & Grayburn, P. 2014, "Cardiovascular drug delivery with ultrasound and microbubbles", *Advanced Drug Delivery Reviews,* vol. 72, pp. 110-126.

van Ewijk, P.A., Schrauwen-Hinderling, V.B., Bekkers, S.C., Glatz, J.F., Wildberger, J.E. & Kooi, M.E. 2015, "MRS: a noninvasive window into cardiac metabolism", *NMR in biomedicine,* vol. 28, no. 7, pp. 747-766.

van Heerebeek, L., Borbely, A., Niessen, H.W., Bronzwaer, J.G., van der Velden, J., Stienen, G.J., Linke, W.A., Laarman, G.J. & Paulus, W.J. 2006, "Myocardial structure and function differ in systolic and diastolic heart failure", *Circulation,* vol. 113, no. 16, pp. 1966-1973.

Vassalli, G., Bueler, H., Dudler, J., von Segesser, L.K. & Kappenberger, L. 2003, "Adeno-associated virus (AAV) vectors achieve prolonged transgene expression in mouse myocardium and arteries in vivo: a comparative study with adenovirus vectors", *International journal of cardiology,* vol. 90, no. 2-3, pp. 229-238.

Waltenberger, J., Claesson-Welsh, L., Siegbahn, A., Shibuya, M. & Heldin, C.H. 1994, "Different signal transduction properties of KDR and Flt1, two receptors for vascular endothelial growth factor", *The Journal of biological chemistry,* vol. 269, no. 43, pp. 26988-26995.

Wang, C., Zheng, J., Sun, J., Wang, Y., Xia, R., Yin, Q., Chen, W., Xu, Z., Liao, J., Zhang, B. & Gao, F. 2015, "Endogenous contrast T1rho cardiac magnetic resonance for myocardial fibrosis in hypertrophic cardiomyopathy patients", *Journal of cardiology,* vol. 66, no. 6, pp. 520-526.

Wang, Y.X., Yuan, J., Chu, E.S., Go, M.Y., Huang, H., Ahuja, A.T., Sung, J.J. & Yu, J. 2011, "T1rho MR imaging is sensitive to evaluate liver fibrosis: an experimental study in a rat biliary duct ligation model", *Radiology,* vol. 259, no. 3, pp. 712-719.

Wild, J.R., Staton, C.A., Chapple, K. & Corfe, B.M. 2012, "Neuropilins: expression and roles in the epithelium", *International journal of experimental pathology,* vol. 93, no. 2, pp. 81-103.

Witschey, W.R., Zsido, G.A., Koomalsingh, K., Kondo, N., Minakawa, M., Shuto, T., McGarvey, J.R., Levack, M.M., Contijoch, F., Pilla, J.J., Gorman, J.H.,3rd & Gorman, R.C. 2012, "In vivo chronic myocardial infarction characterization by spin locked cardiovascular magnetic resonance", *Journal of cardiovascular magnetic resonance : official journal of the Society for Cardiovascular Magnetic Resonance,* vol. 14, pp. 37-429X-14-37.

Wolfram, J.A. & Donahue, J.K. 2013, "Gene therapy to treat cardiovascular disease", *Journal of the American Heart Association,* vol. 2, no. 4, pp. e000119.

Xu, Y., Yuan, L., Mak, J., Pardanaud, L., Caunt, M., Kasman, I., Larrivee, B., Del Toro, R., Suchting, S., Medvinsky, A., Silva, J., Yang, J., Thomas, J.L., Koch, A.W., Alitalo, K., Eichmann, A. & Bagri, A. 2010, "Neuropilin-2 mediates VEGF-C-induced lymphatic sprouting together with VEGFR3", *The Journal of cell biology,* vol. 188, no. 1, pp. 115-130.

Yadav, L., Puri, N., Rastogi, V., Satpute, P. & Sharma, V. 2015, "Tumour Angiogenesis and Angiogenic Inhibitors: A Review", *Journal of clinical and diagnostic research : JCDR,* vol. 9, no. 6, pp. XE01-XE05.

Yamada, Y., Nezu, J., Shimane, M. & Hirata, Y. 1997, "Molecular cloning of a novel vascular endothelial growth factor, VEGF-D", *Genomics,* vol. 42, no. 3, pp. 483-488.

Yamazaki, Y. & Morita, T. 2006, "Molecular and functional diversity of vascular endothelial growth factors", *Molecular diversity,* vol. 10, no. 4, pp. 515-527.

Yang, W., Ahn, H., Hinrichs, M., Torry, R.J. & Torry, D.S. 2003, "Evidence of a novel isoform of placenta growth factor (PlGF-4) expressed in human trophoblast and endothelial cells", *Journal of reproductive immunology,* vol. 60, no. 1, pp. 53-60.

Yao, R., Lecomte, R. & Crawford, E.S. 2012, "Small-animal PET: what is it, and why do we need it?", *Journal of nuclear medicine technology,* vol. 40, no. 3, pp. 157-165.

Yla-Herttuala, S. 2015, "Gene Therapy for Heart Failure: Back to the Bench", *Molecular therapy : the journal of the American Society of Gene Therapy,* vol. 23, no. 10, pp. 1551-1552.

Yla-Herttuala, S. 2013, "Cardiovascular gene therapy with vascular endothelial growth factors", *Gene,* vol. 525, no. 2, pp. 217-219.

Yla-Herttuala, S. & Alitalo, K. 2003, "Gene transfer as a tool to induce therapeutic vascular growth", *Nature medicine,* vol. 9, no. 6, pp. 694-701.

Yla-Herttuala, S., Rissanen, T.T., Vajanto, I. & Hartikainen, J. 2007, "Vascular endothelial growth factors: biology and current status of clinical applications in cardiovascular medicine", *Journal of the American College of Cardiology,* vol. 49, no. 10, pp. 1015-1026.

Yuan, L., Moyon, D., Pardanaud, L., Breant, C., Karkkainen, M.J., Alitalo, K. & Eichmann, A. 2002, "Abnormal lymphatic vessel development in neuropilin 2 mutant mice", *Development (Cambridge, England),* vol. 129, no. 20, pp. 4797-4806.

Yusuf, S., Hawken, S., Ounpuu, S., Dans, T., Avezum, A., Lanas, F., McQueen, M., Budaj, A., Pais, P., Varigos, J., Lisheng, L. & INTERHEART Study Investigators 2004, "Effect of potentially modifiable risk factors associated with myocardial infarction in 52 countries (the INTERHEART study): case-control study", *Lancet (London, England),* vol. 364, no. 9438, pp. 937-952.

Zacchigna, S., Zentilin, L. & Giacca, M. 2014, "Adeno-associated virus vectors as therapeutic and investigational tools in the cardiovascular system", *Circulation research,* vol. 114, no. 11, pp. 1827-1846.

Zarkada, G., Heinolainen, K., Makinen, T., Kubota, Y. & Alitalo, K. 2015, "VEGFR3 does not sustain retinal angiogenesis without VEGFR2", *Proceedings of the National Academy of Sciences of the United States of America,* vol. 112, no. 3, pp. 761-766.

Zhang, T., Maier, L.S., Dalton, N.D., Miyamoto, S., Ross, J.,Jr, Bers, D.M. & Brown, J.H. 2003, "The deltaC isoform of CaMKII is activated in cardiac hypertrophy and induces dilated cardiomyopathy and heart failure", *Circulation research,* vol. 92, no. 8, pp. 912-919.

Zhao, J., Pettigrew, G.J., Thomas, J., Vandenberg, J.I., Delriviere, L., Bolton, E.M., Carmichael, A., Martin, J.L., Marber, M.S. & Lever, A.M. 2002, "Lentiviral vectors for delivery of genes into neonatal and adult ventricular cardiac myocytes in vitro and in vivo", *Basic research in cardiology,* vol. 97, no. 5, pp. 348-358.

Zincarelli, C., Soltys, S., Rengo, G. & Rabinowitz, J.E. 2008, "Analysis of AAV serotypes 1-9 mediated gene expression and tropism in mice after systemic injection", *Molecular therapy : the journal of the American Society of Gene Therapy,* vol. 16, no. 6, pp. 1073-1080.

Zolotukhin, S., Byrne, B.J., Mason, E., Zolotukhin, I., Potter, M., Chesnut, K., Summerford, C., Samulski, R.J. & Muzyczka, N. 1999, "Recombinant adeno-associated virus purification using novel methods improves infectious titer and yield", *Gene therapy,* vol. 6, no. 6, pp. 973-985.

Zoni-Berisso, M., Lercari, F., Carazza, T. & Domenicucci, S. 2014, "Epidemiology of atrial fibrillation: European perspective", *Clinical epidemiology,* vol. 6, pp. 213-220.

APPENDIX:

ORIGINAL PUBLICATIONS AND A MANUSCRIPT (I-III)

I

AAV9-mediated VEGF-B gene transfer improves systolic function in progressive left ventricular hypertrophy

Huusko J, **Lottonen L**, Merentie M, Gurzeler E, Anisimov A, Miyanohara A, Alitalo K, Tavi P, Ylä-Herttuala S.

Molecular Therapy 20(12):2212-2221, 2012.

AAV9-mediated VEGF-B Gene Transfer Improves Systolic Function in Progressive Left Ventricular Hypertrophy

Jenni Huusko[1], Line Lottonen[1], Mari Merentie[1], Erika Gurzeler[1], Andrey Anisimov[2], Atsushi Miyanohara[3], Kari Alitalo[2], Pasi Tavi[1] and Seppo Ylä-Herttuala[1]

[1]*Department of Biotechnology and Molecular Medicine, A. I. Virtanen Institute for Molecular Sciences, Faculty of Health Sciences, University of Eastern Finland, Kuopio, Finland;* [2]*Molecular Cancer Biology Laboratory, Biomedicum, University of Helsinki, Helsinki, Finland;* [3]*Gene Therapy program, Center for Molecular Genetics, University of California San Diego, San Diego, California, USA*

Mechanisms of the transition from compensatory hypertrophy to heart failure are poorly understood and the roles of vascular endothelial growth factors (VEGFs) in this process have not been fully clarified. We determined the expression profile of VEGFs and relevant receptors during the progression of left ventricular hypertrophy (LVH). C57BL mice were exposed to transversal aortic constriction (TAC) and the outcome was studied at different time points (1 day, 2, 4, and 10 weeks). A clear compensatory phase (2 weeks after TAC) was seen with following heart failure (4 weeks after TAC). Interestingly, VEGF-C and VEGF-D as well as VEGF receptor-3 (VEGFR-3) were upregulated in the compensatory hypertrophy and VEGF-B was downregulated in the heart failure. After treatment with adeno-associated virus serotype 9 (AAV9)-VEGF-B_{186} gene therapy in the compensatory phase for 4 weeks the function of the heart was preserved due to angiogenesis, inhibition of apoptosis, and promotion of cardiomyocyte proliferation. Also, the genetic programming towards fetal gene expression, a known phenomenon in heart failure, was partly reversed in AAV9-VEGF-B_{186}–treated mice. We conclude that VEGF-C and VEGF-D are associated with the compensatory LVH and that AAV9-VEGF-B_{186} gene transfer can rescue the function of the failing heart and postpone the transition towards heart failure.

Received 23 March 2012; accepted 26 June 2012; advance online publication 23 October 2012. doi:10.1038/mt.2012.145

INTRODUCTION

Left ventricular hypertrophy (LVH) is a major maladaptive response to chronic pressure overload and an important risk factor for hypertensive patients.[1] It is an early step towards heart failure and increases the risk of subsequent cardiac morbidity and mortality.[2] Initially, LVH is a response to a sustained increased work load where heart mass is increased to maintain circulatory function. Thus, LVH takes place in the early phase of cardiac stress and is accompanied by cardiac remodeling.[3] Compensatory LVH is associated with a thickening of the myocardial wall and maintenance of contractility. When the pathological stress is prolonged, compensatory LVH is accompanied by interstitial fibrosis, contractile dysfunction, altered gene expression, changes in metabolism, and abnormalities in electrophysiology.[2,4] This phase is followed by decompensated hypertrophy that is more prominently associated with a significant increase in the risk for sudden cardiac death or progression to heart failure in humans.[5,6] Although the shift from the compensatory LVH to the pathological LVH is strongly associated with a disruption in the coordination between angiogenesis and cardiomyocyte growth,[7–9] there is very little data available about the expression and role of vascular endothelial growth factors (VEGFs) in different phases of LVH.

VEGFs are among the most powerful regulators of vascular growth.[10] The genes, VEGF-A, -B, -C, -D, -E, and placental growth factor share similar structures but differ in their physiological and biological properties largely due to their different interactions with three specific tyrosine kinase receptors: VEGF receptor (VEGFR)-1, VEGFR-2, and VEGFR-3.[11] VEGF-A, a ligand of VEGFR-1 and -2, is known for its direct strong angiogenic effects.[10,12] VEGF-B is a ligand of VEGFR-1 and NRP-1 and has recently been associated with cardiac angiogenesis[13,14] as well as with specific effects on metabolism, survival, and apoptosis.[15–18] Full-length VEGF-C and VEGF-D are ligands of VEGFR-3 and promote mostly lymphangiogenic effects whereas their processed forms are ligands of VEGFR-2 and increase angiogenesis and vascular permeability.[19–21]

Here, we have studied the progression of LVH and heart failure in an aortic constriction mouse model with echocardiography and related this process to the expression of VEGFs, their receptors, and relevant metabolic genes. Myocardial fibrosis, glycogen accumulation, angiogenesis, proliferation, and apoptosis were also studied, as well as the effects of adeno-associated virus serotype 9 (AAV9)-mediated gene transfer of VEGF-B_{186} on the progression of LVH and gene expression in LVH.

It was found that VEGF-C and VEGF-D were associated with the compensated LVH and that AAV9-VEGF-B_{186} gene transfer was able to rescue the function of the failing heart and postpone the development of heart failure.

Correspondence: *Seppo Ylä-Herttuala, A. I. Virtanen Institute, University of Eastern Finland, P. O. Box 1627, FI-70211 Kuopio, Finland. E-mail: seppo.ylaherttuala@uef.fi*

RESULTS

Progression of LVH

The progression of LVH was followed by echocardiography 2, 4, and 10 weeks after transversal aortic constriction (TAC) operation (**Figure 1**). Aortic constriction was confirmed by measuring a significant decrease in transverse aorta diameter which was later on (2 and 4 weeks after TAC operation) associated with an increase in the mRNA levels of so-called fetal genes, also known as hypertrophic markers, atrial natriuretic peptide (ANP) and skeletal α-actin (data not shown). Two weeks after TAC, compensatory hypertrophy was indicated by an elevated thickness of the anterior wall of the left ventricle (LVAW, **Figure 1d**) and decreased LV internal diameter (**Figure 1e**), while the systolic function measured by ejection fraction (EF, **Figure 1a**) and fractional shortening (FS, **Figure 1b**) were preserved. Decompensatory phase (4 and 10 weeks after TAC) was similarly associated with hypertrophic changes but in addition showed a decrease in EF (**Figure 1a**) and FS (**Figure 1b**) and an increase in LV mass (**Figure 1c**), LVAW (**Figure 1d**) as well as in LV internal diameter (**Figure 1e**). LV volume (**Figure 1f**) did not change significantly. Mortality rate was 18% of which 48% died within the first 24 hours after the TAC operation (n = 128).

Chronic pressure overload effectively triggers endogenous myocardial angiogenesis and causes myocardial fibrosis

Chronic pressure overload triggered physiological angiogenesis in the myocardium indicated by increased mean capillary area (**Figure 2a**) and the number of capillaries per myocyte (**Figure 2b**). The number of capillaries per mm^2 was decreased 2 weeks after TAC, and increased 10 weeks after TAC (**Figure 2c**). The progression of the hypertrophy was seen as a decrease in the amonut of myocytes per mm^2 (**Figure 2d**). Representative pictures of the angiogenic response are shown in **Figure 2e–h**. Progression of hypertrophy was accompanied by increased myocardial fibrosis

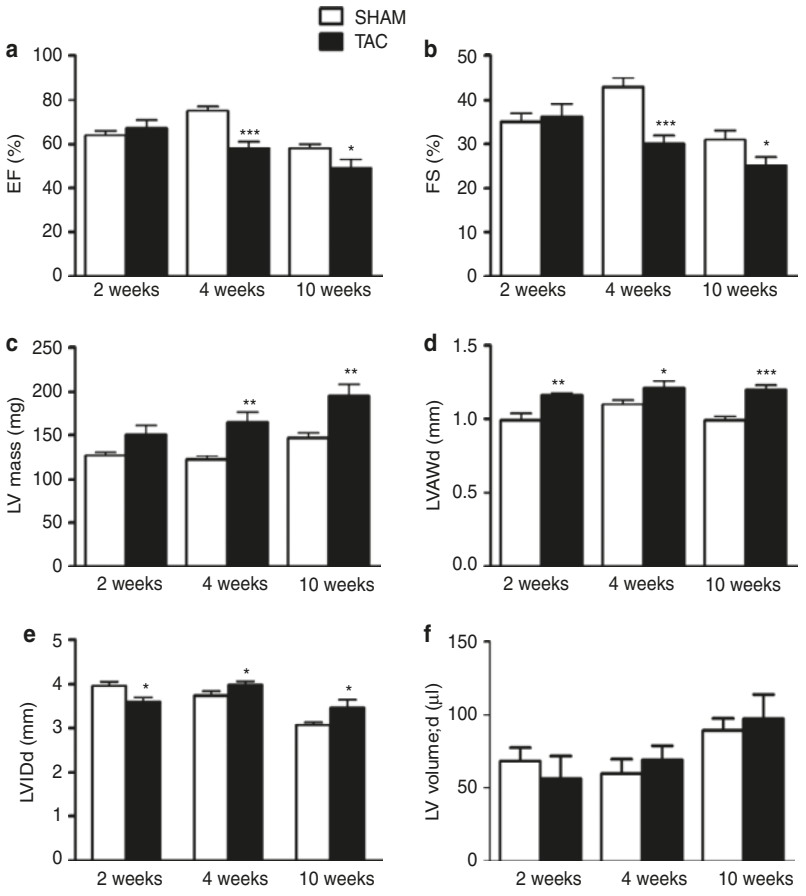

Figure 1 Progression of left ventricular hypertrophy. Myocardial function measured by (**a**) ejection fraction (EF) and (**b**) fractional shortening (FS) was preserved 2 weeks after TAC operation but significantly deteriorated 4 and 10 weeks after the operation. Compensatory hypertrophy was shown as (**d**) increased left ventricle anterior wall thickness during diastole (LVAWd) and (**e**) decreased LV internal diameter during diastole (LVIDd). In heart failure, 4 and 10 weeks after TAC operation, (**c**) LV mass (LV mass), (**d**) LVAWd, and (**e**) LVIDd were increased. (**f**) LV volume did not change significantly. Echocardiographic measurements were done on the day of killing. Results were obtained from parasternal short axis M-mode projections and each time point is compared with the SHAM-operated group of the same time point by Student's t-test. Data in different time points is from individual set of animals and is not therefore compared over time. Mean ± SD, n = 10/group, *P < 0.05, **P < 0.01, ***P < 0.001. TAC, transversal aortic constriction.

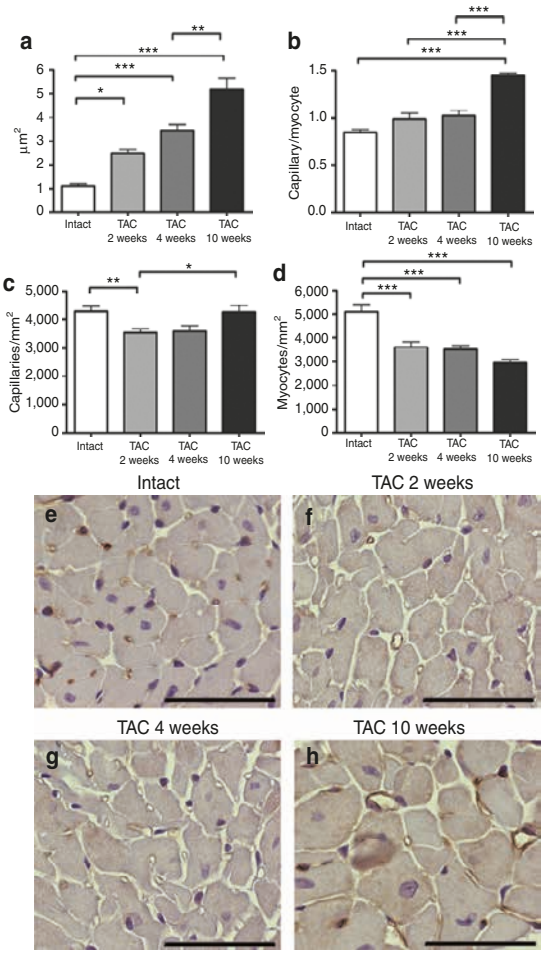

Figure 2 Angiogenic and cardiomyocyte responses to progressive left ventricular hypertrophy (LVH). (**a**,**e**–**h**) Progressive LVH triggered endogenous angiogenesis seen as enlarged capillaries. (**b**) Ten weeks after TAC operation, the number of capillaries per myocyte was significantly increased. Progressive LVH was seen as (**c**) decreased number of capillaries per mm^2 2 weeks after the operation and (**d**) cardiomyocytes per mm^2 in all time points. Quantification was done from five endothelium-stained microscopic fields from each animal at ×400 magnification. Mean ± SEM, n = 6/group (in **a**–**d**), statistical analyses with one-way analysis of variance and Bonferroni's multiple comparison test, *P < 0.05, **P < 0.01, ***P < 0.001. Representative pictures from endothelial stainings with Biotinylated Griffonia (Bandeiraea) Simplicifolia Lectin I, bars 50 μm (in **e**–**h**). TAC, transversal aortic constriction.

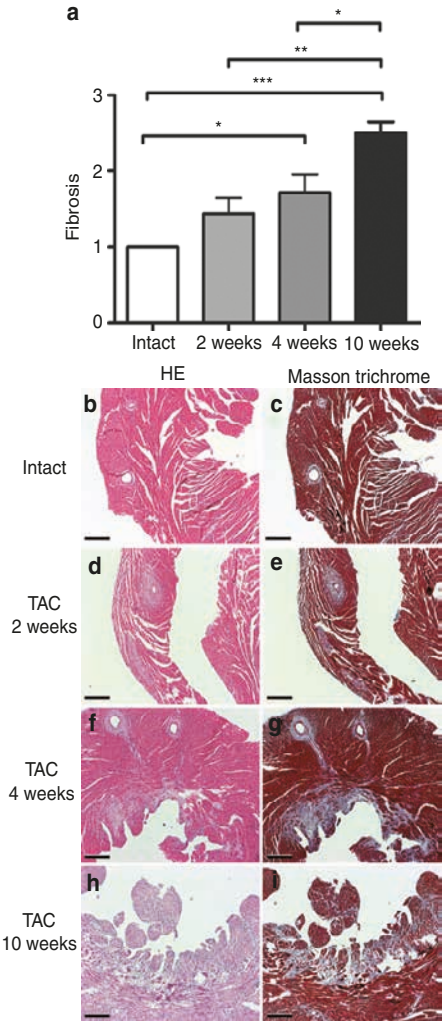

Figure 3 Fibrosis in progressive left ventricular hypertrophy. (**a**–**i**) The amount of fibrosis increased progressively in TAC-operated animals while there was no fibrosis seen in intact animals. Quantification was done in a blinded fashion by three observers screening collagen-stained microscopic sections at ×12.5 magnification using the following grading criteria: 1, minor or no fibrosis; 2, moderate fibrosis; and 3, severe fibrosis. Mean ± SEM, statistical analyses with one-way analysis of variance and Bonferroni's multiple comparison test (n = 6/group), *P < 0.05, **P < 0.01, ***P < 0.001, (**b**,**d**,**f**,**h**) hematoxylin-eosin (HE) staining and (**c**,**e**,**g**,**i**) Masson trichrome staining for collagen, bars 100 μm. TAC, transversal aortic constriction.

(Figure 3) while no difference was seen in glycogen accumulation, proliferation or apoptosis (data not shown). No differences were seen in the angiogenic or cardiomyocytes' response or in the amount of fibrosis between intact animals and sham-operated groups in different time points (**Supplementary Figure S1**).

The expression of VEGF-C, VEGF-D, and VEGFR-3 is increased in compensatory and VEGF-B expression is decreased in decompensatory phase of the LVH

The amount of VEGFs mRNA in LV in all time points were as follows: VEGF-B > VEGF-A >> VEGF-C = VEGF-D (data not shown). No changes in the expression of VEGF-A, VEGF-B, VEGF-C, and VEGF-D was seen 1 day after TAC operation (Figure 4a–d). Interestingly, the expressions of VEGF-C and VEGF-D, growth factors previously unassociated with hypertrophic changes, were significantly increased at the compensatory hypertrophy, 2 weeks after TAC operation (Figure 4c,d) as was their primary receptor VEGFR-3 (Figure 4g). The expression of other receptors remained unchanged (Figure 4e,f,h). While the expression of VEGF-A mRNA remained unchanged and the expression of VEGF-C and VEGF-D mRNAs returned

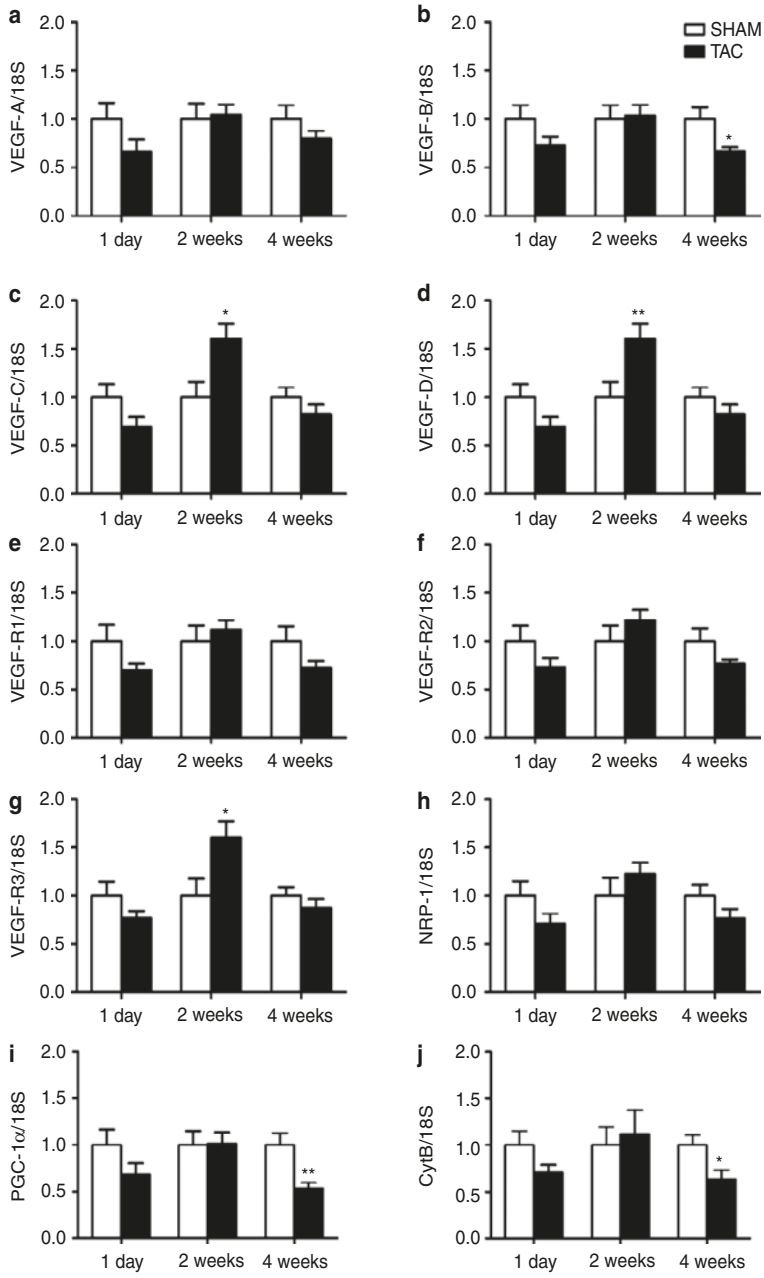

Figure 4 Relative mRNA expression of VEGFs, their receptors (VEGFRs, NRP-1) and mitochodrional genes (PGC-1α, CytB) in progressive LVH. (**a**) Relative expression of VEGF-A mRNA did not change 1 day, 2 or 4 weeks after TAC operation. (**b**) Relative expression of VEGF-B mRNA was decreased 4 weeks after TAC operation and (**c**,**d**,**g**) those of VEGF-C, VEGF-D, and VEGFR-3 mRNAs were increased 2 weeks after TAC operation. (**e**,**f**,**h**) The expressions of mRNA encoding VEGFR-1, VEGFR-2 or NRP-1 were not changed. (**i**,**j**) The expressions of PGC-1α and CytB mRNAs were decreased 4 weeks after TAC operation. mRNA expression of each gene was measured by RT-PCR and normalized to 18S ribosomal RNA as SHAM-operated group of each time point set to one. The relative expression of each gene in TAC-operated animals is compared with that in the SHAM group of the same time point by Student's *t*-test. Mean ± SEM, $n = 6$/group, $^{*}P < 0.05$, $^{**}P < 0.01$. CytB, cytochrome B; LVH, left ventricular hypertrophy; NRP-1, neuropilin-1; RT-PCR, reverse transcription-PCR; TAC, transversal aortic constriction; VEGFR, vascular endothelial growth factor receptor.

to basal level towards the later time point (4 weeks after TAC, Figure 4a,c,d), the expression of VEGF-B mRNA significantly decreased 4 weeks after TAC compared with SHAM-operated animals (Figure 4b).

To evaluate the degree of metabolic remodeling, we measured the mRNA levels of mitochondria associated genes, PGC-1α and CytB, which were both significantly downregulated 4 weeks after TAC (Figure 4i,j).

VEGF-B gene therapy improves systolic function in heart failure

Since VEGF-B expression was decreased at the same time when systolic function of the heart was deteriorated between 2 and 4 weeks after TAC operation, we decided to treat the failing heart with VEGF-B_{186} delivered in AAV9 viral vector (1×10^{10} viral genomes in 10 µl) directly to the anterior wall of the LV. AAV9-LacZ (1×10^{10} viral genomes in 10 µl) was used as a control. The gene transfers were done 2 weeks after the TAC operation in the compensatory phase and animals were killed 4 weeks after the gene transfer. Human VEGF-B_{186} mRNA was detected in the LV 4 weeks after the gene transfer, as expected (data not shown).

Systolic function measured with EF and FS stayed at the normal level in VEGF-B_{186}–treated animals compared with the LacZ controls (**Figure 5a,b**). Also, LV mass did not increase in VEGF-B_{186}–treated group compared with LacZ group (**Figure 5c**) indicating a less severe hypertrophy. No differences were seen in the LVAW thickness during diastole (**Figure 5d**). VEGF-B_{186} gene therapy prevented the dilation of LV internal diameter (**Figure 5e**) as well as the increase in LV volume (**Figure 5f**), known features of heart failure, when compared with LacZ-treated controls.

Gene therapy with hVEGF-B_{186} caused a minimal scaring in the anterior wall of the LV (**Figure 6b–e**) and apparently accelerated the angiogenic response in the myocardium indicated by the faster increase in mean capillary area compared with TAC control animals (**Figure 6a,f,g**). Cardiomyocyte proliferation, indicated by Ki-67 immunostaining, was more prevalent in VEGF-B_{186}–treated group (**Figure 7a,c,d**), and there were less apoptotic cardiomyocytes (measured with cleaved caspase-3 immunostaining) when compared with LacZ-treated group (**Figure 7b,e–h**).

The expression of PGC-1α mRNA (**Figure 8a**) was increased and that of ANP mRNA (**Figure 8c–e**) was decreased after VEGF-B_{186} gene therapy when compared with LacZ-treated group. Also,

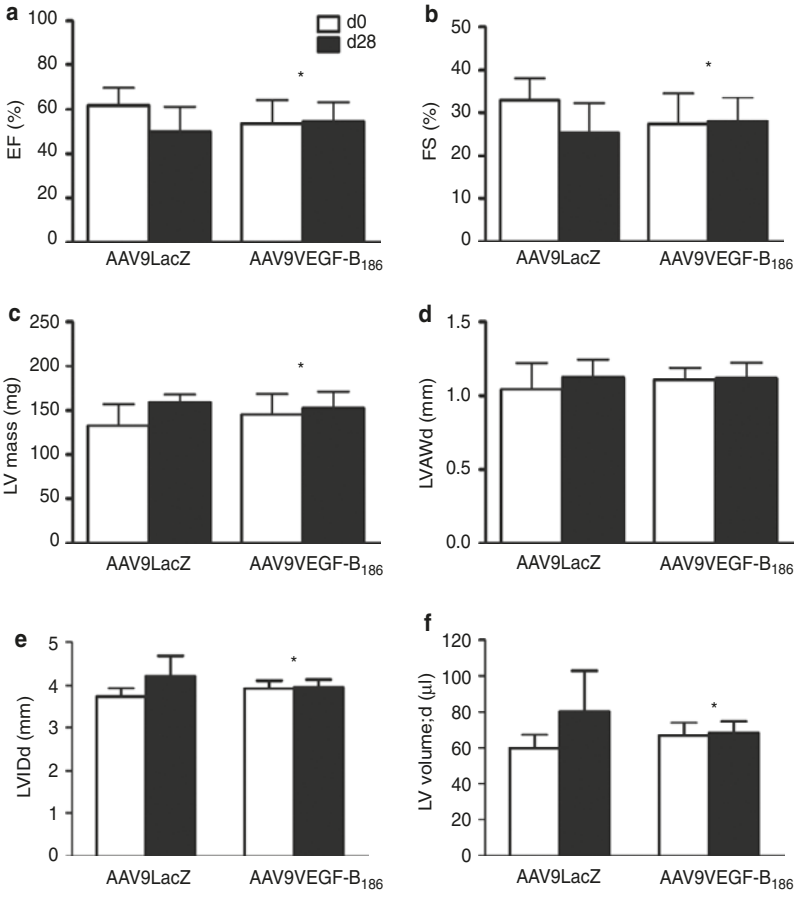

Figure 5 Progression of LVH after AAV9-VEGF-B_{186} gene transfer. AAV9-VEGF-B_{186} gene transfer (1×10^{10} viral genomes in 10 µl) sustained the systolic function ((**a**) EF and (**b**) FS) of TAC-operated mice when compared with AAV9-LacZ treated controls. (**c**) Left ventricle (LV) mass did not increase in VEGF-B_{186} treated group similarly than in LacZ control group (**d**) while LVAWd remained unchanged in both groups. (**e**) LVIDd and (**f**) LV volume stayed at the normal level in AAV9-VEGF-B_{186} treated animals, while both increased in AAV9-LacZ control animals. Echocardiographic measurements were done before the gene transfer and on the day of killing. The results were obtained from parasternal short axis M-mode projections. Mean ± SD, statistical analyses with repeated measurements two-way analysis of variance (n = 8/group), *P < 0.05. AAV, adeno-associated virus; EF, ejection fraction; FS, fractional shortening; LVAWd, left ventricle anterior wall thickness during diastole; LVH, left ventricular hypertrophy; LVIDd, left ventricle internal diameter during diastole; VEGF, vascular endothelial growth factor.

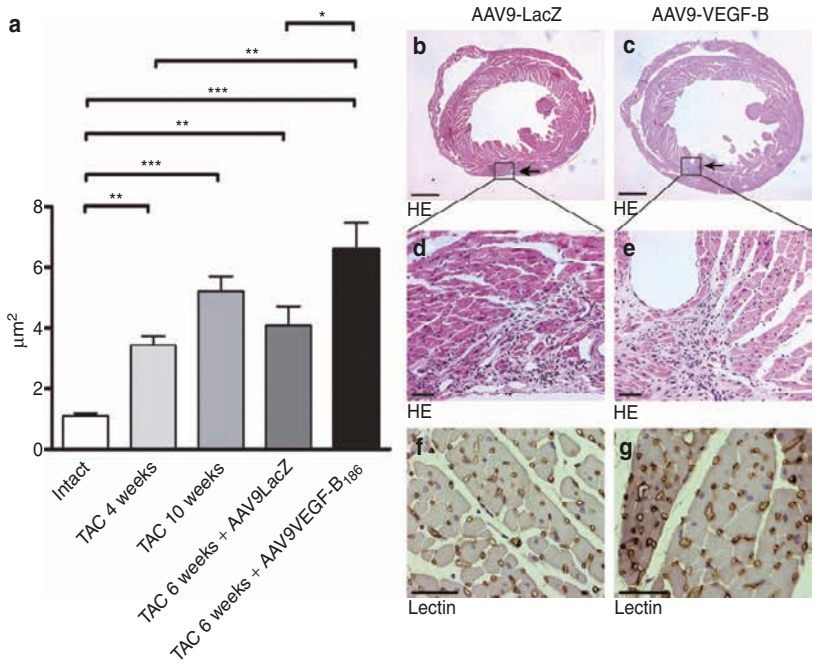

Figure 6 The angiogenic response to AAV9-VEGF-B_{186} gene therapy. (**a**,**f**,**g**) AAV9-VEGF-B_{186} gene therapy significantly increased mean capillary area when compared with AAV9-LacZ group and the response was accelerated compared with the endogenous response of TAC-operated animals. Quantification was done from five endothelium-stained microscopic fields from each animal at ×400 magnification. (**b**–**e**) Gene therapy was done by direct ultrasound-guided injection and caused only a minor needle mark visible in hematoxylin-eosin (HE) staining. Mean ± SEM, statistical analyses with one-way analysis of variance and Bonferroni's multiple comparison test, $n = 4$/group, $^*P < 0.05$, $^{**}P < 0.01$, $^{***}P < 0.001$ (as shown in **a**), bars 1 mm (in **b**,**c**) and 50 μm (in **d**–**g**). HE staining (in **b**–**e**) and endothelium staining with Biotinylated Griffonia (Bandeiraea) Simplicifolia Lectin I (in **f** and **g**). AAV, adeno-associated virus; TAC, transversal aortic constriction; VEGF, vascular endothelial growth factor.

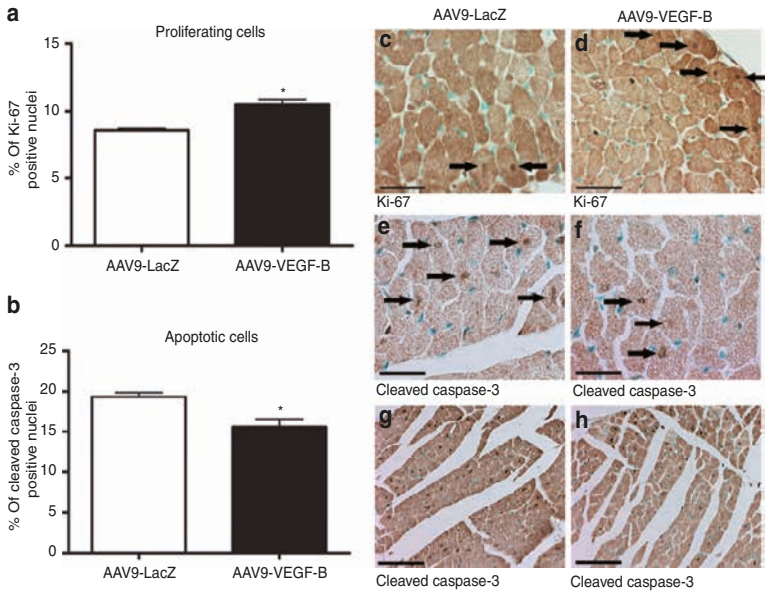

Figure 7 The effect of AAV9-VEGF-B_{186} gene therapy on cell proliferation and apoptosis. AAV9-VEGF-B_{186} gene therapy (**a**,**c**,**d**) increased the number of proliferating cardiomyocytes and (**b**,**e**–**h**) decreased the number of apoptotic cardiomyocytes. Quantifications in **a** and **b** were done from five Ki-67 and cleaved caspase-3 microscopic fields, respectively, from each animal at ×400 magnification. Mean ± SEM, statistical analyses with Student's *t*-test, $n = 4$/group, $^*P < 0.05$ (as shown in **a**,**b**), bars 25 μm (in **c**–**f**) and 50 μm (in **g**,**h**), Ki-67 staining for proliferating cells (**c**,**d**), and cleaved caspase-3 staining for apoptotic cells (**e**–**h**). AAV, adeno-associated virus; VEGF, vascular endothelial growth factor.

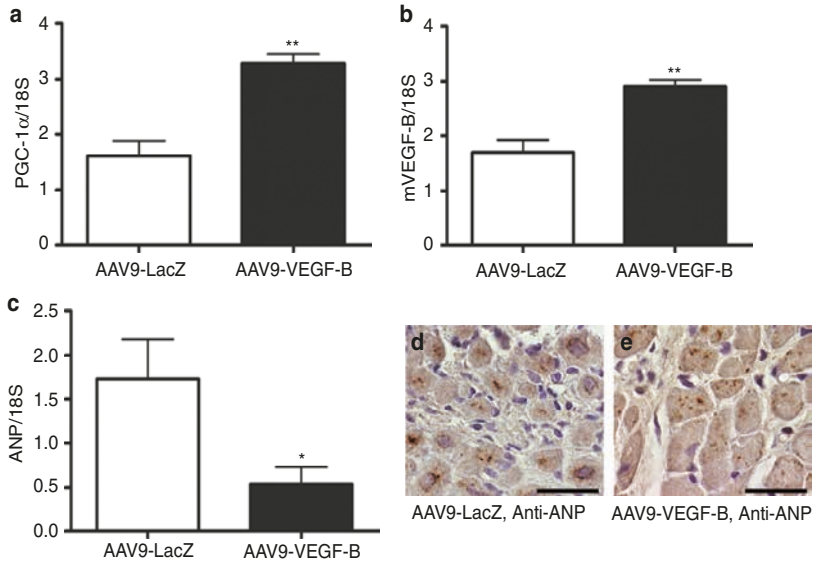

Figure 8 Relative mRNA expression of PGC-1α, mVEGF-B, and ANP after AAV9-VEGF-B$_{186}$ gene therapy. AAV9-VEGF-B gene therapy increased the relative expression levels of (**a**) PGC-1α and (**b**) mVEGF-B and decreased the relative expression of (**c**) ANP mRNA compared with LacZ control group. mRNA expression was measured by quantitative RT-PCR and normalized to 18S ribosomal RNA. Mean ± SEM, statistical analyses with Student's *t*-test, $n = 4$/group, $^*P < 0.05$, $^{**}P < 0.01$. (**d**,**e**) ANP staining, bars 25 µm. AAV, adeno-associated virus; ANP, atrial natriuretic peptide; VEGF, vascular endothelial growth factor.

the expression of endogenous VEGF-B (**Figure 8b**) mRNA was increased in VEGF-B$_{186}$–treated group compared with LacZ group.

DISCUSSION

In the present study, we have identified the expression patterns of mouse VEGFs and their receptors in progressive LVH and treated the failing hearts with VEGF-B$_{186}$ gene therapy to restore VEGF-B expression level. It was found that (i) in the compensatory phase of the LVH, VEGF-C, VEGF-D, and VEGFR-3 were significantly upregulated, (ii) when the LVH shifted towards heart failure, VEGF-B was downregulated, and (iii) by treating the animals with AAV9-mediated VEGF-B$_{186}$ gene transfer in the compensatory phase we could overcome the defects in cardiac functional parameters, reduce metabolism-associated gene expression changes, and reverse the fetal gene expression pattern by lowering the expression of ANP, thus postponing the transition from LVH to heart failure.

In order to study the expression pattern of VEGFs and their receptors, we wanted to cause a chronic, long-term pressure overload recapitulating the different phases of pathological hypertrophy. Hypertrophy was seen in both phases as an increased thickness of the LVAW and an increase in the expression level of hypertrophic marker genes, ANP and skeletal α-actin. Compensatory hypertrophy was followed by heart failure within 4 weeks after TAC operation.

Angiogenesis is considered necessary to support ongoing hypertrophy and is the normal process enabling physiological hypertrophy during normal tissue growth.[9,22] In our model of progressive LVH, a physiological angiogenic response was detected in hypertrophied myocardium. A physiological angiogenic response has also been described earlier.[7,23] Angiogenesis is probably the reason for a slow progression from compensated to decompensated hypertrophy, since myocardium is able to compensate increased energy demands of the growing work load with dilatation of existing capillaries.

VEGF-B was the most abundant member of the VEGF family expressed in the adult myocardium as also described earlier.[24] It has been previously reported that VEGF-A is upregulated 2 weeks after TAC operation[8] but also that VEGF-A transcripts and protein levels remain at the control level 3, 7, and 12 weeks after aortic banding.[25,26] We found VEGF-A levels to stay at the control level at all time points after TAC operation. In contrast to previous findings of upregulated VEGFR-1 levels 3 and 7 weeks after aortic banding,[26] we found no changes in VEGFR-1 or -2 expression.

We show for the first time that in the compensatory phase of the LVH, VEGF-C, VEGF-D, and VEGFR-3 were significantly upregulated and that the expression returned back to control levels as the hypertrophy progresses towards heart failure. VEGF-C and VEGF-D have not so far been associated with cardiac hypertrophy and the activity of these growth factors during chronic pressure overload has remained unclear. In patient data regarding ischemic and dilated forms of cardiomyopathy, VEGF-C has been reported to be upregulated at mRNA and protein levels[27] and both VEGF-C and VEGF-D have been shown to be upregulated after acute myocardial infarction in mice.[28] A recent finding revealed an increase in the number of lymphatic vessels in human hypertrophic myocardium.[29] In gene therapy studies, VEGF-C has been reported to prevent progression of myocardial ischemia by inducing collateral formation in a large animal model.[30] However, the specific roles of VEGF-C and VEGF-D in compensatory hypertrophy need to be studied further.

Strikingly, during the development of heart failure, 2 weeks onwards from TAC operation VEGF-B mRNA expression was

significantly downregulated. Therefore, we hypothesized that we could improve the functional status of the heart by restoring VEGF-B expression. AAV9-mediated, direct gene transfer to LVAW improved the systolic function of the heart by expediting the angiogenic response of the myocardium, lowering the number of apoptotic cardiomyocytes, increasing cardiomyocyte proliferation, and decreasing the overall workload of the heart. We have previously shown that diastolic dysfunction in angiotensin-II–induced LVH could be prevented with adenoviral VEGF-B gene transfer in rats.[16] In this work, the improvements in E/A ratio LV isovolumic relaxation time were suggested to be due to a combined effect of the increased proliferation of cardiomyocytes and an increase in capillary area. Others have also described cardiomyocyte proliferation and renewal in hypertrophy and after injury,[31–33] even though cardiomyocytes have traditionally been regarded as permanently differentiated cells.

In the present study, we wanted to see a long-term gene expression driven by AAV9, which is reported to be cardiotropic.[34] Long-term VEGF-B_{186} expression led, indeed, to a better systolic outcome. It has been previously reported that VEGF-B has an antiapoptotic effect,[18,35] promotes cardiomyocyte proliferation[36] and acts as a protective agent after myocardial infarction.[13,17,35] Recently, Pepe and colleagues[37] reported that AAV9-VEGF-B_{167} treatment delayed the progression of tachypacing-induced hypertrophy towards heart failure *via* a nonangiogenic cardioprotective effect by inhibiting apoptosis.

Metabolic disturbances are known to play a significant role in the transition from compensated to decompensated hypertrophy.[38] It has been previously shown that in heart failure, PGC-1α, a factor associated with mitochondrial biogenesis, is downregulated.[39,40] We also found that PGC-1α and CytB were downregulated at the onset of heart failure 4 weeks after TAC operation. This indicates metabolic remodeling associated with pathological hypertrophy. In AAV9-VEGF-B_{186}–treated animals, PGC-1α levels were higher compared with control group indicating a reduction in metabolic remodeling compared to LacZ-treated controls. This could help heart to better meet its metabolic needs and therefore enhance the functional outcome. Also, we found ANP levels to be reduced in AAV9-VEGF-B_{186}–treated group when compared with control group. ANP is an independent marker of myocardial workload[41] and activity[42] and since AAV9-VEGF-B_{186} gene transfer reduced ANP expression it could indicate that VEGF-B_{186} acts to reduce the overall cardiac workload after TAC. Interestingly, we saw that also the endogenous mouse VEGF-B level was upregulated in VEGF-B–treated animals. Knowing that VEGF-B increases fatty acid uptake *via* endothelium,[15] this upregulation might increase the fatty acid utilization as an energy supply and therefore reduce the energy deprivation in the failing heart.

We conclude that VEGF-C and VEGF-D seem to be associated with the compensatory phase of LVH. Also, VEGF-B level is downregulated at the onset of heart failure and AAV9-mediated VEGF-B_{186} gene therapy improved the functional outcome of the hypertrophied heart by inducing angiogenesis, inhibiting apoptosis, promoting cardiomyocyte proliferation, and altering the expression of metabolism-associated genes in the heart. VEGF-B_{186} is a potential therapeutic target in LVH and for the prevention of heart failure.

MATERIALS AND METHODS

Experimental animals. All animal procedures were approved by The National Animal Experiment Board of Finland and carried out in accordance with the guidelines of The Finnish Act on Animal Experimentation; 128 10–15 weeks old C57BL male mice (Harlan Laboratories, Indianapolis, IN) were used to perform TAC or sham operation. The animals were kept in standard housing conditions in The National Laboratory Animal Center of The University of Eastern Finland. Diet and water were provided *ad libitum*.

TAC. A pressure overload was induced by a modified TAC model.[43] Briefly, mice were anesthetized with medetomidine (1 mg/kg, Domitor; Pfizer, New York, NY) and ketamine (75 mg/kg, Ketalar; Pfizer) subcutaneously and intubated with 0.75 mm polyethylene tube for ventilation (MicroVent; Harvard Apparatus, Holliston, MA). The thorax was opened by cutting the sternum from the midline and transverse aorta was visualized by blunt dissecting. A 7-0 silk suture was placed around the aorta between the brachiocephalicus and the arteria carotis communis sinistra and tied around a 25-G needle, which was subsequently removed. Sham-operated mice went through a similar surgical operation without the ligation. Postoperative analgesic (carprofen (Rimadyl) 5 mg/kg; Pfizer, buprenorphine (Temgesic) 0.05–1 mg/kg; RB Pharmaceuticals Limited, Berkshire, UK) and antisedatative (atipamezole hydrochloride (Antisedan) 0.1–1 mg/kg; Orion Oyj, Espoo, Finland) were given. Animals were killed 1 day, 2, 4 or 10 weeks after the TAC operation.

Echocardiography. Echocardiographic measurements were performed before the TAC operations and at 2, 4, and 10 weeks after the operations using Vevo770 Ultrasound System (VisualSonics, Toronto, Ontario, Canada). A high-frequency ultrasound probe (RMV-707B) operating at 30 MHz, with a focal depth of 12.7 mm was used. The animals were anesthetized with isoflurane (induction: 4.5% isoflurane, 450 ml air, maintenance: 2.0% isoflurane, 200 ml air; Baxter International, Deerfield, IL). EF, FS, LV mass, transverse aorta diameter, and LV diastolic wall thickness were determined from parasternal short axis M-mode measurements. EF was calculated by Vevo770 software (VisualSonics) by using the Teicholz formula.

Immunohistochemistry. Myocardial fibrosis (Masson trichrome, Accustain trichrome stains; Sigma-Aldrich, St Louis, MO), glycogen accumulation (Periodic acid Schiff's glycogen staining), proliferation (Ki-67, ab15580, dilution 1:200; Abcam, Cambridge, UK), apoptosis (Cleaved Caspase-3, Asp175, dilution 1:250; Cell Signaling Technology, Danvers, MA), angiogenesis (endothelium staining, Biotinylated Griffonia (Bandeiraea) Simplicifolia Lectin I, dilution 1:100; Vector Laboratories, Burlingame, CA), and ANP (N-20, SC-18811, dilution 1:100; Santa Cruz Biotechnologies, Santa Cruz, CA) were analyzed from 5 µm thick paraffin-embedded sections fixed with 4% paraformaldehyde in 7.5% sucrose for 4 hours. Capillary area, capillary/myocyte, capillary/mm^2, and myocyte/mm^2 ratios were analyzed from five microscopic fields of endothelium-stained sections at ×400 magnification within each animal as well as the number of proliferating and apoptotic cardiomyocytes from five microscopic fields of Ki-67 and cleaved caspase-3, respectively, stained sections within each animal at ×400 magnification. Glycogen accumulation was quantified from three microscopic fields of glycogen-stained sections within each animal at ×200 magnification. All quantifications were done in a blinded fashion by using AnalySIS software (Soft Imaging System, Muenster, Germany). The number of proliferating and apoptotic cardiomyocytes is presented as a mean percentage of all cardiomyocytes in a field. For proliferation, apoptosis and glycogen accumulation analyzes the microscopic pictures taken from the site of maximum staining in each section. Myocardial fibrosis was analyzed in a blinded fashion by three observers screening collagen-stained microscopic sections at ×12.5 magnification using the following grading criteria: 1, minor or no fibrosis; 2, moderate fibrosis; and 3, severe fibrosis. The result is shown as a mean of all observations.

Quantitative reverse transcription-PCR. Total RNA from cell cultures was isolated using the GenElute Mammalian Total RNA Miniprep Kit (Sigma-Aldrich). cDNA was synthesized using the First Strand cDNA Synthesis Kit (MBI Fermentas, Amherst, NY). Relative expression levels of mRNA encoding mVEGF-A (forward: 5′-GAT CCG CAG ACG TGT AAA TGT TC-3′, reverse: 5′-TTA ACT CAA GCT GCC TCG CC-3′), mVEGF-B (forward: 5′-CCA CTG GGC AAC ACC AAG TC-3′, reverse: 5′-GCT GTG TTC TTC CAG GGA CAT C-3′), mVEGF-C (forward: 5′-TCA GCA AGA CGT TGT TTG AAA TTA C-3′, reverse: 5′-TGA TTG GCA AAA CTG ATT GTG ACT-3′), mVEGF-D (forward: 5′-TGG ACC AGT GAA GGA TTT TTC TTT-3′, reverse: 5′-TGC TCG GAT CTG TTG TTC AGA-3′), VEGFR-1 (forward: 5′-CTT TTC AAG GAC GGC TTT GC-3′, reverse: 5′-GCT CAT GAA TTT GAA AGC GTT TAC-3′), VEGFR-2 (forward: 5′-AAA ACT CTG GAA GAC AGG AAC AAA TT-3′, reverse: 5′-GCC ACA GAC TCC CTG CTT TTA-3′), VEGFR-3 (forward: 5′-TCT CCA ACT TCT TGC GTG TCA-3′, reverse: 5′-CGT TGC TCC GGA GAC TTC TC-3′), NRP-1 (forward: 5′-CTA TGA CCG GCT GGA GAT CTG-3′, reverse: 5′-GCC CAC AAT AAC GCC CAA T-3′), CytB (forward: 5′-CCA CTT CAT CTT ACC ATT TAT C-3′, reverse: 5′-TGA TCC TGT TTC GTG GAG GAA-3′), PGC-1α (forward: 5′-AGC GAC CAA TCG GAA ATC AT-3′, reverse: 5′-GCA AGT TTG CCT CAT TCT CTT CA-3′), ANP (forward: 5′-GAA AAG CAA ACT GAG GGC TCT G-3′, reverse: 5′-CCT ACC CCC GAA GCA GCT-3′), hVEGF-B (forward: 5′-GCC CAG GCC CCT GTC T-3′, reverse: 5′-ACA TCT ATC CAT GAC ACC ACT TTC C-3′), and 18S (forward: 5′-TGG TTG CAA AGC TGA AAC TTA AAG-3′, reverse: 5′-AGT CAA ATT AAG CCG CAG GC-3′) in LV were measured using quantitative reverse transcription-PCR with the ABI 7700 Sequence Detection System (Applied Biosystems, Foster City, CA) using SYBR Green chemistry (Applied Biosystems). The expression levels were normalized to 18S and the results are shown normalized to the expression of sham-operated control group at each time point or compared with the control gene therapy group.

Echocardiography-guided myocardial gene transfer. AAV9-hVEGF-B_{186} or AAV9-LacZ gene transfers were done as described earlier[36] with a dose of 1×10^{10} viral genomes in 10 µl. Gene transfers were done 2 weeks after TAC operation and the animals were killed 6 weeks after the TAC operation. AAV9 vectors were produced in 293T cells using standard plasmid transfection methods and purified through sucrose-cushion ultracentrifugation and an anion-exchange column chromatography (Q-Sepharose; GE Healthcare, Waukesha, WI) followed by concentration through sucrose-cushion ultracentrifugation.[44,45] The final virus pellets were resuspended with a solution which consists of 10 mmol/l Tris-HCl, pH 7.9, 1 mmol/l $MgCl_2$, 3% sucrose and diluted further with sterile phosphate-bufferes saline to the final concentration. Virus titers were determined by measuring the genome copies by real-time quantitative PCR using virus genome DNAs prepared from the purified virus preparations.

Statistical analyses. Results are presented as mean ± SD or ± SEM, statistical significances were evaluated using Student's *t*-test, one-way analysis of variance or repeated measures two-way analysis of variance with Bonferroni's multiple comparison test used as a post-test. The used statistical analyses are specified in the figure legends. $P < 0.05$ was considered statistically significant. The following symbols are used in the figures: $^{*}P < 0.05$, $^{**}P < 0.01$, $^{***}P < 0.001$.

SUPPLEMENTARY MATERIAL

Figure S1. Angiogenic and cardiomyocyte parameters of intact and SHAM-operated mice in different time points.

ACKNOWLEDGMENTS

The study was done in Kuopio, Finland. This study was funded by Finnish Academy, University of Eastern Finland Spearhead Program, Sigrid Juselius Foundation, European Research Council Advanced grant, Finnish Foundation for Cardiovascular Research, Emil Aaltonen Foundation, and The Finnish Cultural Foundation's Northern Savo Fund. The authors like to acknowledge the staff at the Laboratory Animal Center of The University of Eastern Finland for the maintenance of the animals. Anniina Oksman (Charles River Discovery Services, Kuopio, Finland) is acknowledged for help regarding the animal work. The authors declared no conflict of interest.

REFERENCES

1. Katholi, RE and Couri, DM (2011). Left ventricular hypertrophy: major risk factor in patients with hypertension: update and practical clinical applications. *Int J Hypertens* **2011**: 495349.
2. Hunter, JJ and Chien, KR (1999). Signaling pathways for cardiac hypertrophy and failure. *N Engl J Med* **341**: 1276–1283.
3. Rimbaud, S, Sanchez, H, Garnier, A, Fortin, D, Bigard, X, Veksler, V *et al.* (2009). Stimulus specific changes of energy metabolism in hypertrophied heart. *J Mol Cell Cardiol* **46**: 952–959.
4. Lorell, BH and Carabello, BA (2000). Left ventricular hypertrophy: pathogenesis, detection, and prognosis. *Circulation* **102**: 470–479.
5. Levy, D, Garrison, RJ, Savage, DD, Kannel, WB and Castelli, WP (1990). Prognostic implications of echocardiographically determined left ventricular mass in the Framingham Heart Study. *N Engl J Med* **322**: 1561–1566.
6. Frey, N and Olson, EN (2003). Cardiac hypertrophy: the good, the bad, and the ugly. *Annu Rev Physiol* **65**: 45–79.
7. Walsh, K and Shiojima, I (2007). Cardiac growth and angiogenesis coordinated by intertissue interactions. *J Clin Invest* **117**: 3176–3179.
8. Izumiya, Y, Shiojima, I, Sato, K, Sawyer, DB, Colucci, WS and Walsh, K (2006). Vascular endothelial growth factor blockade promotes the transition from compensatory cardiac hypertrophy to failure in response to pressure overload. *Hypertension* **47**: 887–893.
9. Shiojima, I, Sato, K, Izumiya, Y, Schiekofer, S, Ito, M, Liao, R *et al.* (2005). Disruption of coordinated cardiac hypertrophy and angiogenesis contributes to the transition to heart failure. *J Clin Invest* **115**: 2108–2118.
10. Ylä-Herttuala, S, Rissanen, TT, Vajanto, I and Hartikainen, J (2007). Vascular endothelial growth factors: biology and current status of clinical applications in cardiovascular medicine. *J Am Coll Cardiol* **49**: 1015–1026.
11. Ferrara, N (2004). Vascular endothelial growth factor: basic science and clinical progress. *Endocr Rev* **25**: 581–611.
12. Rissanen, TT and Ylä-Herttuala, S (2007). Current status of cardiovascular gene therapy. *Mol Ther* **15**: 1233–1247.
13. Lähteenvuo, JE, Lähteenvuo, MT, Kivelä, A, Rosenlew, C, Falkevall, A, Klar, J *et al.* (2009). Vascular endothelial growth factor-B induces myocardium-specific angiogenesis and arteriogenesis via vascular endothelial growth factor receptor-1- and neuropilin receptor-1-dependent mechanisms. *Circulation* **119**: 845–856.
14. Bry, M, Kivelä, R, Holopainen, T, Anisimov, A, Tammela, T, Soronen, J *et al.* (2010). Vascular endothelial growth factor-B acts as a coronary growth factor in transgenic rats without inducing angiogenesis, vascular leak, or inflammation. *Circulation* **122**: 1725–1733.
15. Hagberg, CE, Falkevall, A, Wang, X, Larsson, E, Huusko, J, Nilsson, I *et al.* (2010). Vascular endothelial growth factor B controls endothelial fatty acid uptake. *Nature* **464**: 917–921.
16. Serpi, R, Tolonen, AM, Huusko, J, Rysä, J, Tenhunen, O, Ylä-Herttuala, S *et al.* (2011). Vascular endothelial growth factor-B gene transfer prevents angiotensin II-induced diastolic dysfunction via proliferation and capillary dilatation in rats. *Cardiovasc Res* **89**: 204–213.
17. Li, X, Tjwa, M, Van Hove, I, Enholm, B, Neven, E, Paavonen, K *et al.* (2008). Reevaluation of the role of VEGF-B suggests a restricted role in the revascularization of the ischemic myocardium. *Arterioscler Thromb Vasc Biol* **28**: 1614–1620.
18. Li, Y, Zhang, F, Nagai, N, Tang, Z, Zhang, S, Scotney, P *et al.* (2008). VEGF-B inhibits apoptosis via VEGFR-1-mediated suppression of the expression of BH3-only protein genes in mice and rats. *J Clin Invest* **118**: 913–923.
19. Achen, MG, Jeltsch, M, Kukk, E, Mäkinen, T, Vitali, A, Wilks, AF *et al.* (1998). Vascular endothelial growth factor D (VEGF-D) is a ligand for the tyrosine kinases VEGF receptor 2 (Flk1) and VEGF receptor 3 (Flt4). *Proc Natl Acad Sci USA* **95**: 548–553.
20. Joukov, V, Pajusola, K, Kaipainen, A, Chilov, D, Lahtinen, I, Kukk, E *et al.* (1996). A novel vascular endothelial growth factor, VEGF-C, is a ligand for the Flt4 (VEGFR-3) and KDR (VEGFR-2) receptor tyrosine kinases. *EMBO J* **15**: 1751.
21. Rissanen, TT, Markkanen, JE, Gruchala, M, Heikura, T, Puranen, A, Kettunen, MI *et al.* (2003). VEGF-D is the strongest angiogenic and lymphangiogenic effector among VEGFs delivered into skeletal muscle via adenoviruses. *Circ Res* **92**: 1098–1106.
22. Tirziu, D, Chorianopoulos, E, Moodie, KL, Palac, RT, Zhuang, ZW, Tjwa, M *et al.* (2007). Myocardial hypertrophy in the absence of external stimuli is induced by angiogenesis in mice. *J Clin Invest* **117**: 3188–3197.
23. Accornero, F, van Berlo, JH, Benard, MJ, Lorenz, JN, Carmeliet, P and Molkentin, JD (2011). Placental growth factor regulates cardiac adaptation and hypertrophy through a paracrine mechanism. *Circ Res* **109**: 272–280.
24. Nash, AD, Baca, M, Wright, C and Scotney, PD (2006). The biology of vascular endothelial growth factor-B (VEGF-B). *Pulm Pharmacol Ther* **19**: 61–69.
25. Hilfiker-Kleiner, D, Hilfiker, A, Kaminski, K, Schaefer, A, Park, JK, Michel, K *et al.* (2005). Lack of JunD promotes pressure overload-induced apoptosis, hypertrophic growth, and angiogenesis in the heart. *Circulation* **112**: 1470–1477.
26. Kaza, E, Ablasser, K, Poutias, D, Griffiths, ER, Saad, FA, Hofstaetter, JG *et al.* (2011). Up-regulation of soluble vascular endothelial growth factor receptor-1 prevents angiogenesis in hypertrophied myocardium. *Cardiovasc Res* **89**: 410–418.
27. Abraham, D, Hofbauer, R, Schäfer, R, Blumer, R, Paulus, P, Miksovsky, A *et al.* (2000). Selective downregulation of VEGF-A(165), VEGF-R(1), and decreased capillary density in patients with dilative but not ischemic cardiomyopathy. *Circ Res* **87**: 644–647.

28. Park, JH, Yoon, JY, Ko, SM, Jin, SA, Kim, JH, Cho, CH *et al.* (2011). Endothelial progenitor cell transplantation decreases lymphangiogenesis and adverse myocardial remodeling in a mouse model of acute myocardial infarction. *Exp Mol Med* **43**: 479–485.
29. Kholová, I, Dragneva, G, Cermáková, P, Laidinen, S, Kaskenpää, N, Hazes, T *et al.* (2011). Lymphatic vasculature is increased in heart valves, ischaemic and inflamed hearts and in cholesterol-rich and calcified atherosclerotic lesions. *Eur J Clin Invest* **41**: 487–497.
30. Pätilä, T, Ikonen, T, Rutanen, J, Ahonen, A, Lommi, J, Lappalainen, K *et al.* (2006). Vascular endothelial growth factor C-induced collateral formation in a model of myocardial ischemia. *J Heart Lung Transplant* **25**: 206–213.
31. Boström, P, Mann, N, Wu, J, Quintero, PA, Plovie, ER, Panáková, D *et al.* (2010). C/EBPß controls exercise-induced cardiac growth and protects against pathological cardiac remodeling. *Cell* **143**: 1072–1083.
32. Hsieh, PC, Segers, VF, Davis, ME, MacGillivray, C, Gannon, J, Molkentin, JD *et al.* (2007). Evidence from a genetic fate-mapping study that stem cells refresh adult mammalian cardiomyocytes after injury. *Nat Med* **13**: 970–974.
33. Bersell, K, Arab, S, Haring, B and Kühn, B (2009). Neuregulin1/ErbB4 signaling induces cardiomyocyte proliferation and repair of heart injury. *Cell* **138**: 257–270.
34. Kho, C, Lee, A, Jeong, D, Oh, JG, Chaanine, AH, Kizana, E *et al.* (2011). SUMO1-dependent modulation of SERCA2a in heart failure. *Nature* **477**: 601–605.
35. Zentilin, L, Puligadda, U, Lionetti, V, Zacchigna, S, Collesi, C, Pattarini, L *et al.* (2010). Cardiomyocyte VEGFR-1 activation by VEGF-B induces compensatory hypertrophy and preserves cardiac function after myocardial infarction. *FASEB J* **24**: 1467–1478.
36. Huusko, J, Merentie, M, Dijkstra, MH, Ryhänen, MM, Karvinen, H, Rissanen, TT *et al.* (2010). The effects of VEGF-R1 and VEGF-R2 ligands on angiogenic responses and left ventricular function in mice. *Cardiovasc Res* **86**: 122–130.
37. Pepe, M, Mamdani, M, Zentilin, L, Csiszar, A, Qanud, K, Zacchigna, S *et al.* (2010). Intramyocardial VEGF-B167 gene delivery delays the progression towards congestive failure in dogs with pacing-induced dilated cardiomyopathy. *Circ Res* **106**: 1893–1903.
38. Ventura-Clapier, R, Garnier, A and Veksler, V (2004). Energy metabolism in heart failure. *J Physiol (Lond)* ***555***(Pt 1): 1–13.
39. Garnier, A, Fortin, D, Deloménie, C, Momken, I, Veksler, V and Ventura-Clapier, R (2003). Depressed mitochondrial transcription factors and oxidative capacity in rat failing cardiac and skeletal muscles. *J Physiol (Lond)* **551**(Pt 2): 491–501.
40. Dai, DF, Hsieh, EJ, Liu, Y, Chen, T, Beyer, RP, Chin, MT *et al.* (2012). Mitochondrial proteome remodelling in pressure overload-induced heart failure: the role of mitochondrial oxidative stress. *Cardiovasc Res* **93**: 79–88.
41. Tavi, P, Laine, M, Weckström, M and Ruskoaho, H (2001). Cardiac mechanotransduction: from sensing to disease and treatment. *Trends Pharmacol Sci* **22**: 254–260.
42. Ronkainen, JJ, Vuolteenaho, O and Tavi, P (2007). Calcium-calmodulin kinase II is the common factor in calcium-dependent cardiac expression and secretion of A- and B-type natriuretic peptides. *Endocrinology* **148**: 2815–2820.
43. Rockman, HA, Ross, RS, Harris, AN, Knowlton, KU, Steinhelper, ME, Field, LJ *et al.* (1991). Segregation of atrial-specific and inducible expression of an atrial natriuretic factor transgene in an *in vivo* murine model of cardiac hypertrophy. *Proc Natl Acad Sci USA* **88**: 8277–8281.
44. Zolotukhin, S, Potter, M, Zolotukhin, I, Sakai, Y, Loiler, S, Fraites, TJ Jr *et al.* (2002). Production and purification of serotype 1, 2, and 5 recombinant adeno-associated viral vectors. *Methods* **28**: 158–167.
45. Gao, G, Qu, G, Burnham, MS, Huang, J, Chirmule, N, Joshi, B *et al.* (2000). Purification of recombinant adeno-associated virus vectors by column chromatography and its performance *in vivo*. *Hum Gene Ther* **11**: 2079–2091.

II

Left ventricular remodelling leads to heart failure in mouse with cardiac-specific overexpression of VEGF-B$_{167}$ -Echocardiography and magnetic resonance imaging study

Lottonen-Raikaslehto L, Rissanen R, Gurzeler E, Merentie M, Huusko J, Schneider JE, Liimatainen T, Ylä-Herttuala S.

Submitted

Left ventricular remodelling leads to heart failure in mouse with cardiac-specific overexpression of VEGF-B_{167}

Echocardiography and magnetic resonance imaging study

Line Lottonen-Raikaslehto[1], Riina Rissanen[1], Erika Gurzeler[1], Mari Merentie[1], Jenni Huusko[1], Jurgen E. Schneider[2], Timo Liimatainen[1], Seppo Ylä-Herttuala[1, 3, 4]

[1]Department of Biotechnology and Molecular Medicine, A. I. Virtanen Institute for Molecular Sciences, Faculty of Health Sciences, University of Eastern Finland, Kuopio, Finland; [2]Radcliffe Department of Medicine, Division of Cardiovascular Medicine, University of Oxford, UK; [3]Gene Therapy Unit, Kuopio University Hospital, Kuopio, Finland; [4]Science Service Center, Kuopio University Hospital, Kuopio, Finland

Short title: Cardiovascular imaging study of left ventricular remodelling

The authors declare no conflicts of interest.

Correspondence:

Seppo Ylä-Herttuala, MD, PhD, FESC

A.I.Virtanen Institute University of Eastern Finland P.O.Box 1627

FI-70211 Kuopio, Finland

Tel. +358-40-3552075

E-mail: seppo.ylaherttuala@uef.fi

ABSTRACT

Cardiac-specific overexpression of vascular endothelial growth factor (VEGF)-B_{167} is known to induce left ventricular hypertrophy due to altered lipid metabolism, in which ceramides accumulate to the heart and cause mitochondrial damage. The aim of this study was to evaluate and compare different imaging methods to find the most sensitive way to diagnose at early stage the progressive left ventricular remodelling leading to heart failure. Echocardiography and cardiovascular magnetic resonance imaging were compared for imaging the hearts of transgenic mice with cardiac-specific overexpression of VEGF-B_{167} and wild-type mice from 5 to 14 months of age at several timepoints. Disease progression was verified by molecular biology methods and histology. We showed, that left ventricular remodelling is already ongoing at the age of 5 months in transgenic mice leading to heart failure by the age of 14 months. Measurements from echocardiography and cardiovascular magnetic resonance imaging revealed similar changes in cardiac structure and function in the transgenic mice. Changes in histology, gene expressions and electrocardiography supported the progression of left ventricular hypertrophy. Longitudinal relaxation time in rotating frame ($T_{1\rho}$) in cardiovascular magnetic resonance imaging could be suitable for detecting severe fibrosis in the heart. We conclude, that cardiac-specific overexpression of VEGF-B leads to left ventricular remodelling at early age and is a suitable model to study heart failure development with different imaging methods.

Key words: Cardiovascular imaging, left ventricular hypertrophy, heart failure, vascular endothelial growth factor –B, mouse ECG

INTRODUCTION

Death rates from cardiovascular diseases have declined, but the burden of the disease remains high despite preventive actions and improved cardiovascular procedures (Go et al. 2014). Aging population and improved survival from other cardiovascular diseases increase the prevalence of heart failure (HF), which has transformed into a chronic disease often with a poor prognosis (Mudd, Kass 2008, Farmakis et al. 2015).

There is a clear need to develop imaging techniques for early diagnostics. Echocardiography has been the golden standard for evaluating left ventricular (LV) function, but the observer dependency and limitations in acoustic access and heart structure visualization impair the accuracy and reproducibility of the method (Jensen 2007). Three-dimensional (3-D) visualization of the LV by cardiovascular magnetic resonance imaging (CMR) has become useful in patients, where it is technically difficult to perform echocardiography and/or LV size and function are abnormal (Bellenger et al. 2000, Amundsen et al. 2011).

T_2-weighted CMR has been used to show the myocardial oedema in acute infarction (Abdel-Aty et al. 2004) and active inflammation in the myocardium (Mirakhur et al. 2013). Decrease in T_2 value has been associated with interstitial collagen accumulation in the myocardium of diabetic mice (Loganathan et al. 2006), but also increased T_2 value has been reported in spontaneously hypertensive rats with increased collagen deposition (Grover-McKay et al. 1991, Caudron et al. 2013). Tissue characterization with late gadolinium enhancement (LGE) is often restricted due to contraindications to gadolinium. T_1 relaxation in the rotating frame of reference ($T_{1\rho}$) is a sensitive marker for macromolecular-water interaction in environment with collagen and proteoglygan

accumulation without the need for exogenous contrast agents (Grohn et al. 2000, Witschey et al. 2012). However, very few studies reporting the use of $T_{1\rho}$ in cardiac diseases have been published. Significant increase in $T_{1\rho}$ time at the infarction site has been reported 1, 3 and 8 weeks after the acute incident (Witschey et al. 2012, Musthafa et al. 2013). A recent study applying $T_{1\rho}$ weighted imaging in patients suffering from hypertrophic cardiomyopathy revealed that the fibrotic area size measured from $T_{1\rho}$ map correlated significantly with LGE positive areas (Wang et al. 2015). Fibrosis in noninfarcted myocardium is associated with pathological remodelling of the heart and the amount of fibrosis has been shown to correlate to hospitalization for HF, death or both. Identification of the myocardial fibrosis would enable the use of therapies, which could reduce fibrosis and prevent adverse outcomes. (Diez et al. 2002, Schelbert et al. 2015.)

The role of vascular endothelial growth factor (VEGF)-B in metabolism and cardiac function has been under investigation in recent years. Unlike transgenic rats expressing the human VEGF-B gene or VEGF-B_{186} isoform, cardiac-specific overexpression of VEGF-B_{167} in mice leads to the accumulation of ceramides in the heart (Karpanen et al. 2008, Kivela et al. 2014). The transgenic (TG) mice show concentric LV hypertrophy without compromising the systolic function of the heart until one year of age (Karpanen et al. 2008).

In this study we showed that structural and functional changes in progressive LV hypertrophy can be detected by echocardiography and CMR. Electrocardiography showed depolarization and repolarization abnormalities connected to structural changes in LV. Elevated natriuretic peptide levels showed initiation of LV remodelling long before clinical signs of deteriorated function. A correlation between diffuse fibrosis grading and $T_{1\rho}$ relaxation time from CMR was found, and to our best knowledge this is one of the first studies using $T_{1\rho}$ in imaging pathological remodelling of the heart.

MATERIALS AND METHODS

Experimental animals

Five to fourteen months old TG male mice with cardiac-specific overexpression of human VEGF-B_{167} on a C57Bl/6J background (n=16) and their wild-type male littermates (n=15) were used to study the heart failure development with echocardiography and CMR. Transgene was targeted to the heart by a myocardium-specific αMHC-promoter (Karpanen et al. 2008). 11 mice were imaged at all timepoints (5, 7, 10, 12 and 14 months) and sacrificed at the age of 14 months. An additional 20 mice in total were imaged and sacrificed either at 5 or 10 months of age to collect histological samples. The animals were kept in standard housing conditions in The National Laboratory Animal Center of The University of Eastern Finland. Diet and water were provided *ad libitum*. All animal procedures were approved by The Animal Experiment Board in Finland and carried out in accordance with the guidelines of the Experimental Animal Committee of the University of Eastern Finland.

Echocardiography and electrocardiogram

Echocardiographic measurements were performed at the age of 5, 7, 10, 12 and 14 months using a Vevo770 Ultrasound System (VisualSonics Inc., Toronto, ON, Canada) and the electrocardiogram

(ECG) was monitored during the echocardiography as described earlier (Huusko et al. 2010). Briefly a high-frequency ultrasound probe (RMV-707B) operating at 30 MHz, with a focal depth of 12.7 mm was used. The animals were anesthetized with isoflurane (induction: 4.5 % isoflurane, 450 ml/min air, maintenance: 2.0 % isoflurane, 200 ml/min air, Baxter International Inc., Deerfield, IL, USA). Ejection fraction (EF), LV mass, LV diastolic wall thickness and LV volume in diastole were determined from parasternal short-axis (SAX) M-mode measurements. EF was calculated by the Vevo770 software by using the Teicholz formula.

Electrocardiogram (ECG) analyses were performed as described thoroughly in Merentie et al 2015 (Merentie et al. 2015). Briefly, an ECG sample of 30 s of each mouse was analyzed and time intervals were measured from the mean curve of the ECG sample with a specially made MatLab analysis program (The MathWorks Inc., MA, USA; Kubios HRV analysis program version 2.0 beta 4, Department of Physics, University of Eastern Finland).

Cardiovascular magnetic resonance imaging

All CMR experiments were performed at 9.4 T magnet, which was equipped with a Varian DirectDrive^{TM} console (Varian Inc., Palo Alto, CA). Mice were placed prone on a pad filled with circulating warm water, and the pad inside the quadrature volume radiofrequency (RF) transceiver with coil diameter of 35 mm (Rapid Biomed, Rimpar, Germany). CMR experiments were performed at 5, 7, 10, 12 and 14 months of age.

The CMR protocol consisted of multi-slice SAX gradient echo cine imaging, T_2-mapping and $T_{1\rho}$ mapping. Cine images were acquired with gradient echo based sequence repetition time 4.6 ms, echo time 2.1 ms, field-of-view 30 x 30 mm2, matrix size 256 x 256 and 1 mm slice thickness. 15-18 cine frames were acquired within the ECG R-R interval and 10 slices covered the whole myocardium. For $T_{1\rho}$ adiabatic, a continuous wave sequence with nominal RF power of 29.3 mT (=1250 Hz), spin-lock durations 0, 18, 36, and 54 ms were applied as previously described (Musthafa et al. 2013). The image readout was achieved by a segmented gradient echo sequence with repetition time 3.0 ms, echo time 1.6 ms, four k-space lines were acquired after 1 s delay and weighting pulse, field-of-view 30 x 30 mm^2, matrix size 128 x 128 points. T_2 was measured similarly as $T_{1\rho}$, but the spin-lock pulse was replaced by adiabatic double spin echo sequence with echo times 0, 7, 14, 21, 28, and 35 ms. $T_{1\rho}$ and T_2 maps were created from 1 mm thick short-axis slice at the middle of the left ventricle.

The data were analyzed as described earlier (Musthafa et al. 2013). Briefly, LV volumes and functional parameters were calculated based on the end-systolic and end-diastolic cine frames. The left ventricle contours in systole and diastole were drawn in each slice from apex to valve level of the heart and the volumes were calculated to obtain end-diastolic and end-systolic volumes (EDV and ESV) of the LV and myocardial wall volume. EF [(1-ESV/EDV) x 100] and LV mass (myocardium wall volume in diastole x conversion coefficient 1.05g/cm^3) were calculated manually. $T_{1\rho}$ and T_2 relaxation maps were reconstructed from image signal intensities and pixel-by-pixel manner and relaxation times were determined from the selected region of interest in a MatLab based platform (The MathWorks Inc., MA, USA; Aedes software package, aedes.ue.fi).

Immunohistochemistry

Heart samples were immersion fixed in 4 % paraformaldehyde-15 % sucrose for 4 hours and in 15 % sucrose overnight. 5 µm thick paraffin-embedded sections were stained to analyse myocardial fibrosis (Masson Trichrome, Accustain trichrome stains, Sigma-Aldrich, USA), apoptosis (Cleaved Caspase -3, Asp175, dilution 1:250, Cell Signaling Technology, USA), proliferation (Ki-67, ab15580, dilution 1:200, Abcam) and glycogen accumulation (Periodic acid Schiff´s glycogen staining, Sigma-Aldrich, USA). The amount of fibrosis was evaluated from Masson Trichrome stained sections in a blinded fashion and graded on a scale 0-3 as follows: 0 = no fibrosis, 1 = minor fibrosis, 2 = moderate fibrosis and 3 = severe fibrosis. The number of apoptotic cells was calculated from five microscopic fields of Cleaved Caspase -3 stained sections and proliferating cells of Ki-67 stained sections within each animal at x400 magnification. Glycogen accumulation was quantified from three microscopic fields of glycogen-stained sections within each animal at x200 magnification. All microscopic pictures were taken from the site of maximum staining in each section. Photographs of the sections were taken with an Olympus AX70 microscope (Olympus, Tokyo, Japan) and Eclipse Ni-E Nikon microscope (Nikon Instruments Inc., NY, USA).

Quantitative RT-PCR

Total RNA was isolated from heart samples with TRI-Reagent (Sigma-Aldrich, St Louis, MO, USA). Quantitative RT-PCR was performed on a StepOnePlus Real-Time PCR system (Applied Biosystems, Carlsbad, CA, USA). Relative mRNA expression of atrial natriuretic peptide (ANP), brain natriuretic peptide (BNP), cardiac troponin T (cTnT) and peptidylprolyl isomerise A (PPIA) were measured using specific Assays-On-Demand systems (Applied Biosystems, Carlsbad, CA, USA). Expression levels were normalized to PPIA.

Clinical chemistry

Sodium, potassium, lactate dehydrogenase (LDH) and cardiac troponin T (cTnT) were measured from plasma samples collected on the sacrification day at 5, 10 and 14 months of age (Movet Oy, Kuopio, Finland).

Statistical analyses

Results are presented as mean ± SD. Data was analyzed using linear mixed model analysis (IBM Corp. Released 2010. IBM SPSS Statistics for Windows, Version 19.0. Armonk, NY: IBM Corp.) or Student´s t-test. Correlations between fibrosis grading and $T_{1\rho}$ relaxation time or fibrosis grading and T_2 relaxation time were studied with the GraphPad Prism5 software by calculating the value of the Pearson correlation coefficient (r). The used analysing method is stated in the figure legends. $P < 0.05$ was considered statistically significant. The following symbols are used in the figures: * $P < 0.05$, ** $P < 0.01$, *** $P < 0.001$.

RESULTS

LV volume and mass were increased and EF decreased in aged TG mice

Heart structure and function in TG mice overexpressing VEGF-B_{167} in a cardiac-specific manner and their WT littermates were observed by echocardiography and CMR in 5, 7, 10, 12 and 14 months of age. LV volume, EF, heart rate (HR) and LV mass showed similar trends in results with both imaging methods.

LV volume (Figure 1 a, b) increased slowly in the TG group and a clear dilatation occurred between 12 and 14 months. LV volume remained unchanged in WT group at all timepoints compared to 5 months baseline. Significant difference between the groups was seen at the age of 14 months, when LV volume measured by echocardiography was 144 μl in TG mice and 79 μl in WT mice compared to CMR measurements of 95 μl and 43 μl. Increase in LV volume in TG mice from 5 to 14 months of age was 89 % ($P < 0.001$) measured by echocardiography and 199 % ($P < 0.001$) measured by CMR. Similarly, LV mass increased slowly in TG group with aging and was significantly different between TGs and WTs at 14 months timepoint detected with echocardiography (TG 215 mg and WT 156 mg) and CMR (TG 172 mg and WT 103 mg) (Figure 1 c, d). Percentage increase in LV mass in TG mice from 5 to 14 months of age was 59 % ($P < 0.01$) measured by echocardiography and 118 % ($P < 0.001$) measured by CMR. At the age of 14 months significantly enlarged cardiomyocytes were detected in TG mice when compared to WT mice. On average TG mice had 74 cardiomyocytes and WT mice had 93 cardiomyocytes in a x400 microscopic view ($P < 0.001$ by Student´s t-test, data not shown). LV anterior wall or posterior wall thickness did not differ significantly between TG and WT mice at any timepoint (data not shown).

Systolic function measured by EF (Fig. 1 e, f) was significantly impaired in the TG group at the age of 14 months as measured by echocardiography (TG EF % 42 and WT EF % 68). However, EF did not differ between TG and WT mice at the earlier timepoints. The decreased EF was also seen with CMR at the 14 months timepoint (TG EF% 53 and WT EF % 63), but the difference compared to WTs was smaller than seen in echocardiography. Decrease in EF in TG mice from 5 to 14 months of age was 34 % measured by echocardiography ($P < 0.001$) and 25 % measured by CMR (P not significant).

Aged TG mice developed diffuse fibrosis in the heart

Progression of LVH led to diffuse myocardial fibrosis in TG mice, whereas WT mice maintained the normal morphology in the heart in all timepoints. Fibrosis was graded from Masson Trichrome stained sections (Figure 2 a-h) and a significant difference between TG and WT mice was detected at 10 and 14 months timepoints (Figure 2 i). No significant differences in TG and WT mice were observed, when average relaxation times from reconstructed $T_{1\rho}$ and T_2 maps from CMR images were compared (data not shown). However, correlation ($r = 0.87$, $^*P < 0.03$) between the fibrosis grading and $T_{1\rho}$ relaxation time in TG mice at the age of 14 months was found in this study (Figure 2 j, h). No correlation was observed between fibrosis grading and T_2 time (data not shown).

Function of the heart deteriorated at the age of 14 months, but no significant differences were observed in glycogen accumulation (TG 4.8 % / WT 3.2 %, evaluated from PAS-stained sections),

number of apoptotic cells (TGs 1.9 / WTs 1.2 %, caspase-3 -staining) or number of proliferating cells (4.0 % / 4.3 %, Ki-67 -staining) when TGs and WTs were compared (data not shown).

LV fibrosis and dilatation in TG mice affected electrical function of the heart measured by electrocardiogram

PQ interval, showing the time from the beginning of atrial depolarization to the beginning of ventricular depolarization, started to prolong after 5 months of age and difference compared to WT mice was significant at 10, 12 and 14 months of age (Fig. 3 a, e-h). TGs had significantly longer QRS time at the age of 14 months indicating changes in ventricular depolarization (data not shown). QRSp time referring to ventricular depolarization and early repolarization was significantly longer in TG mice compared to WT mice at all ages showing that repolarization was affected earlier than depolarization (Figure 3 b, e-h).

QT time, representing the duration of ventricular depolarization and repolarization tended to prolong in TG mice with aging (Figure 3 c, e, g). The corrected QT time QTc [mean QT / $(RR/100)^{1/2}$] (Mitchell, Jeron & Koren 1998) showed the same trend at all timepoints as the absolute value of QT, which is preferred in anesthetized mice (Speerschneider, Thomsen 2013a). TG mice had significantly lower heart rate after 5 months of age compared to WT mice (Figure 3 d).

In TG mice the prevalence of premature atrial complexes was 9 % in 10 months old, 33% in 12 months old and 17 % in 14 months old mice. One out of six TG mice developed second-degree atrioventricular (AV) block at the age of 12 months and at the later timepoint it proceeded to third-degree AV block. In WT mice no premature atrial complexes were detected, however, a single premature ventricular complex was seen in one 14 months old WT mouse during ECG registration. Third-degree AV block was also detected from one WT mouse at the age of 10 months.

Expression of natriuretic peptides increased in TG mice already at the age of 5 months

In TG mice increased expression of ANP mRNA was detected at 5, 10 and 14 months of age (Figure 4 a) and increased expression of BNP at 10 and 14 months of age (Figure 4 b) when compared to WT group. cTnT was decreased in TG group at all timepoints as compared to WT group (Figure 4 c).

There were no differences between TG and WT mice in sodium and potassium levels in plasma at any timepoint (data not shown). LDH was significantly higher in TG group compared to WT at the age of 14 months (TG 746 U/l and WT 292 U/l, $*P < 0.05$, SPSS Linear Mixed Model Analysis), but at earlier timepoints there were no differences (data not shown). Troponin T was measured from plasma but it was undetectable in both groups.

DISCUSSION

HF is a chronic disease with a poor prognosis and there is a clear need to develop imaging techniques for early diagnostics. Therefore we compared echocardiography and different CMR methods in detecting the progression of LVH leading to HF in mice with cardiac-specific overexpression of

VEGF-B_{167}. $T_{1\rho}$ CMR was studied in detecting diffuse myocardial fibrosis. Results from ECG and gene expression analyses were combined to findings from the imaging data.

Technical difficulties in performing echocardiography associated with abnormal LV structure and function have made three-dimensional (3D) visualization of the LV by CMR a favoured method for patients with cardiac disease (Bellenger et al. 2000, Amundsen et al. 2011). In our study both echocardiography and CMR showed the LV mass increase in hypertrophy and LV dilatation attached to HF progression, however, the percentual increases in LV mass and volume from 5 to 14 months of age in TG mice were higher when measured by CMR. Contrary to previously reported concentric LVH in mice with cardiac-specific overexpression of VEGF-B_{167} (Karpanen et al. 2008), we did not detect differences in LV anterior or posterior wall thicknesses between TG and WT mice at any timepoint, which indicates eccentric type of LVH with increased LV volume in this study. TG mice were originally in FVB background and our TG mice were further bred into C57Bl/6J background, which seems to be the differing factor between these studies. Background of FVB or C57Bl has been shown to have influence on the phenotype in other TG mice in previous publications (Rose-Hellekant, Gilchrist & Sandgren 2002, Haluzik et al. 2004), and this may explain by unknown mechanism the different LVH type detected in this study.

Decrease in EF at the age of 14 months in TG mice was detectable with both imaging methods, but echocardiography gave lower values than CMR, which has been shown earlier in infarcted heart (Bellenger et al. 2000). The analysis method differs between echocardiography and CMR, which may explain the differences in results. Echocardiographic measurements are more prone to errors, as the slice selection for one-dimensional M-mode measurements during imaging has a major impact on the outcome. 3D echocardiography has been shown to be more accurate and reproducible in measuring LV volumes and EF than two-dimensional (2D) echocardiography, which is an often used method in adult cardiology (Dorosz et al. 2012). In CMR analysis the whole LV can be analysed objectively without making assumptions about the heart structure (Schneider et al. 2006). In diseased heart CMR would be a preferable imaging method, although echocardiography due to its easy availability can be used for screening mice or patients in the clinic for further imaging.

Fibrosis is associated with pathological remodelling of the LV and HF progression. Early detection of fibrosis would be beneficial in diagnosing heart diseases, following the disease progression and enabling therapies, which could reduce the fibrosis in the heart (Diez et al. 2002). Indeed, diffuse fibrosis detected in the dilated LVs of TG mice at the age of 14 months in this study may explain the function loss in the heart.

T_1 relaxation in the rotating frame of reference ($T_{1\rho}$) is a sensitive marker for macromolecular-water interaction in extracellular space with collagen and proteoglycan accumulation. High contrast with $T_{1\rho}$ has been shown similarly to late gadolinium enhancement (LGE) between myocardial infarction and remote myocardium thus acting like an endogenous contrast agent, and providing an imaging method for patients with contraindications for exogenous contrast agents. (Grohn et al. 2000, Witschey et al. 2012, Musthafa et al. 2013.) $T_{1\rho}$ CMR in cardiovascular diseases has not been widely studied. In hypertrophic cardiomyopathy large fibrotic areas detected with LGE CMR correlated with those measured by $T_{1\rho}$ from the patients (Wang et al. 2015), but in our study diffuse fibrosis did not change the average $T_{1\rho}$ relaxation time of the whole myocardium of the TG mice compared to WTs. However, $T_{1\rho}$ relaxation time tended to be increased and T_2 relaxation time was unaltered in TG mice with significant myocardial fibrosis. Correlation between the severity of the diffuse fibrosis

and $T_{1\rho}$ relaxation time was shown in this study. This indicates that $T_{1\rho}$ CMR might be useful in detecting moderate-severe diffuse fibrosis from the whole myocardium.

14 months old TG mice had widened QRS complex, indicating an increase in the duration of ventricular depolarization, which has been associated with LVH and HF in humans (Oikarinen et al. 2004) and mice (Boulaksil et al. 2010, Speerschneider, Thomsen 2013). QRSp duration, measuring LV depolarization and early repolarization, was prolonged at all timepoints in TG mice compared to WT mice indicating repolarization abnormalities already from 5 months of age in TG mice. Indeed, QRSp duration and LV mass have been shown to correlate in previous studies (Merentie et al. 2015). Time from the start of atrial depolarization to the start of ventricular depolarization (PQ-time) has been shown to be under 55-56 ms in healthy young mice (Merentie et al. 2015, Kaese, Verheule 2012). PQ time > 60 ms has been suggested to refer to the first degree atrioventricular block in mice (Merentie et al. 2015), which was detected from 10 months onwards in TG mice. The electrocardiographic changes associated with cardiac-specific overexpression of VEGF-B have not been shown before according to our knowledge.

Interestingly, in this study TG mice had significantly lower mRNA levels of cTnT already from the age of 5 months, which could indicate contractility defects. cTnT, the subunit which connects the troponin complex to tropomyosin, is known to regulate the calcium-mediated interaction between actin and myosin and has a crucial role in regulating the contractility of the heart (Zhang et al. 2011). Several mutations in the gene coding cTnT are known to cause familial hypertrophic cardiomyopathy or dilated hypertrophy (Gomes et al. 2004). TG mice having lower cTnT expression in the heart have been shown to have increased ANP transcription, interstitial fibrosis and diastolic dysfunction. Mitochondrial dysfunction due to degeneration and lipid accumulation were also observed in mice with reduced levels of cTnT. (Tardiff et al. 1999.) Increased ANP expression and diffuse fibrosis shown in this study and formerly reported mitochondrial dysfunction (Karpanen et al. 2008) in mice with cardiac-specific overexpression of VEGF-B_{167} could be associated with the decrease in cTnT expression.

Natriuretic peptides ANP and BNP, expressed in response to increased wall stretch in the heart and factors regulating hypertrophy, are known to reduce the peripheral resistance and volume load by increasing vasorelaxation, natriuresis, diuresis and lowering blood pressure (Tavi et al. 2001, Kerkela, Ulvila & Magga 2015). The systemic effects of ANP and BNP were shown as lower blood pressure (Karpanen et al. 2008) and heart rate in the studied TG mice compared to WT mice. Detected increase in the ANP and BNP expression has been connected to the remodelling process of the LV leading to cardiac hypertrophy and fibrosis (Kerkela, Ulvila & Magga 2015), which could indicate that in TG mice remodelling was ongoing already at the age of 5 months. Pathological remodelling seems to be associated with long-term overexpression of VEGF-B_{167} isoform in the heart, because LVH induced by overexpression of human VEGF-B gene or VEGF-B_{186} in rat heart does not affect cardiac function or expression of hypertrophic markers even at older age (Kivela et al. 2014).

Diagnostic measurements for diastolic dysfunction were not done in this study, but the increased LV mass due to cardiac hypertrophy in TG mice and elevated expression of natriuretic peptides, especially BNP, refer to HF with preserved EF (HFpEF) (Paulus et al. 2007, Senni et al. 2014). Decreased cTnT expression supports the assumption about HFpEF (Tardiff et al. 1999). Our data indicates that HFpEF may be associated with the development of HF with reduced EF (HFrEF)

featured by LV dilatation in mice with cardiac-specific overexpression of VEGF-B_{167}, although the causality of the HF types is still unknown.

We conclude that cardiac-specific overexpression of VEGF-B_{167} isoform in mice leads to HF. The associated changes to eccentric LV remodelling, namely an increase in LV mass and LV volume and a decrease in EF, could be visualized similarly with echocardiography and CMR. $T_{1\rho}$ CMR showed a clear potential in detecting moderate-severe diffuse myocardial fibrosis.

Acknowledgements

The authors want to thank Marja-Leena Lamidi for the help with statistical analyses, the students from Cardiovascular Imaging group from A.I. Virtanen Institute, University of Eastern Finland, for the help with CMR, Marike H. Dijkstra for the help with molecular biology methods, Kari Alitalo and Riikka Kivelä for the valuable comments and The National Laboratory Animal Center of the University of Eastern Finland (Kuopio campus). This work was supported by Finnish Academy, Sigrid Juselius Foundation, Finnish Foundation for Cardiovascular Research, Ida Montin Foundation and The Finnish Medical Foundation. J.E.S is BHF Senior Basic Science Research Fellow (FS/11/50/29038).

The authors declare no conflict of interest.

References

Abdel-Aty, H., Zagrosek, A., Schulz-Menger, J., Taylor, A.J., Messroghli, D., Kumar, A., Gross, M., Dietz, R. & Friedrich, M.G. 2004, "Delayed enhancement and T2-weighted cardiovascular magnetic resonance imaging differentiate acute from chronic myocardial infarction", *Circulation,* vol. 109, no. 20, pp. 2411-2416.

Amundsen, B.H., Ericsson, M., Seland, J.G., Pavlin, T., Ellingsen, O. & Brekken, C. 2011, "A comparison of retrospectively self-gated magnetic resonance imaging and high-frequency echocardiography for characterization of left ventricular function in mice", *Laboratory animals,* vol. 45, no. 1, pp. 31-37.

Bellenger, N.G., Burgess, M.I., Ray, S.G., Lahiri, A., Coats, A.J., Cleland, J.G. & Pennell, D.J. 2000, "Comparison of left ventricular ejection fraction and volumes in heart failure by echocardiography, radionuclide ventriculography and cardiovascular magnetic resonance; are they interchangeable?", *European heart journal,* vol. 21, no. 16, pp. 1387-1396.

Boulaksil, M., Winckels, S.K., Engelen, M.A., Stein, M., van Veen, T.A., Jansen, J.A., Linnenbank, A.C., Bierhuizen, M.F., Groenewegen, W.A., van Oosterhout, M.F., Kirkels, J.H., de Jonge, N., Varro, A., Vos, M.A., de Bakker, J.M. & van Rijen, H.V. 2010, "Heterogeneous Connexin43 distribution in heart failure is associated with dispersed conduction and enhanced susceptibility to ventricular arrhythmias", *European journal of heart failure,* vol. 12, no. 9, pp. 913-921.

Caudron, J., Mulder, P., Nicol, L., Richard, V., Thuillez, C. & Dacher, J.N. 2013, "MR relaxometry and perfusion of the myocardium in spontaneously hypertensive rat: correlation with

histopathology and effect of anti-hypertensive therapy", *European radiology,* vol. 23, no. 7, pp. 1871-1881.

Diez, J., Querejeta, R., Lopez, B., Gonzalez, A., Larman, M. & Martinez Ubago, J.L. 2002, "Losartan-dependent regression of myocardial fibrosis is associated with reduction of left ventricular chamber stiffness in hypertensive patients", *Circulation,* vol. 105, no. 21, pp. 2512-2517.

Dorosz, J.L., Lezotte, D.C., Weitzenkamp, D.A., Allen, L.A. & Salcedo, E.E. 2012, "Performance of 3-dimensional echocardiography in measuring left ventricular volumes and ejection fraction: a systematic review and meta-analysis", *Journal of the American College of Cardiology,* vol. 59, no. 20, pp. 1799-1808.

Farmakis, D., Stafylas, P., Giamouzis, G., Maniadakis, N. & Parissis, J. 2015, "The medical and socioeconomic burden of heart failure: A comparative delineation with cancer", *International journal of cardiology,* vol. 203, pp. 279-281.

Go, A.S., Mozaffarian, D., Roger, V.L., Benjamin, E.J., Berry, J.D., Blaha, M.J., Dai, S., Ford, E.S., Fox, C.S., Franco, S., Fullerton, H.J., Gillespie, C., Hailpern, S.M., Heit, J.A., Howard, V.J., Huffman, M.D., Judd, S.E., Kissela, B.M., Kittner, S.J., Lackland, D.T., Lichtman, J.H., Lisabeth, L.D., Mackey, R.H., Magid, D.J., Marcus, G.M., Marelli, A., Matchar, D.B., McGuire, D.K., Mohler, E.R., Moy, C.S., Mussolino, M.E., Neumar, R.W., Nichol, G., Pandey, D.K., Paynter, N.P., Reeves, M.J., Sorlie, P.D., Stein, J., Towfighi, A., Turan, T.N., Virani, S.S., Wong, N.D., Woo, D. & Turner, M.B. 2014, "Heart Disease and Stroke Statistics—2014 Update: A Report From the American Heart Association", *Circulation,* vol. 129, no. 3, pp. e28-e292.

Gomes, A.V., Barnes, J.A., Harada, K. & Potter, J.D. 2004, "Role of troponin T in disease", *Molecular and cellular biochemistry,* vol. 263, no. 1-2, pp. 115-129.

Grohn, O.H.J., Kettunen, M.I., Makela, H.I., Penttonen, M., Pitkanen, A., Lukkarinen, J.A. & Kauppinen, R.A. 2000, "Early detection of irreversible cerebral ischemia in the rat using dispersion of the magnetic resonance imaging relaxation time, T1rho", *Journal of cerebral blood flow and metabolism : official journal of the International Society of Cerebral Blood Flow and Metabolism,* vol. 20, no. 10, pp. 1457-1466.

Grover-McKay, M., Scholz, T.D., Burns, T.L. & Skorton, D.J. 1991, "Myocardial collagen concentration and nuclear magnetic resonance relaxation times in the spontaneously hypertensive rat", *Investigative radiology,* vol. 26, no. 3, pp. 227-232.

Haluzik, M., Colombo, C., Gavrilova, O., Chua, S., Wolf, N., Chen, M., Stannard, B., Dietz, K.R., Le Roith, D. & Reitman, M.L. 2004, "Genetic background (C57BL/6J versus FVB/N) strongly influences the severity of diabetes and insulin resistance in ob/ob mice", *Endocrinology,* vol. 145, no. 7, pp. 3258-3264.

Jensen, J.A. 2007, "Medical ultrasound imaging", *Progress in biophysics and molecular biology,* vol. 93, no. 1-3, pp. 153-165.

Kaese, S. & Verheule, S. 2012, "Cardiac electrophysiology in mice: a matter of size", *Frontiers in physiology,* vol. 3, pp. 345.

Karpanen, T., Bry, M., Ollila, H.M., Seppanen-Laakso, T., Liimatta, E., Leskinen, H., Kivela, R., Helkamaa, T., Merentie, M., Jeltsch, M., Paavonen, K., Andersson, L.C., Mervaala, E.,

Hassinen, I.E., Yla-Herttuala, S., Oresic, M. & Alitalo, K. 2008, "Overexpression of vascular endothelial growth factor-B in mouse heart alters cardiac lipid metabolism and induces myocardial hypertrophy", *Circulation research,* vol. 103, no. 9, pp. 1018-1026.

Kerkela, R., Ulvila, J. & Magga, J. 2015, "Natriuretic Peptides in the Regulation of Cardiovascular Physiology and Metabolic Events", *Journal of the American Heart Association,* vol. 4, no. 10, pp. e002423.

Kivela, R., Bry, M., Robciuc, M.R., Rasanen, M., Taavitsainen, M., Silvola, J.M., Saraste, A., Hulmi, J.J., Anisimov, A., Mayranpaa, M.I., Lindeman, J.H., Eklund, L., Hellberg, S., Hlushchuk, R., Zhuang, Z.W., Simons, M., Djonov, V., Knuuti, J., Mervaala, E. & Alitalo, K. 2014, "VEGF-B-induced vascular growth leads to metabolic reprogramming and ischemia resistance in the heart", *EMBO molecular medicine,* vol. 6, no. 3, pp. 307-321.

Loganathan, R., Bilgen, M., Al-Hafez, B. & Smirnova, I.V. 2006, "Characterization of alterations in diabetic myocardial tissue using high resolution MRI", *The international journal of cardiovascular imaging,* vol. 22, no. 1, pp. 81-90.

Merentie, M., Lipponen, J.A., Hedman, M., Hedman, A., Hartikainen, J., Huusko, J., Lottonen-Raikaslehto, L., Parviainen, V., Laidinen, S., Karjalainen, P.A. & Yla-Herttuala, S. 2015, "Mouse ECG findings in aging, with conduction system affecting drugs and in cardiac pathologies: Development and validation of ECG analysis algorithm in mice", *Physiological reports,* vol. 3, no. 12, pp. 10.14814/phy2.12639.

Mirakhur, A., Anca, N., Mikami, Y. & Merchant, N. 2013, "T2-weighted imaging of the heart--a pictorial review", *European Journal of Radiology,* vol. 82, no. 10, pp. 1755-1762.

Mudd, J.O. & Kass, D.A. 2008, "Tackling heart failure in the twenty-first century", *Nature,* vol. 451, no. 7181, pp. 919-928.

Musthafa, H.S., Dragneva, G., Lottonen, L., Merentie, M., Petrov, L., Heikura, T., Yla-Herttuala, E., Yla-Herttuala, S., Grohn, O. & Liimatainen, T. 2013, "Longitudinal rotating frame relaxation time measurements in infarcted mouse myocardium in vivo", *Magnetic resonance in medicine : official journal of the Society of Magnetic Resonance in Medicine / Society of Magnetic Resonance in Medicine,* vol. 69, no. 5, pp. 1389-1395.

Oikarinen, L., Nieminen, M.S., Viitasalo, M., Toivonen, L., Jern, S., Dahlof, B., Devereux, R.B., Okin, P.M. & LIFE Study Investigators 2004, "QRS duration and QT interval predict mortality in hypertensive patients with left ventricular hypertrophy: the Losartan Intervention for Endpoint Reduction in Hypertension Study", *Hypertension,* vol. 43, no. 5, pp. 1029-1034.

Paulus, W.J., Tschope, C., Sanderson, J.E., Rusconi, C., Flachskampf, F.A., Rademakers, F.E., Marino, P., Smiseth, O.A., De Keulenaer, G., Leite-Moreira, A.F., Borbely, A., Edes, I., Handoko, M.L., Heymans, S., Pezzali, N., Pieske, B., Dickstein, K., Fraser, A.G. & Brutsaert, D.L. 2007, "How to diagnose diastolic heart failure: a consensus statement on the diagnosis of heart failure with normal left ventricular ejection fraction by the Heart Failure and Echocardiography Associations of the European Society of Cardiology", *European heart journal,* vol. 28, no. 20, pp. 2539-2550.

Rose-Hellekant, T.A., Gilchrist, K. & Sandgren, E.P. 2002, "Strain background alters mammary gland lesion phenotype in transforming growth factor-alpha transgenic mice", *The American journal of pathology,* vol. 161, no. 4, pp. 1439-1447.

Schelbert, E.B., Piehler, K.M., Zareba, K.M., Moon, J.C., Ugander, M., Messroghli, D.R., Valeti, U.S., Chang, C.H., Shroff, S.G., Diez, J., Miller, C.A., Schmitt, M., Kellman, P., Butler, J., Gheorghiade, M. & Wong, T.C. 2015, "Myocardial Fibrosis Quantified by Extracellular Volume Is Associated With Subsequent Hospitalization for Heart Failure, Death, or Both Across the Spectrum of Ejection Fraction and Heart Failure Stage", *Journal of the American Heart Association,* vol. 4, no. 12, pp. e002613.

Schneider, J.E., Wiesmann, F., Lygate, C.A. & Neubauer, S. 2006, "How to perform an accurate assessment of cardiac function in mice using high-resolution magnetic resonance imaging", *Journal of cardiovascular magnetic resonance : official journal of the Society for Cardiovascular Magnetic Resonance,* vol. 8, no. 5, pp. 693-701.

Senni, M., Paulus, W.J., Gavazzi, A., Fraser, A.G., Diez, J., Solomon, S.D., Smiseth, O.A., Guazzi, M., Lam, C.S., Maggioni, A.P., Tschope, C., Metra, M., Hummel, S.L., Edelmann, F., Ambrosio, G., Stewart Coats, A.J., Filippatos, G.S., Gheorghiade, M., Anker, S.D., Levy, D., Pfeffer, M.A., Stough, W.G. & Pieske, B.M. 2014, "New strategies for heart failure with preserved ejection fraction: the importance of targeted therapies for heart failure phenotypes", *European heart journal,* vol. 35, no. 40, pp. 2797-2815.

Speerschneider, T. & Thomsen, M.B. 2013, "Physiology and analysis of the electrocardiographic T wave in mice", *Acta physiologica (Oxford, England),* vol. 209, no. 4, pp. 262-271.

Tardiff, J.C., Hewett, T.E., Palmer, B.M., Olsson, C., Factor, S.M., Moore, R.L., Robbins, J. & Leinwand, L.A. 1999, "Cardiac troponin T mutations result in allele-specific phenotypes in a mouse model for hypertrophic cardiomyopathy", *The Journal of clinical investigation,* vol. 104, no. 4, pp. 469-481.

Tavi, P., Laine, M., Weckstrom, M. & Ruskoaho, H. 2001, "Cardiac mechanotransduction: from sensing to disease and treatment", *Trends in pharmacological sciences,* vol. 22, no. 5, pp. 254-260.

Wang, C., Zheng, J., Sun, J., Wang, Y., Xia, R., Yin, Q., Chen, W., Xu, Z., Liao, J., Zhang, B. & Gao, F. 2015, "Endogenous contrast T1rho cardiac magnetic resonance for myocardial fibrosis in hypertrophic cardiomyopathy patients", *Journal of cardiology,* vol. 66, no. 6, pp. 520-526.

Witschey, W.R., Zsido, G.A., Koomalsingh, K., Kondo, N., Minakawa, M., Shuto, T., McGarvey, J.R., Levack, M.M., Contijoch, F., Pilla, J.J., Gorman, J.H.,3rd & Gorman, R.C. 2012, "In vivo chronic myocardial infarction characterization by spin locked cardiovascular magnetic resonance", *Journal of cardiovascular magnetic resonance : official journal of the Society for Cardiovascular Magnetic Resonance,* vol. 14, pp. 37-429X-14-37.

Zhang, J., Zhang, H., Ayaz-Guner, S., Chen, Y.C., Dong, X., Xu, Q. & Ge, Y. 2011, "Phosphorylation, but not alternative splicing or proteolytic degradation, is conserved in human and mouse cardiac troponin T", *Biochemistry,* vol. 50, no. 27, pp. 6081-6092.

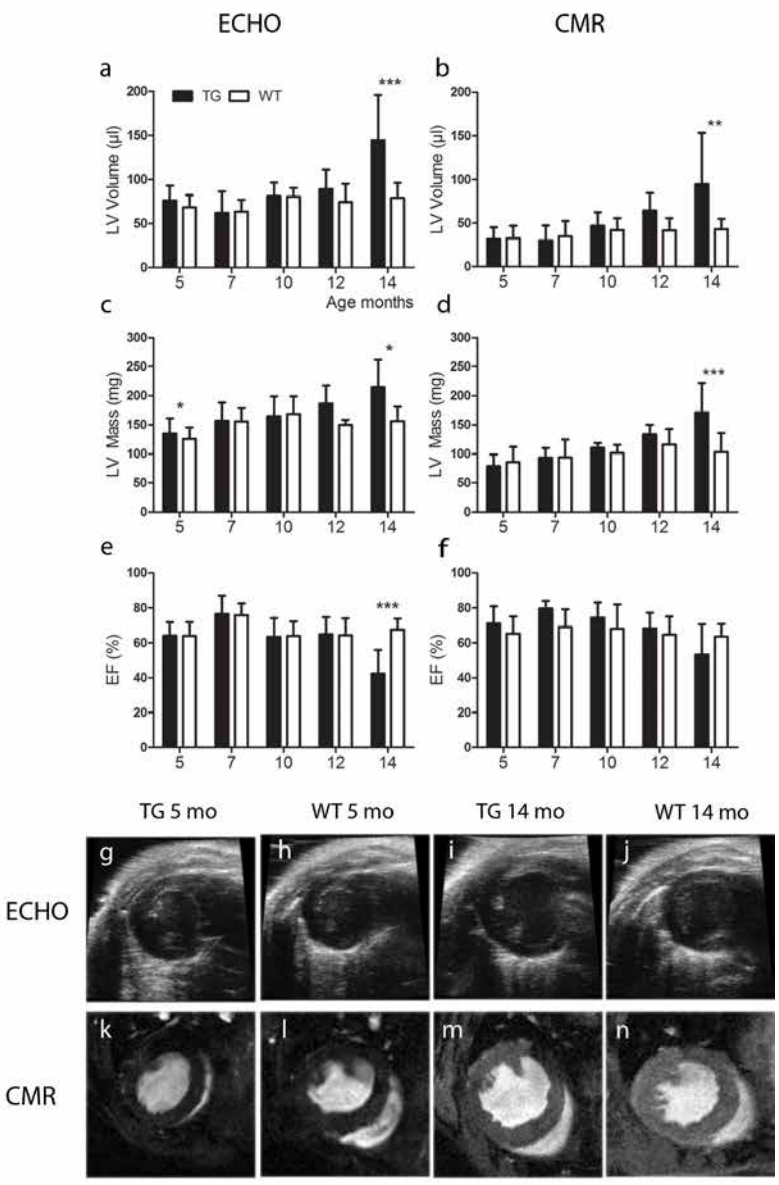

Figure 1. Measurements of cardiac structure and function by echocardiography and CMR. LV volume measured by echocardiography (a) and CMR (b) increased slowly with aging in TG mice and a marked dilatation of the LV was observed at the age of 14 months compared to WT mice. LV mass increased with aging in TG mice and at the age of 14 months the difference compared to WTs was significant measured by both imaging methods (c-d). Ejection fraction (EF), measured with echocardiography, decreased significantly in TG mice at the age of 14 months (e) and the trend was similar when imaged with CMR (f). Representative pictures from TG and WT mice imaged with the echocardiography (g-j) and CMR (k-n) at the age of 5 and 14 months. Mean ± SD, statistical analyses with SPSS Linear Mixed Model Analysis. *P < 0.05, **P < 0.01, ***P < 0.001. TG n=6-11, WT n=5-10.

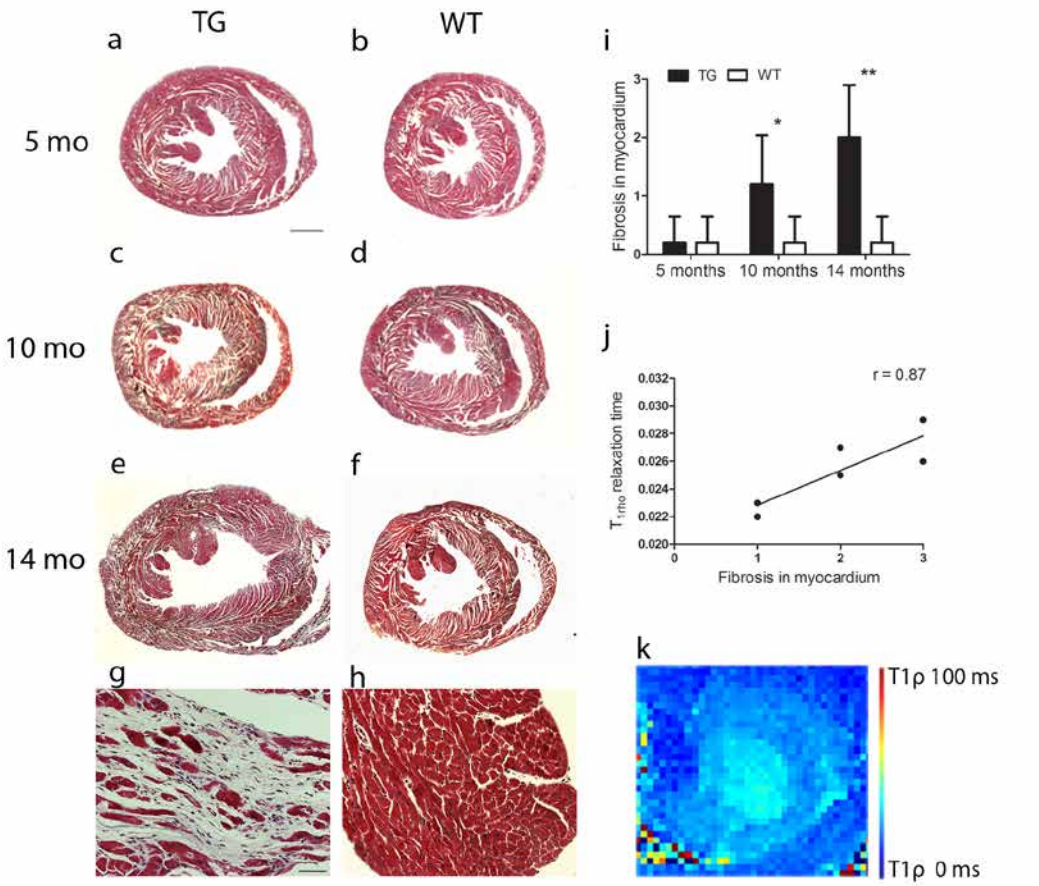

Figure 2. Progression of LVH led to myocardial fibrosis in TG mice. Significant difference in the amount of diffuse myocardial fibrosis was detected from TG mice at the age of 10 and 14 months compared to WT mice, which maintained normal morphology in all timepoints (representative Masson Trichrome stained sections a-h, fibrosis grading i). Fibrosis was graded on a scale 0-3, in which 0 = no fibrosis, 1 = mild fibrosis, 2 = moderate fibrosis and 3 = severe fibrosis (i). Fibrosis grading correlated with $T_{1\rho}$ relaxation time measured from the LV in TG mice by CMR at the age of 14 months (Pearson r = 0.87, *P < 0.03; j). Representative reconstructed $T_{1\rho}$ relaxation time map from 14 months old TG mouse (k). Scale bar 1000 μm (a-f) and 50 μm (g-h). Mean ± SD. TG and WT mice were compared with Student´s t-test at each timepoint. *P < 0.05, **P < 0.01. TG n = 5-6, WT n = 5.

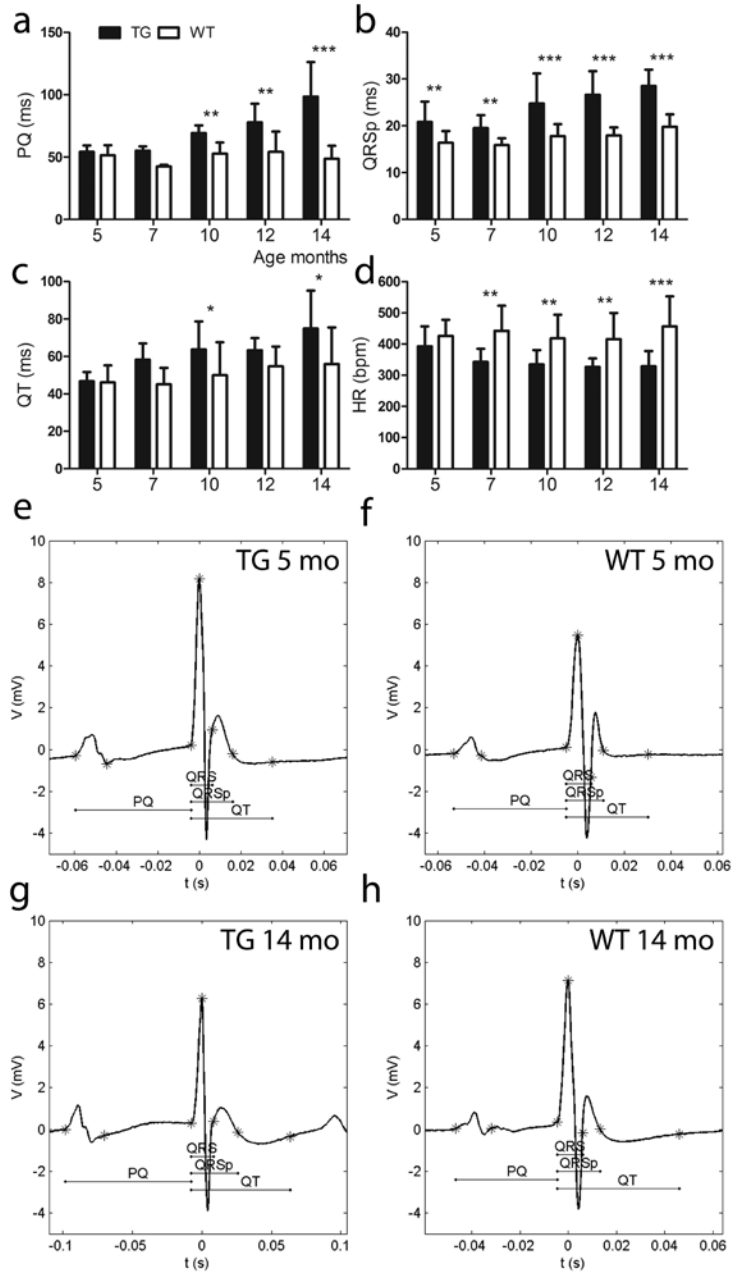

Figure 3. Changes in ECG during LV remodelling. PQ time started to prolong after seven months of age (a) and QRSp time was significantly longer at all ages in TG mice when compared to WT mice (b). TG mice had longer QT time at the age of 10 and 14 months (c) and lower heart rate than WT mice after 5 months of age (d). Representative ECGs from TGs and WTs at the age of 5 months (e-f) and 14 months (g-h). Mean ± SD, statistical analyses with SPSS Linear Mixed Model Analysis. *P < 0.05, **P < 0.01, ***P < 0.001. TG n = 6-11, WT n = 5-10.

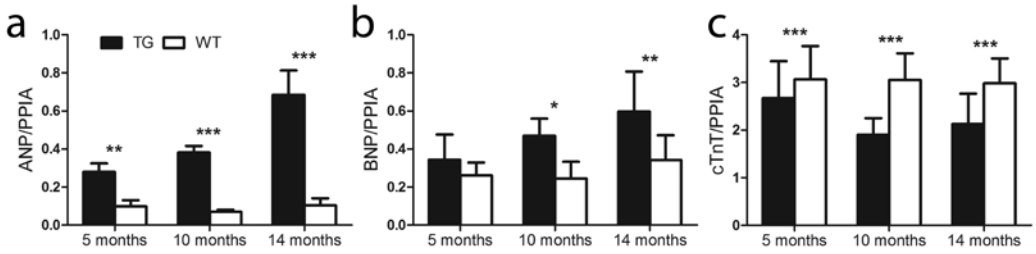

Figure 4. Relative mRNA expression of ANP, BNP and cTnT during LV remodelling. Relative expression of atrial natriuretic peptide (ANP; a) was increased at all ages and brain natriuretic peptide (BNP; b) was increased at the age of 10 and 14 months in TG mice compared to WT mice. The relative expression of cardiac troponin T (cTnT; c) was decreased at all ages among TGs compared to WTs. mRNA expression of ANP, BNP and cTnT were measured by RT-PCR and normalized to PPIA. Mean ± SD, statistical analyses with SPSS Linear Mixed Model Analysis. *P < 0.05, **P < 0.01, ***P < 0.001. TG n = 5-6, WT n = 5.

III

Efficacy and safety of myocardial gene transfer of adenovirus, adeno-associated virus and lentivirus vectors in mouse heart

Merentie M, **Lottonen-Raikaslehto L***, Parviainen V*, Huusko J, Pikkarainen S, Mendel M, Laham-Karam N, Kärjä V, Rissanen R, Hedman M, Ylä-Herttuala S.

Gene Ther 2016 Mar;23(3):296-305.

* Authors with equal contribution.

Gene Therapy (2016), 1–10

www.nature.com/gt

ORIGINAL ARTICLE

Efficacy and safety of myocardial gene transfer of adenovirus, adeno-associated virus and lentivirus vectors in the mouse heart

M Merentie[1], L Lottonen-Raikaslehto[1,8], V Parviainen[1,8], J Huusko[1], S Pikkarainen[1], M Mendel[1,2], N Laham-Karam[1], V Kärjä[3], R Rissanen[1], M Hedman[4,5] and S Ylä-Herttuala[1,6,7]

Gene therapy is a promising new treatment option for cardiac diseases. For finding the most suitable and safe vector for cardiac gene transfer, we delivered adenovirus (AdV), adeno-associated virus (AAV) and lentivirus (LeV) vectors into the mouse heart with sophisticated closed-chest echocardiography-guided intramyocardial injection method for comparing them with regards to transduction efficiency, myocardial damage, effects on the left ventricular function and electrocardiography (ECG). AdV had the highest transduction efficiency in cardiomyocytes followed by AAV2 and AAV9, and the lowest efficiency was seen with LeV. The local myocardial inflammation and fibrosis in the left ventricle (LV) was proportional to transduction efficiency. AdV caused LV dilatation and systolic dysfunction. Neither of the locally injected AAV serotypes impaired the LV systolic function, but AAV9 caused diastolic dysfunction to some extent. LeV did not affect the cardiac function. We also studied systemic delivery of AAV9, which led to transduction of cardiomyocytes throughout the myocardium. However, also diffuse fibrosis was present leading to significantly impaired LV systolic and diastolic function and pathological ECG changes. Compared with widely used AdV vector, AAV2, AAV9 and LeV were less effective in transducing cardiomyocytes but also less harmful. Local administration of AAV9 was safer and more efficient compared with systemic administration.

Gene Therapy advance online publication, 28 January 2016; doi:10.1038/gt.2015.114

INTRODUCTION

The most common cause of death worldwide are cardiovascular diseases, including coronary artery disease and heart failure.[1] Current treatment strategies for ischemic diseases include prevention of disease progression with lifestyle changes and medication, and for patients with critical symptoms, revascularization procedures are applied. However, these conventional therapies cannot be performed for everyone, especially for elderly patients with several comorbidities. Therefore, there is an obvious need to develop efficient and minimally invasive treatment methods for these no-option patients.[2,3] Gene therapy is a promising novel treatment modality for cardiac diseases, and it has shown great potential and efficacy in pre-clinical trials.[2,4–6] Currently, there are five ongoing clinical gene therapy trials aiming to treat patients with coronary artery disease and four trials for developing heart failure treatment. Most commonly, adenovirus (AdV) and adeno-associated virus (AAV) vectors are used for delivering therapeutic genes into myocardium with intracoronary infusion, percutaneous or open-chest intramyocardial injection.[3] In previous cardiovascular clinical trials, the safety has been excellent even in the long-term follow-up.[7,8] However, none of the phase-II/III cardiovascular gene therapy trials have shown clinically relevant positive effects for several reasons, of which low gene transfer efficiency has been associated with several trials. In addition, a lack of a sophisticated efficient delivery method and lack of clinically relevant animal models have contributed to the problem.[2,3,6,9]

AdV vectors have thus far been the most widely used vectors in cardiac gene therapy. They are highly efficient in transducing cardiomyocytes,[4,10] but transgene expression is transient peaking a few days after the gene transfer and lasting for 2–4 weeks.[9,11] AAV vectors are promising gene delivery vectors that provide long-term transgene expression lasting for several months.[11–13] AAV serotype 2 (AAV2) has been commonly used for gene therapy studies, but it has only a moderate transduction efficiency in the heart.[14,15] AAV9 is the most efficient AAV vector of serotypes 1–9 for cardiac gene transfer and has fast onset of gene expression both by systemic route[16] and after direct injection to the left ventricle (LV) wall.[17] Lentivirus (LeV) vectors integrate transgenes into the host genome, thereby providing potential for lifelong expression of the therapeutic protein.[18] LeV has not been widely used for cardiac gene therapy, but it has shown some efficiency in transducing cardiomyocytes in murine models.[18–22] To our knowledge, there are currently no preclinical studies or ongoing clinical trials describing closed-chest/percutaneous intramyocardial gene transfer with AAV or LeV vectors.

In this study, we compared AdV, AAV2, AAV9 and LeV vectors for cardiac gene therapy with regards to transduction efficiency, myocardial damage and cardiac function by transthoracic

[1]Department of Biotechnology and Molecular Medicine, A. I. Virtanen Institute for Molecular Sciences, Faculty of Health Sciences, University of Eastern Finland, Kuopio, Finland; [2]Department of Medical Biotechnology, Faculty of Biochemistry, Biophysics and Biotechnology, Jagiellonian University, Krakow, Poland; [3]Department of Clinical Pathology, Kuopio University Hospital, Kuopio, Finland; [4]Heart Center, Kuopio University Hospital, Kuopio, Finland; [5]Diagnostic Imaging Center, Kuopio University Hospital, Kuopio, Finland; [6]Gene Therapy Unit, Kuopio University Hospital, Kuopio, Finland and [7]Science Service Center, Kuopio University Hospital, Kuopio, Finland. Correspondence: Professor S Ylä-Herttuala, Department of Biotechnology and Molecular Medicine, A. I. Virtanen Institute for Molecular Sciences, Faculty of Health Sciences, University of Eastern Finland, P.O. Box 1627, Kuopio FI-70211 Finland.
E-mail: seppo.ylaherttuala@uef.fi
[8]These authors contributed equal to this work.
Received 20 July 2015; revised 20 October 2015; accepted 21 December 2015; accepted article preview online 24 December 2015

echocardiography (TTE) and electrocardiography (ECG) in order to find the most efficient and safest vector for cardiac gene therapy. We used a sophisticated closed-chest intramyocardial injection method with ultrasound-guidance allowing minimally invasive local gene transfer with one injection through the skin straight into the LV wall. The gene transfer efficacy, safety and biodistribution after systemic AAV9 injections with three viral doses was studied. We show here that compared with widely used AdV vector, AAV2, AAV9 and LeV were not only less effective in transducing cardiomyocytes but also less harmful. Local administration of AAV9 was found to be safer and more efficient compared with systemic administration.

RESULTS

In vivo toxicity

During the follow-up of 28 days, two mice from the AAV9 LacZ intravenous (i.v.) 10^{12} dose group were found dead at day 26. The cause of death remains unknown, but on the previous day, one of the mice was unwilling to move and the body temperature was lower than normal. We did not notice any changes in the behavior of animals in the other treatment groups. There were no macroscopic abnormalities in the collected organs (lung, liver, spleen, kidneys, rectus femoris muscle or testis) at day 28. Changes in the weights of the mice in all groups were within 10% of the d0 weight during the follow-up, indicating that the mice did not have any serious welfare problems.

Transduction efficiencies

Intramyocardial gene transfer of AdV LacZ, AAV2 LacZ, AAV9 LacZ and LeV green fluorescent protein (GFP) led to local transgene expression close to the injection needle tract (Figures 1a–d, arrows). The transduction efficiency in the maximally transduced area near the needle tract in intramyocardially injected mice was quantified as the percentage of transgene-positive cardiomyocytes (Figure 1k). Gene transfer with AdV LacZ resulted in the highest transduction efficiency at d28 (Figures 1e and k). Earlier at d6, the transduction efficiency was slightly lower being 38 ± 9% (data not shown). The transduction efficiencies of AAV2 and AAV9 were at similar level compared with each other but about 50% lower than AdV transduction efficiency at d28 (Figures 1f, g and k). With LeV, the transduction efficiency was about 25% of AdV efficiency (Figures 1h and k). Corresponding to the localization of GFP immunostained cells near the needle tract, GFP-positive cells could be visualized also with native green fluorescence in LeV GFP-injected hearts (data not shown).

After systemic administration of AAV9 LacZ, the transgene expression could be seen throughout the myocardium (Figures 1i and j). For comparing the transduction efficiencies of intramyocardial injections with i.v. injections, the transgene-positive cell coverage was quantified as the size of the transduced area (percentage of the LV area). The transduced area was the largest 6 days after AdV delivery (19 ± 7% of the LV area, result not shown), decreasing toward d28 time point (Figure 1i). Intramyocardial gene transfer of AAV2 LacZ resulted in 10 ± 8%, AAV9 LacZ in 15 ± 3% and LeV GFP in 7 ± 3% transduced areas at d28. In the AAV9 LacZ i.v. group, the transduced area size was 8 ± 8% with the 10^{12} dose and decreased markedly with decreasing doses (Figure 1l).

Myocardial damage

To evaluate the myocardial damage associated with the gene transfers, the amount of fibrosis and inflammation was analyzed from the myocardium. From the intramyocardially injected hearts, the size of the fibrotic scar area was quantified (percentage of the LV area) and amount of inflammation scored with the scale of 0–3. Intramyocardial gene transfer produced a local fibrotic scar area with lymphocyte-intensive inflammatory reaction at the injection site in the LV wall 28 days after the gene transfer (Figures 2c–f, arrows). Apart from the local injury site and its instant vicinity, the morphology of the myocardium was normal in all the study groups. Size of the scar area was the largest after both 'empty' AdV cytomegalovirus (CMV) carrying no transgene and AdV LacZ injection, followed by AAV9 and AAV2 (Figure 2a). LeV led to the smallest scar in the LV wall. Only a minimal scar area (about 1% of the LV area) representing the needle tract was seen in the Needle and NaCl control groups. Similar trend between the groups was seen in the amount of inflammatory cells within the scar area (Figure 2b); both AdV gene transfers led to a severe inflammation followed by AAV9 gene transfer. After AAV2 and LeV injections, mild-to-moderate amount of inflammation was seen. In the Needle and NaCl groups, a few lymphocytes were present in the needle tract, and in addition, a few hypertrophic and/or degenerated myocytes were seen near the needle tract in 50% of the mice in the NaCl group (data not shown). Also, after AdV, AAV2 and AAV9 gene transfers, some degenerated and hypertrophic cardiomyocytes were present around the scar area in all the samples. Instead, in the LeV group a few hypertrophic cardiomyocytes were seen around the scar only in about 30% of the samples. Small amounts of lipofuscin pigment, which is an intralysosomal undegradable waste product accumulating as a response to oxidative damage,[23] was found within few cardiomyocytes in the scar area of intramyocardially treated groups apart from AdV LacZ (data not shown).

With systemic AAV9 injection, both fibrosis and inflammation were assessed by scoring with the scale of 0–3. I.v. administration of AAV9 LacZ with 10^{12} dose led to diffuse fibrosis throughout the myocardium, the amount of which was scored to be moderate (Figures 2g, i and j). In the AAV9 10^{11} and 10^{10} groups, there was only minor fibrosis, if any, seen as small focal spots of the scar tissue and morphology appeared to be mainly normal (Figures 2g, k and l). Similarly, the amount of inflammatory cells, mainly lymphocytes, was moderate in myocardium after AAV9 LacZ 10^{12} treatment and was decreased to modest to none in the 10^{11} and 10^{10} groups (Figure 2h). In the 10^{12} dose group, a few degenerated and hypertrophic cardiomyocytes were seen around the fibrotic areas; instead, in the 10^{11} and 10^{10} dose groups, morphology was mainly normal (data not shown). No lipofuscin pigment was seen in the AAV9 LacZ i.v. injected groups (data not shown).

LV size and function

The effects of the gene transfers to the LV size and function were quantified with echocardiography. In the intramyocardially injected hearts, acute edema at the injection site was seen as an increase in LV anterior wall (LVAW) thickness in diastole 6 days after gene transfers especially in the AdV CMV and AdV LacZ groups, and also to a smaller extent in the NaCl, AAV2 and LeV groups (Figure 3a). In addition, AdV LacZ gene transfers led to thinning of the LVAW at d28 owing to fibrosis at the injection sites (Figures 3a, g and j). In the AdV LacZ group, the LV end-diastolic diameter (LVEDD, Figure 3b) and LV volume (data not shown) were increased at d28, indicating LV dilatation. Also systolic LV function measured as Teicholz ejection fraction (EF) was significantly decreased in the AdV LacZ group at d28 owing to almost akinetic LVAW at the site of the injection scar, instead the LV posterior wall (LVPW) was contracting normally (Figures 3c, g and j).

Intramyocardial injection of AAV2 or AAV9 did not change the LVEDD (Figure 3b) or the systolic function (Figure 3c). AAV9 caused diastolic dysfunction to some extent, as the left atrium (LA) area (Figure 3d) and mitral valve (MV) *E/A* ratio was somewhat increased (Figure 3e). LeV did not change the LVEDD (Figure 3b) and it did not affect the cardiac function (Figures 3c–e). Also, in the AAV2, AAV9 and LeV groups, a local hypokinetic spot was seen at the injection site in the LVAW corresponding to the size of the

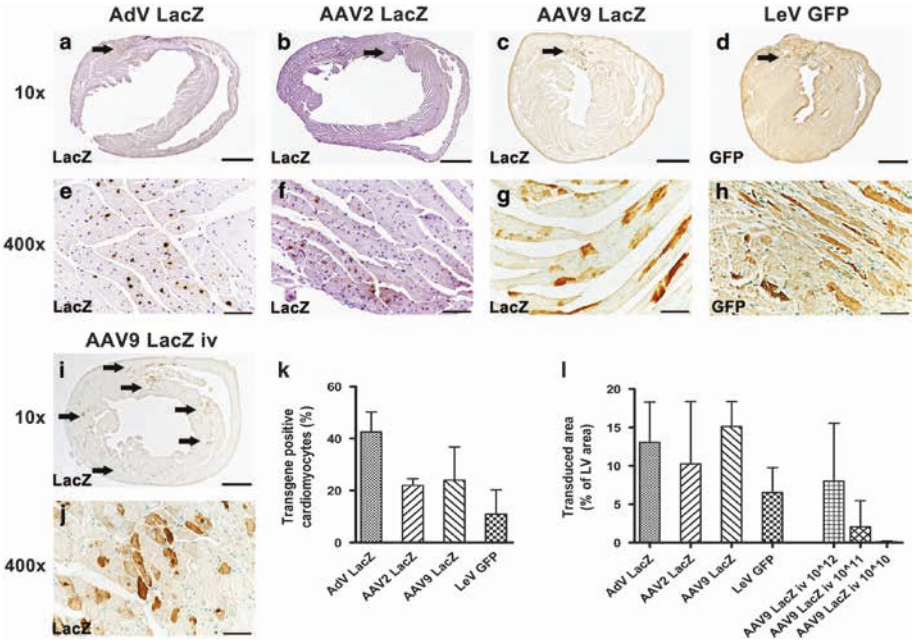

Figure 1. Gene transduction efficiencies of the viral vectors in the myocardium 28 days after gene transfer. Representative images of immunohistological stainings of the transgene expression after intramyocardial delivery of AdV LacZ (**a**, **e**), AAV2 LacZ (**b**, **f**), AAV9 LacZ (**c**, **g**) and LeV GFP (**d**, **h**) with the local transgene expression close to the needle track in the LVAW (arrows). LacZ stainings from the LacZ-transduced groups (**a**–**c**, **e**–**g**, **i**, **j**) and GFP stainings of LeV GFP-transduced group (**d**, **h**) seen with ×10 (**a**–**d**, **i**, scale bar 1000 μm) and ×400 (**e**–**h**, **j**, scale bar 50 μm) magnifications. Quantification of transgene-positive cardiomyocytes in the maximally transduced area near the needle tract (**k**). Representative images of LacZ-stained histological sections after systemic administration of AAV9 LacZ (10^{12} dose) with global diffuse transgene expression in the whole myocardium (**i**, **j**). The quantified size of the transduced area (percentage of LV area) after intramyocardial and systemic gene transfer (**l**). Results are represented as mean ± s.d., $n = 5$ per group, except in AdV LacZ and LeV GFP $n = 7$.

scar, leaving other parts of the LV non-affected or even hyperkinetic.

Surprisingly, intramyocardial injection of NaCl led to dilatation of LV (Figure 3b) and decrease in systolic function (Figure 3c) seen in TTE as global hypokinesia (Figures 3f and i), although the myocardial damage was minimal at the histological level (Figures 2a–c). The injection site at the LVAW could be visually detected in TTE only in one mouse out of six as a small hypokinetic spot in the LV wall (data not shown).

After systemic gene transfer of AAV9 LacZ with 10^{12} dose, the systolic LV function was significantly decreased at d28 (Figures 3c, h and k). The decreased EF was a result of global hypokinesia of the LV owing to extensive fibrosis (Figures 2g, i and j). A significant increase in the LA area (Figures 3d, l and m) and an increase in MV *E/A* ratio (Figures 3e, n and o) was seen, indicating severely impaired diastolic function. The increased *E/A* ratio was explained by a marked decrease in MV *A* peak, whereas no significant changes were seen in MV *E* peak (Figures 3n and o, data not shown). No significant changes were seen in TTE results in the groups of AAV9 LacZ i.v. gene transfers with viral doses of 10^{11} and 10^{10} viral genomes (vg) during the follow-up (data not shown).

Electrocardiogram

To further characterize the function of the LV, the ECG signal (lead II) was analyzed. The heart rate of the mice varied between 420 and 520 b.p.m. during the isoflurane anesthesia (data not shown). There were no significant changes in the ECG parameters in the NaCl group at d28 apart from shortened PQ time and an increased S amplitude, evidently due to a higher heart rate and an increased LV volume, respectively (Figures 4a–c). There were no changes in QRS time in any of the groups, meaning that there were no marked defects in ventricular depolarization. However, there was significant increase in QRSp time in the AdV CMV group and also to some extent in the AAV9 LacZ i.v. 10^{12} group at d28 ($P = 0.056$ compared with d0), indicating changes in the beginning of repolarization. Decreased *R* amplitude was seen in AdV CMV, AdV LacZ, LeV GFP and most markedly in the AAV9 LacZ i.v. 10^{12} groups, which most likely can be explained by the scar tissue. The most extensive changes in ECG parameters were seen in AAV9 LacZ i.v. 10^{12} treated mice, which exhibited significantly increased *P* and *Q* wave durations and decreased *P*, *R* and *S* wave amplitudes at d28 compared with baseline (Figures 4a, d and e) as signs of increased LA size and fibrotic LV. In addition, some signs of disturbances in repolarization were seen as a disappearance of the *J* wave and JT depression in 50% of the mice at d28 in the same study group (Figures 4d and e). In all the other groups, the ECGs curves were normal in shape and no arrhythmias were detected at day 28 (data not shown).

Biodistribution

For comparing the biodistribution of the systemic AAV9 LacZ gene transfer to intramyocardial gene transfer, the expression of LacZ transgene was quantified from the safety tissues 28 days after local or systemic injection of AAV9 LacZ. Table 1 depicts that AAV9 LacZ i.v. gene transfer with 10^{12} dose led to LacZ transgene expression above the detection limit in all the tested kidney, liver and testis samples at d28. Transgene expression was also detected in 90% of the spleen samples and 30% of the lung samples but in none of the rectus femoris muscle samples of the 10^{12} dose group. By reducing the systemic viral dose by 10- and 100-fold, the number of transgene positive samples was markedly reduced

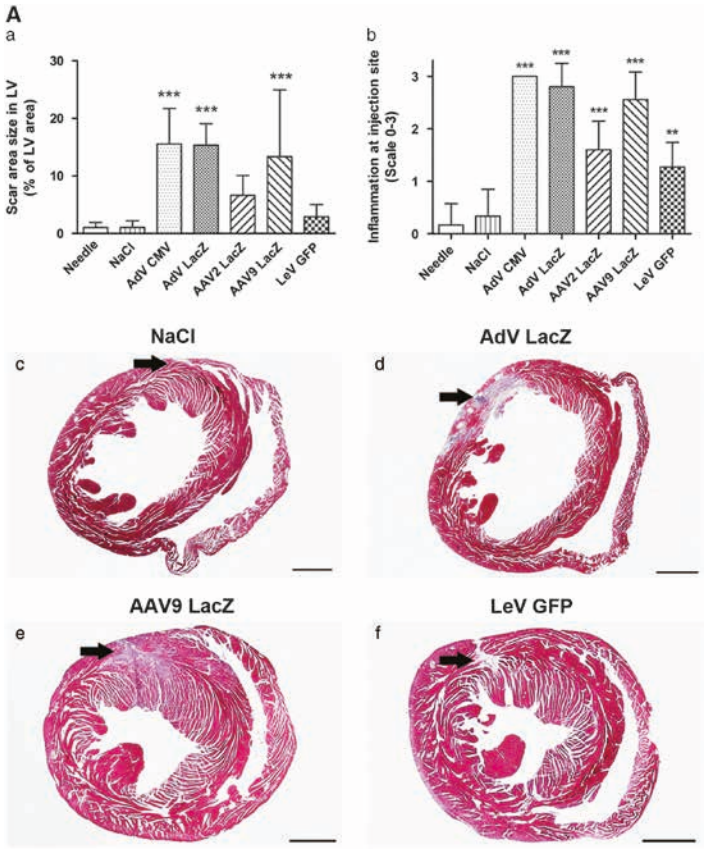

Figure 2. Myocardial damage 28 days after intramyocardial (**A**) and systemic (**B**) gene transfer. Local fibrotic scar with lymphocyte-intensive inflammatory reaction in the LV wall after intramyocardial injection of NaCl (**c**), AdV (**d**), AAV9 (**e**) and LeV (**f**) seen in the representative Masson trichrome-stained sections of hearts (magnification ×10, scale bar 1000 μm). The size of the local scar area in the LV wall (**a**, quantified from Masson trichrome-stained sections) and the amount of inflammation at the injection site (**b**, scored with the scale 0–3, where 0, no inflammation; 1, minor inflammation; 2, moderate inflammation; and 3, severe inflammation). Amount of diffuse fibrosis (**g**) and lymphocyte-intensive inflammation (**h**) after systemic AAV9 LacZ gene transfer with decreasing viral doses scored with the scale 0–3 (0, no fibrosis per inflammation; 1, minor fibrosis per inflammation; 2, moderate fibrosis per inflammation; and 3, severe fibrosis per inflammation). Representative Masson trichrome-stained sections of AAV9 LacZ i.v. 10^{12} vg dose (**i**, **j**) and 10^{11} vg dose (**k**, **l**) with ×10 (**i**, **k**; scale bar 1000 μm) and ×100 (**j**, **l**; scale bar 250 μm) magnifications. Results are shown as mean ± s.d., one-way ANOVA with Dunnet's *post hoc* test, $^{**}P < 0.01$, $^{***}P < 0.001$ compared with NaCl-injected hearts (**a**) or 10^{12} dose group (**b**). $n = 6$ per group, except in AAV9 LacZ (**a**, **b**) $n = 9$, in LeV GFP $n = 10$ (**a**, **b**) and in AAV9 LacZ i.v. 10^{12} $n = 9$ (**g**, **h**).

in all other tissues except the liver, in which the transgene expression was detected in all the studied samples 28 days after i.v. injection. Although in the liver a clear dose–response was seen in the LacZ expression, the relative amount of LacZ mRNA expression was 5.4 in the 10^{12} group, 3.8 in the 10^{11} group and 1.0 on average in the 10^{10} group. After intramyocardial delivery of AAV9 LacZ, 80% of the liver samples were positive for transgene expression, but the level of expression was really low, 16-fold lower than in the AAV9 LacZ i.v. 10^{12} group with a relative value of 0.3 compared with the i.v. 10^{10} group. Also, low levels of transgene expression were detected in 10% of the lungs and testes, but no transgene expression was seen in the kidney, spleen or rectus femoris muscle after intramyocardial AAV9 LacZ injection.

Histology of the safety tissues after AAV9 LacZ gene transfer

To study the histological outcome of the biodistribution of AAV9 LacZ transgene, the morphology of the safety tissues after systemic and intramyocardial gene transfer of AAV9 LacZ was examined. Histological morphology was essentially normal in the safety tissues in all the study groups apart from the liver, in which some minor changes were seen (data not shown). There were mild-to-moderate amounts of 'dropout' necrosis in the liver samples in all the AAV9 LacZ injected samples, that is, single hepatocytes near the central veins were replaced by a few inflammatory cells, mostly lymphocytes. In addition, in some liver samples of AAV9 LacZ i.v. injected mice, there were lighter stained hepatocytes seen in zone three near the central vein, but no actual ballooning degeneration was present. In one AAV9 LacZ i.v. 10^{11} dose liver sample a minor amount of microvesicular steatosis was seen, and in one AAV9 LacZ i.v. 10^{12} dose liver sample some mitoses were present. Bile ducts were normal in all the samples. No fibrosis was seen in the Masson trichrome-stained sections in any of the safety tissues.

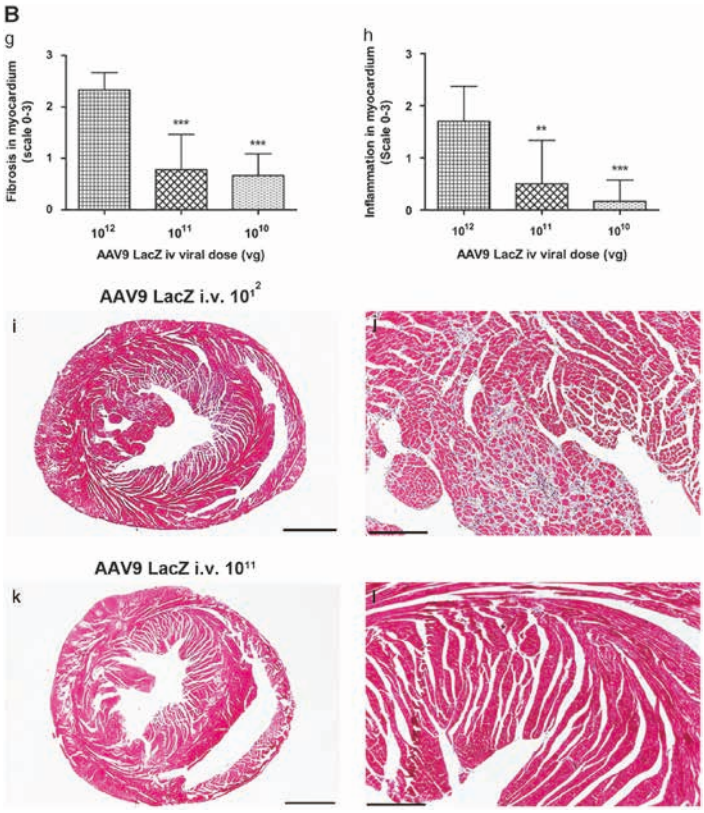

Figure 2. Continued.

DISCUSSION

Gene therapy has great potential for the treatment of cardiac diseases, such as coronary artery disease and heart failure. However, the optimal delivery of transgenes to the heart remains a challenge and the efficiency of the gene transfer vectors and delivery methods needs to be improved without forgetting the safety aspects. Local transfer of the gene drug straight into the target tissue is considered more efficient than systemic administration, and in local administration unnecessary side effects in non-target tissues caused by systemic administration can be minimized.[6,11] In addition, optimal gene transfer method should cause as little trauma as possible. In clinical intramyocardial gene therapy studies, the focus has shifted from the intramyocardial injections, which require thoracotomy, to using more sophisticated minimally invasive percutaneous catheter injections allowing more precise and local intramyocardial gene transfer.[6,9,24] For these reasons, we wanted to exploit sophisticated closed-chest intramyocardial gene delivery setting, in which the injections are carried out straight to LV wall through the chest with ultrasound guidance. With the minimally invasive injection method utilized here, it is possible to avoid the traumatic open-chest procedures, which are often used in preclinical studies, and also mimic more closely the human percutaneous approach. To our knowledge, this is the first time that the three most widely used viral vectors in cardiac gene therapy have been compared side by side with the same method and, furthermore, the first time that AAV and LeV gene transfers have been studied with this gene transfer method. In addition, we wanted to compare the effects of systemic AAV9 injection to intramyocardial injection.

AdV vectors are known to be efficient in delivering transgenes into cardiomyocytes.[11] Accordingly, we demonstrated that transduction efficiency was the best after AdV gene delivery compared with AAV and LeV and the transduced area was similar in size as seen with previous study using the same injection method.[25] The transduction efficiency of AAV2 and AAV9 was somewhat lower compared with AdV gene transfer, which is consistent with earlier study in mouse cardiomyocytes, although in titer-matched comparison AAV transduction efficiency reached the efficiency of AdV vector.[26] AAV9 has been reported to have high cardiac tropism and superior efficiency in transducing cardiac cells compared with other AAVs. Instead, the transduction efficiency of AAV2 has been shown to be poorer compared with AAV9.[15] In our study, AAV2 was as efficient in transducing cardiomyocytes as AAV9, but AAV2 produced a smaller scar and less inflammation, suggesting that AAV2 would be a better choice for intramyocardial gene transfer from the safety perspective. In our study, the systemic AAV9 injection led to transduction of cardiomyocytes throughout the myocardium, but the efficiency did not reach the levels reported by others.[27,28] Neither of the studies reported any myocardial damage after i.v. injection with the same dose of 1×10^{12}.

The main limitation of using LeV in cardiovascular approaches has been low transduction efficiency and low titers of virus preparations,[11,29] which is consistent with our findings and explains why a smaller viral dose was used with LeV vector compared with AdV and AAV. In addition, with the current LeV production methods, the LeV preparations with LacZ transgene had even lower titers owing to larger size of the LacZ gene in comparison to the GFP gene. Therefore, we were forced to use

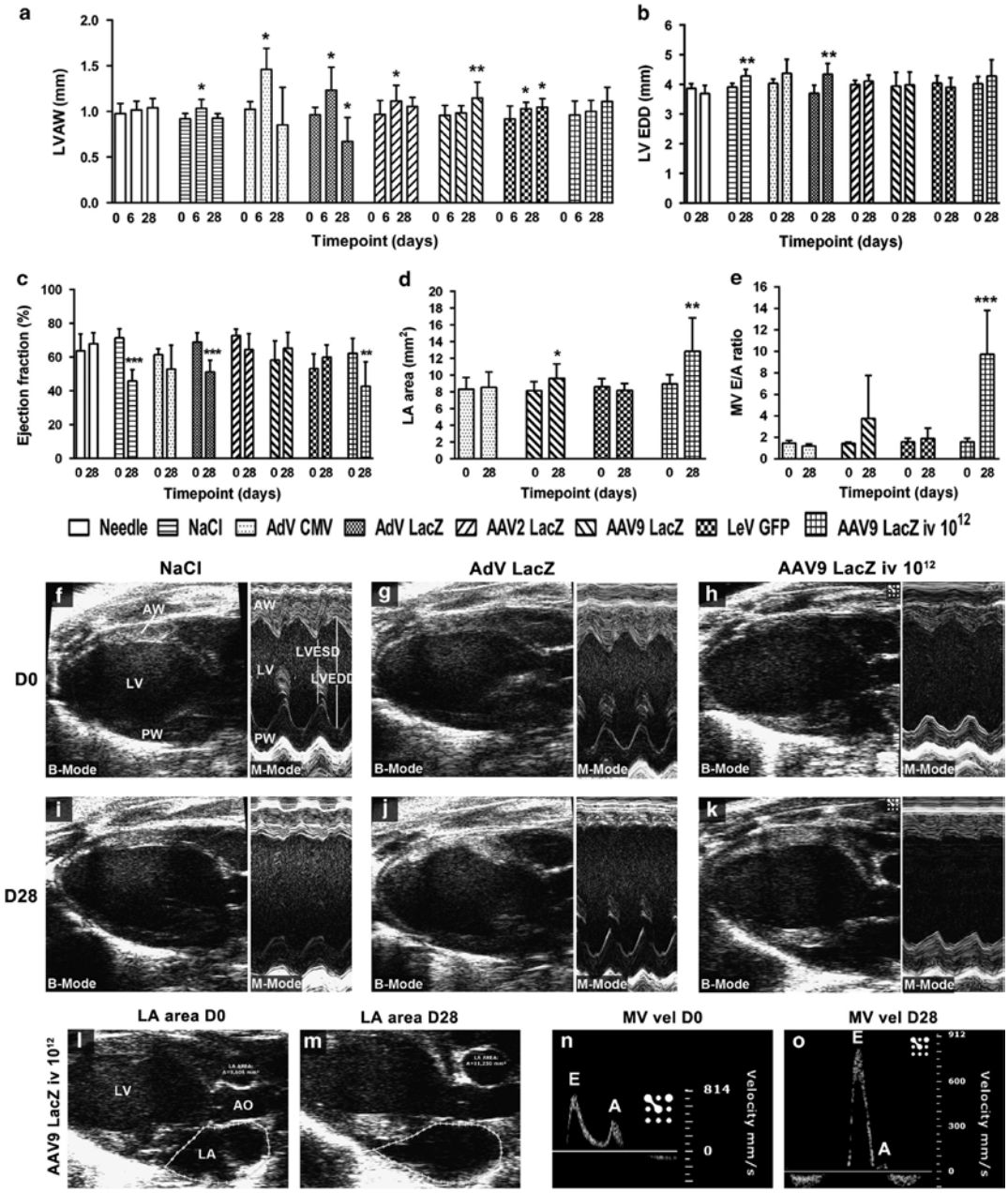

Figure 3. Echocardiography measurements of LV dimensions and function. LVAW thickness in diastole (**a**), LVEDD (**b**), ejection fraction (**c**), LA area (**d**) and MV *E/A* ratio (**e**) at d28. Representative B-Mode (long axis view) and M-Mode (short axis view) images of intramyocardially injected NaCl (**f**, **i**), AdV LacZ (**g**, **j**) and i.v. injected AAV9 LacZ 10^{12} dose (**h**, **k**) before the gene transfers at day 0 (D0, **f**, **g**, **h**) and 28 days after the gene transfer (D28, **i**–**k**). Representative long axis view B-Mode images of LA area at D0 (**l**) and D28 (**m**) and Doppler images of mitral valve flow velocities at D0 (**n**) and D28 (**o**) of the AV9 LacZ i.v. 10^{12} group. Results are expressed as mean ± s.d., $n = 6$ per group, except $n = 9$ in AdV LacZ and AAV9 LacZ i.v. 10^{12}, $n = 10$ in AAV9 LacZ and $n = 11$ in LeV GFP. One-way ANOVA with Dunnet's *post hoc* test (**a**) or Student's *t*-test (**b**–**e**) was used, $^{*}P < 0.05$, $^{**}P < 0.01$, $^{***}P < 0.001$ compared with day 0 value within each group. MV vel, mitral valve flow velocity; *E*, *E* peak representing passive diastolic filling; *A*, *A* peak representing atrial contraction.

a

	Time (days)	NaCl (n=6)	Ad CMV (n=6)	Ad LacZ (n=4)	AAV2 LacZ (n=6)	AAV9 LacZ (n=10)	LV GFP (n=14)	AAV9 LacZ iv 10^{12} (n=9)
P dur (ms)	0	16,7 ± 2,0	13,2 ± 1,3	15,1 ± 0,5	17,3 ± 2,4	17,0 ± 2,4	14,6 ± 1,7	15,9 ± 0,8
	28	16,3 ± 1,8	13,9 ± 1,1	14,9 ± 1,2	17,1 ± 2,2	16,9 ± 2,3	14,5 ± 2,1	17,3 ± 1,7*
PQ (ms)	0	44,4 ± 2,3	42,1 ± 3,3	44,0 ± 4,1	44,2 ± 4,2	45,1 ± 2,7	43,8 ± 2,4	43,3 ± 4,1
	28	40,9 ± 2,7*	44,4 ± 1,6	39,5 ± 1,9	44,5 ± 3,6	44,7 ± 5,1	43,1 ± 3,2	46,0 ± 6,0
Q dur (ms)	0	0,4 ± 0,6	0,7 ± 0,8	0,6 ± 0,7	1,0 ± 0,8	1,1 ± 1,4	0,6 ± 1,0	1,0 ± 1,3
	28	0,5 ± 0,8	0,4 ± 0,7	0,6 ± 0,7	0,6 ± 0,7	1,0 ± 1,4	0,5 ± 0,9	2,9 ± 1,4**
QRS (ms)	0	10,5 ± 0,5	10,0 ± 0,8	10,5 ± 0,7	10,4 ± 1,6	11,1 ± 1,8	11,2 ± 0,9	10,8 ± 0,7
	28	11,3 ± 1,4	9,8 ± 0,3	10,5 ± 0,5	10,6 ± 1,1	10,8 ± 1,4	10,5 ± 0,8	12,3 ± 2,6
QRSp (ms)	0	16,8 ± 1,2	14,0 ± 0,9	15,4 ± 1,6	15,5 ± 1,9	16,3 ± 2,1	15,3 ± 1,2	15,0 ± 1,0
	28	16,2 ± 1,4	15,5 ± 1,1*	17,3 ± 1,1	16,6 ± 1,2	16,5 ± 2,2	15,2 ± 1,0	18,2 ± 4,9
QTc (ms)	0	41,2 ± 5,0	39,2 ± 1,6	41,4 ± 2,5	41,0 ± 1,4	42,1 ± 5,6	40,7 ± 2,9	40,3 ± 3,8
	28	42,0 ± 1,3	40,1 ± 5,0	40,8 ± 1,8	38,3 ± 3,7	41,5 ± 3,9	40,2 ± 2,7	38,3 ± 6,0
Amp P (mV)	0	1,0 ± 0,3	1,1 ± 0,2	1,3 ± 0,2	0,9 ± 0,2	1,4 ± 0,4	1,3 ± 0,3	1,3 ± 0,2
	28	1,1 ± 0,3	1,1 ± 0,2	1,1 ± 0,2	0,9 ± 0,2	1,2 ± 0,5	1,3 ± 0,3	1,0 ± 0,2**
Amp R (mV)	0	7,1 ± 1,3	8,5 ± 1,9	9,5 ± 1,5	7,7 ± 1,4	9,3 ± 3,0	11,6 ± 2,3	11,9 ± 2,7
	28	8,1 ± 1,6	5,7 ± 2,2*	5,7 ± 0,8**	8,2 ± 1,3	8,3 ± 2,3	9,7 ± 1,6*	5,5 ± 2,4***
Amp S (mV)	0	-2,9 ± 1,1	-3,6 ± 2,0	-4,7 ± 2,2	-3,5 ± 1,1	-3,2 ± 1,3	-5,3 ± 2,0	-4,5 ± 1,4
	28	-4,8 ± 1,3*	-2,5 ± 1,2	-3,7 ± 1,9	-2,7 ± 1,3	-2,8 ± 1,2	-4,5 ± 1,9	-1,6 ± 0,4***

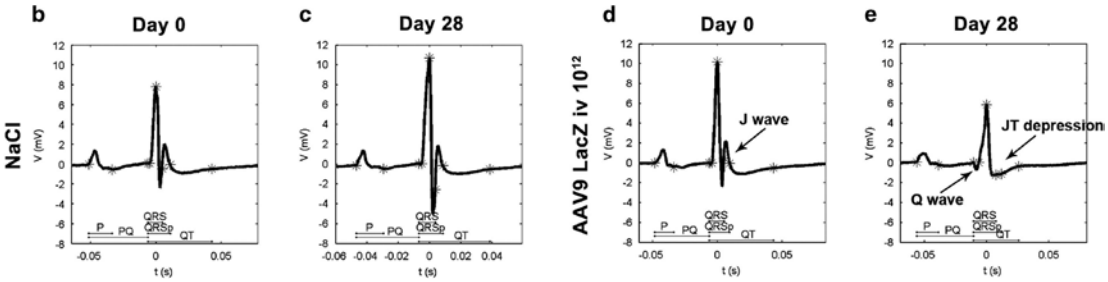

Figure 4. ECG measurements at d0 and d28 (**a**). Representative ECG of NaCl injected at baseline (**b**) and at d28 (**c**) and of systemic AAV9 injected with 10^{12} dose at baseline (**d**) and at d28 (**e**). Results are shown as mean ± s.d. Student's *t*-test $*P < 0.05$, $**P < 0.01$, $***P < 0.001$ compared with day 0 value within each group. Number of mice in each group is indicated in the upper row of table **a**. P dur, duration of P wave; Q dur, duration of Q wave; Amp, amplitude.

Table 1. Biodistribution of AAV9 LacZ transgene expression in AAV9 LacZ i.v. groups compared with AAV9 LacZ intramyocardial (i.m.) gene transfer group at d28 measured by quantitative RT-PCR

Group	*Kidney*	*Liver*	*Lungs*	*Spleen*	*Rectus femoris muscle*	*Testis*
AAV9 LacZ i.v. 10^{12}	9/9	10/10	3/10	9/10	0/10	10/10
AAV9 LacZ i.v. 10^{11}	2/6	6/6	1/6	1/6	1/6	5/6
AAV9 LacZ i.v. 10^{10}	1/6	6/6	0/6	2/6	0/6	1/6
AAV9-LacZ i.m.	0/10	8/10	1/10	0/10	0/10	1/10

Abbreviations: AAV, adeno-associated virus; i.v., intravenous; RT-PCR, reverse transcriptase-PCR. The results are shown as tissue samples expressing the transgene/all analyzed samples in the treatment group.

different marker gene in LeV injections making it more challenging to compare the LeV group to AdV and AAV groups, in which the transgene, promoter and viral dose were the same. In the LeV construct, the GFP gene was driven by phosphoglycerate kinase-1 (PGK) promoter. With a stronger promoter, transduction efficiency could be possibly improved, namely, the CMV promoter has shown to drive higher enhanced GFP expression levels than the PGK promoter with LeV vectors in adult rat cardiomyocytes.[20] Taking these into consideration, transduction efficiency of about 11% after LeV gene transfer in the immediate proximity of the needle track with the highest possible dose of $1–4 \times 10^7$ transducing units was found to be good, even though it was the lowest compared with AdV and AAVs. Approximately, the same transduction efficiency[20] and also transduction efficiencies of even up to 40% have been reported in rat models.[19,21]

Intramyocardial viral gene transfer resulted in inflammation and fibrosis at the injection site, which were the largest after intramyocardial AdV gene transfer and the smallest after LeV gene transfer. The immune reactions associated with AdV vectors are generally known, and the inflammatory effects in the mouse myocardium after intramyocardial gene transfer have been previously reported by us[10] and others.[25] However, optimal low doses of AdVs produced according to good manufacturing practice protocols cause only little inflammation in myocardium, and AdVs have proven to be safe in preclinical and clinical trials.[7,8,11,30,31] In contrast to AdVs, AAV vectors are associated with low immunogenicity in murine models,[12,13,32,33] and in general, no adverse cardiac effects have been reported with intramyocardial AAV2[34] and AAV9[17,35] injections. However, the immunogenicity of AAV has recently become apparent in clinical trials, and the

immune responses are currently profiled more thoroughly in preclinical models.[32,33] Consistently with our findings, Fleury *et al*.[20] reported that after intramyocardial injection with LeV the tissue inflammation was significantly milder compared with AdV vectors in rats. They suggest that immune responses to the VSV-G envelope protein, enhanced GFP, and contaminants that copurify with vector particles may account for tissue inflammation.[20] In our study, GMP grade viral vectors were used, which should reduce adverse effects caused by potential contaminants.

Acute inflammatory responses secondary to needle injury are thought to be a drawback of direct needle injections.[24] But only minor myocardial damage was seen herein and also previously with intramyocardial NaCl/phosphate-buffered saline (PBS) injections with this injection method.[10,25] Despite the really small tissue damage that NaCl injection produced, it surprisingly led to LV dilatation and a decrease in EF owing to global hypokinesia. Instead, in the needle group in which no liquid was injected into the myocardium, no change in LV function was seen, although the tissue damage was similar as in the NaCl group. Also, intramyocardial gene transfers of AAV2, AAV9 and LeV did not impair the systolic function of the LV, even though larger fibrotic areas were present in the LV wall, suggesting that the closed-chest intramyocardial gene transfer method itself does not explain the worsening of the EF in the NaCl group. The mechanism behind this phenomenon remains unknown, but this should be taken into consideration in the future studies when using saline injections as controls.

Efficient transduction of myocardial cells has been achieved in small animals with systemic AAV9 delivery,[16,27,35] but no major adverse effects have been previously reported. Therefore, the severe cardiac fibrosis leading to impaired LV function and even to deaths as a result of systemic AAV9 gene transfer with 10^{12} vg dose, which is generally used in preclinical studies, was an unpleasant surprise. Previously, it has been reported that after AAV9-CMV-LacZ i.v. gene transfer of 1×10^{12} viral particles (vp) there was no inflammation, no changes in LV function and the survival rate of mice was 100% after 12 weeks follow-up.[34] Consistently with our findings, significant inflammatory cell infiltration in the heart was seen after AAV6-CMV-LacZ i.v. delivery of 1×10^{12} vg dose, but it was thought to be due to widespread expression of a bacterial protein (β-gal) and not associated with viral components.[36] Instead, in our study it seems that LacZ transgene did not induce the tissue inflammation and damage, at least in the case of AdV as the amount of fibrosis and inflammation was similar in the AdV CMV group carrying no transgene compared with the AdV LacZ group. According to our results, AAV9 i.v. dose of 10^{12} vg is too high to be used safely in mouse cardiac gene transfers. Decreasing the viral dose 10- and 100-fold not only significantly decreased the tissue damage but also reduced the transgene expression to barely detectable levels. Although not feasible gene transfer method for human studies,[11] systemic AAV9 delivery is generally used in preclinical trials with small animals and the harmful effects should be carefully addressed when assessing the effects of the gene transfer in the future.

Mouse ECG has not been widely studied and as far as is known, there are no reports of preclinical cardiac gene transfer studies with ECG data. Previously, we have reported that AdV gene transfers and NaCl injections do not to have any effects on surface ECG 6 days after the gene transfer.[10] Also, in this study there were no marked changes in the surface ECG (lead II) of intramyocardially injected mice. The most dramatic changes were seen after systemic AAV9 LacZ 10^{12} gene transfer. *P* wave duration was increased most likely as a consequence to an increased LA area, as seen in humans.[37] Formation of deeper *Q* waves, an increase in *Q* duration together with marked decreases in *P*, *R* and *S* amplitudes together with repolarization disturbances are probably caused by myocardial fibrosis. QRSp time, which measures the depolarization and early repolarization of ventricles, was somewhat increased in both AdV groups and AAV9 LacZ i.v. 10^{12} groups, possibly indicating that repolarization is somewhat disturbed. This could also be explained by fibrosis, which was the most abundant in these groups.

Reducing the harmful side effects of AdV or improving the transduction efficiency of the safer AAV and LeV vectors will be needed in the future. Modifications of the AdV vector have improved the safety in mouse studies.[25,38] Also, third-generation AdV might be less immunogenic with longer-lasting transgene expression, but their potential in human trials has not been tested.[9] As AAV and LeV intramyocardial injections were well tolerated, several injections could be carried out to increase the transduction efficiency.

The immune responses to the vector can limit the vector transduction, duration of gene expression or result in immune clearance of transduced cells. There are differences in the development of immune response against viral vectors, transgene products and the gene-modified cells between animal models and humans, which sets challenges in translating the results into clinical studies.[29,32,33] Although mouse models are invaluable in understanding the biological function of transferred genes and the viral vectors, information derived from small animal models should be extrapolated with caution to human therapies.

In summary, compared with AdV, which is widely used, AAV2, AAV9 and LeV were less effective in transducing cardiomyocytes but also less harmful. Local administration of AAV9 was safer and more efficient compared with the systemic administration. Our findings emphasize the importance of the careful evaluation of the possible adverse effects of viral vectors and delivery methods in gene therapy trials. We also encourage to further study the potential of LeV vectors in cardiac gene therapy.

MATERIALS AND METHODS

Experimental animals

Altogether 112 C57Bl/6J male mice (Harlan Laboratories, Indianapolis, IN, USA), 8–15 weeks of age, were used for the experiments. The number of mice in each group is indicated in the figure legends. The sample size was mainly six at minimum to ensure high enough statistical power. More mice per group was taken initially for the experiments, and experiments were repeated, if necessary, to get at least 5–6 mice per group successfully analyzed at the end. The preestablished exclusion criterion was that the mice into which the gene transfer was not successfully performed were excluded (that is, if no needle mark was seen in the histology). Mice were randomized for the study groups, and the analyses were performed in a blinded manner. All animal procedures were approved by The National Animal Experiment Board of Finland (reference number for the license was ESAVI-2011-003264) and carried out in accordance with the guidelines of The Finnish Act on Animal Experimentation. The animals were kept in standard housing conditions in The National Laboratory Animal Center of The University of Eastern Finland, Kuopio, Finland. Diet and water were provided *ad libitum*.

Viral constructs

AdV vectors were the first-generation serotype five replication-deficient, E1a/b- and E3-deleted preparations, in which the LacZ transgene with a nuclear localization signal (NLS) was driven by the CMV promoter. For evaluating possible harmful effects of the LacZ transgene itself, an 'empty' AdV CMV construct carrying only the CMV promoter without an actual transgene was used. AdV were produced as previously described.[10]

AAV2 vectors were produced according to a previously described protocol[39] with some modifications. Briefly, 293T cells were transfected with AAV2 vector plasmid with calcium phosphate precipitation. Cells were harvested 48–72 h after transfection. Viral vector was released from cells by three freeze-thaw cycles and the vector-containing media was purified by iodixanol-gradient centrifugation and heparin-affinity chromatography. Fractions containing the purified vector were collected and dialyzed against PBS. The purified vector was stored in PBS at −70 °C until use. AAV9 production was carried out as previously described.[40] In AAV2 and AAV9 vectors, the LacZ was under the CMV promoter and in AAV2 it carried a NLS, whereas in AAV9 expression was cytoplasmic.

Third-generation HIV-1-based LeVs were prepared with the standard calcium phosphate transfection method of 293T cells as previously described.[41] In the LeV, the GFP transgene was under the human PGK promoter.

Gene transfer

The gene transfer procedures were performed for normal non-diseased mice with healthy hearts for assessing the role of plain therapy in the myocardium. Mice were anesthetized with isoflurane inhalation (induction: 4.5% isoflurane, 450 ml min^{-1} air, maintenance: 2.0% isoflurane, 200 ml min^{-1} air; Baxter International, Deerfield, IL, USA). TTE-guided intramyocardial gene transfer of AdV CMV, Ad LacZ, AAV2 LacZ, AAV9 LacZ and LeV GFP to the anterior wall of LV in a closed-chest manner were carried out as previously described by us.[10] Briefly, injections were carried out with a 30-gauge disposable needle in a 50-µl Hamilton syringe connected to a micromanipulator system (Fujifilm VisualSonics Inc., Toronto, Ontario, Canada). The needle was penetrated through the chest in between the ribs and inserted intramyocardially into the LV wall without entering the lumen of LV. Injections of viral constructs in 10 µl volume were carried out and visualized in TTE images. For postoperative analgesic, carprofen (50 mg ml^{-1}, Rimadyl, Pfizer Inc., NY, USA) was given.

In AdV CMV and AdV LacZ gene transfers viral dose of 1×10^{10} vp and in AAV2 LacZ and AAV9 LacZ gene transfers 1×10^{10} vg diluted with sterile 0.9% NaCl in 10 µl volume were used. In LeV GFP gene transfers, 10 µl of non-diluted viral preparations with the highest possible titers were used corresponding to a viral dose of $1.3–4 \times 10^{7}$ transducing units. For controlling the effect of intramyocardial injection itself, a group of mice received 10 µl sterile 0.9% NaCl. The mechanical effect of a plain needle was controlled by performing the injection otherwise similarly but without any injected solution. For i.v. delivery of AAV9 LacZ, three decreasing doses were used: 1×10^{12}, 1×10^{11}, and 1×10^{10} vg in 200 µl volume injected via tail vein.

Transthoracic echocardiography and electrocardiography

TTE measurements were carried out under isoflurane anesthesia, as described earlier,[10] with Vevo 2100 Ultrasound Systems (Fujifilm VisualSonics Inc.) before the gene transfer (d0) and 6 (d6) and 28 days (d28) after the gene transfer. The MS-400 high-frequency ultrasound probe operating at 18–38 MHz was used. Briefly, for TTE and ECG measurements, mice were placed in supine position on a heated platform (THM100, Indus Instruments, Houston, TX, USA) for maintaining the body temperature at 36–37 °C (monitored via rectal probe). To obtain the ECG signal, the paws of the mice were connected to the electrode pads on the platform by using ECG gel and fixed with a skin tape. The recorded ECG represents the standard limb lead II. Heart rate and respiration were monitored during anesthesia via ECG pads.

LV dimensions (LVAW, LVPW, LVEDD) and EF, were determined from parasternal short-axis *M*-mode measurements of TTE. EF was calculated by the Vevo software with the Teicholz formula and LV mass with the formula: $1053 \times ((\text{LVEDD;d+LVPW;d+LVAW;d})^3 - \text{LVEDD}^3)$. The area of the LA was determined with the 2D area tool from parasternal long-axis view *B*-mode image taken more laterally than the normal long-axis view to visualize the LA at its largest point. The MV flow velocities were measured with the aid of the color Doppler signal from the apical four-chamber view.

The raw data of ECG was analyzed with a Matlab-based ECG analysis program (Kubios HRV, version 2.0 beta 4, Department of Physics, University of Eastern Finland, Kuopio, Finland), which was modified specially for analyzing mouse ECG.[42] The time intervals *P* wave duration, PQ time, *Q* wave duration, QRS and QRSp width, QTc time (mean QT/(mean RR/100)$^{1/2}$) and amplitudes of *P*, *R* and *S* wave were analyzed from the mean curve generated from a 30-s ECG recording. In mouse ECG, there is an additional wave in the early repolarization right after the QRS complex called J wave,[43] and QRSp time is measured from the beginning of the QRS complex to the point where J wave returns to the isoelectric line.

Histology

Mice were killed 28 days after the gene transfer and tissue samples of the heart, lungs, liver, spleen, kidneys, quadriceps femoris muscle and testis were collected. In addition, 6 days after AdV LacZ gene transfer heart tissue was harvested for histology to study the time point of the highest transgene expression. After PBS perfusion, tissues were fixed with 4% paraformaldehyde in 7.5% sucrose for 4 h and kept in 15% sucrose overnight. Histological stainings were carried out from 5-µm thick paraffin-embedded sections apart from the LeV GFP heart samples, which were frozen to OCT (Optimal Cutting Temperature, Tissue-Tek, Sakura Finetek, Torrance, CA, USA) and cut to 8-µm thick frozen sections. Hematoxylin/eosin (HE) stainings were used to find the injection site from the intramyocardially injected hearts and for studying general histology in all the samples. The immunohistological and Masson trichrome stainings were performed on sections next to the section with the needle tract. Myocardial scar area/fibrosis was analyzed from Masson trichrome (Accustain trichrome stains; Sigma-Aldrich, St Louis, MO, USA) stained sections. Transduction efficiency was evaluated from LacZ-stained (rabbit anti-beta-galactosidase polyclonal antibody, dilution 1:2500, Merck Millipore, Darmstadt, Germany) sections of AdV LacZ- and AAV2/9 LacZ-transduced hearts and from GFP-stained (rabbit Anti-GFP antibody, ab 290, dilution 1:1500, Abcam, Cambridge, UK) sections of LeV GFP-transduced hearts.

The number of transgene-positive cardiomyocytes in intramyocardially injected hearts was quantified from LacZ- or GFP-stained sections from five microscopic fields at ×400 magnifications from each animal. The size of the transduced area (percentage of the LV area) was quantified from ×12.5 magnifications. All quantifications were carried out in a blinded manner by using the AnalySIS software (Soft Imaging System, Muenster, Germany). The amount of transduced cardiomyocytes is presented as a mean percentage of all cardiomyocytes in a field in maximally transduced area, that is, right next to the needle track in intramyocardially injected hearts. Green fluorescence from LeV GFP-transduced hearts was evaluated with a fluorescence microscope from frozen sections mounted in Vectashield Hard-Set Mounting Medium with DAPI (Vector Laboratories, Inc., Burlingame, CA, USA), which counterstains the DNA allowing the visualization of nucleai with the blue fluorescence.

Myocardial damage associated with the intramyocardial and systemic gene transfer was evaluated by an experienced pathologist from the HE-stained heart sections with largest amount of damage. The general histological morphology was analyzed, and the samples were scored with the following scale: 0–3 for inflammation with the following scoring criteria: 0, no inflammation; 1, minor amount of inflammatory cells (few cells); 2, moderate amount of inflammatory cells (tens of cells); and 3, large amount of inflammatory cells (several tens to hundreds of cells). The given scores were proportioned within the data. The scar area size in the LV wall (percentage of the LV area) of intramyocardially injected mice was quantified from ×12.5 magnified Masson-stained sections in a blinded manner with the AnalySIS software (Soft Imaging System). Myocardial fibrosis in the i.v. injected mouse hearts was analyzed in a blinded manner by three independent researchers from Masson trichrome-stained microscopic sections on a scale 0–3 using the following scoring criteria: 0, no fibrosis; 1, minor fibrosis (just the needle tract); 2, moderate fibrosis; and 3, severe fibrosis. The given scores were proportioned within the data. The results are shown as a mean ± s.d. of all observations.

The general histological morphology of safety tissues of AAV9 LacZ intramyocardially and i.v. injected mice was evaluated from HE-stained paraffin-embedded sections. The liver samples of AAV9 LacZ-injected mice were scored by the pathologist in terms of dropout necrosis, amount of lymphocytes/eosinophilic granulocytes in the dropout necrotic area, ballooning degeneration, microvesicular steatosis and morphology of bile ducts on the scale 0–3 (none–minor–moderate–large amount). In addition Masson trichrome stainings were carried out for detecting possible fibrosis.

Biodistribution

Biodistribution of AAV9 LacZ transgene expression was determined from the safety tissues of AAV9 LacZ i.v. injected mice and compared with the group that received AAV9 LacZ intramyocardially. The studied organs were kidney, liver, lungs, spleen, rectus femoris muscle and testis. Total RNA from the tissues was isolated with TRI-Reagent (Sigma-Aldrich). RNA samples were DNAse treated by the DNA Free Kit (Ambion by Life Technologies, Carlsbad, CA, USA) and reverse transcribed using Revertaid (Thermo Fischer Scientific, Waltham, MA, USA). Quantitative real-time PCR was performed with a StepOnePlus Real Time PCR system (Applied Biosystems, Foster City, CA, USA). LacZ mRNA expression levels in the tissues were determined using specific TaqMan Gene Expression Assay for LacZ (Mr03987581_mr; Applied Biosystems) and related to PPIA housekeeping gene expression levels (Mm03302254_g1; Applied Biosystems).

Statistical analyses

Statistical analyses were carried out with Student's paired *t*-test in the Excel Software 2010 (Microsoft Corporation, Redmond, WA, USA) when comparing two groups/time points and with one-way analysis of variance with Dunnet's *post hoc* test in the GraphPadPrism 6.0 software (GraphPad Software, Inc., La Jolla, CA, USA) when comparing three or more groups/

time points. The tests used are indicated in the figure legends. *P*-value < 0.05 was considered statistically significant, and the following symbols were used for *P*-values: $^{*}P < 0.05$, $^{**}P < 0.01$, $^{***}P < 0.001$. Results are expressed as mean ± s.d.

CONFLICT OF INTEREST

The authors declare no conflict of interest.

ACKNOWLEDGEMENTS

This work was supported by grants from Finnish Academy, ERC, Finnish Foundation for Cardiovascular Diseases, Sigrid Juselius Foundation and Kuopio University Hospital, Summit (Grant Agreement number 115006, IMI). We thank Sari Järveläinen, Tiina Koponen, Tuula Salonen, Anne Martikainen and Seija Sahrio for technical assistance and the staff at The National Laboratory Animal Center of the University of Eastern Finland (Kuopio campus) for maintenance of the animals. pDG helper plasmid was a kind gift from Dr Jürgen A Kleinschmidt, (German Cancer Research Center, Heidelberg, Germany).

REFERENCES

1 Lozano R, Naghavi M, Foreman K, Lim S, Shibuya K, Aboyans V *et al.* Global and regional mortality from 235 causes of death for 20 age groups in 1990 and 2010: a systematic analysis for the Global Burden of Disease Study 2010. *Lancet* 2012; **380**: 2095–2128.
2 Dragneva G, Korpisalo P, Yla-Herttuala S. Promoting blood vessel growth in ischemic diseases: challenges in translating preclinical potential into clinical success. *Dis Model Mech* 2013; **6**: 312–322.
3 Halonen PJ, Nurro J, Kuivanen A, Yla-Herttuala S. Current gene therapy trials for vascular diseases. *Expert Opin Biol Ther* 2014; **14**: 327–336.
4 Lahteenvuo JE, Lahteenvuo MT, Kivela A, Rosenlew C, Falkevall A, Klar J *et al.* Vascular endothelial growth factor-B induces myocardium-specific angiogenesis and arteriogenesis via vascular endothelial growth factor receptor-1- and neuropilin receptor-1-dependent mechanisms. *Circulation* 2009; **119**: 845–856.
5 Rutanen J, Rissanen TT, Markkanen JE, Gruchala M, Silvennoinen P, Kivela A *et al.* Adenoviral catheter-mediated intramyocardial gene transfer using the mature form of vascular endothelial growth factor-D induces transmural angiogenesis in porcine heart. *Circulation* 2004; **109**: 1029–1035.
6 Yla-Herttuala S. Cardiovascular gene therapy with vascular endothelial growth factors. *Gene* 2013; **525**: 217–219.
7 Hedman M, Muona K, Hedman A, Kivela A, Syvanne M, Eranen J *et al.* Eight-year safety follow-up of coronary artery disease patients after local intracoronary VEGF gene transfer. *Gene Therapy* 2009; **16**: 629–634.
8 Muona K, Makinen K, Hedman M, Manninen H, Yla-Herttuala S. 10-year safety follow-up in patients with local VEGF gene transfer to ischemic lower limb. *Gene Therapy* 2012; **19**: 392–395.
9 Hedman M, Hartikainen J, Yla-Herttuala S. Progress and prospects: hurdles to cardiovascular gene therapy clinical trials. *Gene Therapy* 2011; **18**: 743–749.
10 Huusko J, Merentie M, Dijkstra MH, Ryhanen MM, Karvinen H, Rissanen TT *et al.* The effects of VEGF-R1 and VEGF-R2 ligands on angiogenic responses and left ventricular function in mice. *Cardiovasc Res* 2010; **86**: 122–130.
11 Rissanen TT, Yla-Herttuala S. Current status of cardiovascular gene therapy. *Mol Ther* 2007; **15**: 1233–1247.
12 Zaiss AK, Liu Q, Bowen GP, Wong NC, Bartlett JS, Muruve DA. Differential activation of innate immune responses by adenovirus and adeno-associated virus vectors. *J Virol* 2002; **76**: 4580–4590.
13 Gruchala M, Roy H, Bhardwaj S, Yla-Herttuala S. Gene therapy for cardiovascular diseases. *Curr Pharm Des* 2004; **10**: 407–423.
14 Wasala NB, Shin JH, Duan D. The evolution of heart gene delivery vectors. *J Gene Med* 2011; **13**: 557–565.
15 Zacchigna S, Zentilin L, Giacca M. Adeno-associated virus vectors as therapeutic and investigational tools in the cardiovascular system. *Circ Res* 2014; **114**: 1827–1846.
16 Zincarelli C, Soltys S, Rengo G, Rabinowitz JE. Analysis of AAV serotypes 1-9 mediated gene expression and tropism in mice after systemic injection. *Mol Ther* 2008; **16**: 1073–1080.
17 Prasad KM, Smith RS, Xu Y, French BA. A single direct injection into the left ventricular wall of an adeno-associated virus 9 (AAV9) vector expressing extracellular superoxide dismutase from the cardiac troponin-T promoter protects mice against myocardial infarction. *J Gene Med* 2011; **13**: 333–341.
18 Li Q, Xie J, Li R, Shi J, Sun J, Gu R *et al.* Overexpression of microRNA-99a attenuates heart remodelling and improves cardiac performance after myocardial infarction. *J Cell Mol Med* 2014; **18**: 919–928.
19 Zhao J, Pettigrew GJ, Thomas J, Vandenberg JI, Delriviere L, Bolton EM *et al.* Lentiviral vectors for delivery of genes into neonatal and adult ventricular cardiac myocytes in vitro and in vivo. *Basic Res Cardiol* 2002; **97**: 348–358.
20 Fleury S, Simeoni E, Zuppinger C, Deglon N, von Segesser LK, Kappenberger L *et al.* Multiply attenuated, self-inactivating lentiviral vectors efficiently deliver and express genes for extended periods of time in adult rat cardiomyocytes in vivo. *Circulation* 2003; **107**: 2375–2382.
21 Niwano K, Arai M, Koitabashi N, Watanabe A, Ikeda Y, Miyoshi H *et al.* Lentiviral vector-mediated SERCA2 gene transfer protects against heart failure and left ventricular remodeling after myocardial infarction in rats. *Mol Ther* 2008; **16**: 1026–1032.
22 Turunen MP, Husso T, Musthafa H, Laidinen S, Dragneva G, Laham-Karam N *et al.* Epigenetic upregulation of endogenous VEGF-A reduces myocardial infarct size in mice. *PLoS One* 2014; **9**: e89979.
23 Terman A, Brunk UT. The aging myocardium: roles of mitochondrial damage and lysosomal degradation. *Heart Lung Circ* 2005; **14**: 107–114.
24 Katz MG, Fargnoli AS, Williams RD, Bridges CR. Gene therapy delivery systems for enhancing viral and nonviral vectors for cardiac diseases: current concepts and future applications. *Hum Gene Ther* 2013; **24**: 914–927.
25 Toivonen R, Koskenvuo J, Merentie M, Soderstrom M, Yla-Herttuala S, Savontaus M. Intracardiac injection of a capsid-modified Ad5/35 results in decreased heart toxicity when compared to standard Ad5. *Virol J* 2012; **9**: 296–422X-9-296.
26 Vassalli G, Bueler H, Dudler J, von Segesser LK, Kappenberger L. Adeno-associated virus (AAV) vectors achieve prolonged transgene expression in mouse myocardium and arteries in vivo: a comparative study with adenovirus vectors. *Int J Cardiol* 2003; **90**: 229–238.
27 Inagaki K, Fuess S, Storm TA, Gibson GA, Mctiernan CF, Kay MA *et al.* Robust systemic transduction with AAV9 vectors in mice: efficient global cardiac gene transfer superior to that of AAV8. *Mol Ther* 2006; **14**: 45–53.
28 Bostick B, Ghosh A, Yue Y, Long C, Duan D. Systemic AAV-9 transduction in mice is influenced by animal age but not by the route of administration. *Gene Therapy* 2007; **14**: 1605–1609.
29 Rincon MY, VandenDriessche T, Chuah MK. Gene therapy for cardiovascular disease: advances in vector development, targeting, and delivery for clinical translation. *Cardiovasc Res* 2015; **108**: 4–20.
30 Wirth T, Hedman M, Makinen K, Manninen H, Immonen A, Vapalahti M *et al.* Safety profile of plasmid/liposomes and virus vectors in clinical gene therapy. *Curr Drug Saf* 2006; **1**: 253–257.
31 Yla-Herttuala S, Rissanen TT, Vajanto I, Hartikainen J. Vascular endothelial growth factors: biology and current status of clinical applications in cardiovascular medicine. *J Am Coll Cardiol* 2007; **49**: 1015–1026.
32 Hareendran S, Balakrishnan B, Sen D, Kumar S, Srivastava A, Jayandharan GR. Adeno-associated virus (AAV) vectors in gene therapy: immune challenges and strategies to circumvent them. *Rev Med Virol* 2013; **23**: 399–413.
33 Basner-Tschakarjan E, Bijjiga E, Martino AT. Pre-clinical assessment of immune responses to adeno-associated virus (AAV) vectors. *Front Immunol* 2014; **5**: 28.
34 Meloni M, Descamps B, Caporali A, Zentilin L, Floris I, Giacca M *et al.* Nerve growth factor gene therapy using adeno-associated viral vectors prevents cardiomyopathy in type 1 diabetic mice. *Diabetes* 2012; **61**: 229–240.
35 Bish LT, Morine K, Sleeper MM, Sanmiguel J, Wu D, Gao G *et al.* Adeno-associated virus (AAV) serotype 9 provides global cardiac gene transfer superior to AAV1, AAV6, AAV7, and AAV8 in the mouse and rat. *Hum Gene Ther* 2008; **19**: 1359–1368.
36 Gregorevic P, Blankinship MJ, Allen JM, Crawford RW, Meuse L, Miller DG *et al.* Systemic delivery of genes to striated muscles using adeno-associated viral vectors. *Nat Med* 2004; **10**: 828–834.
37 Hazen MS, Marwick TH, Underwood DA. Diagnostic accuracy of the resting electrocardiogram in detection and estimation of left atrial enlargement: an echocardiographic correlation in 551 patients. *Am Heart J* 1991; **122**: 823–828.
38 Li Q, Guo Y, Tan W, Stein AB, Dawn B, Wu WJ *et al.* Gene therapy with iNOS provides long-term protection against myocardial infarction without adverse functional consequences. *Am J Physiol Heart Circ Physiol* 2006; **290**: H584–H589.
39 Zolotukhin S, Byrne BJ, Mason E, Zolotukhin I, Potter M, Chesnut K *et al.* Recombinant adeno-associated virus purification using novel methods improves infectious titer and yield. *Gene Therapy* 1999; **6**: 973–985.
40 Huusko J, Lottonen L, Merentie M, Gurzeler E, Anisimov A, Miyanohara A *et al.* AAV9-mediated VEGF-B gene transfer improves systolic function in progressive left ventricular hypertrophy. *Mol Ther* 2012; **20**: 2212–2221.
41 Makinen PI, Koponen JK, Karkkainen AM, Malm TM, Pulkkinen KH, Koistinaho J *et al.* Stable RNA interference: comparison of U6 and H1 promoters in endothelial cells and in mouse brain. *J Gene Med* 2006; **8**: 433–441.
42 Merentie M, Lipponen JA, Hedman M, Hedman A, Hartikainen J, Huusko J *et al.* Mouse ECG findings in aging, with conduction system affecting drugs and in cardiac pathologies: Development and validation of ECG analysis algorithm in mice. *Physiol Rep* 2015; **3**: pii: e12639.
43 Liu G, Iden JB, Kovithavongs K, Gulamhusein R, Duff HJ, Kavanagh KM. In vivo temporal and spatial distribution of depolarization and repolarization and the illusive murine T wave. *J Physiol* 2004; **555**: 267–279.

LINE LOTTONEN-RAIKASLEHTO

Heart failure (HF) is a severe syndrome, which is expected to increase in the near future. The aim of this thesis work was to determine the expression levels of vascular endothelial growth factors and their receptors in progressive left ventricular hypertrophy leading to HF and to compare echocardiography and magnetic resonance imaging in HF development. Efficacy and safety of different viral vectors were evaluated to find the best candidate for cardiac gene therapy studies.

UNIVERSITY OF
EASTERN FINLAND

uef.fi

**PUBLICATIONS OF
THE UNIVERSITY OF EASTERN FINLAND**
Dissertations in Health Sciences

ISBN 978-952-61-2089-8
ISSN 1798-5706